LONDON'S GLOBAL UNIVERSITY

The interplay between HCV E1E2 glycoproteins and host receptors regulates entry efficiency and antibody evasion.

Mphatso Dumisani Kalemera

A thesis submitted in fulfilment of the requirements for the degree of Doctor of Philosophy

Institute of Immunity and Transplantation

Division of Infection and Immunity

University College London

August 2021

ORINGINALITY STATEMENT

‘I, Mphatso Dumisani Kalemera, hereby confirm that the work presented in this thesis is my own. To the best of my knowledge, it contains no materials previously published or written by another person, or substantial proportions of material which have been accepted for the award of any other degree. Where information has been derived from other sources, I confirm that this has been indicated in the thesis. Please note, I use the plural pronouns throughout thesis rather than singular. This is a matter of preference and does not mean experiments precluding results were performed by anyone besides myself. Indeed, any contribution made to the research in this thesis by others at UCL or elsewhere is explicitly acknowledged within and highlighted the methodology and in the data figure legends.'

Signed: 

Date: 03/08/2021

Abstract

Structural and computational analyses indicate that neither E1 nor E2 (E1E2), the entry proteins of hepatitis C Virus (HCV), fall into the three classes of viral membrane fusion proteins described so far. Consequently, the detailed molecular mechanisms of HCV entry/fusion have remained elusive, so too have the structural features on E1E2 that may govern and antibody resistance. The hypervariable region1 (HVR-1) of E2 has been identified as a lynchpin for HCV humoral immune evasion and was assumed to shield the CD81 binding site from neutralising antibodies. Here, rather than acting as a simple shield, we demonstrate that HVR-1 possesses an autoregulatory function that suppresses the activity of E1E2 on free virions. This function of HVR-1 is achieved via its intrinsic conformational flexibility and high entropy. Significantly, our data suggest that interactions with SR-B1, another HCV host receptor, stabilise HVR-1, which turns off the safety catch mechanis and primes E1E2 for engagement to CD81, a prerequisite molecular event in HCV entry. As such, HVR-1 functions akin to a safety catch on E1E2 activity. Fittingly, mutations that reduce the entropy of HVR-1, and its genetic deletion, turn off the safety catch to generate hyperreactive HCV that exhibits enhanced entry. However, improvements in entry are offset by reduced thermostability and acute sensitivity to neutralising antibodies. Therefore, the HVR-1 safety catch determines the efficiency of virus entry and maintains resistance to antibodies.

We also show in this work that interactions between E2 and CD81 are detrimental to the production of HCV pseudoparticles. Genetic ablation of the HCV receptor from producer cells enhanced or rescued the infectivity of most of patient clones tested without altering virion antigenic properties. We also saw improvement in SARS-CoV1/2 pseudoparticle infectivity following CD81 deletion, indicating CD81 also regulates pseudoparticle production through mechanisms other than binding viral glycoproteins.

Impact Statement

HCV is a significant human pathogen infecting more than 70 million people worldwide, of whom the majority are chronically infected. Current estimates by the World Health Organisation suggest around half a million patients succumb to the disease annually, mostly due to complications arising from cirrhosis or liver cancer. Transmission continues unabated with incidence rates rising in North America as most infected individuals are unaware of their status. The recent development of curative direct-acting antivirals has revolutionised HCV therapy as well as raised the possibility of eliminating HCV. Nonetheless, the high cost of treatment, the risk of reinfection following successful treatment and poor awareness of HCV status in high-risk groups necessitate the development of a prophylactic vaccine.

Most approved viral vaccines work by inducing antibodies that in turn bind to proteins on the surface of viruses and block their entry into target cells. In most cases antibodies target viral entry proteins, these are molecular machinery that, through interactions with host receptors, drive viral penetration of the cellular lipid membranes. Timely examples of vaccines are the current crop of SARS-CoV2 vaccines which function by inducing antibodies against SPIKE, the coronavirus entry protein, and prevent its engagement to ACE2, an essential SARS-CoV2 receptor. By blocking viral entry protein interactions with host receptors antibodies prevent structural changes within the entry proteins which would otherwise coalesce the viral and cellular bilayers. Designing vaccines for any virus requires substantial knowledge of how the entry protein, including its structure and the specific outcomes of entry protein-receptor binding events. For HCV, a significant portion of this information remains unknown because E1E2, the HCV entry proteins, are unique in that they don't fit into the three currently defined structural classes of viral fusion machinery.

This work addresses two, as it emerged, intertwined features of E1E2: the sequence of its engagement to host receptors and how they resist antibodies to establish a chronic infection. The work proposes a novel mechanism through which viruses can maintain antibody resistance coined the 'entropic safety catch'. This mechanism helps explain how a short peptide tail such as HVR-1 can regulate the global antibody sensitivity of E1E2. This is the first account of peptide tail conformational flexibility and entropy regulating viral antibody resistance. However, it is possible convergent evolution has led other viral entry proteins to acquire safety

catches of their own in the evolutionary arms race against humoral immunity. And regarding vaccine development, the work suggests incorporation of the safety catch mechanism (HVR-1 function) into immunogens may be necessary to overcome the poor immunity of E1E2 constructs observed to date.

Dedication

I would like to dedicate this thesis to my late parents, Margaret Titha Daza and Joseph Kalemera, and to my sister Heather Nanzunga Gill.

Acknowledgements

I would like to thank Dr Joe Grove for the opportunity to undertake a PhD in his lab and for his guidance with matters regarding technical expertise, scientific presentation and intellectual stimulation, and his kindness and friendship throughout my time at UCL. I would also like to thank other members of the Grove lab for their technical assistance, scientific discussion and friendship, in no order, Machaela Palor, Lenka Stejskal, Lucas Walker, Samuel Dicken, Piya Mindal, Tobias Starling and Nicole Finardi.

From the division, I would like to thank Dr Laura McCoy, Dr Clare Jolly and Prof David Sansom for sitting on my thesis committee. Additionally, I am grateful to Dr Lucy Thorne for technical training and kind support, as well as Scott Layzell, Erin Waters, Houman Houshidar and Cayman Williams for their friendship and providing comical relief from the barrage of scientific discussions.

I would also like to thank our collaborator Adrian Shepard (Birkbeck College) for supervising the computational part of the work described here, which, in turn, was undertaken by Lenka Stejskal. I would like to express my gratitude for Chris Illingworth (Cambridge University), for collaborating with us to generate a mathematical model of HCV entry, which informed much of the work performed in this thesis.

I would like to thank my friends outside the lab for the support offered during these past five years. Particularly, Matthew Judge for proof-reading the majority of my written work, Jamie Polius for mixing the soundtracks to my thesis writing. And Sarah Wilson, Victor Robinson, Ross Dlima, Trifon Dimov and Bartek Glab for being my emotional tethers during turbulent times.

Finally, I would like to thank my family Heather, Lee, Annie, Selina, Thoko, Chiku and Tundo, for being my biggest (and loudest) supporters. This thesis would not have materialised without your encouragement and love!

Publications arising during PhD

2021, Dicken SJ*, Murray MJ*, **Kalemera MD***, Stejskal L*, Thorne LG, Reuschl AK, Forrest C, Ganeshalingham M, Muir L, Palor M, McCoy LE, Jolly C, Towers GJ, Reeves MB and Grove J. Characterisation of B.1.1.7 and Pangolin coronavirus spike provides insights on the evolutionary trajectory of SARS-CoV-2 Preprint, bioRxiv

2020, Stejskal L*, **Kalemera MD***, Palor M, Walker L, Daviter T, Lees WD, Moss DS, Kremyda-Vlachou M, Kozlakidis Z, Rosenberg W, Illingworth C, Shepherd AJ and Grove J**.** An Entropic Safety Catch Controls Hepatitis C Virus Entry and Antibody Resistance Preprint, **bioRxiv**

2020, Kalemera MD, Capella-Pujol J, Chumbe A, Underwood A, Bull RA, Schinkel J, Sliepen K, Grove J**.** Optimized cell systems for the investigation of hepatitis C virus E1E2 glycoproteins **J Gen Virol**; doi:10.1099/jgv.0.001512

2019, Kalemera M, Mincheva, D, Grove J, Illingworth CJ. Building a mechanistic mathematical model of hepatitis C virus entry **PLoS Comput Biol** 15(3): doi.org/10.1371/journal.pcbi.1006905

Presentations during PhD

2019, HCV balances the opposing selective pressures of neutralising antibody evasion and efficiency of entry by conformationally tuning the E2 glycoprotein. (Oral) HCV 2019, Seoul, South Korea

2019, HCV balances the opposing selection pressures of antibody evasion and efficiency of entry. (Oral) 17th UK Hepacivirus and Flavivirus Meeting, Lake District, UK

2018, HCV entry is a numbers game. (Oral) 16th UK Hepacivirus and Flavivirus Meeting, Lake District, UK

Table of Contents

List of Figures

List of Tables

1 Introduction

1.1 Preface

Hepatitis C virus (HCV) is an enveloped positive-sense, single-stranded RNA virus with a greatly restricted species tropism. Humans are the only known natural host of the virus and infection of chimpanzees has only been observed within the confines of a laboratory (1). The cloning and discovery of HCV was a significant event in medical history because HCV has been determined to be the major etiological agent of viral hepatitis alongside hepatitis B virus (HBV) (2). Thirty years after its discovery HCV remains a leading indicator for liver transplantation despite there being curative treatment (3). In the UK and most developed countries, parenteral infection is now the main route of HCV transmission with the majority of infections stemming from intravenous drug use (IVDU) (4,5).

Following blood-to-blood transmission, HCV is transported to the liver by the circulatory system. Here, interactions between the virus envelope proteins and receptors on hepatocytes culminate in membrane fusion, delivering the viral genome and initiating viral translation and replication (6). Following infection, some patients clear HCV in the acute phase of disease without the need for medical intervention; however, HCV persists in approximately 65-80% of patients, resulting in chronic hepatitis (7–9). The continued presence of HCV RNA in a patient's bloodstream past six months post-infection qualifies as chronic HCV infection (10). The disease progresses slowly, taking years or decades before symptoms become apparent. The morbidity and mortality of chronic HCV are often attributed to complications such as cirrhosis and hepatocellular carcinoma (HCC) which materialise due to frequent bouts of immune-mediated inflammation within the infected liver (11).

The mechanisms that govern whether HCV persists in some and is cleared in others are incompletely understood. Nonetheless, ex-vivo studies suggest clearance is dependent on both the cellular and humoral arms of the adaptive immune response. Robust $CD8^+$ T cell responses directed toward the non-structural proteins of HCV and the early appearance of neutralizing antibodies have both been observed in patients who speedily cleared infection (12–18). By contrast, the early appearance of $CD8^+$ escape mutants is often observed in subjects who develop persistent infection (19,20). Viral diversification, driven by the humoral immune response, similarly leads to the emergence of variants that are highly resistant to neutralising antibodies (21,22). Recently, a CD8+ T cell-based vaccine in phase II clinical trials failed to prevent

chronic infection in injection drug users (23). Effective control of HCV will likely require a combination vaccine composing the HCV structural and non-structural proteins to elicit both CD8+ and B cell responses since no predilection to either response is observed in patients who clear acute infection.

The interplay between HCV and the host cell during infection is complex with multifaceted consequences, yet understanding it is crucial for the development of effective control strategies, such as a vaccine. This thesis will focus on the evolutionary 'arms race' between HCV and the humoral immune response, exploring how the virus conformationally tunes its major glycoprotein E2 to balance the opposing selective pressures of the need for efficient entry with the requirement to evade neutralising antibodies.

1.1.1 Origins and classification

HCV is a member of the *Flaviviridae* family which also includes a host of arboviruses carrying significant disease burden such as Zika virus and Dengue virus, which are the causal agents of congenital zika syndrome and dengue fever, respectively (24). HCV is classified to a separate genus (*hepacivirus*) from the arboviruses (genus *flavivirus*) within the *Flaviviridae* family. Few viral species are classified to *hepacivirus* genus alongside HCV, these include GB virus B (GBV-B) which causes acute hepatitis in tamarins and a number of non-primate, rodent and bat hepaciviruses (Fig 1.1) (25,26).

The origins of HCV remain mysterious. However, since humans are continuously exposed to diverse animal viruses via direct contact with domestic or wild animals, it is highly likely HCV emerged from a zoonotic event. Before 2011, GBV-B was the only known member of the *hepacivirus* genus beside HCV (27). In the time since, the exploration of potential hosts unrelated to non-human primates has led to the discovery of many hepacivirus species which can be classed into equine, rodent, bovine and shark hepaciviruses (Fig 1.1) (28). Notably, the discovery of Wenling shark virus, a shark hepacivirus, greatly expands the potential host range of hepaciviruses and may lead to the discovery of additional novel hepaciviruses in non-mammalian hosts (29). Indeed, a novel reptilian hepacivirus was recently identified through metagenomic mining in a preprint (30)!

The recent discoveries of novel hepacivirus species have provided new insights into the origins and the evolution of the *hepacivirus* genus. Indeed, it is now possible to make well-informed speculations as to the possible zoonotic source for HCV (31–33). Equine hepacivirus (EqHV) is currently the closest genetic relative to HCV, it's possible EqHV spilt over into humans from horses and has undergone speciation to become what we now recognise as HCV (34). Alternatively, the two viral species may share a common ancestor. The fact that EqHV exhibits very low sequence diversity supports the latter hypothesis. If EqHV were the direct ancestor of HCV, it means EqHV would have jumped into humans, rapidly evolved and diversified all the while remaining phylogenetically stagnant in horses which seems unlikely (28). However, species-specific immune factors may account for the gap in diversity between HCV and EqHV.

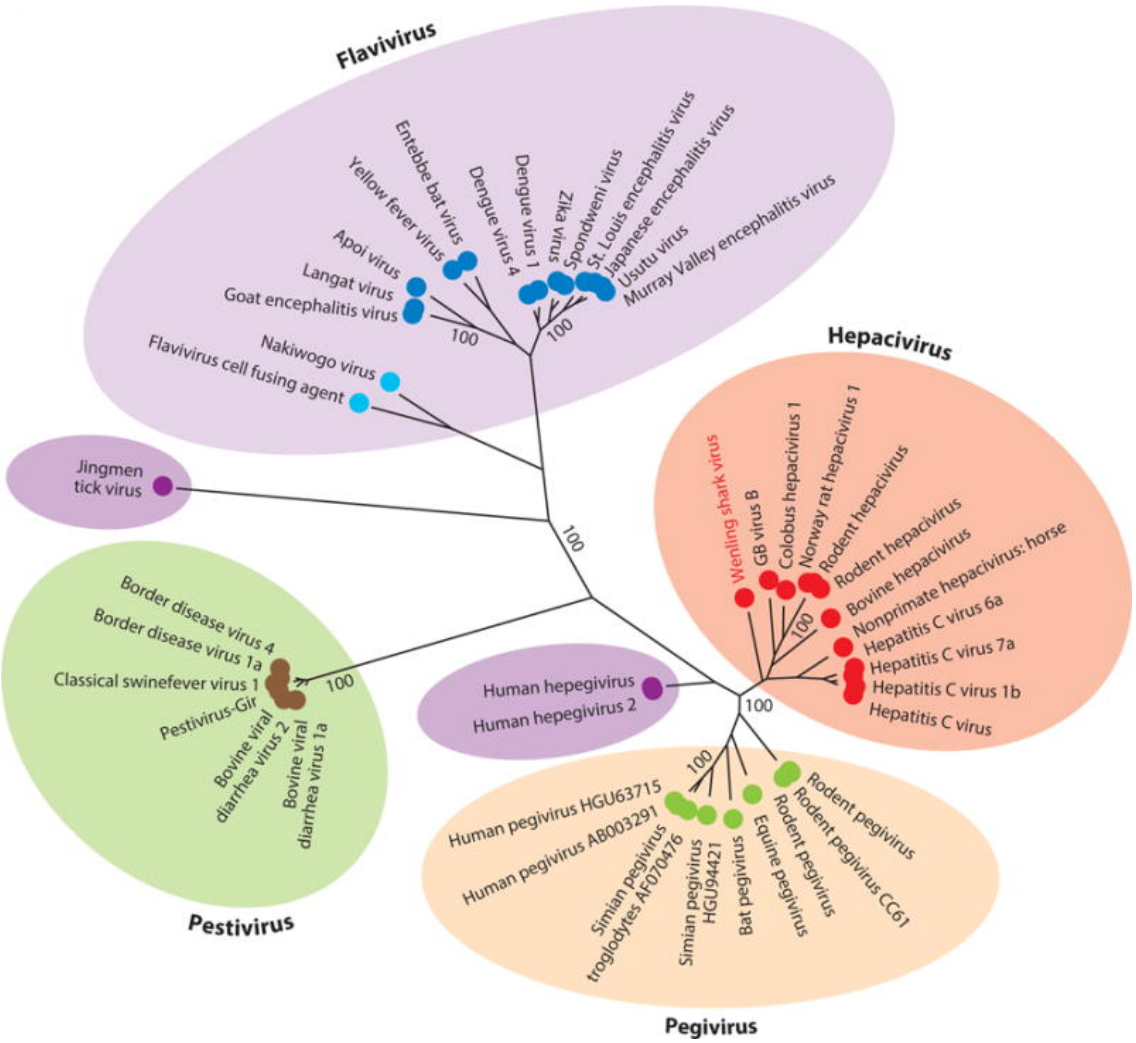

Figure 1.1 Classification of the Flaviviridae family into four major genera. The tree is drawn according to phylogenetic analysis of ns3 (helicase) gene sequences and representative members of each genus are shown. The figure is taken from a review by Hartlage et al (28).

The high species specificity of hepaciviruses and their propensity for persistence suggests long-term coevolution and extensive host adaptation. This, combined with the seemingly wide range of hepacivirus hosts, raises the possibility that, throughout their history, ancestral hepaciviruses infected many different animals and possibly spilt over into others, including humans, before host speciation (35). Extensive screening of animals for hepacivirus infection is required to identify the origin of HCV and provide clarity to the puzzle of hepaciviral evolution. Indeed, it is likely that undersampling has led to the long phylogenetic separation (high genetic separation) currently observed between the various hepacivirus lineages.

Consistent with extensive host adaptation, HCV is an exceptionally diverse virus, with seven major genotypes (numbered 1-7) (Fig 1.2, below) and an eighth under debate (36,37). The HCV genotypes are further subclassified into subtypes (labelled alphabetically [a, b, c etc.]). HCV classification is defined by nucleotide sequence heterogeneity. Clones share 65–70% sequence identity within a genotype and 75–80% homology within a subtype (38–41). Genetic variability is unevenly distributed across the genome (42). Regions corresponding with viral enzymatic function (such as translation and replication) are highly conserved as is the region encoding the viral capsid; in these two regions, distant clones share up to 90% and 80-88% sequence identity, respectively (43,44). The most variable region within the HCV genome is that encoding the envelope glycoproteins (45). Here, sequences comprising the hypervariable regions 1 and 2 (HVR-1 and HVR-2) exhibit the least homology with only 50% identity between different isolates (46).

Further sequence diversity is observed within individual hosts since the error-prone nature of HCV replication permits the emergence and coexistence of minor genetic variants (47). This population of minor intra-host variants share 98% homology and are commonly referred to as a quasispecies. It is generally presumed that the emergence of quasispecies during infection enables HCV to rapidly adapt to the changing, and hostile, environment produced by the immune response (48).

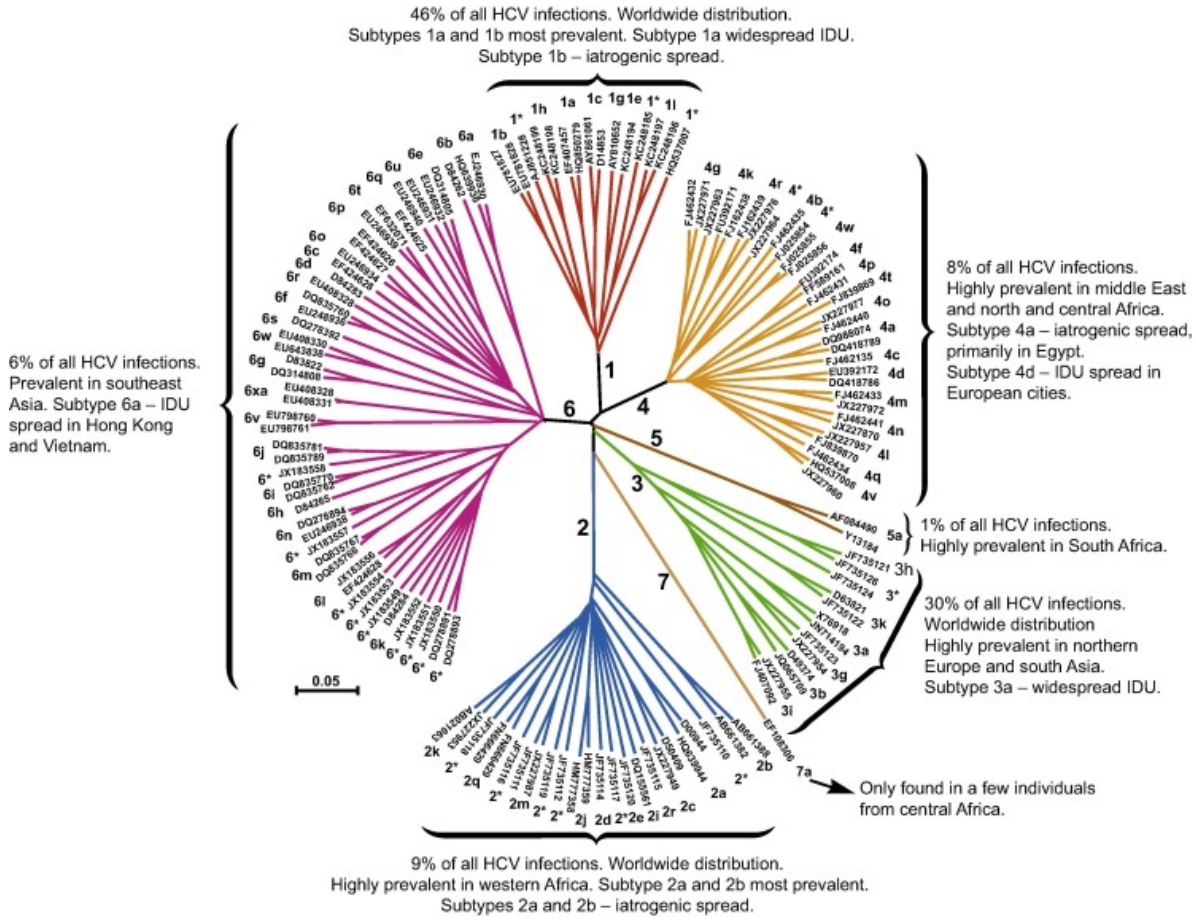

Figure 1.2 Classification of HCV into 7 major genotypes and numerous subtypes. The tree is drawn according to phylogenetic analysis of the open reading frame (nucleotide) sequences. The overall prevalence and geographical distribution for each major genotype are indicated. The illustration is from a review by Jens Bukh (37).

1.1.2 Natural history of HCV infection

Unlike HBV acute HCV infection is asymptomatic in 75% of patients and consequently goes undiagnosed is most individuals (49,50). Current estimates indicate between a quarter and a third of individuals who contract HCV will clear the virus within six months with the remainder developing chronic infection. Chronic hepatitis C, like all forms of viral hepatitis, progresses slowly with continuing fibrosis due to recurrent bouts of immune-mediated inflammation of the infected liver. Unchecked fibrosis progresses to cirrhosis with liver failure, and finally HCC. Annually, HCC is estimated to manifest in 1–4% of established HCV-associated cirrhosis cases (7,9).

Factors thought to contribute to the natural clearance of HCV include female sex, Caucasian ethnicity, infection with a genotype 1 strain, restricted diversity of viral

quasispecies and patient age (8,51–53). Humoral immune responses appear to weaken with age as the serum of young patients tends to possess a stronger neutralizing effect and is often more effective in neutralizing a broader panel of clones (54,55). The emergence of a broad adaptive immune response in the early stage of infection is associated with clearance of HCV (56–58). However, owing to HCV's great diversity and repeated exposure through IVDU in high-risk persons, clearance does not provide sterilising immunity and re-infection with heterologous and even homologous genotype variants is common (59).

Polymorphisms in immune genes are also known to impact disease progression. Several genome-wide association studies (GWAS) have established a strong correlation between spontaneous HCV clearance and response to IFN-treatment versus polymorphisms in the *IL28B* gene, which encodes for the cytokine interferon-λ3 (IFN-λ3). The IFN-λ3 rs12979860 single nucleotide polymorphism (SNP) was associated with clearance in six different cohorts. Additionally, specific alleles of two SNPs in human leukocyte antigen *(HLA)-DQB1* and *HLA-DQA2* genes, rs2395522 A and rs2395522 G, have been shown to regulate neutralizing antibody (nAb) breadth (18,60). HLA-DQ is a heterodimer of the type MHC class II present on antigen-presenting cells (APC) and is important for antigen presentation to $CD4^+$ T helper cells. Osburn et al. found that the neutralizing activity against genotype 1 viruses was broader in plasma derived from patients carrying the rs2395522 A or rs2395522 G alleles, irrespective of whether they were infected with a genotype 1, 2 or 3 virus (18). A later study further supported the link between the expression of the rs2395522 A allele in genotype 1-infected patients and their development of broadly-neutralizing antibodies (60). Notably, the sites of both SNPs are located outside the protein coding region of the *HLA-DQ* gene suggesting that they may regulate gene transcription in a manner that in-turn broadens nAb responses (18). However, it should be noted that neither SNP has been associated with HCV clearance in GWAS analysis so whether host genetics truly influence the breadth and potency of nAb remains ambiguous.

1.1.3 Epidemiology

Although epidemic jaundice had been reported by both the Greeks and Romans, it was not until the mid-20^{th} century that it was determined that viral etiological agents

cause hepatitis. Teams in Germany, England and the USA employed human 'volunteer' experiments and confirmed the transmissibility of two distinct forms of viral hepatitis through their clinical and epidemiological characteristics. Patients whose plasma could transmit hepatitis for only up to 45 days post-infection were deemed to have hepatitis A and patients whose incubation period lasted over 60 days were regarded to have hepatitis B (61).

The first of the viruses to be discovered was one responsible for chronic disease, and it was appropriately named hepatitis B virus. Its discovery was a drawn-out process lasting nearly nine years from the point a key antigen (HBs) was identified to the point an association between said antigen and post-transfusion hepatitis was established in 1972 (62). By the mid-1970s, hepatitis A virus (HAV) was discovered and shown to result in an almost entirely acute disease which rarely led to conditions like jaundice or cirrhosis, as expected. Screening for HAV and HBV and the subsequent exclusion of infectious donors only resulted in a 25-50% fall in post-transfusion hepatitis cases indicating further causal agents were yet to be identified. Disease not attributable to HAV or HBV was collectively termed non-A non-B hepatitis. The discovery of HCV by Houghton and colleagues in 1989, and subsequent screening efforts confirmed HCV as the major causative agent for viral hepatitis alongside HBV (2). Notably, the cloning of plasma-extracted HCV nucleic acid into an expression vector symbolised a paradigm shift in the approach for identifying infectious agents. It was the first time in history that a pathogen was identified using a direct molecular biology approach without tissue culture, serology, or immune-electron microscopy.

By the mid-1990s, the mandatory practice of screening blood for HAV, HBV and HCV reduced transfusion-related hepatitis transmission to exceedingly low levels in industrialised countries (4,63). In these countries, good aseptic practice has also led to transmission events associated with surgical, dental and perinatal medical procedures occurring only sporadically during local breaches of infection control and hygiene measures (64). As mentioned previously, IVDU has now become the main source of incident HCV infections in industrialised countries (63). There are over 16 million practising injection drug users worldwide and among them, HCV infection prevalence ranges from 45% to >90% and annual incidence rates are 6-40% (65). Frequent HCV transmission following intranasal recreational drug use is also observed (66). This mode of transmission appears to be facilitated by damaged incurred to the

nasal mucosa following long-term use of substances like cocaine or ketamine, which induce bleeding. Sexual intercourse is now regarded as a route of HCV transmission in Europe, North America and Australia (67–72). Incident infections are predominantly reported in men who have sex with men; in this group, individuals who are HIV positive appear to be most at risk (73).

IVDU is prevalent in some lower-income countries and is predicted to contribute to HCV transmission (74,75), nevertheless most new infections in these countries are suspected to occur through the iatrogenic route (76). In Egypt, where HCV prevalence in people aged 15 to 59 stands at over 12%, most infections can be traced back to syringe reuse during mass-treatment campaigns in the 1960-70s to combat schistosomiasis (77). Similarly, ongoing epidemics in central African countries, where HCV prevalence rates are notably high among people >50 years, are widely suspected to have originated from mass-treatment efforts or vaccination campaigns in the late 20th century (78–80).

At the turn of the 21st century, 130-170 million people were estimated to be HCV positive (translating to a global prevalence of 2.2-3.0%) (81). By 2014, estimates were revised down to around 100 million due to improved mathematical modelling and maybe an early reflection of the curative impact of direct-acting antivirals (DAAs) (82). The WHO global hepatitis report in 2017 estimated 71 million people are living with chronic HCV infection (83).

HCV prevalence varies geographically. Industrialised countries generally report low prevalence (≤2%), with northern European nations, in particular, possessing rates of only 0.4% or lower (84). Countries with the highest prevalence (≥5%) are mainly low-middle income countries such as aforementioned Egypt, Pakistan (~6.8%), Nigeria (3.1-8.4%), Georgia (~6.7%) (85–88). The modern-day geographic distribution of the HCV genotypes is complex (89). Genotypes 1a, 1b, 2a and 3a are distributed globally. The rapid spread of these epidemic subtypes is largely acknowledged to have occurred in the decades before the discovery of HCV by way of blood transfusion and mass vaccination and treatment campaigns of infectious diseases (90–92). The majority of HCV subtypes are largely endemic: endemic genotype 1 and 2 are largely restricted to West Africa, 3 to South Asia, 4 to Central Africa and the Middle East, 5 to Southern Africa and 6 to South East Asia (90,93,94)

Recent estimates suggest ~182,400 people in the UK were living with chronic HCV infection in 2015 (95). Modelling predicts this figure to have fallen to ~143,000

by year-end of 2018 (96). Qualitative RT-PCR of UK cohorts frequently identify genotypes 1 and 3 as the most prevalent in the UK, with subtypes 1a and 3a often overrepresented (95,97,98). The most comprehensive of such studies found genotype 1 to account for nearly half of all cases (46.8%), followed by 3 (35.8%), 2 (4.4%) with genotypes 4, 5 and 6 only accounting for 3.3%, when taken together (98).

Infection with multiple strains (2 or more) is common and can be established simultaneously or sequentially. Surveillance analyses of high-risk groups in different regions have reported that the rate of multiple strain infections ranges from 5 to 25% (99–101). Reinfection, with an identical or different strain of HCV, following clearance is very common amongst people who use injectable drugs (PWID) as they are frequently exposed by way of sharing injection equipment (102). The exceptional diversity of HCV and the limited protective immunity generated toward the virus are also factors for multiple infection and reinfection (84,102).

1.1.4 Treatment

Since acute infection with HCV is predominantly asymptomatic a substantial number of patients begin treatment regimen only when the disease has advanced to a stage at which liver complications become apparent. Currently, combination DAA therapy is the standard HCV treatment. DAAs are relatively new, having been approved as the standard of care (SOC) for chronic HCV only in the last decade. Before this, the SOC was a combination of pegylated interferon-alpha (PEG IFN-α) and ribavirin administered for 24- to 48-weeks depending on genotype (103,104). Viral eradication rates remained suboptimal during this era as sustained virologic responses (SVR12), a period where HCV RNA is undetectable in blood for ≥12 weeks, were identified in 50-75% of patients (105). Patients with genotype 1 infection, in particular, presented a clinical challenge as SVR12 rates following a 48-week course of PEG IFN-α stood at a measly 40% (106). Side effects of PEG IFN-α regimens include flu-like symptoms, cytopenia and, more concerningly, given the regimen length and IDVU history of many patients, depression and anxiety (105).

Combination DAA therapy is the superior SOC for patients living with chronic HCV as SVR12 rates exceeding 95% have been reported in numerous cohort studies (107). Furthermore, unlike PEG IFN-α regimens, combination DAA therapy (with the occasional ribavirin supplementation) can achieve pan-genotypic effectiveness and

side effects are minor/fewer during/after the standard 12-week and present little psychiatric morbidity (102,108,109). In the UK DAA therapy provided by the NHS consists of a single drug regimen of or a combination of protease (NS3) inhibitor (simeprevir, paritaprevir, glelcaprevir voxilaprevir), NS5A inhibitor (ledipasvir, ombitasvir, pibrentasvir, velpatasvir), polymerase (NS5B) inhibitor (dasabuvir, sofosbuvir) and/or ribavirin (95,96).

In 2016, when the curative capabilities of DAA therapy became clear, the WHO called for the elimination of viral hepatitis as a major public health threat by 2030 (i.e. a 90% and 60% fall in the incidence and mortality rates, respectively) (110). Despite this, the high cost of DAA therapy (~£12,000 per 12-week course) and underdiagnosis due to the asymptomatic nature of acute infection present significant hurdles for meeting these targets (111). Furthermore, reinfection rates are high among PWID and many clinicians and insurance providers are reluctant to approve DAA therapy for this group citing poor cost-effectiveness (102,112). Together, these obstacles necessitate the development of a prophylactic vaccine to prevent future cases and get us closer to achieving elimination by 2030 (113). A review of HCV vaccine development and trials will follow in the upcoming sections.

1.1.5 Basic virology

Despite the many efforts made toward understanding HCV and the development of new technologies that enable the comprehensive study of a single virion, we have limited information on the HCV virion structure. The consensus from independent ultrastructural analyses of full-length cell culture HCV is that virions are structurally irregular, lack obvious surface features and are pleiomorphic in size (ranging from 50 to 80 nm) (model shown in Fig 1.3). In vitro molecular studies show that virions are encompassed by an endoplasmic reticulum (ER)-derived envelope (lipid bilayer), in which the E1E2 glycoproteins are embedded as heterodimers (114–116). The lipid bilayer surrounds an icosahedral core/capsid (30-40 nm) which contains the 9.6 kilobase (kb) positive sense, single-stranded RNA genome of HCV (117).

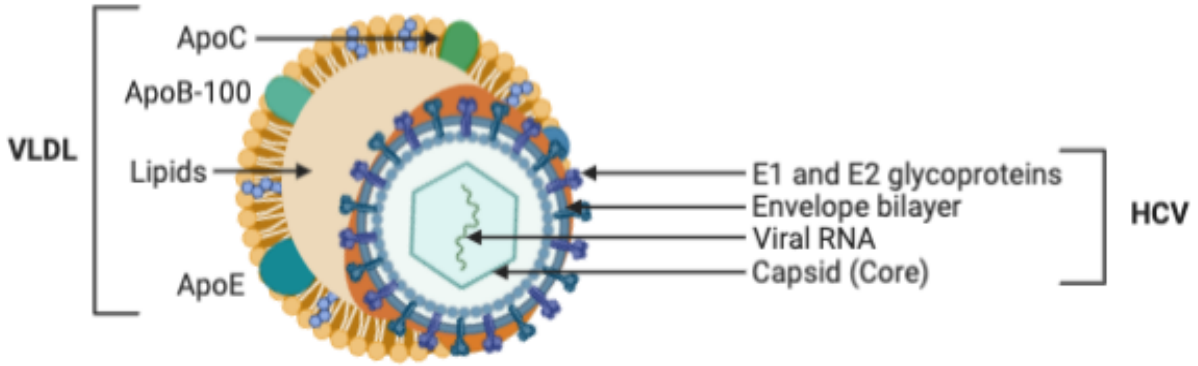

Figure 1.3. A model of the HCV lipoviralparticle (LVP). The HCV particle consists of an endoplasmic reticulum-derived envelope within which the E1 and E2 glycoproteins are anchored. The envelope surrounds an icosahedral capsid, formed by the viral core protein, which contains the positive-stranded RNA genome. Highly infectious particles are a hybrid of HCV virion and VLDL components named LVP. The apolipoprotein constituents of LVP are illustrated in the diagram. Diagram produced in BioRender.

The difficulty of resolving the HCV structure is largely due to the virion's unique lipid composition (115). Mass spectral analyses established that the lipid composition of HCV particles resembles that of very low- and low-density lipoproteins (VLDL, LDL) (115,116). Infectious particles, isolated from both patient sera and cell culture, have a low density, are rich in cholesterol and triglycerides and contain host apolipoproteins (Apo) such as ApoB, ApoA-I, ApoE and ApoCs (Fig 1.3) (116,118,119), consequently, the HCV particle is often considered a lipoviralparticle. HCV particle association with lipoprotein components serves a critical purpose in the viral life cycle, hijack of host apolipoproteins, in particular, allows for efficient propagation in hepatocytes (120,121).

1.1.6 Translation and replication

Following successful entry, which will be discussed extensively in upcoming sections, the translation of the HCV genome is initiated. The 9.6 kb positive single-stranded RNA genome encodes a long open reading frame (ORF) which is flanked by two untranslated regions (UTRs) (Fig 1.4 A). The UTRs harbour the signals for viral protein and RNA synthesis and signals to coordinate both processes (122). The UTRs also harbour crucial cis-acting elements that protect the viral genome from host anti-viral factors. Notably miR-122, a liver-specific miRNA, interacts with such elements and

recruits Argonaute 2 to the 5' end of the viral genome, thereby stabilising and protecting HCV RNA from degradation by 5' exonucleases (123,124).

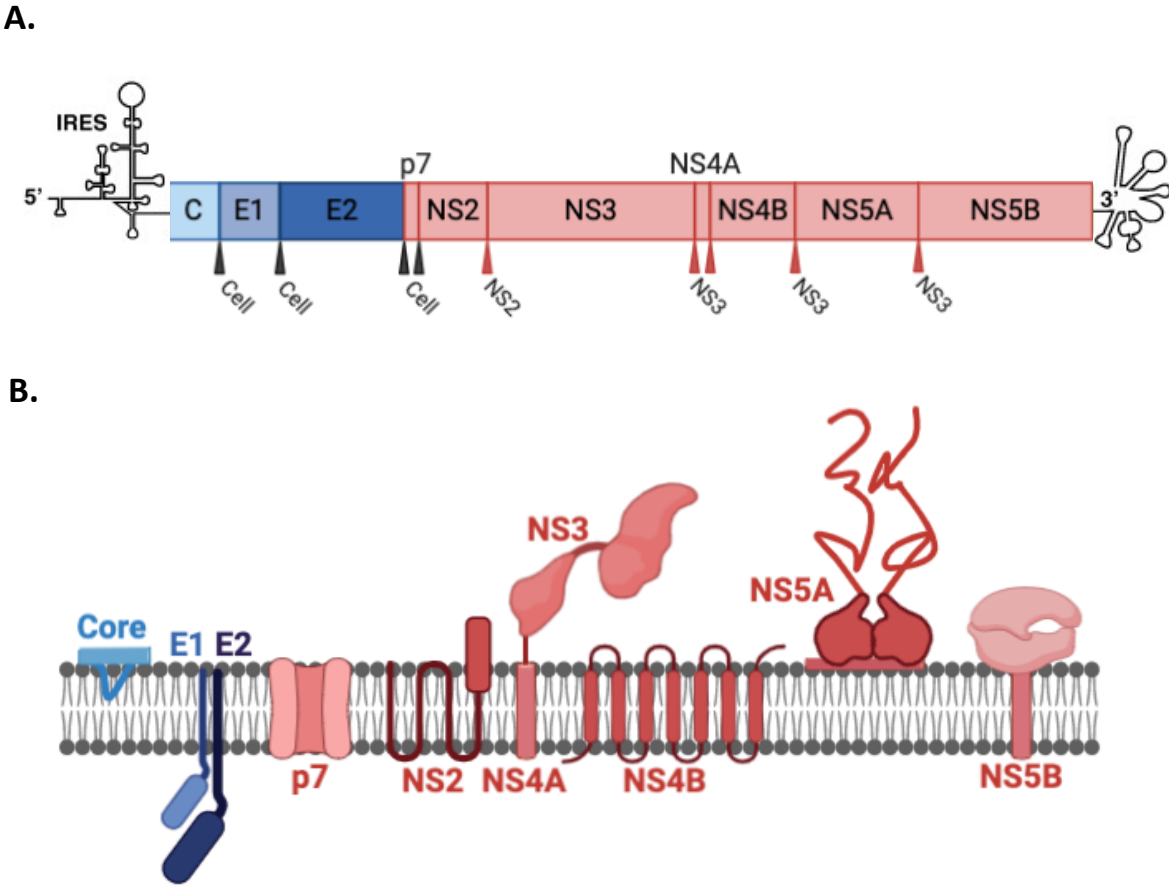

Figure 1.4. HCV virus replicon and membrane organisation of viral proteins. (**A**) The RNA genome of HCV is positive-stranded, containing a single open reading frame flanked by highly structured 5' and 3' untranslated regions (UTRs). Translation of a single polyprotein is initiated at the internal ribosomal entry site (IRES). The polyprotein is cleaved by cellular (black arrowheads) or viral proteases (red arrowheads). (**B**) Membrane association of HCV proteins. Functional domains of non-structural proteins face the cytosol whereas the globular domains of the entry proteins E1 and E2 face the ER lumen. Diagram produced in BioRender.

Translation of the HCV ORF is initiated through an internal ribosomal entry site (IRES) in the 5' UTR. Directly binding to this site places ribosomes close to the start codon of the ORF. The translated polyprotein is processed cotranslationally and posttranslationally by host and viral proteases into ten distinct products. The structural proteins (core [C], envelope [E] 1 and E2) are in the N-terminal third and the non-structural (NS) proteins occupy the remainder (Fig 1.4 B) (122). The viral RNA-dependent RNA polymerase (RdRP) NS5B, together with the non-structural protein NS3/4A, NS4B and NS5A are the minimal machinery required for HCV translation and replication (125).

Typically, HCV amino acid residues are numbered using absolute nomenclature, i.e., based on the HCV polyprotein with numbering starting from the first residue of the core protein continuing to the end of NS5B. In this system, residues comprising the E2 glycoprotein in the reference isolate, H77, are numbered 384-746 (126).

The function of the non-structural proteins will only be discussed briefly here as these are beyond the scope of this study, but a detailed overview can be found elsewhere (127). NS2 is a viral cysteine protease involved in both viral polyprotein maturation and particle assembly (128). NS3 has two domains which perform independent functions; one domain is an essential serine protease that cleaves the NS3 to NS5B region of the viral polypeptide (see Fig 1.4 A) (129). The other domain forms the HCV helicase which unwinds duplex RNAs formed during viral replication. NS4A is membrane protein that interacts with NS3 thereby anchoring the enzyme which has no transmembrane domain of its own (129). Indeed, most HCV proteins are membrane-associated (Fig 1.4 B), and some have functions linked to host membrane reorganisation. Accordingly, viral proteins induce the extensive rearrangement of host cell ER membrane during infection, resulting in 'membranous webs' with vesicles that provide a protected environment for HCV replication and assembly (Fig 1.5) (130,131). Although most proteins in the replication complex contribute to membranous web formation, it is NS4B and NS5A that are key in its biogenesis and maintenance.

NS4B is a highly hydrophobic ER membrane integral protein (132). It possesses amphipathic helices in both its N and C terminal domains which it uses to induce membrane curvature, a crucial early step in membranous web formation (133). Furthermore, in vitro experiments suggest NS4B binds the negative HCV strand at the 3' end via an arginine-rich motif (134). This interaction may serve to recruit negative-strand viral RNA, the template for positive strand genomes, to sites of replication.

Comprised of three domains separated by low complexity sequences and anchored to the membrane, NS5A is perhaps the most enigmatic of the HCV proteins (135). The N-terminal domain I is the best characterised, it contains both an RNA and a zinc (Zn^{2+}) binding domain which are essential for replication. In contrast, the two C-terminal domains are predicted to be intrinsically disordered. The NS5A interactome represents a feat in viral genetic economy; the viral protein interacts with dozens of cellular proteins, in fact too many to engage simultaneously. It is thought intrinsic disorder and differential phosphorylation creates diverse pools of NS5A, separated

both spatially and temporally, that play different roles and interact with different subsets of host factors (136). Examples of key host factors interacting with NS5A include cyclophilin A, an is essential cofactor for membranous web formation, and phosphateidyinositol-4-phosphate-kinase-III alpha which bridges virion assembly with lipid metabolism (137–139).

The viral RNA-dependent RNA polymerase (RdRP) NS5B produces an antigenome negative-strand intermediate from which progeny positive-strand genomes are produced (140,141). Follow-up rounds of translation of positive-strand genomes result in ≥1,000 fold excess of viral proteins over the viral genome (140), and finally viral genomes are packaged into newly assembling virions (142).

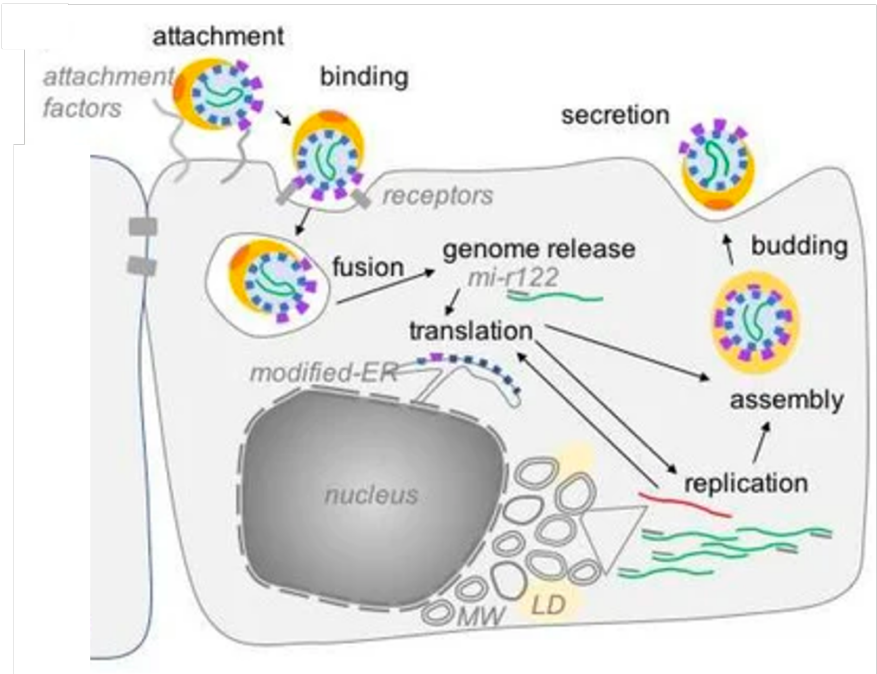

Figure 1.5. The HCV life cycle. The different steps of the HCV life cycle are indicated in black. ER endoplasmic reticulum, MW membranous web. LD lipid droplets. The negative strand intermediate is shown in red. Adapted from Alazard-Dany et al (127).

1.1.7 Assembly, budding and secretion

HCV assembly occurs near the membranous web at assembly sites derived from ER-membranes and close to lipid droplets (143). Initiation of particle assembly is thought to require the release of replicated genomes from the web to the lipid droplets where the core protein, the foundation of the virion capsid, accumulates following biosynthesis (144). A key role for NS5A in controlling the transition from replication to

assembly is well described, most notably, it is involved in RNA genome delivery to core proteins (145). NS2 and p7 also play central role in virus assembly via their interactions with various viral structural and non-structural proteins (127,144). Notably, they control the spatial-temporal recruitment of the envelope glycoproteins E1E2, NS3 and NS5A to assembly sites, thereby correctly bringing together key viral actors required for assembly (146–149).

Since HCV core locates to the cytosolic side of the ER membrane to access lipid droplets, nascent viral particles must transfer across the ER lumen to access the secretory pathway. At this stage, particles acquire their envelope, with unmodified viral glycoprotein embedded, by budding into the ER lumen. Fittingly, roles in HCV particle release have been described for components of the ESCRT (endosomal sorting complex required for transport) pathway (150–152). As the HCV particles transit through the secretory pathway, E1 and E2 undergo post-translational modification. Notably, E1 and E2 on purified HCVcc particles harbour both high mannose and complex Asn-linked glycans, indicating they are processed via the Golgi apparatus, where glycan modification is known to occur (153).

As mentioned previously, the lipid composition of HCV virions resembles that of VLDLs. It is likely HCV hijacks the VLDL assembly pathway for virion maturation and eventual release (154). HCV particles acquire their characteristic low buoyant density as they traverse the secretory pathway by interacting with ApoE-rich VLDL or HDL particles (155,156). Of note is the important role of the p7 ion channel which protects viral particles in transit from exposure to low pH by neutralising the acidification of otherwise acidic intracellular compartments. For a detailed comprehensive review of the HCV life cycle please see reviews (130,142,157,158). An overview of anti-HCV responses during natural infection are discussed in the succeeding section.

1.2 Immune responses to HCV

Upon transmission of a virus into a new host, innate immunity acts as the first line of defence. Innate immunity is initiated upon detection of unspecific pathogen-associated molecular patterns (PAMPS) by host pattern-recognition receptors. Innate immunity acts immediately upon infection and its activation is crucial for the induction and regulation of the adaptive immunity, which takes four to eight weeks to take effect

upon primary HCV infection (159). Adaptive immunity targets pathogens more specifically and provides immunological memory. Effective interplay between innate and adaptive arms of immunity are predicted to influence disease outcome. However, gauging the innate immune response's contribution to HCV clearance has proven challenging since acute HCV is largely asymptomatic. Conversely, a quick, strong, broad and persistent adaptive response correlates positively with spontaneous HCV clearance (159,160).

1.2.1 HCV innate immune response

During HCV infection, viral RNA is the major PAMP inducing an innate immune response (161). Intracellular viral RNA is recognised by RIG-I and the Toll-like receptor 3 (TLR3) recognises double-stranded RNA products within endocytic membranes (122). RIG-I sensing results in the phosphorylation of the transcription factor interferon-regulatory factor (IRF-3), which activates the IFN-β promoter (162). Similarly, the signalling cascade initiated upon recognition by TLR3 culminates in the activation of IRF-3 and nuclear factor kappa B (NF-κB), driving IFN-β transcription (163). IFN-β released into the extracellular space by infected cells binds the IFN-α/β receptors IFNAR1/2 on nearby cells, activating the Janus Kinase-1/signal transducers and activators of transcription (JAK/STAT) pathway which culminates in the activation of a set of IFN-stimulated genes (ISGs) (161). ISG transcription induces an antiviral state promotes and the secretion of multiple IFN types. Characterised by the expression of restriction factors that impede viral entry and viral as well as degrades viral genetic material (164).

HCV infection is often chronic, indicating it has evolved some effective mechanisms to counter the host innate response. To this end, several HCV non-structural proteins interact with host innate and signal transduction factors to attenuate the antiviral state (165). NS3/4A can induce the cleavage of transducers involved in TLR signalling, particularly TLR-domain containing adapter-inducing IFN-β (TRIF), to inhibit TLR3 signalling. Additionally, the NS3/4A protease directly cleaves MAVS (Mitochondrial antiviral signalling protein) attenuating RIG-I mediated IFN-β expression (166). These interferences allow HCV to successfully overcome the innate immune response, which becomes insufficient to eliminate the virus (167).

Natural killer (NK) cells comprise the majority of innate cells in the human liver. NK cells are an important component of innate immunity and participate in HCV clearance. NK cells produce IFN-γ which primes $CD4^+$ T as well as limits HCV replication through ISG induction (168). Upon contact with infected hepatocytes, NK cells release granules filled with granzymes and TNF-related apoptosis inducing ligand (TRAIL), leading to lysis of the infected cell (169). NK cells are sometimes thought of as a 'bridge' between the innate and adaptive arms of immunity as they are implicated in dendritic cell (DC) maturation (170). DCs process and present antigens via MHC I and II, leading to the activation of $CD8^+$ and $CD4^+$ T cells, respectively. So, NK cells can affect the ability of DCs to prime effector T cells by editing DC function (170). Notably, NK cells are activated during acute HCV infection, irrespective of the clinical outcome (171).

1.2.2 HCV adaptive immune response

Adaptive immunity constitutes the last barrier to HCV infection. The innate immune response allows for the activation of APCs such as DCs, discussed above, and the secretion of cytokines that induce the cellular and humoral arms of the adaptive immune response. Cellular immunity involves $CD4^+$ helper T cells ($CD4^+$ T_H) and $CD8^+$ cytotoxic T lymphocytes (CTLs), whereas humoral immunity involves antibody-producing B cells.

1.2.2.1 Cellular immune response

$CD4^+$ T_H cells primarily play an immunoregulatory role during viral infection. They express co-stimulatory receptors such as CD40L and produce the cytokine IL-4 and IL-21 during naïve B cell selection and through affinity maturation of activated B cells, thus influencing antibody production (172). $CD4^+$ T_H cells also secrete IFN-γ and IL-2, which limit HCV replication and regulate lymphocyte proliferation/turnover (both $CD4^+$ and $CD8^+$), respectively (173). Generally, a robust $CD4^+$ T cell response is a prerequisite for HCV clearance. Accordingly, individuals who clear infection have $CD4^+$ T_H cells that recognise more epitopes in HCV non-structural proteins as well as produce more IL-2 and IFN-γ upon stimulation (174,175). Moreover, reduced or delayed $CD4^+$ help correlated with HCV chronicity in both chimpanzees and patients (14,176).

Within the $CD4^+$ compartment, $CD25^+FOXP3^+$ regulatory T cells (Tregs) are a key subpopulation. They play a fundamental role in moulding immune responses by suppressing activation and proliferation of effector lymphocyte populations ($CD4^+$ T_H cells, CTLs and NK cells) as well as macrophages and DCs through superior secretion of IL-10. The number of Tregs in peripheral blood was found to correlate inversely with HCV viral load (177). Furthermore, a more recent study found a larger HCV-specific Treg population with elevated IL-10 production in patients with chronic infection, whereas clearers were characterised by increased IFN-γ secreting $CD4^+$ T_H cell numbers (178). However, such simplistic correlation studies on patients after clinical outcome is known offer little insight regarding Treg role in limiting infection. Indeed, their elevated numbers may be the result of a previously exacerbated inflammatory response as HCV spreads in the liver. A small animal model that is both faithful to human HCV disease progression and amenable to genetic manipulation would provide clarity as to whether Treg function aids or limits hepatitis C transition from an acute to chronic condition.

CTLs induce ordered cytolysis in target cells via the release of granzymes, perforin, Fas ligand and TRAIL. In addition to lysing of infected hepatocytes, CTLs also limit HCV replication via their secretion of IFN-γ and TNF-α (179). As with $CD4^+$ T_H cells, an early, broad CTL response is thought to promote spontaneous viral clearance, with clearers targeting a broader range of non-structural protein epitopes (180–182). On the other hand, narrow immunodominant CTL responses with heightened magnitude may serve to drive immune escape of transmitted/founder viruses during acute infection (183). Notably, $CD8^+$ T cell exhaustion is often observed in chronic hepatitis C (184). Exhaustion-committed HCV-specific $CD8^+$ cells are characterised by the upregulation of effector function inhibitory receptors such as PD-1, impaired proliferation and antiviral cytokine expression, repressive transcriptional reprogramming and defective effector function and memory development (185). A better understanding of the molecular mechanism influencing the breadth and kinetics of the cellular immune response will inform rational vaccine development.

1.2.2.2 Humoral immune response

Unlike T lymphocytes which undergo development in the thymus, B cells develop in the bone marrow before migrating to secondary lymph organs. HCV-specific B cell activation likely occurs in liver draining lymph nodes, where follicular naïve B cells will

present HCV antigens to follicular $CD4^+$ T_H cells, which in turn activate the B cells, as discussed above. Activated B Cells either mature into short-lived plasma cells, which are essentially antibody factories, or develop into the germinal centre. Humoral immunity is refined within the germinal centre, with antibodies undergoing class switch from high avidity, pentameric immunoglobulin M (IgM) to high affinity, monomeric IgG. Long lived plasma cells and memory B cell subpopulations emerge from germinal centres. For HCV, antibodies mainly target epitopes on the E1E2 heterodimer which is present at the surface of the virion particle, with E2 bearing the larger share of immunodominant epitopes.

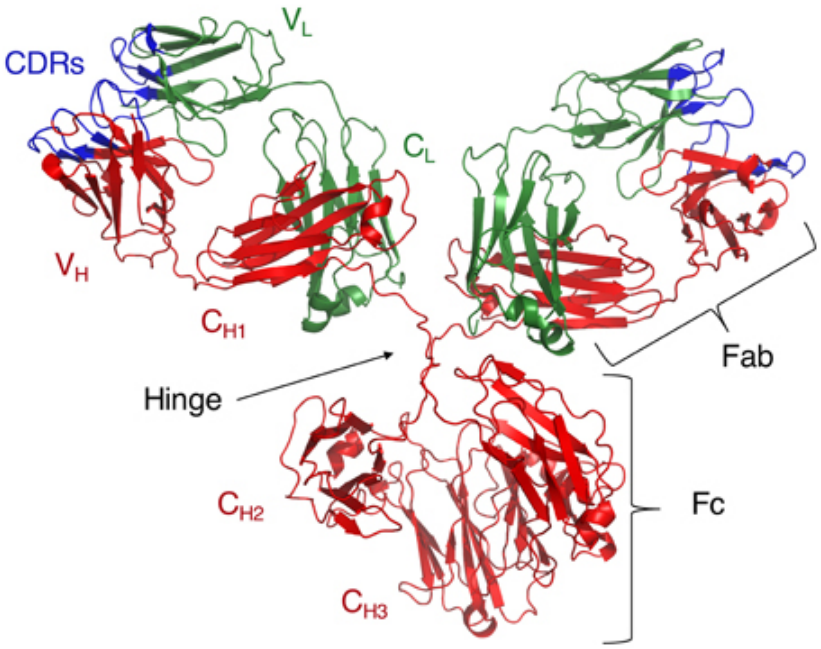

Figure 1.6. Crystal structure of intact IgG_1 (PDB: 1IGY). Adated from Janda et al (186).

Antibodies are Y-shaped structures, composed of two light chains and heavy chains which essentially mirror each other on a central axis (Fig 1.6). Antibodies have two fragment antigen-binding (Fab) domains, comprised of variable and constant regions, and the fragment-crystallisable (Fc) domain, which consists of only constant regions (186). At the very tip of the variable regions are the complementarity determining regions (CDRs), which are the points of antigen engagement and the most variable part of the molecule. The heavy chain determines isotype (IgM, IgA, IgE, IgD and IgG) and the light chains are classified as either Kappa or Lambda. Isotypes differ in their function, size, complement cascade initiation and Fc receptor binding. IgGs

are the most abundant of the antibody isotypes as well as the most important in containing primary and preventing subsequent viral infections.

Secreted antibodies function by neutralising their target, binding antigens on the virus surface and blocking entry, or through FcR-dependent signalling pathways, culminating in complement activation or antibody-dependent cell-mediated cytotoxicity (187,188). The role of humoral immunity in controlling HCV is incompletely understood. However, results from a longitudinal study of German women accidentally exposed to the same HCV strain in a single-source outbreak suggest that spontaneous clearance coincides with the early emergence of neutralising antibodies (17,189–191). On the other hand, chronic infection was characterised the absence of neutralising antibodies. The epitopes targeted by neutralising antibodies are reviewed in more detail later (Chapter 1.6). The pathway and receptors that facilitate HCV entry are discussed in detail in the following section.

1.3 HCV entry

Viruses, both non-enveloped and enveloped, share common features and routes of entry, generally beginning with attachment to the cell surface and culminating with the delivery of the viral genome into the host cell (192). Viruses have evolved an array of strategies to successfully achieve this but in all cases, the process consists of four generic steps, attachment, receptor engagement, penetration and uncoating. Attachment occurs via low specificity interactions with ubiquitous cell surface molecules and is rapidly followed by the high-affinity engagement of viral entry proteins to bona fide receptors. For viral genomic material to access host replicative machinery in the cell interior, viruses must first penetrate cellular membranes. Finally, once at the appropriate cellular environment viruses uncoat their capsids to expose their viral genome for replication to commence (193).

To execute the above processes a viral particle must be robust enough to resist environmental and immune-induced hazards as it traverses the target cell. However, the particle is also required to relinquish its genome when the opportunity arises. Thus, to successfully infect a naïve cell, a virion must exist in an equilibrium between stability and fragility. Viruses have evolved to exist as metastable structures to counter this evolutionary quandary. The entry proteins of circulating virions are yet to attain the minimum free energy conformation and consequently reach their target cell primed for

conformational changes. Said changes are triggered upon receptor engagement and irreversible conformational transitions prepare the particle for the next stage in viral entry. Further stimuli prompt temporal changes in structure until the ultimate event of uncoating. In this way, metastability allows a virus to respond appropriately to host cell microenvironments as it progresses through its entry pathway (193).

1.3.1 HCV receptors

The cell surface components that viruses bind to group into two general types depending on the outcome of the interaction. Attachment factors bind particles and concentrate viruses at the cell surface. Receptors actively promote entry by triggering conformational changes on the viral particles, activating signalling cascades and promoting internalization (193). Additionally, entry cofactors are proteins that don't necessarily interact with the virion but support virus entry by acting in concert with receptors or by activating signalling cascades (194,195). Often receptors are internalised along with the virus during endocytic uptake and may actively participate or facilitate viral fusion. The following section will detail the biological function of key HCV receptors in order of their discovery (196,197).

1.3.1.1 CD81

The first of the HCV receptors to be identified was the tetraspanin cluster of differentiation 81 (CD81) (198). The 236 residues of CD81 organise into the typical features of a tetraspanin, two extracellular loops anchored by four α-helical transmembrane domains (Fig 1.7) (199). Structural analyses of CD81 revealed it possesses a cholesterol-binding pocket that likely regulates the conformational switch of the large extracellular loop (200). Tetraspanins play an important role in membrane organization, interacting among themselves and with other transmembrane proteins to create extensive cholesterol-rich complexes on the cell surface called tetraspanin webs (201). These microdomains are functionally significant. Interactions between CD81 and its partners influence immune cell activation and differentiation, cell-cell adhesion, and it has been implicated in sperm-egg membrane fusion.

CD81 is ubiquitously expressed and localises mainly at the basolateral surface of hepatocytes, protruding a mere 3.5 nm from the lipid bilayer. The E2 glycoprotein binds the large extracellular loop of CD81. Mutagenesis has determined residues

F186, I182, N184, L162 are involved in E2 engagement, with mutation of F186 abolishing the E2-CD81 interaction entirely. Notably, African green monkey CD81 does not bind soluble E2 (sE2) but supports HCV infection of human cells suggesting cell-free E2-CD81 interaction does not predict infection (202). Furthermore, our recent work also indicates that cholesterol sensing by CD81 also regulates infection (203). Here we found that CD81 in a closed conformation, mimicking a cholesterol-bound state, proved a superior adapter for HCV infection.

Epitope mapping on E2 with monoclonal antibodies and CD81-LEL has identified the putative CD81 binding residues. These include G436-WLAGLF-Y443, Y527, W529, G530, D535 and residues within 613-618, as well as W420 though other hydrophobic residues are sufficient at this position (204–206). However, without of a crystal structure of E2 in complex with CD81, it's impossible to deduce the precise molecular interaction.

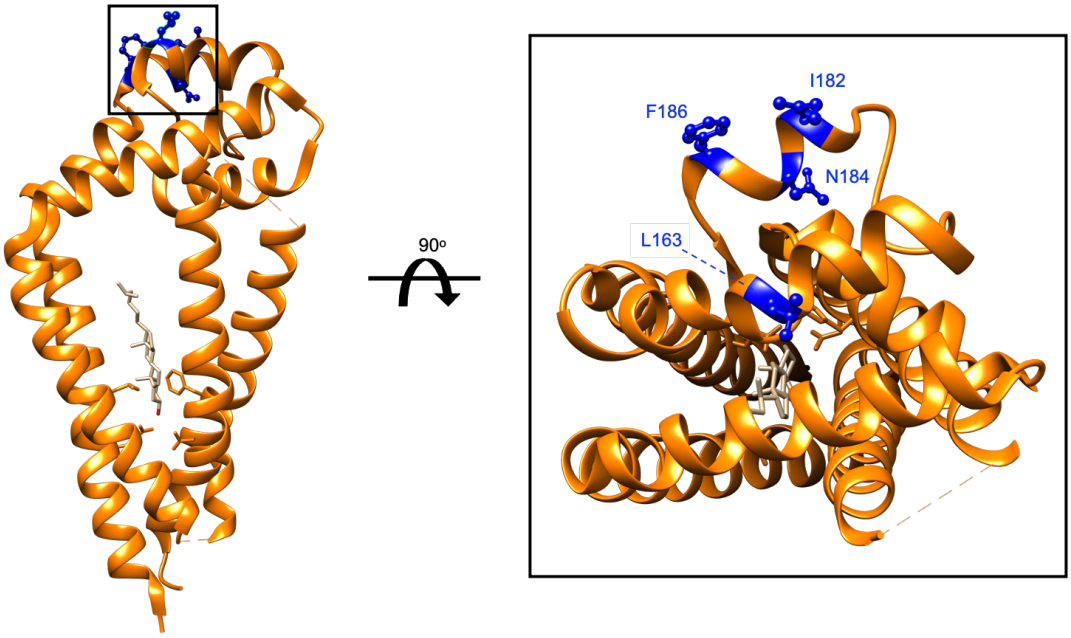

Figure 1.7. Structure of the tetraspanin CD81 (PDB: 5TCX). Residues determined to interact with E2 are shown in blue.

1.3.1.2 SR-B1

The second HCV receptor to be identified was scavenger receptor class B member 1 (SR-B1). It is a multi-ligand membrane receptor protein with systemic expression but is enriched in the liver and steroidogenic tissue (207). SR-B1 has two transmembrane

domains, with a large extracellular domain that is suspected, based on its homology with LIMP-2, to arrange into an antiparallel β-fold decorated with many short α-helical segments (Fig 1.8) (208,209). SR-B1 has a key involvement in lipid metabolism binding and allowing selective uptake of ligands such as high-density lipoproteins (HDL), LDL and VLDL. In the liver, uptake of cholesterol by SR-B1 from HDL allows for selective sorting and, if necessary, its conversion into bile salts and subsequent removal by biliary secretion (207,210).

Like CD81, SR-B1 was identified as an HCV receptor via its binding to sE2 (211). To this regard, CD81 and SR-B1 are considered the true HCV receptors as they bind the HCV particle directly via E2. E2-SR-B1 interactions are predicted to occur via the hypervariable region 1 as deletion of this domain ablates sE2 binding to CHO cells transduced to express human SR-B1 (212). Interestingly, the major SR-B1 ligand HDL can enhance HCV infection in vitro in a genotype-dependent manner. Additionally, this phenotype required the lipid transfer activity of SR-B1 (213–215). It has been proposed SR-B1 lipid transfer activity could modify the lipoprotein profile of the virion, liberating the particle from associated lipoproteins (see Figure 1.3) (216,217).

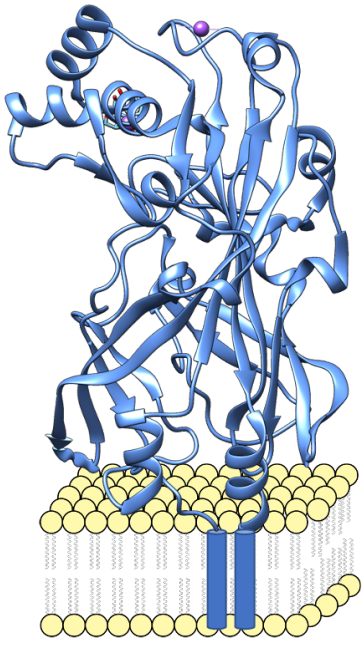

Figure 1.8. Homology model of the SR-B1 ectodomain. Model is based on the structure of LIMP-2 (PDB: 4Q4B), which, like SR-B1, is a member of the CD36 superfamily.

It has been shown that SR-B1 is dispensable for HCV entry and, consequently, it was thought other lipoprotein receptors may fulfil a similar role to SR-B1 during HCV entry. Indeed, HCV infectivity of an SR-B1 and LDL receptor (LDL-R) receptor double knock-out hepatoma cell line could be rescued by exogenous expression of either one of the two receptors, suggesting they contribute redundantly to HCV infection (218). However, LDL-R is not known to engage the HCV glycoproteins, and it was recently found that antibody-mediated blockade of SR-B1 and LDLR did not synergistically inhibit HCV infection in vitro (219). Moreover, HCV entry requires cholesterol uptake (220) and LDL-R lipid uptake is realised via endocytosis, inconsistent with the accepted model of tight-junctional internalization of HCV (142,221).

1.3.1.3 The tight junction components Claudin and Occludin

Claudin-1 (CLDN1) was identified as a potential HCV entry cofactor by Charles Rice's lab in 2007 following the screening of a hepatocyte cDNA library in HEK293 cells. Subsequent CLDN1 complementation in these cells made them permissive for HCV pseudoparticle (HCVpp) infection indicating it was indeed an essential entry cofactor (222). CLDN6 and CLDN9 can also mediate HCV entry in Huh-7 cells; however, they are weakly expressed in authentic hepatocytes and thus may not support infection in vivo, unlike CLDN1 which is highly prevalent in liver tight junctions.

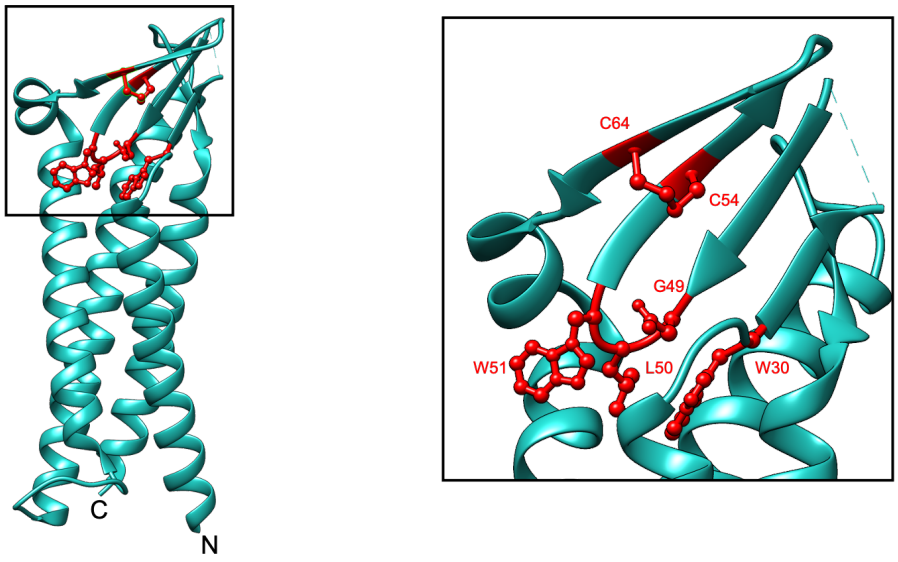

Figure 1.9. Homology model of CLDN1. Model is based on the structure of murine claudin-15 (PDB: 4P79). Residues determined to essential for HCV entry by alanine scanning mutagenesis are shown in red.

A similar cDNA cloning strategy by the same group identified OCLN as an entry cofactor that conferred HCVpp entry into murine cells transduced to express CD81, SR-B1 and CLDN1. (223). The importance of CLDN1 and OCLN's role in HCV entry was further highlighted in a later study which showed CRISPR-engineered deletion of either protein abrogated HCV infection of Huh-7 cells (218).

CLDN1 and OCLN are key constituents of tight junctions. They are four-pass transmembrane proteins with extracellular domains that interact with their equivalent on the opposing membrane on neighbouring cells to form branching strands (Fig 1.9). Tight junctions are intercellular adhesion complexes present in all epithelia and endothelia that function to control paracellular permeability (224). Under an electron microscope, they appear as a series of very close membrane appositions (so-called 'kissing points') of adjacent cells. The claudin family is thought to be the most crucial for mediating tight junction formation and permeability, whereas OCLN plays an essential role in barrier function and junction stability.

In the liver, tight junctions physically separate the basolateral membrane, which is bathed by blood flow, and the apical membrane, which forms the bile canaliculi, to create the blood-biliary barrier. As OCLN is primarily localised to tight junctions in polarised hepatocytes, it is likely HCV particles translocate from the basolateral surface to access it. The importance of HCV particle localisation to hepatocyte tight junctions is controversial. Abrogation of tight junction formation renders Huh-7 cells less susceptible to HCV infection. However, the ectopic expression of OCLN mutants defunct for tight junction localisation restored HCV infection in polarised OCLN knock-out Huh7 cells, suggesting the virion engages non-junctional CLDN1 and OCLN and is internalised at the lateral membrane. These observations suggest HCV infection requires functional tight junctions, but the virion does not necessarily need to access them for successful entry. Nonetheless, the most comprehensive study of HCV particle and receptor/entry cofactor colocalization to date clearly demonstrated virion and OCLN colocalised at the tight junction (225).

In addition to the bona fide the entry factors CD81, SR-B1, CLDN1 and OCLN, a startling number of proteins have been suggested to play a role in HCV entry (211,221,223). These include epidermal growth factor receptor (EGFR), Niemann Pick C1-like 1 cholesterol receptor (NPC1L1), transferrin receptor (TfR1), Ab1 tyrosine kinase and IFN-α/β receptor IFNAR2, to name a few (226–228). EGFR signalling is thought to contribute to receptor complex formation and particle endocytosis and

NPC1L1 likely contributes to HCV entry through its role as a cholesterol receptor (225,229). However, there is little mechanistic insight regarding the roles of the other proposed 'entry factors', thus their significance is debatable (221).

1.3.2 Entry mechanism of cell-free HCV particles

HCV circulates in the blood of infected patients and thus makes direct contact with the basolateral surface of hepatocytes, the cell type permissive for its replication (142). The HCV virions transiently attach to the cell surface, allowing for receptor binding and initiation of entry. HCV is internalised via clathrin-mediated endocytosis. Many enveloped viruses have appropriated the endocytic pathway for entry into epithelial cells; however, few have evolved to take as intricate a route to arrive at this stage as HCV does. Of currently well-studied viruses, only group B coxsackieviruses and HCV are known to internalise at tight junctions (195).

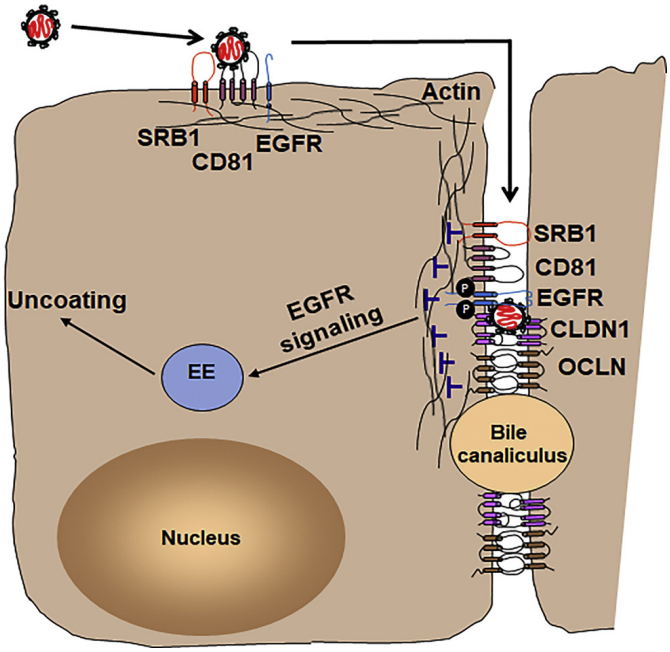

Figure 1.10 Cell-free virion HCV entry. Following attachment by HSPG and LDLR, HCV proceeds in a spatially coordinated manner via specific interactions with SR-B1, CD81, CLDN1 and OCLN. The virion is then internalised via clathrin-dependent endocytosis, realised through EGFR signalling. The entry process finalises when the viral and endosomal envelopes fuse to release the capsid, containing the RNA genome, into the hepatocyte cytosol. Baktash et al (224).

HCV entry is a multifaceted process facilitated by the interactions of virion-associated E1E2 glycoproteins and lipoprotein components with a panel of cell surface receptors (Fig 1.10) (116,142). HCV initially attaches to cells via interactions between virion-associated ApoE and both the LDL receptor (LDLR) and glycosaminoglycans present on heparin sulphate proteoglycans (HSPG) (230). The glycoproteins on membrane-bound viral particles then physically interact with the receptors SR-B1 and CD81. Interaction with CD81 triggers the formation of a receptor complex also comprising CLDN1 and OCLN. EGFR also plays a crucial role in regulating the entry process (225). The differential subcellular localization (basolateral or tight junction) of these entry cofactors partly explains the temporally-regulated manner of HCV entry (225,231–234). CD81, SR-B1, EGFR and CLDN1 not only bind or associate with the HCV virion but also interact with each other, it is likely this allows them to form an HCV receptor/cofactor complex that is essential for ensuing viral internalization (221,225,235).

Following attachment, HCV E2 is widely suspected to first bind the extracellular domain of SR-B1 (211,222). The interaction with SR-B1 has been proposed to be required for E2's subsequent engagement with CD81 (198). The exact mechanism of this 'priming' step remains unknown; however, the lipid transfer activity of SR-B1 may facilitate exposure of the CD81 epitope on E2 (236). It's also plausible that the SR-B1-E2 interaction may induce or stabilise a conformation of E2 favourable for CD81 binding (236). CD81 engagement is a critical step in the entry HCV process. CD81 engagement activates signalling pathways that promote virion internalization such as EGFR dimerization (225,237). Signalling events culminate in the reorganization of the actin cytoskeleton leading to the virion-coreceptor complex (SR-B1, CD81 and EGFR) translocating to the tight junction. Here EGFR-dependent association between CD81 and CLDN recruits the latter into the virion-receptor/cofactor complex (225,228).

CLDN1 recruitment is crucial for HCV internalization at the tight junction (222). CLDN1 has two extracellular loops (EL1 and EL2) and residues within a small but highly conserved region of EL1 are vital for HCV entry (238). Direct interactions between CLDN1 and the HCV virion remain unproven, however, genetic evidence following culture adaptation of HCV in a CLDN1-ablated cell line suggest CLDN1 interacts with E1. Molecular interactions between CLDN1-EL1 and HCV E1E2 complexes have been confirmed by co-immunoprecipitation, whereas attempts to prove any between CLDN1-EL1 and E2 alone have failed (239).

OCLN is last the of the HCV receptors to colocalise with the virion in polarised 3D hepatoma cell cultures (225). There is no evidence for a direct interaction between OCLN and the viral particle. Nonetheless, the crucial role of OCLN in HCV entry is highlighted by the observation that of the known receptors currently, it and CD81 represent the minimum set of species-specific factors needed for viral uptake into mouse or hamster cells (221,223). Time of addition studies indicate OCLN and CLDN act at a late post-binding step preceding fusion, consistent with their tight junction localization (222,223,240).

As post-binding roles have been suggested for SR-B1, involving its lipid transfer activity, and CD81, in priming the viral fusion machinery (216,241,242), it is likely the formation and maintenance of the receptor/cofactor complex, also comprising CLDN1 and OCLN, is a prerequisite for successful HCV entry. Ultimately, the virion-receptor/cofactor complex is internalised via clathrin-mediated endocytosis triggered through EGFR signalling (225,243). Internalised HCV-coreceptor complexes are trafficked to Rab5-comprised endosomal compartments, where the low pH induces fusion between viral envelope anchoring the conformationally rearranged viral glycoprotein and bound endosomal membrane (241). Following fusion, the HCV genome is presumably released into the host cytosol, where RNA translation and viral replication are initiated (244).

1.3.3 Cell-to-cell transmission

HCV particles can infect hepatocytes through cell-free entry or via cell-to-cell transmission. The cell-free route is considered the classical route as it is by far the better characterised of the two and the route used to establish primary infection in a new host (245). However, following production infection, HCV can propagate to neighbouring cells independent of the classical route.

In tissue culture, HCV can be restricted to cell-to-cell transmission when infected cells are cocultured with naïve cells in the presence of neutralising antibodies. In one such study, while transmission of cell-free viral transmission was reduced by 95%, neutralising antibodies were found to have minimal effect on curbing the spread of infection (246). Accordingly, this route of spread is thought to be important for neutralising antibody escape (247,248). Moreover, HCV infected cells were found as clusters in liver biopsies of patients, indicating cell-to-cell spread as the predominant

mode of HCV transmission in vivo (249). Although most HCV entry factors described to date have been implicated in cell-to-cell spread; the mechanism governing this process remain unknown, but might involve exosomes (250).

Having reviewed the HCV entry players on the cellular end, the following sections will review the players on the viral end, viral fusion proteins. Beginning with an overview of their general function before exploring the different structural classes described to date before arriving at a comprehensive review of the HCV E1 and E2 glycoproteins in the penultimate sections of the introduction.

1.4 Viral fusion proteins

The envelope (lipid bilayer) of animal viruses like HCV serves to protect the viral genome until its delivery to the cytoplasm of target cells (251). As such, during infection enveloped viruses must induce the fusion of the viral envelope with the cell membrane of their target cell to deliver their genomic material (252). This process is catalysed by specialised viral fusion proteins expressed on the surface of virions. Notably, many viral fusion proteins are often multimeric or multidomain, with the monomeric subunits (or single domains) performing specified functions which include receptor engagement, conformational rearrangement and anchoring the fusion peptide. Hydrophobic and ubiquitous to all viral fusion proteins, the fusion peptide is a short segment that gets buried into the host membrane, thereby bridging the viral and cellular membranes. Broadly speaking, viral fusion protein-receptor engagement triggers conformational changes in the viral fusion protein that expose the fusion peptide and lead to the coalescence of the viral and cellular membranes.

The first crystal structure of a viral fusion protein was solved for the influenza A virus hemagglutinin (HA) protein in 1981 (253). In the following forty-years as an increasing number of viral fusion protein X-ray structures were solved, it became apparent that many otherwise unrelated viruses possess related fusion proteins. We now group viral fusion proteins into at least three classes which show astonishing differences in tertiary and quaternary structure between them. This observation indicates that the corresponding gene had either been horizontally exchanged among viruses or had actually been acquired from an ancient gene pool shared with cells – since the shared structural homology is also observable in the ancient eukaryotic gamete fusion protein HAP2 (254).

1.4.1 Triggers of envelope-cell membrane fusion

Specific interactions with the target cell trigger an exothermic fusogenic conformational change of the viral fusion protein, irreversibly transiting it from a metastable, activated prefusion state to its lowest-energy, post-fusion conformation (252). These conformational change triggering interactions can be grouped into several broad categories (255). In the first category, fusion is triggered by specific receptor interactions with the fusion protein or a companion viral glycoprotein. In some cases, sequential interactions with a primary receptor then a co-receptor are necessary as exemplified by HIV Env, which first binds CD4 before it can engage CCR5 or CXCR4 (256). Viruses in this category can fuse directly with the plasma membrane.

In the second category, fusion protein-receptor interactions at the cell surface lead to the endocytosis of the virion and viral membrane-endosome fusion is triggered by the binding of protons in the low pH environment of the late endosome (257). In the third category, interactions at the cell surface also lead to endocytosis; however, proteolytic processing of the fusion protein and subsequent binding of a secondary internal receptor is required to trigger fusion. Furthermore, the fusion proteins of some non-enveloped viruses are thought to require an activating redox reaction to trigger cell-to-cell fusion, it's possible some enveloped viruses use a similar mechanism to fuse their viral envelope with target cell membrane (258).

1.4.2 The fusogenic conformational change

All three classes of viral fusion proteins adopt a hairpin-like arrangement in their post-fusion state, juxtaposing the target-membrane insertion element with its viral transmembrane anchor. The energy released during the conformational transition is used to overcome repulsive forces between the two juxtaposed membranes as they come closer together by the required dehydration of the lipids to allow for direct interaction between the bilayers (259,260). As the membranes come within ~3 nm of each other, said dehydration force is felt and increases very steeply the closer they become. This prevents direct membrane contacts and acts an effective barrier for an overall exergonic (i.e., releasing of free energy) fusion which would otherwise occur spontaneously.

During the conformational transition, the fusion protein first adopts a transient, extended intermediate conformation in which a hydrophobic segment, called the ‘fusion peptide’ (class I) or ‘fusion loop’ (class II or III), projects out to insert into the cell membrane (Fig 1.11 B) (261). This extended state is unstable and thus collapses into a more energetically favourable hairpin-like conformation, in which the hydrophobic segment inserted in the cell membrane is relocated near the viral transmembrane anchor of the fusion protein. This brings the outer leaflets of the two membranes within 1 nm, thereby overcoming the dehydration force and allowing direct membrane apposition (262). Membrane fusion then commences, firstly via the creation of a hemifusion step where the lipids of the outer leaflets coalesce, followed by the formation of a fusion pore(s) by the merging of the inner leaflets and then expansion of the pore(s) to complete fusion. As such, viral entry proteins can be viewed as spring-loaded conformational machines that require specific molecular cues (e.g., receptor binding, fall in endosomal pH) to trigger their function.

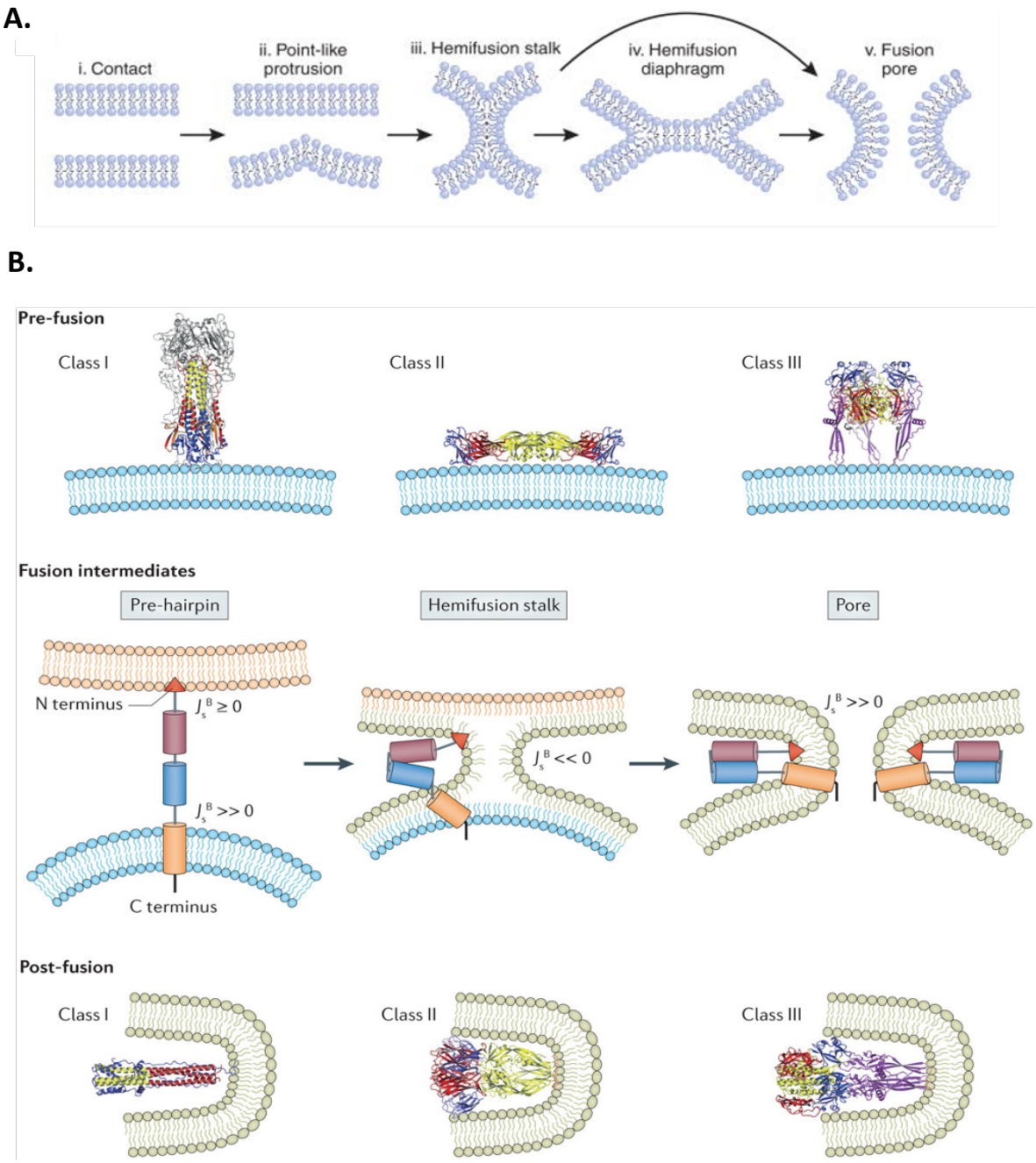

Figure 1.11. Fusion via hemifusion mechanism of lipid bilayers. (**A**) (i) initial contact; (ii) point-like protrusion bringing the outer leaflets of the two apposed membranes in close contact; (iii) formation of a hemifusion stalk, merging only the outer leaflets without affect the inner leaflets of the bilayers; (iv) expansion of the stalk leads to the formation of a hemifusion diaphragm; (v) finally fusion pore forms in the diaphragm or directly from the hemifusion stalk. Adapted from Chernomordik and Kozlov, 2008 (259). (**B**) Representative pre- and post-fusion conformations of class I-III viral fusion proteins (top and bottom rows, respectively). Middle row: a cartoon diagram depicting the transition from the extending pre-hairpin intermediate to the hairpin-like fold of a schematic model of a class I protein. For simplicity, only one monomer is shown but the pre-hairpin intermediates are always trimeric. As the crystal structures of fusion intermediates are yet to be solved, the models are based on experimental evidence. The bilayer spontaneous curvature (J_S^B) of the viral and cellular membranes are indicated to highlight the dramatic changes in membrane curvature during the fusion process. Adapted from Vigant et al (260).

1.4.3.1 Class I fusion proteins

Class I viral fusion proteins arrange into non-covalently linked homotrimers in both their pre- and post-fusion states (252). They are type I single-pass transmembrane proteins synthesised as a monomeric precursor, of which the N terminus is generated upon signal peptidase cleavage after translocation into the ER. The precursor undergoes further maturation to generate an N-terminal surface subunit (e.g., HIV gp120) and a C-terminal subunit containing the transmembrane domain (e.g., HIV gp41) (262). The two subunits are often linked through disulphide bonding or non-covalent interactions.

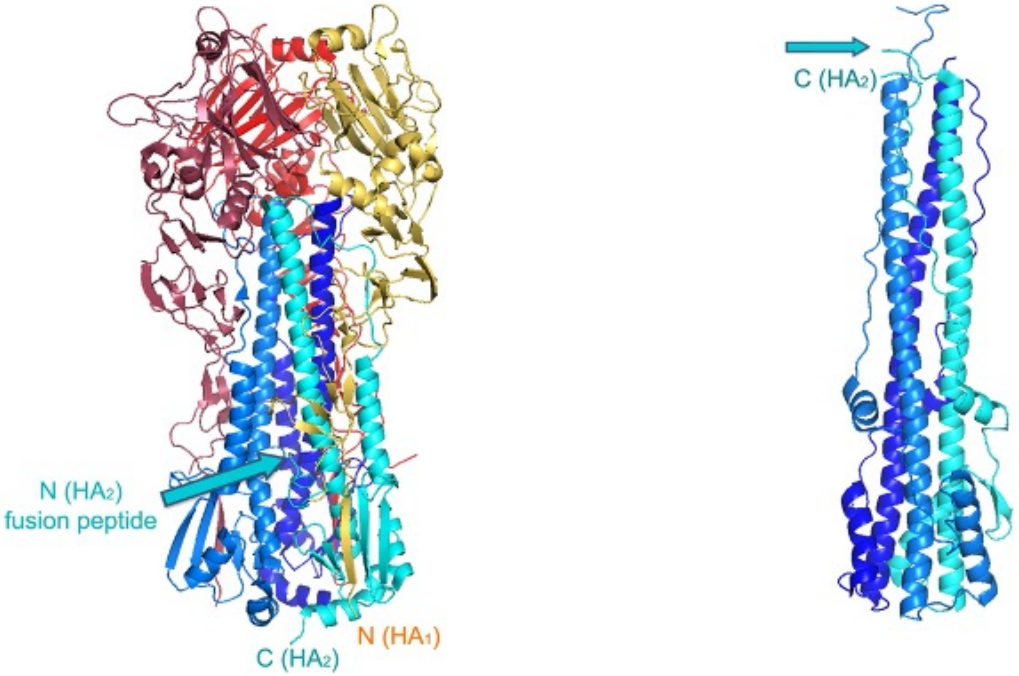

Figure 1.12. Representative structure of a class I fusion protein. Pre- and post-fusion conformations (left and right, respectively) of the influenza haemagglutinin (HA) ectodomain (PDB: 2YPG and 1QU1). HA_1 chains, the N-terminal subunits, are coloured in shades of red/gold and HA_2 chains, the C-terminal subunits, are shown in shades of blue. The N terminus of HA_1 and the C terminus of HA_2 are labelled. The cyan arrow indicates the position of fusion peptides inserted near the threefold axis in the pre-fusion form (on the left). Figure adapted from Harrison, 2015 (259).

Parallel trimeric coiled-coils in the post-fusion C-terminal subunit are a hallmark of class I fusion proteins. The long and short α-helices of the coiled-coil run antiparallel to each other and complete a trimeric post-fusion hairpin, thereby making a trimeric post-fusion 6-helix bundle (Fig 1.12). The fusion peptide is at or near the N-terminal end of the long post-fusion helix of the C-terminal subunit and is spring-loaded underneath the N-terminal subunit trimer cap. Receptor engagement disrupts the

trimer contacts of the N-terminal subunit, allowing the long helix of C-terminal subunit to spring out, thereby exposing the fusion peptide for insertion into the host cell membrane.

The diverse group of viruses carrying class I viral membrane proteins includes influenza viruses, coronaviruses, Ebola virus and HIV, all of which cause devasting disease. Moreover, class I viral fusion protein are ubiquitous in host endogenous retroviruses (ERV). Most remarkably, a series of paradigm-shifting papers across several labs have shown that the virally derived 'syncytin' proteins, vital for the formation of the mammalian placenta, are class I fusion machines (263,264). Indeed, it would appear the class I fusion proteins of ERVs are an archetypal demonstration of virus-host coexistence.

1.4.3.2 Class II fusion proteins

Unlike their class I equivalents, class II viral fusion proteins do not arrange into independent trimers on the viral membrane, instead they assemble into dimers that encase the entirety of the viral membrane (252). Class II proteins are expressed within a polyprotein precursor containing at least two proteins, although they are more often part of a single polypeptide precursor which encodes all ten or so virally encoded proteins as seen in flaviviruses. The fusion protein forms a heterodimer with the upstream companion glycoprotein, and both are anchored in the viral envelope by their own transmembrane domain.

Class II viral fusion proteins do not possess long α-helices and instead have β-sheets as their dominating secondary structure. They have three structured domains termed I, II and III. Domain I is a β sandwich with 'up and down' topology with connections between adjacent β sheets forming long protrusions to form domain II, which anchors the fusion loop at the distal end of the first protrusion (Fig 1.13). Domain III has an Immunoglobulin superfamily fold and is connected to domain I and the transmembrane region, the C terminal of the protein, by a linker and a 'stem' region, respectively. The ectodomain is organised into a long rod with domain I at the centre and is flanked by domains II and II at either end. In the post-fusion state, the rod bends in half with domains I and II packed centrally and flanked by domain III and the stem which are packed externally. This forms a trimeric hairpin, analogous to the 6-helix bundle observed in class I proteins albeit with a fundamentally different structure.

Arthropod-borne (arboviruses) make up the majority of important, and more often emerging, human pathogens which possess class II viral fusion proteins. They include flaviviruses such tick-borne encephalitis viruses, the mosquito-transmitted haemorrhagic fever agents dengue virus and yellow fever virus and the neurotropic and teratogenic Zika virus. They also include alphaviruses such as Chikungunya virus, which causes severe arthralgia. Furthermore, viruses in the recently defined *Bunyavirales* order also have class II viral fusion proteins.

Bunyaviruses with potential to cause significant disease burden include the mosquito-borne haemorrhagic fever agent Rift valley fever virus and the tick-borne biosafety IV pathogen Crimean-Congo haemorrhagic virus. Recently, structural and functional homologs of class II viral fusion proteins have been discovered in eukaryotes. EFF-1 from *C. elegans* is a somatic cell-cell fusion protein that potentiates the construction of syncytia which are necessary for skin formation during embryogenesis (265). The glycoprotein HAP2 drives gamete fusion (sperm/egg fusion) and is almost ubiquitous in the main eukaryotic branches (266).

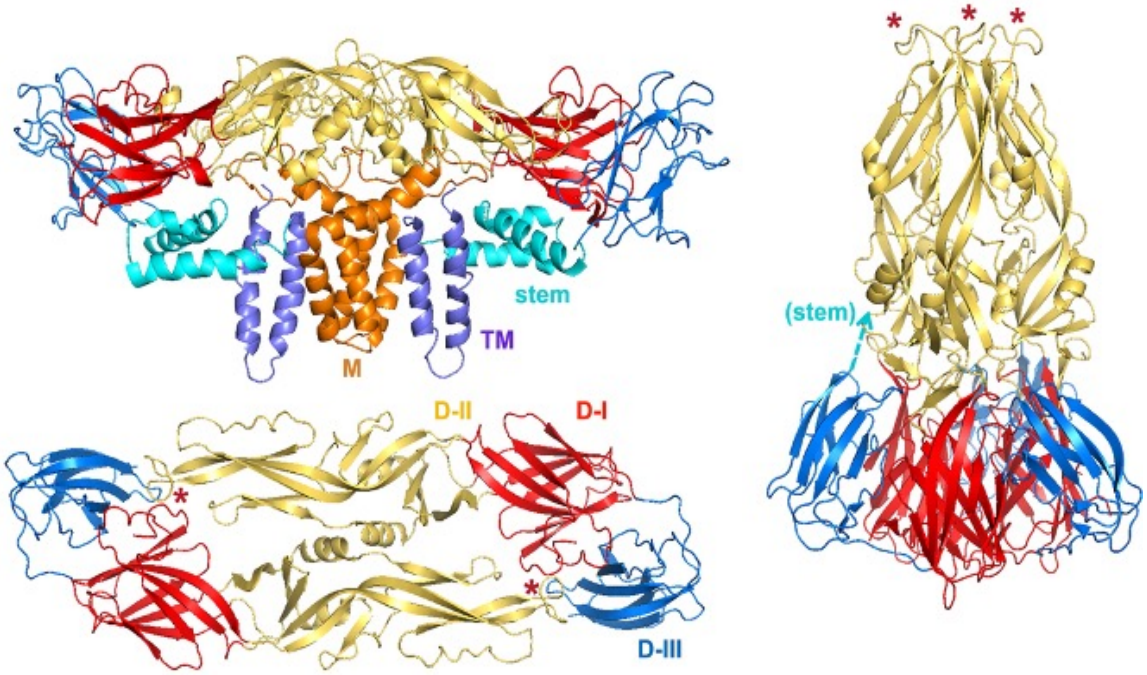

Figure 1.13 Representative structure of a class II fusion protein. Pre- and post-fusion conformations (left and right, respectively) of dengue virus type 2 E protein. The tangential ('side') view shows a cryo-EM model of a dimer of the complete E and M polyprotein chains (PDB: 3J27); the radial ('top') view shows just the stem-less ectodomain (1OAN). Colouring: domain I: red; domain II: yellow; domain III: blue; stem: cyan; transmembrane anchor: slate and M: orange. The dashed cyan arrow on the post-fusion trimer (1OK8) represents where the stem emerges from. The red asterisks indicate the positioning of the fusion loops. Figure adapted from Harrison, 2015 (259).

1.4.3.3 Class III fusion proteins

Class III viral fusion proteins appear to be a combination class I and II fusion proteins, with a central coiled-coil in the post-fusion state, which bears an N-terminal fusion domain that is enriched for β sheets, reminiscent of domain II of class II proteins (Fig 1.14). They are trimeric in both their pre- and post- fusion states, except for the vesicular stomatitis virus (VSV) glycoprotein G which can sometimes be observed as a monomer on the virus surface (267). Unlike their class I counterparts, class III viral fusion proteins do not require activating proteolytic cleavage to mature. However, they behave like class I proteins, regarding ectodomain arrangement, since they do not encase the viral envelope with glycoprotein assemblies.

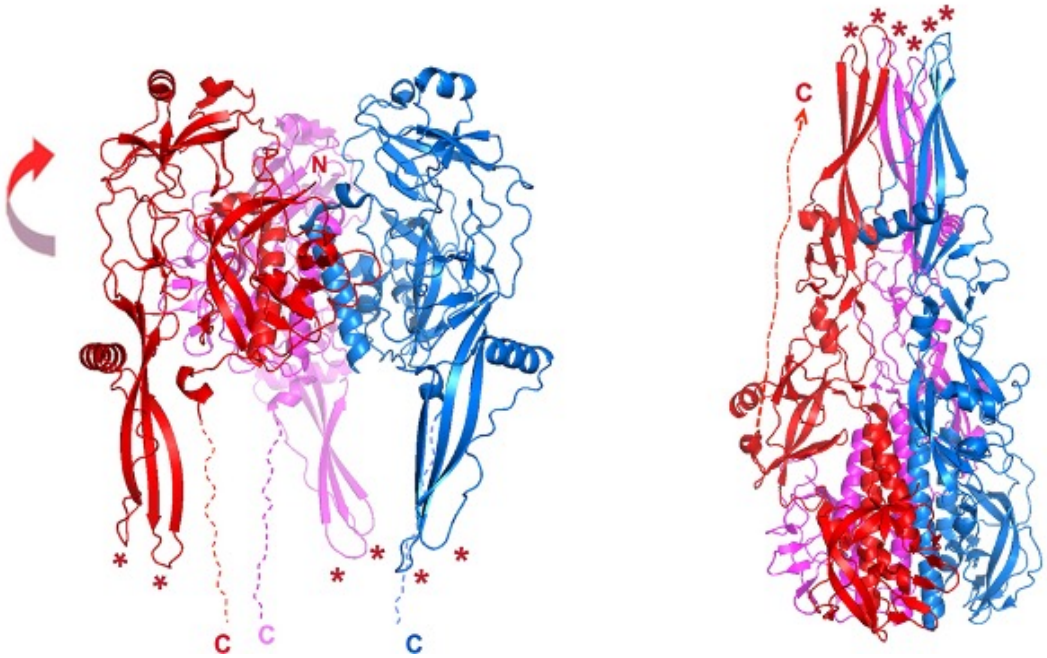

Figure 1.14. Representative structure of a class III fusion protein. Pre- and post-fusion conformations (left and right, PDB: 2J6J and 2CMZ, respectively) of the VSV G ectodomain. The three monomeric chains are shown in red, blue and magenta. Dashed lines show the location of a disordered C terminal segment that connects the folded protein to the transmembrane anchor. Only the red-subunit C-terminal segment is displayed in the post-fusion conformation on the right. The curved red arrow indicates that in the transition from the conformation on the left to the one on the right, the domain bearing the fusion loop (red asterisks) flips over 180° to engage the host cell membrane. Figure adapted from Harrison, 2015 (259).

VSVG is the prototypical class III fusion protein, the virus itself is zoonotic and causes livestock disease characterised by vesicular lesions. VSV belongs to the *Rhabdoviridae* family which also includes the rabies lyssavirus, a neurotropic virus responsible for oft-irrecoverable rabies in humans and animals. In a clear

demonstration of convergent evolution viruses, the glycoprotein B (gB) of the HSV-1 and CMV (and presumably all *Herpesviridae*) were also very recently determined to have class III fold (268,269), despite their vast phylogenetic distance to VSV. Furthermore, viruses belonging to the *Bornaviridiae* family have been suggested to possess class III viral fusion proteins, although this is yet to be experimentally confirmed.

Having now reviewed the three defined structural classes of viral entry machinery, the succeeding sections will concentrate specifically on the HCV glycoproteins E1 and E2. The subsections will discuss the structural features of E1E2, particularly focusing on their conformational landscape and how this relates to their entry function and immunogenicity.

1.5 HCV envelope glycoproteins E1 and E2

Once host ER signal peptidases cleave E1 and E2 from the viral polyprotein, the two glycoproteins form a heterodimer which is postulated to arrange into a functional higher-order oligomer on the virion surface and orchestrate HCV entry (270,271). C-terminal transmembrane domains anchor E1 and E2 to the ER membrane, the ectodomain of either protein extends into the ER lumen (272). The transmembrane domains are also pivotal for heterodimerisation. Moreover, ER-retention of the E1E2 heterodimer keeps it near the HCV non-structural protein-induced membranous web, where HCV replication and virus assembly happen.

Based on HCV's classification as a *Flaviviridae,* it was assumed HCV E1E2 were functionally similar to the flavivirus E proteins. However, most evidence indicates considerable deviation in both their structure and functionality (252). Most significantly, the HCV E1E2 heterodimer does not group together with other flavivirus E proteins as a class II fusion machine (273,274). Also, unlike flavivirus envelope proteins, E1 and E2 are highly glycosylated, possessing up to 5 and 11 potential sites, respectively (275). Glycans account for nearly half the mass of the E1E2 heterodimer. Glycans are linked to an asparagine (Asn) within the Asn-X-Thr/Ser motif (276). Roles for glycans in correct E1E2 folding and dimerization, receptor interactions and antibody sensitivity have been demonstrated (275,277–279).

We currently only have partial crystal structures for the E2 core domain, the N-terminal of E1 and the E1E2 heterodimer are is yet to be solved (273,274,280). This

has hindered comprehensive scrutiny of the interactions between E1 and E2 themselves and those they share with receptors and antibodies, as well as their functionality. Despite this, the full-length cell culture system, the pseudoparticle system and soluble envelope glycoproteins have allowed us to uncover some functional properties of E1E2 (281–283).

1.5.1 The E1 glycoprotein

Of the two glycoprotein partners, E1 is the more mysterious, with little known of its function and even less of its structure (284). Difficulties with expressing correctly folded E1, in the absence of E2, have prevented determination of the complete E1 structure and prevented studies to potentially confirm its direct binding to any of the HCV receptors described to date (285). Regardless, it is known that E1 is essential for viral entry and current evidence suggests that is contains the HCV fusion peptide (274,284,286).

At 192 amino acids in length, E1 is much smaller than E2, which is approximately 365 amino acids depending on the genotype. It has an N-terminus ectodomain of approximately 160 residues and has been found to exist as a trimer on the surface of cell culture-derived HCV particles (271). Pan-genotypic bioinformatics analysis of E1 sequences reveals conserved protein domain organization (286), comprising an N-terminal domain (NTD) (strain H77 polyprotein amino acid residues 192-239), a putative fusion peptide (res. 272-290), a highly conserved region (res. 302-329) and the C-terminal transmembrane domain (CTD) (res. 350-381). Aside from the CTD, which anchors E1 in the host-derived lipid bilayer, the (predicted) specific contribution(s) of said conserved domains to virus entry and antibody sensitivity are largely elusive or unvalidated (284).

The E1 glycoproteins of all currently sequenced HCV strains harbours four Asn-linked glycans at residues 196, 209, 234 and 305 (287). A fifth glycosylation site at position 250 is specific to genotypes 1b and 6, while one at position 299 is specific to genotype 2b (288,289). E1 glycosylation is crucial for its folding and functionality. Site-directed mutagenesis of E1 Asn-linked sites has produced E1 impaired for heterodimerization with E2 and led to impaired incorporation of E1 into viral particles (290). A role in epitope masking for viral envelope-associated glycoprotein is also well documented (279). In accordance, removal of glycans N305 and N209 has been

shown to improve anti-E1 humoral responses, with deletion of the latter even improving the immunogenicity of the E1E2 heterodimer (291,292).

The notion that E1 may contain the putative HCV fusion peptide gained support following the resolution of the E2 core domain structure which revealed the peptide was not present in E2, as it would be if E2 functioned synonymously to flaviviral E (274,293). The E1 amino acid sequence analysis suggests the E1 NTD may contain a fusion peptide-like domain; however, the published structure does not resemble any fusion protein conformation (Fig 1.15) (294). More recently, escape mutations following cell culture adaptation of a genotype 2a strain of HCV in the presence of likely HCV fusion inhibitor suggests residues 272-290 comprise, harbour or are adjacent to the putative fusion peptide (295). Although, given the strong cooperation between E1 and E2 during virus assembly and entry, the fusogenic components of the glycoprotein unit may be realised only in the context of the heterodimer (287,296).

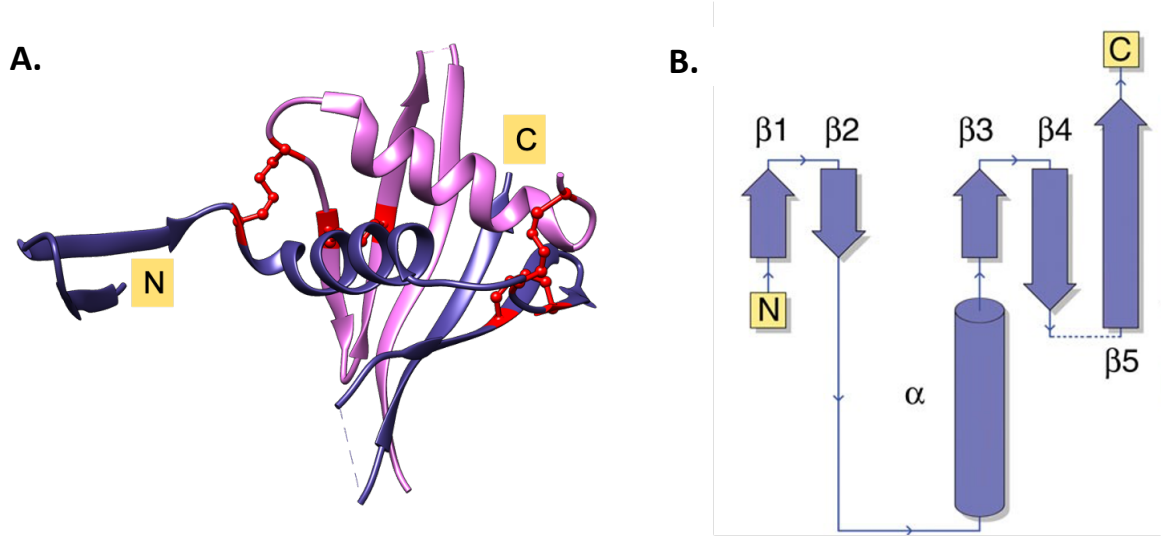

Figure 1.15. Crystal structure of the E1 N-terminal ectodomain (PDB: 4UOI). (**A**) Cartoon representation of a E1 NTD dimer. Chains are coloured in deep purple and magenta. Red residues represent cysteines involved in intra- and intermolecular disulphide bonding. (**B**) Topology of an E1 NTD monomer, corresponding to the deep purple chain in **A**. **B** adapted from Omari et al 2014 (291).

A direct interaction between E1 and any one of the known HCV receptors is not yet confirmed. However, it has been proposed that the role of E1 in the viral entry steps preceding membrane fusion is to maintain E2 in a functional conformation, thus modulating E2-receptor interactions. Indeed, CLDN1 has been shown to interact to E1E2 and not E2 on, as discussed previously (239). Additionally, cross talk between E1 and E2 has been observed in several studies. In these studies the mutation of any

of the conserved cysteines (removal of disulphide bridges) in E1 as well as several NTD residues, and the mutation of several C terminal domain residues affected interactions with CD81 and SR-B1, respectively (239,297,298).

1.5.2 The E2 glycoprotein

The functional properties of E2 have been extensively studied. It is regarded as the major HCV envelope glycoprotein, directly interacting with receptors to facilitate entry, as mentioned above. The physical interactions E2 shares with CD81 and SR-B1 are biochemically verifiable and E2-CD81 engagement is thought to initiate the formation of a coreceptor complex that temporally coordinates downstream entry events (see section 1.2.3) (198,211,225). E2 is the major immunogen for anti-HCV humoral immune responses and is thus the focus of most B-cell vaccine development efforts (299). Evidence suggests the mechanism for HCV neutralisation is the blockade of the interactions between E2 with its cognate binding partners, with the most potent and broadly neutralizing antibodies (nAbs) blocking E2-CD81 interactions (277).

1.5.2.1 The E2 core structure

Deciphering the structure of complexed HCV envelope glycoproteins remains a challenge despite recent advancements in crystallography methods. This is partly due to difficulties arising from overexpression of either or E1 and E2 monomers or heterodimers which often yields misfolded or aggregated protein. The innate properties of the heterodimer also pose a major challenge. The transmembrane domain of E2 is required for the correct folding of the E1 ectodomain and the oligomeric status of the authentic virion-associated heterodimer is unknown. Currently, only the ectodomain of E2 is amenable for thorough structural characterization since it folds correctly as a soluble protein (300,301).

E2 and antigen-binding fragment (Fab) co-crystallization approaches were utilised by two independent groups to solve the partial structures of E2 from the prototypical strains, H77 (genotype 1a) and J6 (2a) (PBB ID: 4MWF and 4WEB, respectively) (273,274). In both studies, the soluble E2 ectodomain (sE2) was genetically engineered to exclude the flexible regions. Overall, the two structures were in good agreement and revealed the basic domain organization of E2. The core domain exists as a globular structure with a central immunoglobulin (Ig)-like β-

Sandwich around which functional domains such as the front layer (FL) (res. 421-459), the back layer (BL) and the CD81 binding loop (res. 519-535) are organised (Fig 1.16).

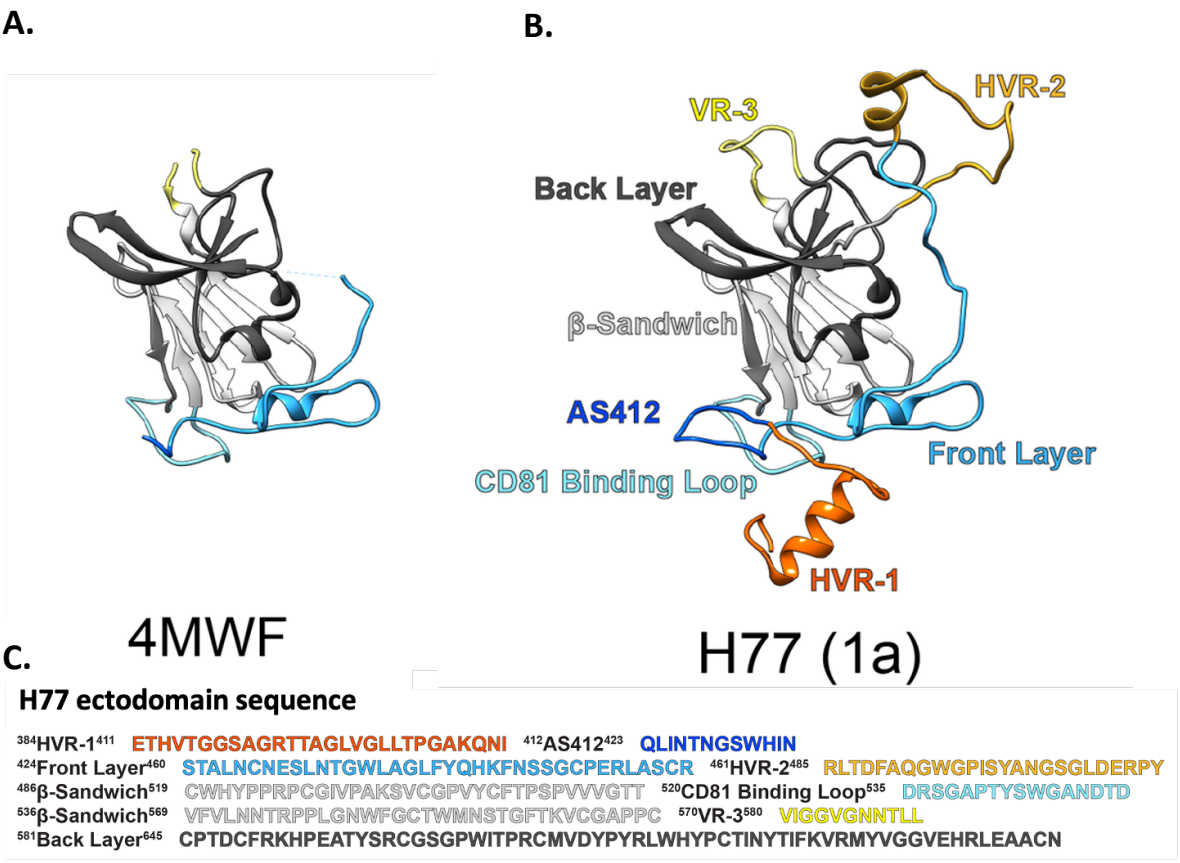

Figure 1.16 Structure and model of the E2 ectodomain. (**A**) Partial structure of H77 E2 (PDB: 4MWF). (**B**) Complete ectodomain model of H77 minus the stem. Annotations denote colour-coding of regions. (**C**) Amino acid sequence of E2, residues are coloured according to their corresponding region in **B**. Adapted from Stejskal et al (327).

The FL is an N-terminal stretch that is mostly extended loops with at least one truncated helix that packs against the central β-Sandwich and contributes to CD81 binding (280). The BL has high β-sheet content and is thought to harbour membranotropic segments which potentially play a role in membrane fusion (302). The CD81 binding loop is intrinsically flexible as highlighted its contrasting resolution in the aforesaid structures (273,274). In 4WEB, where an anti-BL Fab was used, the CD81 binding loop is disordered. On the other hand, the loop is stabilised by the AR3C Fab in 4MWF. The structural integrity of the overall fold is provided by an extensive hydrophobic core and by several disulphide bridges which cross-link the central β-Sandwich and bridge the flanking regions.

1.5.2.2 E1E2 is outside the three classes of fusion proteins

As touched on earlier, HCV was anticipated to possess a class II viral fusion protein given the genomic organisation of HCV is the same as that of other flaviviruses, displaying two envelope glycoproteins in tandem (E1 and E2) within the polyprotein precursor (252). Going by flavivirus analogy, E2 was postulated to be the fusion protein as it the larger of the two glycoproteins and is downstream on the polyprotein precursor. However, the crystal structures of the core fragments of E2 and complete models revealed it does not possess a class II viral fusion protein fold, nor indeed class I or III (Fig 1.17) (274,293). Furthermore, the E1 and E2 heterodimer (E1E2) is also unlikely to undergo class I conformational transition because it possesses two transmembrane domains, whereas the class I fusion heterodimer is a single-pass transmembrane (252).

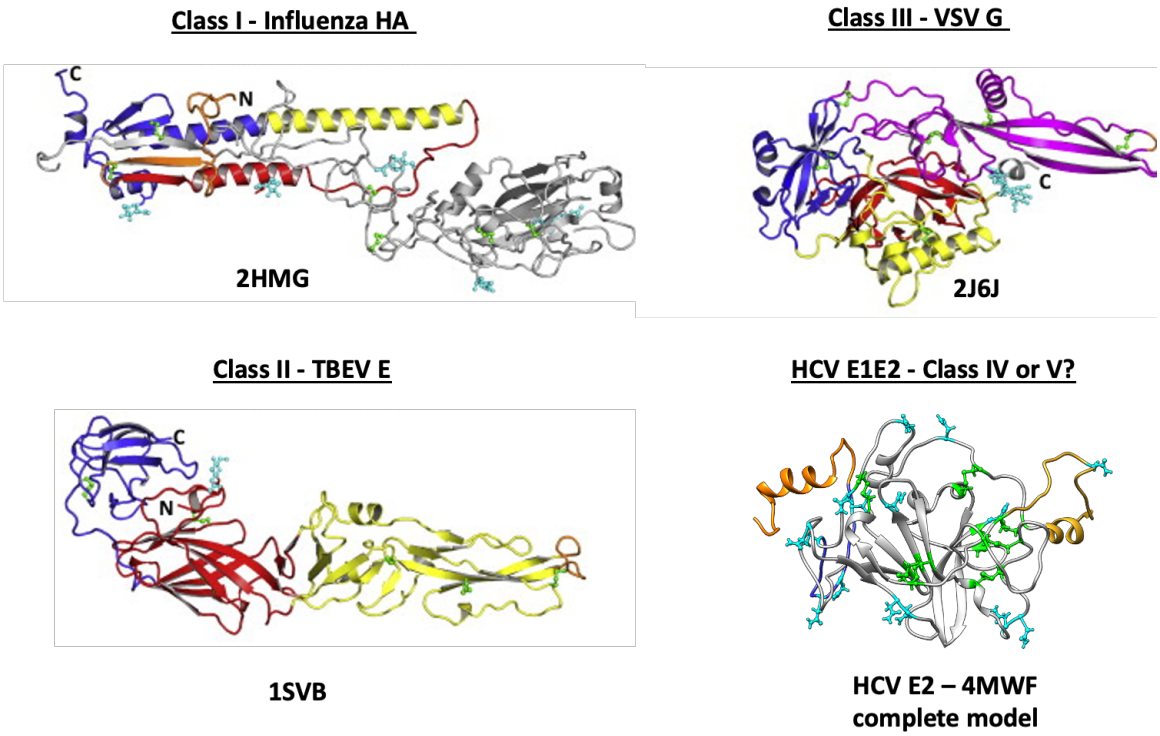

Figure 1.17. Representative pre-fusion structures of the ectodomains of viral fusion/entry proteins. Parentheses below structures: PDB references. In the Class I-III structures, the fusion motifs are coloured orange and the colour shade indicate domains. Sites of potential Asn-linked glycosylation are shown in cyan and disulphide bonds in green. Adapted from Li & Modis (300).

Notably, structural and bioinformatic analyses suggest the fusion proteins of the *Flaviviridae* family genera *Hepacivirus*, *Pestivirus* and *Pegivirus* all fall outside the three classes of fusion protein characterised so far (196,197,252). To this end, in 2013,

two independently solved crystal structures of the E2 protein of bovine diarrhoea virus revealed that it did not bear the hallmarks of any of the three defined classes of viral fusion proteins (196,197). Consisting of two Ig-like domains followed by an elongated β-stranded domain and a membrane anchor, it bears no resemblance to HCV E2 (Fig 1.16) (273). The drastically different structural organisation between BVDV E2 and HCV E2 suggests the *Flaviviridae* family possibly contains putative class IV and V fusion (303). Nonetheless, like HCV the fusion peptide/loop of BVDV is predicted to be in E1, so the fusion mechanism may yet prove to be conserved between the two viruses.

Given the above observations, it is unclear how the fusion machinery of HCV works, and the structure-to-function relation of E1E2 heterodimer cannot be predicted by simple analogy to other viruses. The structure of an E1E2 heterodimer and a clear cryo-EM 3D reconstruction of the HCV virion are necessary to provide clarity in these matters.

1.5.2.3 Variable regions

E2 possesses three variable regions, hypervariable regions 1 (HVR-1) and 2 (HVR-2 and variable region-3 (VR-3 or intergenotypic-VR) that together comprise ~25% of the E2 sequence and thus significantly contribute to the high diversity of HCV. Indeed, the HVR-1 and HVR-2 sequence segments exhibit the greatest variability in the genome (44). Notably, all E2 structures solved so far indicate the three variable regions reside outside the conserved core (Figs 1.16 & 1.18). HVR-1 is composed of the first 27 residues (26 for several genotype 6 subtypes) at the N-terminal of E2 but there is no structural information for this region. The overall basic charge of HVR-1 is highly conserved despite the high sequence diversity of this region, possibly to regulate interdomain interactions or SR-B1 binding (304). HVR-1 is predicted to contain the putative SR-B1 binding site as deletion of HVR-1 abolishes E2-SR-B1 interactions (305,306). A large body of evidence indicates HVR-1 is a prime target of humoral response during natural infection (307,308). Antibodies generated following either immunization with E2 or natural infection are often directed toward HVR-1 and are typically non-neutralizing or exhibit strain-specific neutralization (285,309).

It was long assumed that the HVR-1 shielded the CD81 binding site since its deletion was found to increase HCVpp sensitivity to nAb targeting cross-subtype conserved epitopes (213). However, it was recently shown that HVR-1 protects a

much wider variety of epitopes, including those in the back layer of E2 and even epitopes available only in the context of an E1E2 heterodimer (310,311). Moreover, HVR-1 deletion does not improve E2's immunogenic properties as one would expect if it were indeed an epitope shield (312). Consequently, the field has moved away from the notion of the simple HVR-1 epitope shield.

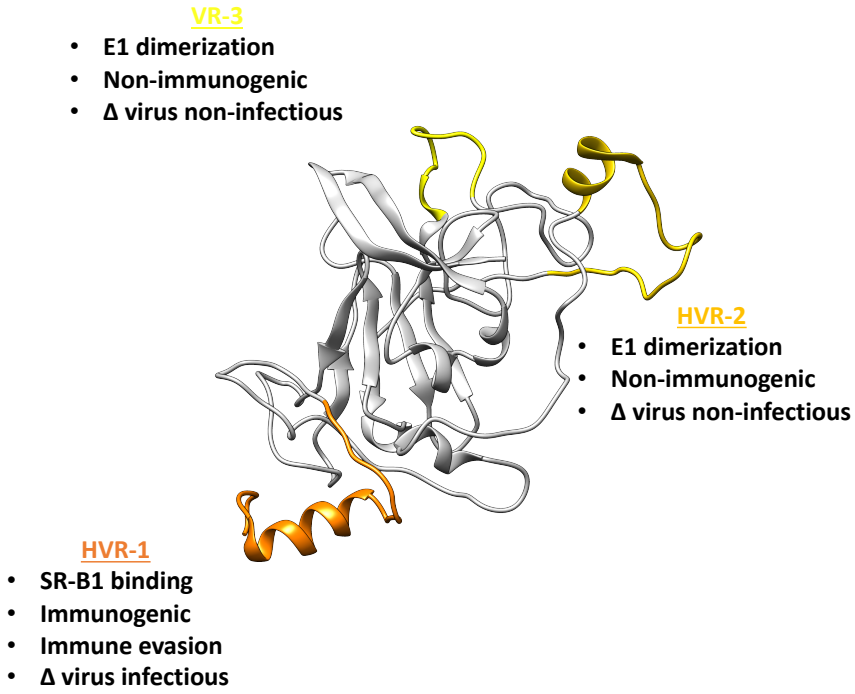

Figure 1.18. Model of the E2 ectodomain with variable regions highlighted. Proposed functions of the variable region are indicated. Δ virus: virus missing indicated variable region.

Less is known of the functional properties of HVR-2 and VR-3 (285). The HVR-2 (res. 461-481) is not essential for protein fold nor does it directly participate in receptor interactions (273,313). Sequence identity within this region exhibits great intergenotypic variation, ranging from 39% genotypes 1a and 1b to over 90% in genotype 5a (313). VR-3 is the shortest (H77 res. 570-580) of the variable regions and relatively conserved within genotypes but displays a high degree of intergenotypic variation both in length (ranging 10-15 residues) and sequence (313). E2 deleted of either HVR-2 or VR-3 fails to dimerise with E1 and ΔHVR-2 and ΔVR-3 HCVpp are non-infectious, as a result (314). Unlike HVR-1, HVR-2 and VR-3 do not appear to be the targets of an antibody response, which may mean they are not susceptible to immune selection (313). The role for HVR-1 in E2 immune evasion and entry are explored in more detail in the following subsections.

1.5.2.4 E2 Asn-linked glycans

Up to 11 Asn-linked glycosylation sites can be detected in E2 sequences. Nine are conserved across the HCV genotypes and are positioned at residues (in H77) 417, 423, 430, 448, 532, 566, 576, 623, and 645. The remaining two at positions 476 and 540 are also conserved except in genotype 1b, and genotypes 3 and 6, respectively (279). This high degree of conservation despite the E2 sequence being the most variable in the HCV genome suggests glycans play an essential role in the HCV life cycle.

Asn-linked glycans heavily influence the native fold of protein (315). Even without accounting for glycan interactions with ER chaperones, the presence of these large polar saccharides alone will guide protein orientation. Interactions between the chaperone calnexin and the HCV glycoproteins have been demonstrated (316,317); however, the exact contribution of these interactions to protein fold remain unknown (279). In the case of E2, a role in protein folding and E1E2 heterodimerization has been demonstrated for the glycans at N476, N556 and N623, independent of their potential interactions with calnexin (318).

Glycans can also influence virus entry by moderating glycoprotein-receptor affinity. Loss of the glycan at N532 through site-directed mutagenesis led to an increase in particle infectivity for authentic full-length cell culture HCV (HCVcc) (275). This mutant was found to be sensitive to neutralization by the soluble large extracellular loop of CD81 (sCD81), suggesting an improved affinity for CD81. Indeed, a soluble form of E2 devoid of the glycan at N532 exhibits higher affinity for CD81 (319). In contrast, loss of the glycan at N540 greatly reduced particle infectivity; however, the exact mechanism could not be determined (275). It is possible the glycan at this position may influence infectivity by modulating protein conformation. To this end, a recent study by Prentoe and colleagues suggested Asn-linked glycans may cooperate with HVR-1 to modulate envelope conformations (311).

Many viruses reduce the immunogenicity of their envelope proteins by employing a glycan shield to mask conserved functional epitopes (320). Glycans are mostly non-immunogenic as they are host-derived autoantigens; thus, nAbs either avoid or evolve to accommodate carbohydrate sidechains on viral glycoproteins (321). Appropriately, when modelled onto the E2 core structure, seven of 11 glycans present in H77 are presented on the neutralizing face of E2 (Fig 1.19) (293). This suggests

glycans potentially restrict the generation of nAbs to this region which is implicated in CD81 binding. Based on the H77 core stricture, the neutralizing face is a predominantly hydrophobic surface that includes the N-terminal antigenic site 412 (AS412), most of FL and the CD81 binding loop and consists of largely conserved residues (322). The glycans at N417, N532 and N623 were found to obscure the E1E2 heterodimer from CD81 and their deletion increased HCVpp sensitivity to nAbs. In the context of HCVcc, the glycans at N423 and N448 also affected nAb sensitivity (275).

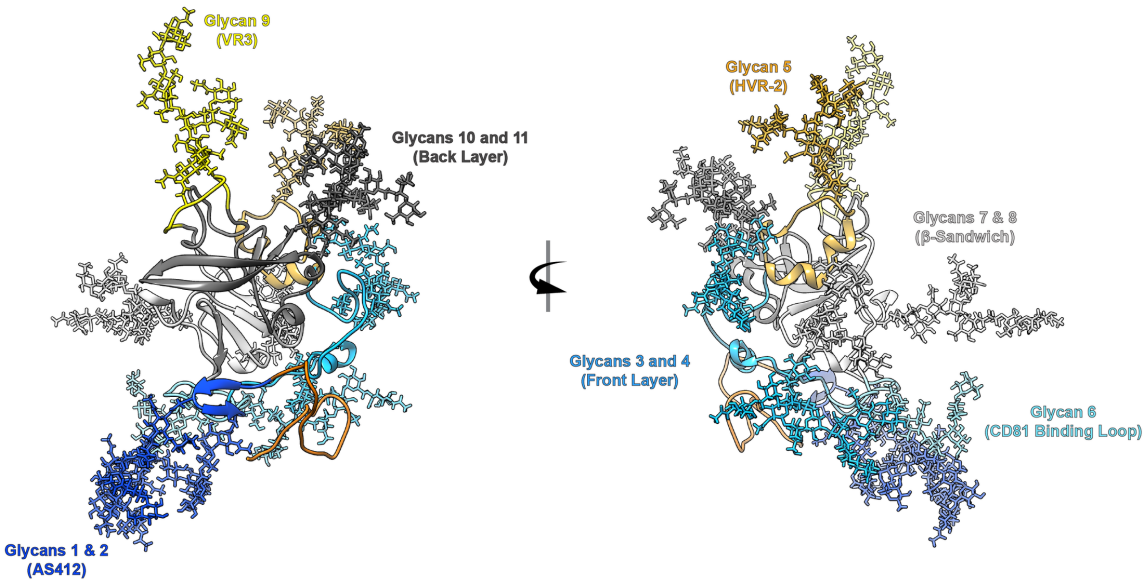

Figure 1.19. Model of glycosylated J6 E2 ectodomain. Glycans are colour coded according to their protein region, consistent with the coding shown in Fig **1.15**. Curved arrow indicates 200° rotation. Adapted from Stejskal et al (327).

Some have questioned the simple model of glycans modulating immune evasion through steric hindrance alone (322). Although modelling predicts extensive glycan shielding of the neutralizing face of E2 (293), this surface remains accessible on native virions and is immunogenic, more so during natural infection than post-vaccination (309). Furthermore, the neutralizing face of E2 is accessible to nAbs with different angles of approach, suggesting it is not obstructed by glycans (322,323). Soluble proteins, including viral glycoprotein ectodomains (324,325), undergo large-scale movements of secondary structures, subunits or domains that define a native-state ensemble of structures (326). Molecular dynamics (MD) simulations suggest Asn-linked glycans can stabilise glycoprotein structures and reduce glycoprotein dynamics (327). In the case of E2, it was recently suggested Asn-linked glycans on E2 contribute to immune evasion not only by steric hindrance of key epitopes but also

by modulating the stability of functional E2 conformations (311). In this study, in addition to increasing nAb sensitivity, the sum removal of three glycans from E2 (J6, genotype 2a) reduced the virion stability at 37°C, indirectly suggesting this mutant preferably occupied a conformation distinct to J6 wildtype E2. A direct study of sE2 or particle-associated E2 conformation transition is required to validate this observation.

1.5.2.5 Disulphide bonds

HCV E2 has 18 cysteine residues that are strictly conserved across the HCV genotypes. Most of the residues are predicted to participate in intramolecular disulphide bonding within E2. Sixteen cysteine residues in the first E2 structure, 4MWF, participate in an intramolecular disulphide bond (293). A disulphide bond between C459 and C486, the two cysteines not participating in a disulphide bond in 4MWF, is present in more recent structures (280). Interestingly, these recent structures also exhibit different disulphide bonding patterns around VR-3 compared to 4MWF. This may signify intrinsic heterogeneity in the disulphide bonding patterns of cysteines within E2. Actually, there is evidence for intermolecular disulphide bonding between E1 and E2 cysteines. Vieyres et. al found that virion associated E1E2 heterodimers formed large covalent complexes stabilised by disulphide bonds (153). Furthermore, attempts to biochemically deduce the disulphide bond linkages with E2 have reported different cysteine pairings (328,329). The environment of the endocytic pathway, through which HCV egress is realised, is highly oxidizing and compatible with disulphide bond reshuffling which may account for the observed disulphide bond heterogeneity (284).

Nonetheless, heterogeneous E2 disulphide bonding is unlikely to affect overall protein fold, due to its extensive hydrophobic core and disulphide bonding between secondary structure elements (280,284,293). Modelling E2 with bonding patterns taken from the first E2 structure (293) or from Flyak et. al (280) did not change protein behaviour during MD simulations (Fig 1.20) (330). In addition to scaffolding the three-dimensional structure of E2, disulphide bonding within E2 also contributes to heterodimerization with E1 as any Cys to Ala mutation in E2 severely decreased or abolished said interaction (331). Notably, despite its apparent conformational flexibility, E2 has high thermal stability compared to other viral glycoproteins and some suggest this is attributable to the dense network of disulphide bonds within the E2 (323).

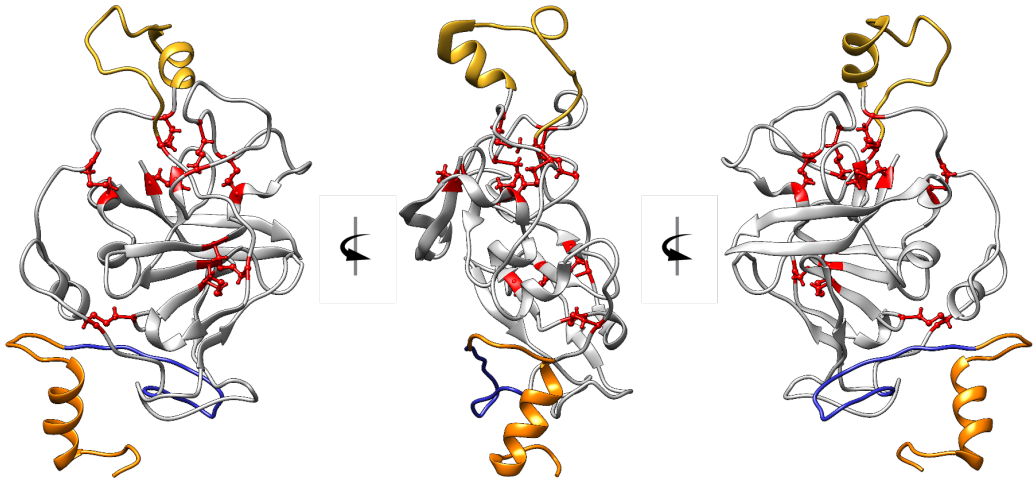

Figure 1.20. Disulphide bonding in H77 E2 ectodomain model. Red residues represent cysteines involved in intramolecular disulphide bonding. The HVR-1, AS412 and HVR-2 are coloured according to **Fig 1.16 B** to aid orientation. Curved arrow indicates 90° rotation.

1.6 Antibody epitopes in E1E2

Since viral entry proteins are often the most prominent proteins of the virions, they are also the principal target nAbs. As mentioned earlier, nAbs block HCV infection by blocking the interaction between E1E2 and the receptors SR-B1 and CD81 (332–334). It was initially thought humoral immunity played only a minor role in HCV elimination, partly because clearance in chimpanzees was strongly associated with cellular immune responses (14,182). However, in the last decade, it has become increasingly clear that the kinetics of the emergence of broadly neutralising antibodies (bnAbs) influence the outcome of infection. Additionally, in the chronic stages of infection, concurrent HCV evolution to escape humoral immunity may lead the virus off an 'evolutionary cliff', where accumulated mutations render E1E2 not fit-for-purpose (17). This brief subsection will outline the key antibody epitopes of the HCV entry machinery as well as discuss their suitability to rational immunogen design.

The immunogenic epitopes on E2, and to a lesser extent E1, are well characterised. These epitopes, though wholly overlapping, have been given varying nomenclature (e.g., AR 1-5 and domains A-E by different groups who've isolated and characterised their cognate monoclonal antibodies (mAbs). To avoid confusion, in this work, the epitope nomenclature is identical to the protein region (see Table 1.1), i.e., we refer to the epitope cover residues 412-423 as AS412, not as Epitope I (335) or Domain E (336).

Table 1.1 Epitopes targeted by neutralising antibodies

Protein	Name	Position (AA res.) [a]	mAb example	Epitope class	DOI
E1	**Unnamed**	**313-327**	IgH505	Linear	Meunier 2008
			IgH526	Linear	
E2	**HVR-1**	**384-411**	H77.16	Linear	Sabo 2011
			HEPC98	Conformational	Mankowski 2016
			J6.36	Conformational	Sabo 2011
	AS412	**412-423**	AP33	Linear	Clayton R 2002
			H77.39	Conformational	Sabo 2011
			HC33.1.53	Conformational	Wang 2011 JBC
			HCV-1	Conformational	Morin plos Path
	Front layer *	**424-460**	AR3A	Conformational	Law 2009
			AR3B	Conformational	Law 2009
			AR3C	Conformational	Law 2009
			AT12-009	Conformational	Merat 2016
			HC84.24	Conformational	Keck 2012
			HC84.26	Conformational	Keck 2013
			HEPC3	Conformational	Flayk 2018
			HEPC43	Conformational	Flayk 2018
	Back layer	**581-645**	AR2A	Conformational	Giang 2012
E1E2	**AR4/AR5**	**E1 (201-206) & E2 (Back layer and Stem)**	AR4A	Conformational	Giang 2012
			AR5A	Conformational	Giang 2012

[a] Amico acid numbered in reference to the polyprotein of the H77 isolate. *All mAbs listed here also target the CD81 binding loop.

As it is the minor and less prominent of the two HCV glycoproteins, E1 is weakly immunogenic and mAbs with epitopes targeting it are rarely isolated. The patient-derived antibodies IgH505 and IgH526 are to date the only anti-E1 mAbs to demonstrate appreciable broad-spectrum neutralising activity in an HCVpp screen (337). Consistent with E1's putative role as the HCV fusogen, the two antibodies were found to neutralise the virus at a post-receptor engagement step (338). Additionally, the E1/E2 heterodimerisation-dependent epitope AR4/AR5 encompasses residues 201-206 in E1 (339). It's important to note that the difficulty in isolating anti-E1 mAbs is likely due to their rarity as much as it is due to the difficultly of expressing correctly folded E1 *sans* E2, as previously mentioned.

Consistent with a model where HVR-1 is displayed prominently relative to the rest of E2, vaccination of small animals with E2 or E1E2 constructs induces a high proportion of anti-HVR-1 responses. These antibodies neutralise HCV by preventing E2 engagement with SR-B1 (340,341). However, anti-HVR-1 antibodies isolated in the chronic phases of infection are typically weakly neutralising (309). Nonetheless, intriguingly, evidence suggests that in some patients, clearance of HCV during the

acute phase is associated with the emergence of autologous, narrow but potently neutralising antibodies (15,342). Acute-phase sera from some clearers was shown to effectively neutralise autologous transmitted/founder virus in a recent study by Walker et al (15). This implies that anti-HVR-1 responses play a role in controlling HCV in the early stages of infection; however, the region's genetic variability and intrinsic disorder (discussed in the next section) make it an unworkable epitope with regards to broad-acting vaccine design.

Antibodies targeting the AS412 largely bind a linear epitope, and immunisation of mice and rats has yielded some particularly potent anti-AS412 mAbs, including 3/11, AP33 and mAb24. Most of these antibodies contact some or all resides spanning 413-420 in E2 and, notably, W420 has been implicated in CD81 engagement. However, antibodies toward AS412 come by very rarely during natural infection, with ELISA studies indicating that less than 2.5% of patients with chronic HCV develop antibodies that bind this region (343,344). Antibodies with the prefix HC33 are the best-characterised anti-AS412 mAbs and several exhibit broad-spectrum activity (345). Taken together with its epitope linearity and high conservation, this broad activity makes AS412 an attractive candidate for antigen mimicry and rational vaccine design (346–348). Indeed, potent anti-AS412 mAbs could yet be observed in acute clearers since they are yet to be investigated using the current cutting-edge mAb isolation techniques.

Composing the front layer and the binding loop (res 520-525), the discontinuous conformational epitope of the CD81 binding face is the main target of most HCV bnAbs described to date (see Table 1.1 for examples). The mode of action for these antibodies is the prevention of CD81 engagement since their E2-surface footprint significantly overlaps with the CD81 contact residues. Residues within this epitope that are frequently targeted include some with pangenotypic incidence such as W529, G530 and D535, all of whom are indispensable for HCV entry (349). With its limited escape potential, high conservation, and frequent elicitation of bnAbs, the CD81 binding face is intensely investigated for the mechanisms underlying its immunogenicity. A discussion of the genetic and structural features of said bnAbs, and approaches to rationally design immunogen candidates to elicit them, can be found in the general discussion (Section 6.4). Next, the intrinsic flexibility of the E2 epitopes is reviewed in detail, as is the impact of said dynamism on antibody and receptor engagement.

1.7 The Intrinsic structural flexibility of E2

Crystal structures indicate 60% of the E2 ectodomain adopts no obvious secondary structure, suggesting E2 may exhibit a great degree of flexibility in aqueous solution (280,293). In recent years crystallographic studies using short antibody-recognised E2 peptides have uncovered the molecular intricacies of antibody-epitope interactions, highlighting great structural heterogeneity within E2's functional subunits.

1.7.1 Antigenic site 412

Structural evidence indicates AS412 is remarkably disordered despite high genetic conservation across the genotypes. This region has been found to adopt three distinct conformations when co-crystallised with cognate Fabs. The human nAb HCV1, mouse nAbs AP33 and mAb24, and the humanised and affinity matured nAbs MCRT.10V362 and hu5b3.V3 bound AS412 peptides adopting a similar β-hairpin conformation (e.g., PDB: 4DGY) (Fig 1. 21 A) (350–354). In contrast, the Fab of the rat nAb 3/11 recognises the same peptide in an extended configuration which protrudes into a cleft between the heavy and light of the Fab as a closed loop (Fig 1.21 B) (355). And lastly, the AS412 peptide forms an anti-parallel β-sheet with strand F of the heavy chain of Fabs from the HC33 group of human nAbs, with the remainder of the peptide recognised as an extended coil (Fig 1.21 C) (356). The intrinsic flexibility of AS412 was further highlighted in an electron microscopy study which found the Fab of the mAb HCV1 could engage the peptide from multiple angles (323).

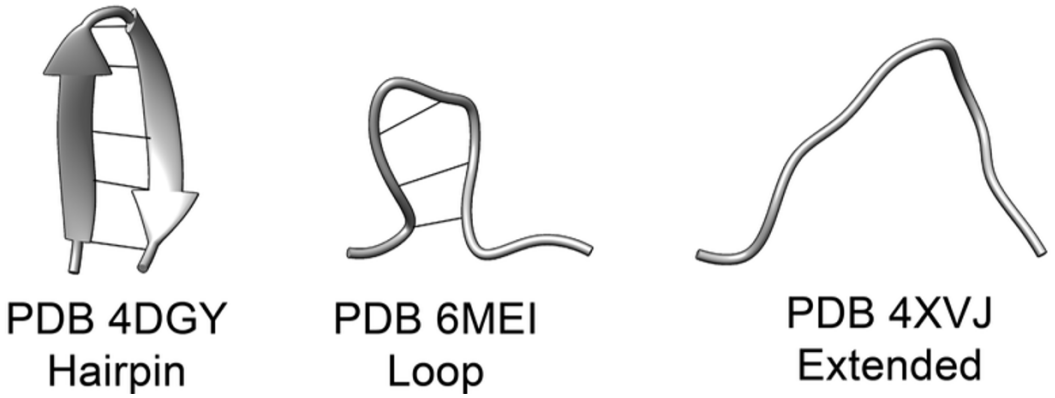

Figure 1.21. Conformational differences in crystallised AS412. Representative structures of AS412 in a β-hairpin (PDB: 4DGY), closed loop (PDB 6MEI) or extended (PDB: 4XVJ) conformation. Adapted from Stejskal et al (327).

adopts an ensemble of well-defined conformations (357). The AS412 peptide readily adopted a regular secondary structure in solution and all multiform conformational

states it adopted in Fab co-crystals mentioned above were detected as part of the structural ensemble during MD simulations of the peptide. Furthermore, Stejskal et. al very recently observed the Fab-bound conformations in their simulations of the complete E2 ectodomain (330). These simulations suggest the Fab-bound conformations represent snapshots captured from a dynamic equilibrium of distinct states. Notably, Augestad et al recently reported that the AS412 is skewed toward the β-hairpin conformation when E2 functionally adopts a theoretical 'closed' fold, typified by resistance to nAbs (346).

Notably, *in silico* predictions of the peptide alone suggest a β-hairpin conformation comparable to the one observed in AP33 (356). Indeed, β-hairpin configuration was the most commonly observed during MD simulations and is the most prevalent in AS412 peptide-Fab complexes (330,358). Together, these findings suggest the β-hairpin is the preferred, but highly unstable configuration of AS412. Considering the high degree of genetic conservation of this region across the genotypes, it's likely the transitions in AS412 conformation are important for function, allowing it to readily convert between configurations following a model of "induced-fit" binding to CD81 or nAb. Moreover, this intrinsic flexibility could account for the limited humoral responses observed in patients toward AS412.

1.7.2 The front layer

Fab-peptide co-crystals have similarly informed our current understanding of the dynamic behaviour within the E2 front layer. The structures available for this region fall into two classes, peptide complexed with potent patient-derived nAb and peptide complexed weakly with non-nAbs (358). When crystallised with the potent nAbs HC84.1 and HC84.27, a peptide spanning encompassing 434-446 forms a short α-helix which spans residues W437-F442 with the C-terminal residues adopting an extended conformation (359,360). This short α-helix is also present in AR3C Fab-E2 core structure (293). An even shorter α-helix is observed a few residues upstream in two structures when a peptide with similar residue coverage was complexed with the Fabs of murine-derived non-nAbs mAb #8 and mAb 12. Interestingly, residues W437 and L438 crucial for binding to murine non-nAbs are solvent-inaccessible in 4MWF suggesting a conformational transition is required to expose these two residues to make them available for binding (361,362). Superposition of the respective peptide-Fab structures at the N-terminal, which is anchored in the central β-Sandwich, predicts

the C-terminal α-helix has to flip out to permit for mAb 8 binding (358). Hydrogen deuterium exchange mass spectrometry (HDXMS) have confirmed structural flexibility within the front layer including the putative CD81 binding site which overlaps with the epitopes of many bnAbs (323). Flexibility within the front layer could be attributed to a hinge constituted by conserved glycine at position 436, which may permit for some degree of rotation of the α-helices.

More recently, Law and colleagues identified a novel conformation of the FL whereby it is displaced upon antibody binding to expose residues in the BL for direct antibody interactions (363). In this study, mutation of the BL Y613 and W616 residues reduced CD81 binding suggesting a direct interaction between CD81 and the E2-BL. These findings suggest BL residues may directly engage CD81, opposing long-held view that the BL does not contribute to the receptor binding epitope. However, conformational transitions to expose the BL may simply disrupt the CD81 binding site and not necessarily bring BL in contact with CD81 itself. Further studies are needed to elucidate the importance of this process to receptor binding and, by extension, HCV entry. Additionally, nAbs from infected human were able to engage this BL-exposed conformation, indicating it exists in vivo and is biologically relevant.

1.7.3 The CD81 binding loop

The poor resolution of an already-resolved segment of the CD81 binding loop in the second crystal structure of the E2 core suggests the loop is intrinsically disordered (274). In 4WEB, residues 524-535 are disordered and the phenylalanine at position 537 is solvent-exposed. Indeed, F537 is buried in the Fab-peptide interface of a complex between a short peptide consisting of residues 532-540 and the non-nAb DAO5 (364). By contrast, F537 is inaccessible to solvent, buried inside a hydrophobic core of an Ig-like domain in 4MWF (273). Collectively, these findings suggest a model where the CD81 binding loop transitions between configurations to allow hydrophobic sidechains buried within E2 secondary structure to flip inside-out and become solvent-exposed. Infection experiments using cross-competing Fabs suggest both binding loop configurations, where F537 is buried or accessible, are simultaneously displayed on HCVpp.

1.7.4 The hypervariable region 1

All three variable regions present in E2 are highly flexible and adopt heterogeneous conformations as indicated by HDXMS experiments of complete E2 ectodomain (323). In emphasis, HVR-2 and VR-3 are present as loops lacking obvious secondary structure when a genotype 1b strain 1b09 E2 ectodomain is co-crystallised with the Fab of HEPC3 (a bnAb) (280). However, only the very C-terminal segment of HVR-1 is resolved in this structure, suggesting this region to be exceptionally flexible. By performing MD simulations of complete of H77, J6 and 1b09 ectodomains, we recently reported that HVR-1 bears the hallmarks of an intrinsically disordered protein region (IDPR) (330). In the study, intrinsic disorder predictions of genotype 1-6 consensus sequences further supported this assertion. Strikingly, dynamic cross-correlation analysis, a way to measure intramolecular interactions during MD simulations, provided evidence that motions within HVR-1 are communicated throughout E2.

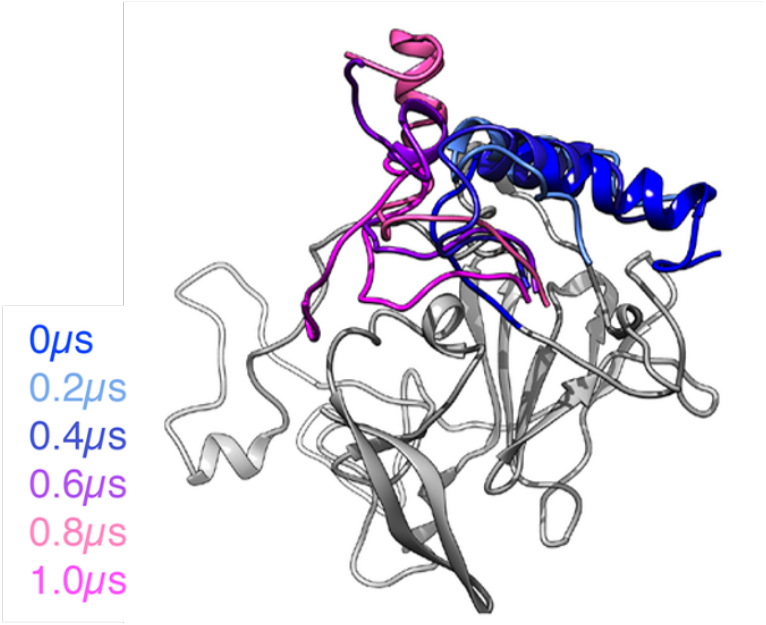

Figure 1.22. Flexibility of HVR-1. 200 ns snapshots taken from a single representative trajectory for the complete H77 E2 model. HVR-1 is color-coded by time. The remainder of E2 is shown in grey for T=0 μs snapshot alone. Adapted from Stejskal et al (327).

As mentioned before, HVR-1 accumulates mutations during natural infection, particularly toward the C terminus. Prentoe and colleagues recently reported that residues 400-404 in HVR-1 influence the global E1E2 conformational landscape (346). They observed that polymorphisms within this sequence broadly regulated nAb sensitivity, suggesting that mutations that accumulate here during chronic infection may protect HCV from nAbs targeting non-HVR-1 epitopes. MD simulations of HVR-

1-AS412 peptides revealed that nAb protective polymorphisms in 400-404 stabilised a β-hairpin AS412 conformation. β-hairpin fold in AS412 skewed E1E2 to a theoretical 'closed' state, which though favourable for nAb evasion, is likely to be detrimental for CD81 engagement. The authors suggest SR-B1 engagement may aid nAb resistant 'closed' HCV to engage CD81. Taken together with Stejskal et al, this data suggests HVR-1 regulates global E2 or E1E2 conformation dynamics, possibly influencing protein function.

As with its intrinsic sequence heterogeneity, the conformational plasticity of HVR-1 is proposed to contribute to its role as an immune decoy. In contrast, HVR-2 and VR-3 are not immune decoys as demonstrated by the fact they are not susceptible to immune selection during natural infection. Although little is known of its functional properties, mutagenesis and evolutionary analyses are consistent in their prediction that HVR-2 is present at the interface of the E1-E2 heterodimer (302,365,366). Therefore, despite HDMXS and MD simulations highlighting HVR-2 flexibility in E2 monomers, it is likely constrained in the biologically relevant context of a virus particle. HVR-2 burial in the E1-E2 interface could also explain why the region isn't immunogenic in natural infection but modulates binding of E2-antibody binding following animal vaccination with E2 ectodomain based constructs (285,367).

1.8 Hypothesis and aims

To reiterate, it is impossible to determine the HCV fusion mechanism by structural analogy since E1E2 do not fall into any of the three described classes of fusion protein. The difficulty of the task of deciphering the E1E2 structure-to-function relationship is further compounded by the lack of a crystal structure for the heterodimer. As such, we elected to employ a multidisciplinary approach in our quest to understand E1E2. This integrated approach yielded two significant studies.

Firstly, in Kalemera et al (219), using a combination of in vitro experimentation and mathematical modelling we found that HCV entry can proceed via two routes, one mediated by SR-B1 and one independent of it (Fig 1.23). While the majority of virus traverses the former route, we hypothesise that SR-B1 dependency introduces a rate-limiting step, as corroborated by the inefficient entry we observed. Another key takeaway was that our data implied that SR-B1 primes E1E2-CD81 interactions.

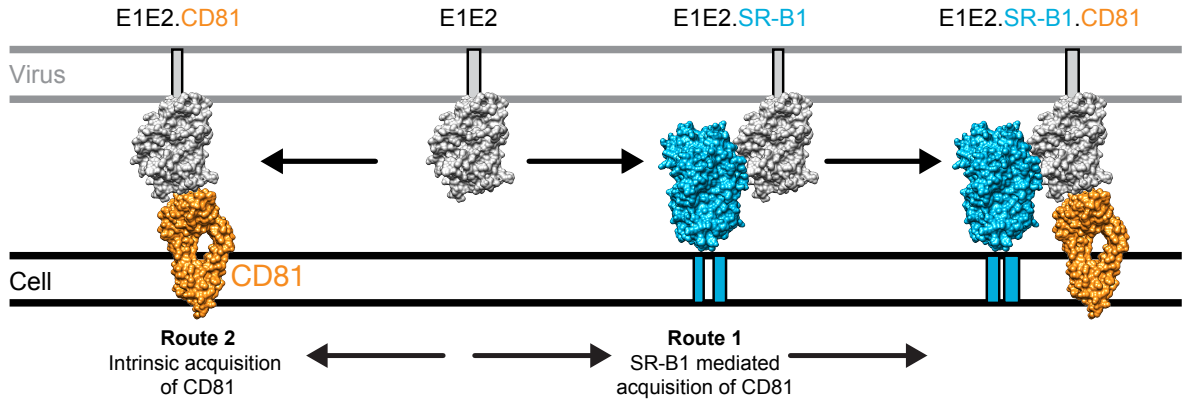

Figure 1.23. The two routes of HCV entry. E1E2-receptor interactions at the cell surface, as recreated in our model (218). To achieve entry E1E2 must acquire CD81, this can occur via two routes. Route 1 SR-B1 mediated: prior binding to SR-B1 primes E1E2 for interaction with CD81. Route 2 intrinsic binding: E1E2 interact with CD81 without prior engagement of SR-B1 Once sufficient molecules of CD81 have been acquired, the virus particle proceeds along the entry pathway. Molecular cartoons are based on previously published structures and are drawn to scale.

Secondly, in Stejskal et al, by performing MD simulations and confirmatory biophysical measurements, we found that flexibility and intrinsic disorder are conserved features of the E2 ectodomain (see section 1.7.4, above) (330). Strikingly, we observed that motions within HVR-1, the most conformationally dynamic region, were communicated throughout E2. As previously mentioned, HVR-1 bears the hallmarks of an IPDR; these contribute significantly to protein biology by influencing protein-protein interactions and regulating protein function. Therefore, it is possible HVR-1 has evolved to be disordered to perform or refine a particular function of E2 (330).

1.8.1 Overarching hypotheses

The experimental design in chapters three and four of this thesis was guided by the key takeaways from the abovementioned works and addressed three key hypotheses. Firstly, we hypothesised that SR-B1 dependency reduces HCV entry efficiency. Stemming from this, we theorised that HCV evolved to require priming by SR-B1 to evade neutralising antibodies. Lastly, we hypothesised that HVR-1 conformational entropy regulates E1E2 function.

1.8.2 Aims

The fundamental purpose of this study was to the identify the molecular mechanisms that determine HCV entry efficiency and nAb evasion. The specific aims of this thesis were:

1. Establish how HCV entry efficiency and, by extension, SR-B1 dependency is intrinsically linked to nAb evasion.
2. Identify structural features that may control entry efficiency and nAb evasion.
3. Apply our understanding of E1E2-receptor interactions to increase the representation of circulating HCV strains in vaccine efficacy screens.

This work has the potential to provide insights to E1E2 structure-to-function relationship and could thus inform rational B-cell vaccine efforts.

2 Materials and methods

2.1 Antibodies

Table 2.1. The details of the antibodies used in this study

2.131 (anti-CD81)	Jane Mckeating	10.12688/wellcomeopenres.12058.1
AP33	Arvind Patel	10.1128/JVI.76.15.7672-7682.2002
AR2A	Mansun Law	10.1073/pnas.1114927109
AR3A	Mansun Law	10.1038/nm1698
AR3B	Mansun Law	10.1038/nm1698
AR3C	Mansun Law	10.1038/nm1698
AR4A (E1E2)	Mansun Law	10.1073/pnas.1114927109
AR5A (E1E2)	Mansun Law	10.1073/pnas.1114927109
AT12-009	Tim Beaumont	10.1371/journal.pone.0165047
CBH-23	Steven K H Foung	10.1128/JVI.02200-09
CBH-4B	Steven K H Foung	10.1128/JVI.78.17.994-9232.2004
CBH-7	Steven K H Foung	10.1128/JVI.78.17.994-9232.2004
Goat anti-human IgG (HRP)	Jackson Immunoresearch	N/A
Goat anti-mouse Alexxa Flour 647	ThermoFisher	N/A
Goat anti-mouse IgG (HRP)	CST	N/A
Goat anti-rabbit Alexxa Flour 647	ThermoFisher	N/A
H77.16	Michael S Diamond	10.1128/JVI.00586-11
H77.39	Michael S Diamond	10.1128/JVI.00586-11
HC1	Steven K H Foung	10.3390/v3112127
HC84.26	Steven K H Foung	10.1371/journal.ppat.1002653
HEPC3	James Crowe	10.1172/jci.insight.92872
HEPC43	James Crowe	10.1172/jci.insight.92872
IgH505 (E1)	Jens Bukh	10.1128/JVI.01872-07
J6.36	Michael S Diamond	10.1128/JVI.00586-11
mAb S38 (NS5A)	Jane Mckeating	10.1128/JVI.01569-08
Rabbit anti-SR-B1 sera	Thierry Huby	10.1096/fj.05-4728fje
StrepMAB classic	IBA LifeSciences	N/A

[a.] Unless otherwise stated otherwise, the antibodies listed above are specifically anti-E2.

2.2 Reagents and kits

Unless specified, all kits were used according to manufacturer's instructions.

2.3 Cell lines and culture

The receptor knock-out Huh-7 cell lines were a kind gift from Prof. Yoshiharu Matsuura (Osaka University) (218), and HeLa-ACE2 cells were kindly gifted by Dr. James Voss (SCRIPPS) (368). Huh-7 cells were acquired from Apath LLC and Caco-2 from ATCC. All aforementioned cells were grown at 37°C in Dulbecco's Modified Eagle Medium (DMEM) (Gibco) supplemented with 10% foetal calf serum (FCS), 1% non-essential amino acids (Gibco) and 1% penicillin/ streptomycin (P/S) (Gibco). HEK 293T (ATCC) and $293T^{CD81KO}$ cells adapted to suspension were maintained in FreeStyle™ medium, as were 293-F cells (Invitrogen). All suspension cell lines were maintained in a shaking incubator (125 rpm) at 37°C and 8% CO_2.

2.4 Isolation of patient IgG *(Joe Grove)*

Blood samples were collected from HCV+ patients under ethical approval: "Characterising and modifying immune responses in chronic viral hepatitis"; IRAS Number 43993; REC number 11/LO/0421. Extracted serum was heat inactivated, filtered and diluted 1:1 in PBS. Total IgG was captured using a HiTrap™ protein G column (Cytiva), eluted in pH 2.7 glycine buffer and buffer exchanged into PBS. For experiments, batches of pooled IgG were created by equimolar combination of IgG from two patient samples.

2.5 Generation of J6/JFH-1 cell culture proficient HCV

Plasmid encoding cell-culture proficient full-length J6/JFH-1 (HCVcc) was purchased from Apath LLC. To initiate infection, viral RNA was electroporated into Huh-7.5 cells using a BTX830 (Harvard Instruments). From 3-7 days post electroporation, cell culture supernatants containing infectious J6/JFH-1 HCVcc were harvested every 3-5 hours. Short harvest times limit the opportunity for virus degradation thereby preventing the accumulation of non-infectious particles. To ensure maximum reproducibility between experiments, a standardised stock of experimental virus was generated by pooling the harvested supernatants.

2.6 HCVcc adaptation experiments

In the first adaptation experiment (Chapter 3, performed by Joe Grove), a continuous culture of J6/JFH-1 HCVcc was established in Huh-7.5 cells. Infected cells were passaged twice weekly, and the culture was supplemented with an excess of uninfected target cells whenever infection breached 90% of cells. Throughout the experiment, culture supernatant was harvested, clarified by centrifugation, and stored culture supernatants at -20°C for analysis by next-generation sequencing (NGS). From the point of initial electroporation, the adaptation experiment was continued for up to 20 weeks. Viral RNA was isolated from stored supernatant using QIAamp® Viral RNA kits, per the manufacturer's instructions.

For the adaptation plus or minus IgG selection (Chapter 4), a serial passage strategy was employed. Huh-7.5 cells were electroporated with the J6/JFH genome and the next day medium was replaced with DMEM 3% FCS plus or minus HCV+ patient IgG at 100 µg/ml. Once 90-100% of cells were determined to be infected, the culture supernatant was harvested, clarified by centrifugation, and used to infect fresh Huh-7.5 cells. Typically, this was done every week. Again, culture supernatants were frozen at -20°C at regular intervals for future analysis by NGS.

2.7 Site-directed mutagenesis

Substitutions observed in the culture adaptation were introduced into pD603-J6 E1E2 plasmids using the Q5 Site-Directed Mutagenesis Kit (New England BioLabs) and confirmed by Sanger sequencing (Eurofins). Mutations were then introduced into the J6/JFH-1 vector by use of restriction enzymes (New England BioLabs).

2.8 HCVcc infections

Huh-7.5 and receptor KO Huh-7 cells were seeded at 1.5 x 10^4 cells per well of a 96 well plate 24 hours prior to the experiment. A day later, to quantify infectious titres, cells were challenged with a two-fold serial dilution of virus stock (1/4 down to 1/64) in DMEM supplemented with 3% FCS (infection medium). For standard infections, cells were challenged with virus stock diluted 1/2 in infection medium. Cells were incubated with viral supernatants for only five hours before the cells were subsequently washed, and fresh medium was added. From thence, infections were allowed to proceed for 48 (Huh-7.5 cells) or 72 (Huh-7 lines) hours before reading out. To measure HCVcc

replication by fluorescence microscopy, cells were fixed with 100% methanol and stained for viral NS5A protein with mAb S38. HCV foci-forming units (FFU) were quantified by manual counting and percentage of infection determined by automated analysis of fluorescence micrographs (369).

2.9 Next generation sequencing (*Lenka Stejskal*)

RNA was extracted from cell culture supernatants containing HCVcc by a BioRobot MDx instrument using QIAamp Virus RNA extraction Kits. Extracted RNA samples were amplified as described (370) processed locally within the UCL Hospital Virology laboratories for PCR library preparation and Next Generation Sequencing using Illumina MiSeq equipment (371) were trimmed of adaptors and low-quality reads using Trimmomatic V.0.33 (372). The quality of the sequence files was then assessed using the FastQC program. The resulting FASTQ files were then aligned to the indexed reference J6/JFH-1 HCVcc genome using the BWA-MEM algorithm (Burrows Wheeler Aligner (373)), converted into Sequence Alignment Map (SAM) files, which were further compressed into BAM files (binary versions of SAM files), sorted by reference coordinates and indexed using SAMtools. The duplicate sequences were then removed by Picard Tools and indexed again using SAMtools. Basecalling for each position in the genome was extracted from the indexed file. Positions of interest were identified as those with at least 1000 reads available with variance in nucleotide base composition of ≥ 5%.

2.10 Antibody-mediated receptor blockade

To limit the availability of receptor, Huh-7.5 cells seeded for infection were pre-incubated at 37°C with 50 µl DMEM supplemented with 3% FCS containing a serial dilution of either rabbit-SR-B1 serum or 2.131 (anti-CD81). One hour later, wells were washed twice with PBS and then challenged with virus for infection following the protocol outlined in section 2.7.

2.11 Lentiviral-mediated receptor overexpression

To generate lentiviral vectors, HEK293T cells were transfected with three plasmids: an HIV packaging construct (pCMV-dR8.91), VSV-G envelope plasmid (pMD2.G) and a dual promoter transfer plasmid encoding GFP in combination with SR-B1 or CD81

(pDual SR-B1 or CD81 plasmids are available from Addgene: https://www.addgene.org/Joe_Grove/). Supernatants containing viral vectors were collected at 48- and 72-hours post-transfection. At least 96 hours before an experiment, Huh-7.5 were transduced with lentivirus vectors diluted in complete medium and 24 hours prior to study the cells were seeded into a 96 well plate for infection, as described above (section 2.7).

2.12 Neutralisation assays

Huh-7.5 cells were seeded at 1.5 x 10^4 cells per well of a 96 well plate 24 hours prior to the experiment. On the following day, a volume of virus stock was incubated in triplicates with a dution series of anti-E2 antibody or sCD81 prior to infection. Virus-antibody or virus-sCD81-LEL mixtures were incubated for 1 hour at 37˚C and were added to Huh-7.5 cells and infection was allowed to proceed for 72 hours. To measure HCVcc replication, cells were fixed with 100% methanol and stained for viral NS5A protein. The percentage of infected cells was determined using the ImageJ Infection Counter plugin (369).

2.13 Fluorescence microscopy

To quantify infection assay plates were imaged using a Nikon Ti inverted microscope fitted with a motorised encoded stage for plate-reading. A 4 mm by 4 mm area of each well was acquired by image stitching using an ORCA Flash 4 sCMOS camera (Hamamatsu), with 405 nm and 647 nm fluorescence illumination provided by a PE4000 LED unit (CoolLED) through a multi-band excitation/emission filter cube (Semrock). To ensure optimal imaging, software-based autofocusing was performed prior to acquiring each well. The number of foci in each image was quantified manually using the counting tool in FIJI/ImageJ (374).

2.14 Generation of CD81 knock-out cell lines

HEK 293T^{CD81KO} cell lines were established by following the Invitrogen TrueGuide™ sgRNA CRISPRMAX™ transfection protocol. Briefly, 293T cells were first transfected with one of the following CD81 sgRNAs: CRISPR661076_CR, CRISPR661085_CR and CRISPR661093_CR (Thermo Fisher Scientific). Seventy-two hours later, the cells were then sorted on a FACSAria™ II instrument (BD Biosciences) to obtain CD81-/-

populations. Cells were then expanded for 48 hours before dilution for single cell cloning and expansion in a 96 well plate. Knock-out of CD81 was confirmed by flow cytometry and Western blot.

2.15 Production of sE2 *(Machaela Palor & Lenka Stejskal)*

Soluble E2 comprises residues 384-661 of the HCV genome, flanked by an N-terminal tissue plasminogen activator signal sequence and a C-terminal Twin- Strep-tag. HEK 293T^{CD81KO} cells (375) were transduced with lentivirus encoding sE2. Cell culture media, containing sE2, were harvested every 24 hours for up to 6 weeks. The harvested supernatants were frozen immediately at -80°C. High purity monomeric sE2 was generated by sequential affinity purification using StrepTactin-XT columns (IBA Lifesciences) and size-exclusion chromatography using the HiPrep™ 16/60 Sephacryl® S-200 HR gel filtration column (Cytiva). The concentration of the monomer fraction was then determined by Nanodrop (Thermo Fisher Scientific) using theoretical molecular weight and extinction coefficient.

2.16 Soluble E2 binding assay

CHO cells were first transduced to express human SR-B1 or CD81 following the the protocol outlined in section 2.10. Seventy-two hours later, the cells were harvested, washed and resuspended to single-cell populations in PBS. The cells were then preincubated in ‘traffic stop’ buffer, PBS + 1% bovine serum albumin (BSA) and 0.01% sodium azide; this component prevents receptor internalisation. All subsequent steps are performed in traffic stop buffer. Cells were pelleted and then resuspended in a serial dilution of sE2. Following an hours’ incubation at 37°C, cells were washed twice and incubated with 3 µg/ml StrepMab classic (for CHO-huSR-B1) or J6.36 (for CHO-huCD81) followed by an anti-mouse Alexxa Fluor 647 secondary. After a final wash, the cells were fixed in 1% formaldehyde and analysed by flow cytometry. To measure cell surface expression of human receptors post-transduction, cells were stained for SR-B1 or CD81 and signal was detected using an anti-rabbit or anti-mouse Alexxa Fluor 647 secondary, respectively.

2.17 Flow cytometry

Fluorescence signals were measured on either the LSR II or LSR Fortessa machines (Becton Dickinson) and data was analysed using FlowJo 10.6 software (FlowJo). The

lentiviral vectors, described above, also express GFP from a separate promoter; therefore, this GFP signal was used as an independent measure of transduction to identify positive cells during analysis.

2.18 Enzyme-linked immunosorbent assay (ELISA)

Purified Strep-II-tagged sE2 monomers (1.0 µg/mL diluted in TRIS buffered saline, TBS) was coated for 2 hours at room temperature on 96-well Strep-TactinXT coated microplates (IBA LifeSciences). Plates were washed with TBS twice before incubating with serially diluted mAbs and sCD81 (R&D systems) in casein blocking buffer (Thermo Fisher Scientific) for 90 min. After three washes with TBS, a 1:3000 dilution of HRP-labelled goat anti-human IgG in casein blocking buffer was added for 45 min. After washing the plates five times with TBS+0.05% Tween-20, plates were developed by adding develop solution (1% 3,3',5,5'-tetraethylbenzidine (Sigma-Aldrich), 0.01% H_2O_2, 100 mM sodium acetate, 100 mM citric acid) and the reaction was stopped after 3 min by adding 0.8 M H_2SO_4. Absorbance was measured at 450 nm.

2.19 Generation of HCV pseudoparticles

To generate HCVpp, HEK 293T or HEK 293T^{CD81KO} cells were co-transfected with three plasmids: an HIV (pCMV-dR8.91) or MLV (phCMV-5349) packaging construct, a luciferase reporter plasmid and an expression vector encoding the appropriate viral glycoprotein. For all experiments, a non-enveloped control (empty plasmid) was employed as a negative control. Supernatants containing HCVpp were collected at 48- and 72-hours post-transfection.

2.20 Entry Kinetics assay

Huh-7.5 cells were seeded at 1.5 x 10^4 cells per well of a 96 well plate 24 hours prior to experiment. HCVpp were preincubated with magnetic nanoparticles (ViroMag, OZ Biosciences) for 15 min. Media on Huh-7.5 cells was changed to infection medium with or without 3 µg/ml purified anti-CD81 at t = -30 min (Figure 4A). At t = -15 min, media was replaced with 50 µl magnetized HCVpp (plus anti-CD81 for t = -30 and -15 time points) and the plate was placed on a Super Magnetic Plate (OZ Biosciences) for 15 min at 37°C, per manufacturer's instructions. At t = 0, cells were washed twice, and from there on the synchronised infection chased with a saturating receptor blockade

by adding 3 μg/ml anti-CD81 mAb 2.131 at the indicated time points. Infection was assayed after 72 hours using the SteadyGlo reagent kit and a GloMax luminometer (Promega).

2.21 Cell-to-cell spread

Prior to the experiment, Huh-7.5 cells were electroporated with HCV RNA transcripts. Three days later, electroporated cells were trypsinized and mixed with target, naïve uninfected Huh-7.5 cells at 1:5 ratio prior to plating at 7.5 x 10^5 cells per well in a 12 well plate. Cells were maintained in infection medium containing 10 μg/ml pooled HCV^+ patient IgG to prevent cell-free spread. Cells were harvested and fixed with 1% formaldehyde every 24 hours post mix up to 96 hours. Once the experiment was complete, the cells were stained for viral NS5A followed by an anti-mouse Alexa Fluor 647 secondary to quantify spread by flow cytometry.

2.22 Soluble E2 limited proteolysis

Soluble E2 (0.2 mg/ml) were reacted with Endoproteinase GluC (New England Biosciences) at 1:50 (w/w) ratio in TBS buffer (50 mM Tris-HCl, 50 mM Glu-Glu) at 37 °C for up to 4 hours. Aliquots of proteolysis mixtures were quenched by laemli boil at specific intervals and the kinetics of digestion determined by non-reducing SDS-PAGE (4–20% acrylamide) followed by western blot. Each experiment was probed with both HVR-1 (J6.36) and AS412 (H77.39) targeting monoclonal antibodies.

2.23 Polyacrylamide gel electrophoresis

For Blue native PAGE gels (Chapter 5 only), 5 μg sE2 was mixed with PBS and 4x loading dye (a mix of 500 μl 20x MOPS Buffer (1M MOPS + 1M Tris, pH 7.7), 1000 μl 100% glycerol, 50 μl 5% Coomassie Brilliant Blue G-250, 600 μl milli-Q) and directly loaded onto a 4-12% Bis-Tris NuPAGE gel (Thermo Fisher Scientific). The gels were run for 1 hour at 200 V at 4°C using NativePAGE Running Buffer (Invitrogen). BN-PAGE gels were stained using the Colloidal Blue Staining Kit according to the manufacturer's instructions (Life Technologies). For SDS PAGE, 5 μg of sE2 was mixed with loading dye (25 mM Tris, 192 mM Glycine, 20% v/v glycerol, 4% m/v SDS, 0.1% v/v bromophenol blue in milli-Q water) and incubated at 95°C for 5 min prior to loading on a 4-12% Tris-Glycine gel (Invitrogen). For reducing SDS-PAGE,

dithiothreitol (DTT; 100 mM) was included in the loading dye and loaded on MiniPROTEAN 4-12% gels (BioRad) or a Novex 10-20% Tris-Glycine gel (Thermo Fisher Scientific). Gels were run in a buffer containing 25 mM Tris, 192 mM glycine and 0.5% SDS for 1 hour at 200 V. Coomassie blue staining of SDS-PAGE gels was performed using the PageBlue Protein Staining Solution (Thermo Fisher Scientific).

2.24 Western blotting

Run samples on SDS-PAGE gels were transferred onto a nitrocellulose membrane. The blots were blocked in PBS + 2% milk solution + 0.1% Tween-20 and then probed sequentially with an anti-E2followed by a goat anti-mouse secondary conjugated to horseradish peroxidase. Chemiluminescence signal was activated using the SuperSignal™ kit (ThermoFisher) and then measured on a Chemidoc MP machinery (BioRad).

2.25 Circular dichroism spectroscopy (*Lenka Stejskal*)

Circular dichroism experiments were performed using the B23 nitrogen-flushed Module B end-station spectrophotometer at B23 Synchrotron Radiation CD BeamLine located at Diamond Light Source. They were performed by the BeamLine lab manager as a mail-in service. Four scans of protein samples in 50 mM NaF and 20mM NaH2PO4 and Na2HPO4 pH 7.2 were acquired in the far-UV region (175 - 260 nm) in 1 nm increments using an integration time of 1 sec, 1 nm bandwidth and pathlength of 0.00146 cm, at 20°C. Results obtained were processed using CDApps v4.0 software. The scans were averaged, and spectra have been normalized using average amino acid molecular weight which was calculated for each sample. Spectra presented are difference spectra meaning the buffer baseline has been subtracted from the observed spectra and zeroed between 253 – 258 nm. Secondary structure deconvolution from CD spectra was carried out using the CDApps CONTINLL algorithm and SP29 reference data set referencing 29 soluble protein structures.

2.26 Nano differential scanning fluorimetry (*Lenka Stejskal*)

The melting temperature (Tm) of sE2 (1mg/ml) was calculated using the Prometheus NT.48 (Nanotemper) during heating in a linear thermal ramp (1°C, 20 – 90°C) with an excitation power of 30%. The fluorescence at emission wavelengths of 350 and

330 nm was used to determine changes in tyrosine and tryptophan environments. The Tm was calculated by fitting the Boltzmann sigmoidal curve to the first derivative of the fluorescence ratios (350/330 nm).

2.27 Mathematical modelling *(Chris Illingworth)*

We applied a mathematical model described in Kalemera et al (219) to the novel data generated by this study. Our model uses a series of differential equations to describe the processes via which HCV particles, having bound to the cell membrane, acquire CD81 and SR-B1 receptors. Viruses are modelled as uniformly having N_e E2 proteins available to bind cellular receptors. We consider an E2 protein as being either bound or unbound to CD81. If it is unbound to CD81 we consider whether it is bound or unbound to SR-B1; once E2 is bound to CD81 we are unconcerned about its binding to SR-B1. Thus, we represent the population as existing on a grid of points M_{ij}, indicating viruses that have i copies of E2 bound to CD81 and j copies of E2 bound to SR-B1 but not to CD81. All viruses begin at the point M_{00}, then progress through the grid (see Figure 5 in Kalemera et al) (219).

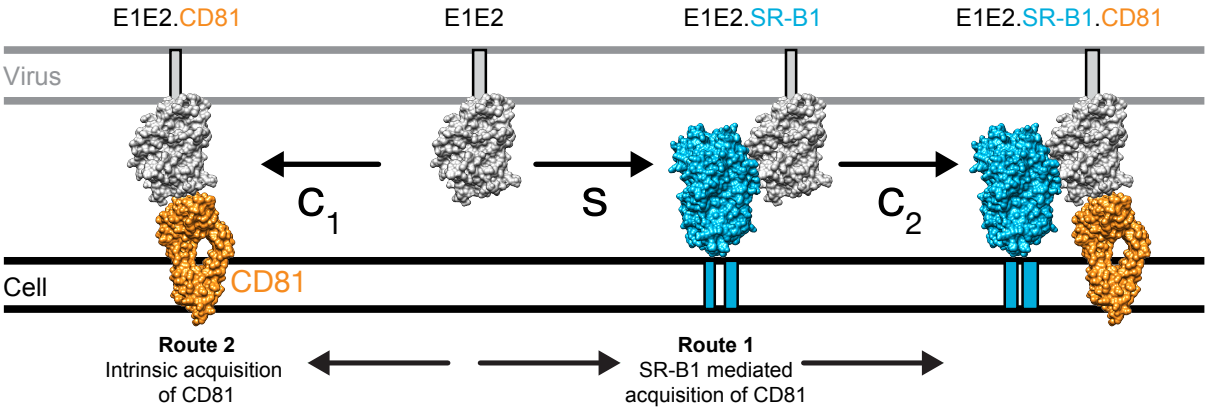

Figure 2.1 Mathematical modelling of HCV entry. E1E2-receptor interactions at the cell surface, as recreated in our model. To achieve entry E1E2 must acquire CD81, this can occur via two routes. Route 1 SR-B1 mediated: prior binding to SR-B1 (at rate s), primes E1E2 for interaction with CD81 (at rate c2). Route 2 intrinsic binding: E1E2 interact with CD81 without prior engagement of SR-B1 (at rate c1). Once sufficient molecules of CD81 have been acquired the virus particle proceeds along the entry pathway (including endocytosis and fusion) at rate e. Molecular cartoons are based on previously published structures and are drawn to scale.

At the point M_{ij}, viruses have N_e-i-j free E2. We suppose that they bind SR-B1 at some rate, s (Fig 2.1). Viruses bind CD81 via two specific processes. Firstly, viruses bind CD81 via an SR-B1 independent process at the rate c_1. SR-B1 engagement

provides a priming mechanism, which facilitates a second SR-B1-mediated acquisition of CD81, occurring at the rate c_2. Viruses which gain a pre-specified threshold number of CD81 receptors pass at some rate, e, into the down-stream process of viral entry. Viruses die at constant rate d, which is arbitrarily pre-specified; in our model all other processes occur at some rate relative to this value. Viruses gaining entry to the cell are modelled as being in the state E, while viruses which are dead are modelled as being in the state D.

Our model considers data from a number of states in which the number of CD81 and SR-B1 receptors has been altered (Fig 3.4 and 3.5). In a given system we model the proportion of CD81 receptors as pc, and the proportion of SR-B1 receptors as ps, where the value in unmodified cells is 1 in each case.

Following the above, we obtain the following equations for viral progress across the membrane:

$$\frac{dD}{dt} = d\sum_{ij} M_{ij}$$

$$\frac{dE}{dt} = e\sum_{j} M_{rj}$$

$$\frac{dM_{ij}}{dt} =$$

$$\frac{1}{N_e}\left[p_c\left(c_1\left(N_e-i-j+1\right)M_{i-1j}+c_2 j M_{i-1j+1}\right)+p_s s\left(N_e-i-j+1\right)M_{ij-1}\right]-$$

$$\frac{1}{N_e}\left[\left(p_c\left(c_1\left(N_e-i-j\right)M_{i-1j}+c_2 j\right)+p_s s\left(N_e-i-j\right)\right)M_{ij}\right]-dM_{ij}-eI_{ir}M_{ij}$$

where I_{ir}=1 if i=r and I_{ir}=0 if ir, and the system has the initial conditions D=0, E=0, M_{00}=1, and M_{ij}=0 for all i>0 and j>0, and the system is bounded by the constraints 0 i r and 0 j N_e.

Given a set of input parameters, a fourth-order Runge-Kutte scheme with adaptive step size was used to propagate the system until the sum of terms D+E was greater than 0.999, indicating that 99.9% of the simulated viruses had either

died or gained entry. The probability P that a single virus gains entry to a cell was then calculated as

$$P(p_c, p_s, c_1, c_2, s, e) = \frac{E}{D+E}$$

An optimisation procedure was run to fit the model to data from experiments. As in a previous publication, experiments modelling viral entry were performed in replicate. To estimate the values p_c and p_s, indicating the extent of available receptor, we used fluorescence microscopy measurements of receptor blockade/over-expression performed in parallel with the infection experiments, as previously described (219). These values were normalised to the range 0 to 1 in the case of receptor knockdown experiments, or above 1 in the case of overexpression experiments; 1 being the availability in unmodified cells.

We now consider data describing a level of receptor availability (p_c, p_s) and a number of observed foci of infection; using the index i we term the latter value o_i. Given a knowledge of the number of input particles and the number of cells observed in a well, this can be understood in terms of a probability of a given cell being infected by the virus. Observations were modelled as being distributed according to a double Poisson distribution with mean $_i$ and parameter

$$\log L = \log\left[\theta^{0.5} e^{-\theta\mu_i}\left(\frac{e^{-o_i} o_i^{o_i}}{o_i!}\right)\left(\frac{e\mu_i}{o_i}\right)^{\theta o_i} C\right]$$

where

$$\frac{1}{C} = 1 + \left(\frac{1-\theta}{12\theta\mu_i}\right)\left(1 + \frac{1}{\theta\mu_i}\right)$$

An estimate of the dispersion parameter was calculated by fitting a single value i to each set of values oi arising from the same level of receptor availability with no other constraint on the i. This parameter was then used in the likelihood function to fit values

i=niP (pc, ps, c1, c2, s, e), where ni is the number of cells observed in a well and P (pc, ps, c1,c2, s, e) is the probability of viral entry calculated from the differential equation model described above; parameters c1, c2, s, Ne, and e were optimised to give a maximum likelihood fit to the data.

2.28 Molecular dynamic simulations (*Lenka Stejskal*)

The complete model of the J6 E2 ectodomain was generated as previously described (330). For simulations of the mutant glycoprotein, the respective amino acid substitutions were modelled in using Modeller (376).

We performed MD simulations in explicit solvent using the Amber 16 GPU-based simulation engine (377). The model was solvated in a truncated octahedral box using OPC water molecules. The minimal distance between the model and the box boundary was set to 12 Å with box volume of 4.2×10^5 Å^3. Simulations were performed using the ff14SB force field on GPUs using the CUDA version of PMEMD in Amber 16 with periodic boundary conditions. CONECT records were created using the in-house MakeConnects.py script to preserve the disulphide bonds throughout the simulations. MolProbity software was used to generate physiologically relevant protonation states.

Minimisation and equilibration: The systems were minimised by 1000 steps of the steepest descent method followed by 9000 steps of the conjugate gradients method. Sequential 1ns relaxation steps were performed using the Lagevin thermostat to increase the temperature from 0 to 310 K, with initial velocities being sampled from the Boltzmann distribution. During these steps, pressure was kept constant using the Berendsen barostat. All atoms except for the modelled residues, hydrogen atoms and water molecules were restrained by a force of 100 kcal/mol/Å^2. The restraint force was eventually decreased to 10 kcal/mol/Å^2 during subsequent 1ns equilibration steps at 310 K.

A further minimisation step was included with 1000 steps of the steepest descent method followed by 9000 steps of the conjugate gradients method with all backbone atoms restrained by a force of 10 kcal/mol/Å^2. The systems were then subjected to four 1ns long equilibration steps at constant pressure with stepwise 10-fold reduction of restraint force from 10 to 0 kcal/mol/Å^2. All minimisation and equilibration stages were performed with a 1fs time step.

Production runs: An initial 1μs production run was simulated under constant volume and temperature using the Langevin thermostat. SHAKE was used in all but the minimisation steps; this, in combination with hydrogen mass repartitioning, permitted 4 ft time-steps during the production runs. Short-range cutoff distance for van der Waals interactions was set to 10 Å. The long-distance electrostatics were calculated using the Particle Mesh Ewald Method. To avoid the overflow of coordinates, iwrap was set to 1. Default values were used for other modelling parameters. To achieve independent repeat simulations, we performed steps to decorrelate the output from the equilibration process. Initial velocities were generated from the Boltzmann distribution using a random seed. The coordinates, but not velocities, from the final equilibration step were used as input for a short (40ns) production run. The coordinates, but not velocities, from this run were used for a second 4ns production run. This was followed by a 1 μs production run. This process was repeated for each independent simulation.

The MD trajectories were analysed using scripts available in cpptraj from Amber Tools 16. For RMSF/RMSD analyses, the average structure generated from the given trajectory was used as the reference structure. The analyses were performed using the backbone Cα, C and N atoms unless otherwise stated.

2.29 Molecular modelling

Molecular model visualisation was performed with UCSF Chimera (378).

2.30 Statistical analysis

All statistical analysis was performed in Prism 7.0 (GraphPad). In the majority of cases ordinary one-way ANOVA was performed using Dunnett's multiple comparison test, using WT virus as a control. Data were also analysed using paired or unpaired t-tests, spearman's correlation or curve fit F-test, and data were fitted using by linear regression, hyperbola of log (inhibitor) vs. response (four parameters) function or the sigmoidal curves where X is log(concentration) function. Please see figure legends for accompanying analyses.

3 Evolution of HCV to optimise virus entry is offset by increased sensitivity to antibodies

3.1 Introduction

Previous work has shown that cell-culture adaptation of HCV gives rise to variants that exhibit both increased infectious titres and altered sensitivity to neutralising antibodies compared to wildtype strains (248,379,380). These are often point-mutations that do not necessarily map to critical receptor binding epitopes or nAb epitopes. The mechanisms underpinning these changes are not understood but the changes in global nAb sensitivity point to conformational changes in E1E2 following culture-adaptation. Additionally, our previous work indicates that SR-B1 is dispensable for entry (see Fig 1.23) and that SR-B1 dependency exerts a fitness cost on the virus by making virus entry less efficient (219). Based on these observations, we hypothesise that HCV performs a balancing act between opposing selection pressures: the necessity to evade neutralising antibodies vs the benefits of efficient entry. We propose that any given HCV strain exists on a spectrum between neutralising antibody evasion and optimal entry and that the SR-B1 priming step helps the virus achieve this delicate balance.

The results presented in this chapter are largely the phenotypic analyses of HCV mutants that arose during a prior cell-culture adaptation experiment. Cell-culture adaptation has long been used in molecular virology to gain insights into the factors that underly efficient viral replication. E1E2 mutations present in the successful, fixated lineage were characterised for their impact on HCV infectivity, receptor dependency and antibody sensitivity.

The specific aims were to:

1. Determine the cell entry phenotype of HCV E1E2 polymorphisms following cell-culture adaptation.
2. Examine whether the polymorphisms affected E1E2 reactivity to activating stimuli.
3. Determine the antibody sensitivity of the E1E2 polymorphisms and establish whether antigenicity and entry phenotypes of HCV are linked.

3.2 HCV explores evolutionary pathways to optimise virus entry

We first established a continuous culture of J6/JFH-1 HCVcc in Huh-7.5 cells. J6/JFH-1 is a chimeric infectious clone composed of structural components (Core, E1, and E2) and p7 from the J6 strain and non-structural components from the JFH-1 strain, the latter permitting efficient propagation in hepatoma cell lines. Culture supernatant from the adaptation was routinely harvested and viral adaptation to Huh-7.5 cells was monitored by next-generation sequencing (NGS). By day 42, NGS analyses revealed the accumulation of various polymorphisms throughout the genome. The viral entry proteins, E1E2, were particularly enriched for non-synonymous substitutions when compared to other coding regions with comparable length (Fig 3.1 A), suggesting optimisation of virus entry. Notably, some substitutions occurred at highly conserved sites (e.g., G406S, S449P) (Fig S1 in appendix), indicating in-vitro replication does not recreate the evolutionary constraints present during authentic patient infection. This is likely a reflection of the complete absence of an adaptive immune response during culture adaptation.

Over a dozen mutations were present at > 5% frequency (Fig S1) within E1E2 by day 42, including I438V in E2 and I262L in E1 (Fig 3.1 B). The I438V mutant later reached fixation and established a lineage with additional A524T (E2) and M356V (E1) mutations emerging sequentially, with the former rapidly achieving fixation. Interestingly, establishment of the I438V lineage was associated with the loss of other variants from the population (see I262L in Fig 3.1 B), suggesting the successful lineage possessed a ‘fitness’ advantage.

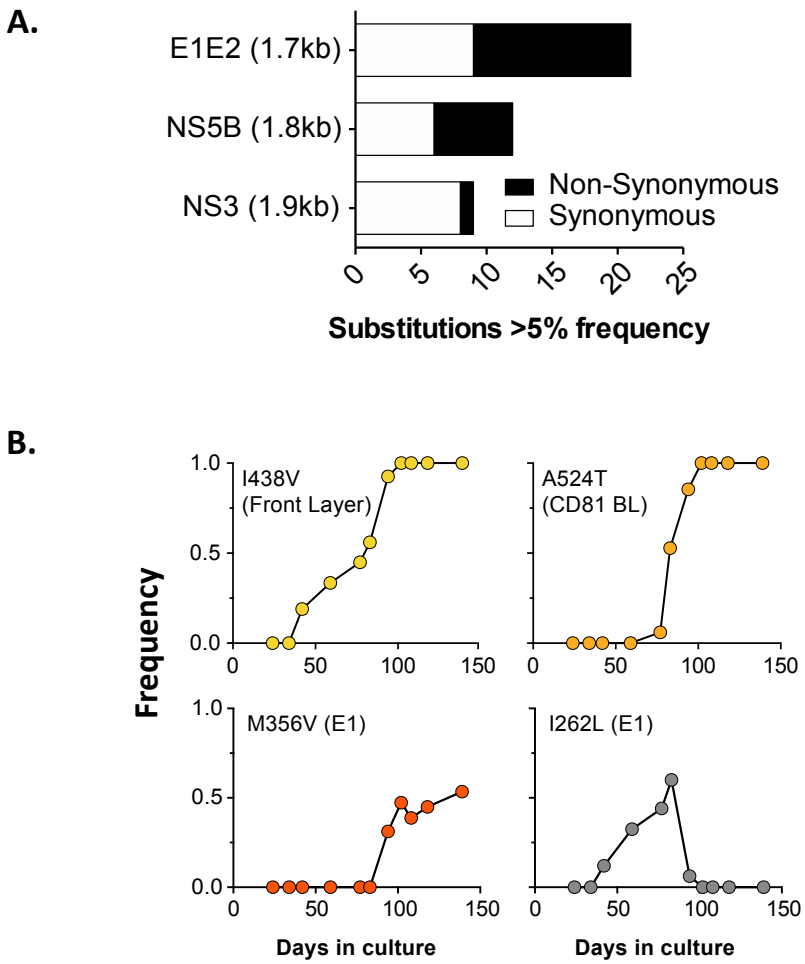

Figure 3.1. HCV accumulates mutations in E1E2 during culture adaptation. J6/JFH-1 HCVcc was continuously propagated in Huh-7.5 cells for 20 weeks with viral evolution monitored by NGS. (**A**) The proportion of synonymous/silent (white) and non-synonymous (black) substitutions present at > 5% frequency in the population, in three coding regions of comparable length: E1E2 (glycoproteins), NS5B (RNA polymerase and NS3 (protease). (**B**) The frequency of example mutations throughout the culture experiment. By day 100, all viruses possessed the I438V A524T E2 mutations, ~50% had an additional mutation in E1 (M356V), whilst a previously prevalent mutation (I262L) had been lost from the population. Data in A and B generated by Joe Grove.

We then introduced the mutations observed in the I438V lineage into the WT backbone by reverse genetics. To assess the effect that the accumulation of mutations in the successful lineage has on viral infectivity, we compared the infectivity of the three clones to WT. We quantified infectious titres by manually counting foci of infected Huh-7.5 cells and obtained values were corrected for differences in the content of genomic HCV RNA present in the viral harvests. We found that the addition of each mutation increased infectivity in a stepwise manner with the I438V and I438V A524T mutant being two- and three-fold more infectious than WT virus, respectively (Fig 3.2).

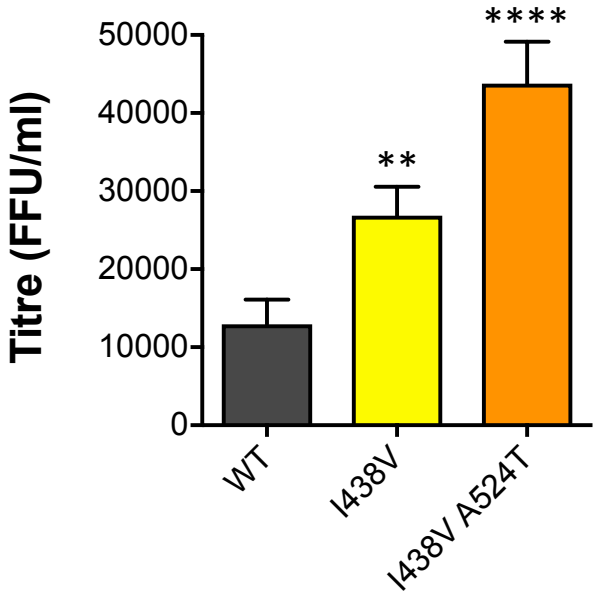

Figure 3.2. E1E2 mutations arising from cell-culture adaptation enhance HCV infectivity. The infectious titres of WT, I438V and I438V A524T HCVcc, expressed as foci forming units per ml, values were normalised for in input particle numbers (RNA genomes). Error bars indicate the standard error of the mean (SEM), asterisks denote statistical significance, ANOVA (GraphPad Prism).

3.3 Culture-adapted HCV is less dependent on SR-B1 for entry

To investigate whether the adaptive variants exhibit altered receptor usage during cell entry, we infected Huh-7 cells CRISPR/Cas9-engineered to not express the critical HCV entry factors (CD81, SR-B1, CLDN1 and OCLN). Although frameshift of the target genes and deficiencies of protein expressions in the KO cells were previously confirmed by the Matsuura lab (217), we also reconfirmed ablation by western blot (Fig 3.3 A). Infection was quantified relative to that observed in the parental Huh-7 cell line (Fig 3.3 B). WT and mutant viruses were equally dependent on CD81, CLDN1 and OCLN as their deletion abrogated entry of all HCV strains tested. SR-B1 dependency, however, decreased in mutant viruses in a manner that mirrored virus titre, as evidenced by the stepwise increase in infection of SR-B1 KO cells (Fig 3.2 B, SR-B1 KO lane).

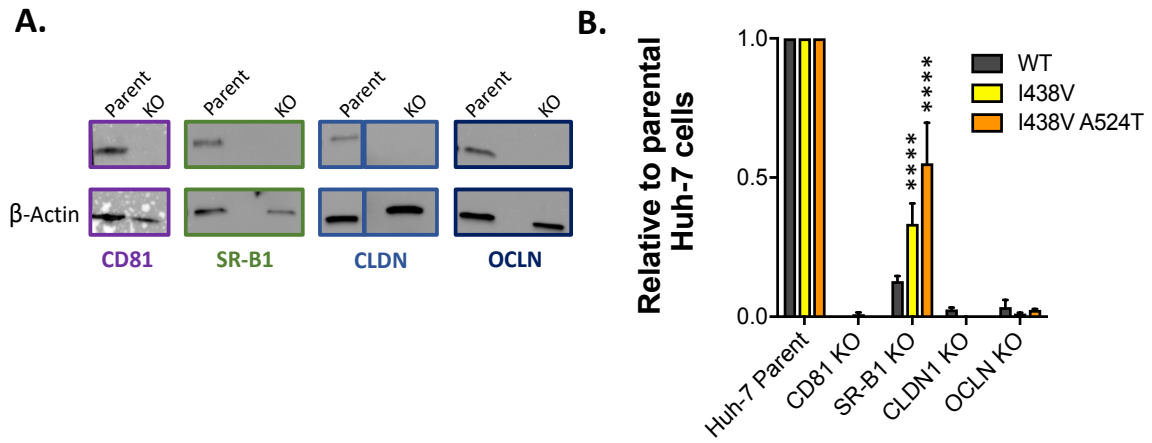

Figure 3.3. HCV evolves to increase infectivity through altered receptor dependency. (A) Entry factor knockout in CRISPR-engineered cells was reconfirmed by Western blot analysis **(B)** WT and mutant HCV infection of parental Huh-7 cells and those CRISPR/Cas9 engineered to knock out the stated HCV entry factor. To aid direct comparison of each mutant, infection values have been expressed relative to that observed in parental Huh-7 cells**.** Error bars indicate the standard error of the mean (SEM), asterisks denote statistical significance, ANOVA (GraphPad Prism). Data in subfigure A was generated by Lucas Walker.

We found that the third mutation in the lineage (M356V, in E1) conferred a further increase in infectivity (Fig 3.4 A), but no further reduction in SR-B1 dependency (Fig 3.4 B). We next investigated the relative contribution of each mutation to the reduced SR-B1 dependency phenotype of the lineage. To do this, we performed reverse genetics to generate M356V and A524T single mutant clones and determined their infectious titres and their ability to infect receptor KO Huh-7 cells. The titres and infection of SR-B1 knock-out cells by M356V and A524T single mutants was

comparable to WT (Fig 3.4 C & D). This finding indicates that there is a hierarchical interdependency between the mutations observed in this lineage, seeing as the M356V and A524T substitutions need to be in the context of the preliminary I438V mutation to contribute to SR-B1 independency and increased infectivity. Thus, the double E2 mutations (I438V A524) were necessary and sufficient to confer altered receptor dependency, therefore subsequent investigations were focused on this mutant. Overall, these data indicate that cell-culture adaptation reduces the requirement for SR-B1 during HCV entry.

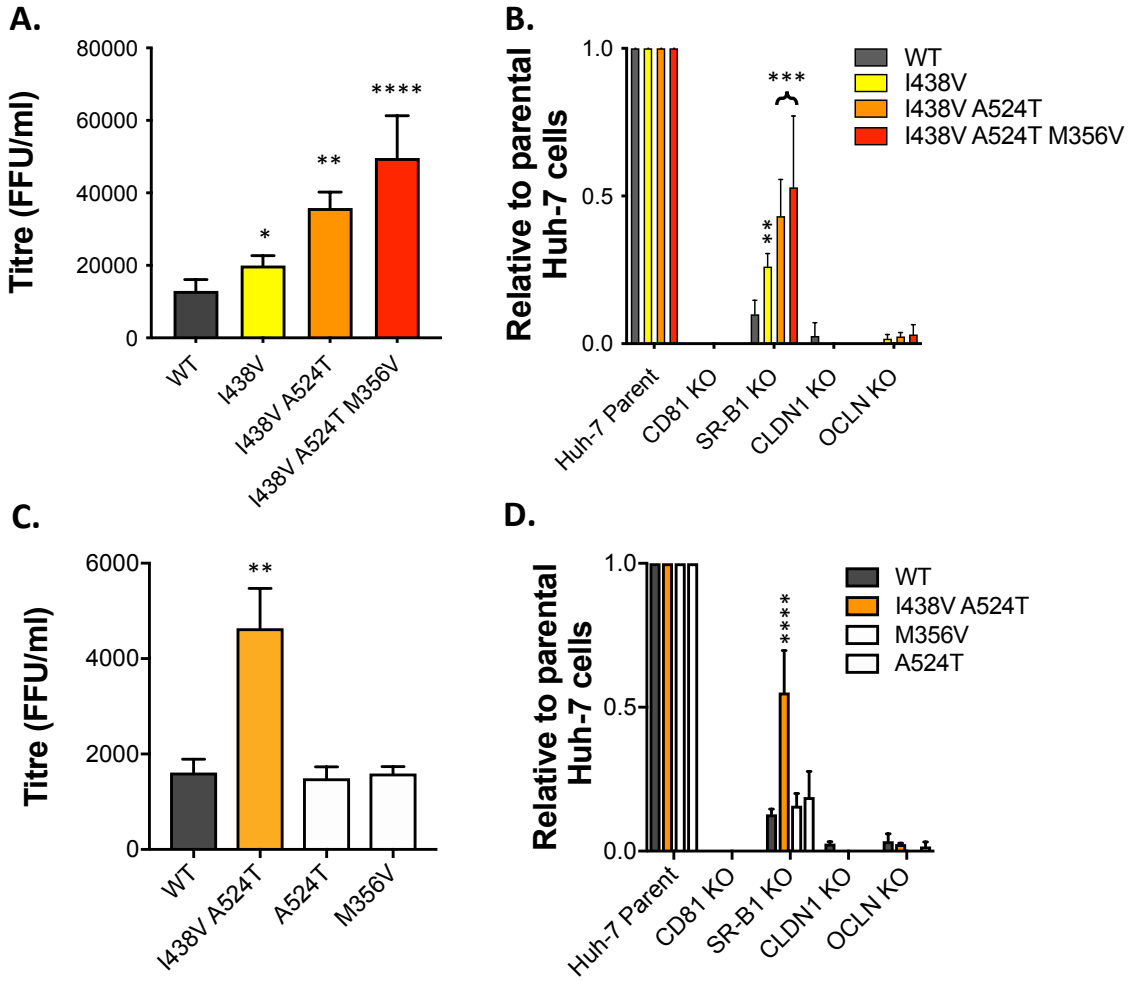

Figure 3.4. HCV evolves to enhance infectivity through altered receptor dependency. (**A**) The infectivity of WT, I438V, I438V A524T and I438V A524T M356V HCVcc, expressed as foci forming units per ml, values were normalised for in input particle numbers (RNA genomes). (**B**) WT and mutant HCV infection of parental Huh-7 cells and those CRISPR/Cas9 engineered to knock out the stated HCV entry factor. (**C**) The infectivity of WT, I438V A524T, A524T and M356V HCVcc, expressed as foci forming units per ml. (**D**) WT, I438V A524T, A524T and M356V infection of parental Huh-7 cells and those CRISPR/Cas9 engineered to knock out the stated HCV entry factor**.** In all cases, error bars indicate the standard error of the mean (SEM), asterisks denote statistical significance, ANOVA (GraphPad Prism).

3.4 Characterising HCV receptor dependency by blockade

So far, only SR-B1 and CD81 have been reported to interact directly with the HCV entry machinery, via E2 (211,381). The precise molecular basis of E2-receptor interactions are yet to be defined at the structural level. Nonetheless, mutational and antibody blocking experiments have demonstrated that SR-B1 binding occurs via the N-terminal HVR-1 (Fig 1.16 B) whilst the CD81 binding site is thought to be composed of three discontinuous regions: antigenic site 412 (AS412), the front layer, and the CD81 binding loop, (Fig 1.16 B) (211,293). Our previous work, and others', suggest that SR-B1 is the initial receptor for HCV and is likely to prime subsequent stages of entry (including interaction with CD81) via an unknown mechanism (route one in Fig 1.23) (219,222,240,346).

We evaluated the relationship of WT and I438V A524T HCV with SR-B1 and CD81 using a variety of techniques. First, we performed receptor blockade where Huh-7.5 cells were preincubated with antibodies targeting SR-B1 or CD81 which interfere with E2-SR-B1 and E2-CD81 interactions, respectively, thereby blocking HCV infection (382,383). Antibody treated cells were then challenged with WT or I438V A524T HCV and infectivity was determined 48 hours post-infection. A parallel plate was set up to quantify antibody binding by fluorescence microscopy allowing us to infer the amount of receptor available for HCV entry during virus challenge (Fig 3.5 A-D). Serial dilutions of each antibody revealed (near) saturation at high concentrations suggesting complete receptor blockade, i.e. no receptors were available for entry as they are occupied by antibodies (Fig 3.5 C & D). Absolute blockade of CD81 equally negated infection of both viruses (Fig 3.5 F), whereas the I438V A524T mutant was largely resistant to inhibition by anti-SR-B1 (Fig 3.5 E). The CD81 blockade results corroborate observations in the receptor knock-out studies (Fig 3.3 B & 3.4 B), and other studies showing CD81 to be indispensable for HCV entry (223,225,283).

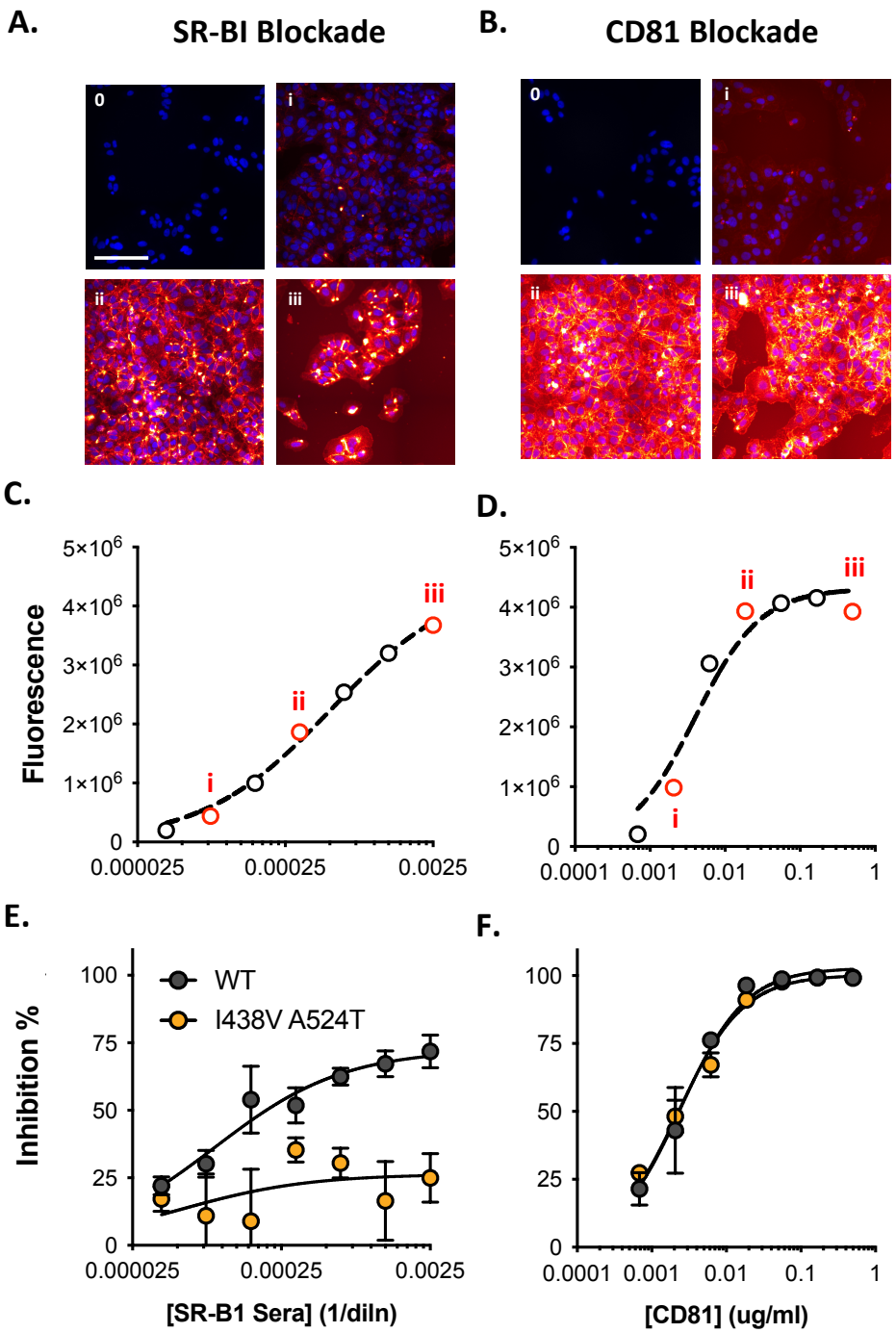

Figure 3.5. I438V HCV is resistant to antibody mediated SR-B1 blockade. Huh-7.5 cells were pre-treated with anti-SR-B1 serum or an anti-CD81 mAb to limit receptor availability prior to infection. Example fluorescent micrographs of (**A**) SR-B1 and (**B**) CD81 blockaded cells, the images are representative of the annotated data points in **C** and **D**. Scale bar = 50 µm. Binding of (**C**) anti-SR-B1 and (**D**) anti-CD81 to receptors was quantified using fluorescence microscopy (measured by arbitrary units), and receptor saturation was achieved at high antibody concentrations. Data points represent the mean of three technical replicates. Infection by WT and I438V A524T HCVcc of (**E**) SR-B1 or (**F**) CD81 blockaded is expressed as % inhibition relative to infection of untreated cells. Data points represent the mean of three independent experiments. For all curves, the data was fitted with a hyperbola function and the curves compared by statistical testing to confirm significance difference (F-test, GraphPad Prism), error bars indicate standard error of the mean.

3.5 Characterising HCV receptor dependency by overexpression

We next investigated the impact of SR-B1 or CD81 overexpression on the entry of WT and I438V A524T HCV. We transduced Huh-7.5 cells with lentiviral vectors to introduce SR-B1 or CD81. These cells were then challenged with virus following the protocol outlined above. Again, a parallel plate was set up to evaluate the receptor availability at the point of virus challenge by fluorescence microscopy (Fig 3.6 A & B). Up to three times greater cell surface expression of both SR-B1 and CD81 was achieved at the point of infection (Fig 3.6 C & D). WT virus exhibited a strong response to the increased availability of SR-B1 and CD81, reaching a 3-4 fold enhancement relative to untreated cells (Fig 3.6 E & F, grey bars). In contrast, the I438V A524T virus was less responsive to increased CD81 levels, although it did exhibit a dose-response to increasing CD81 levels (Fig 3.6 F). The infectivity of the I438V A524T mutant was even less affected by SR-B1 overexpression. Taken together, the blockade and over-expression data indicate that HCV, in cell-culture, will evolve to become less dependent on SR-B1 for entry, whereas CD81 remains critical for the process.

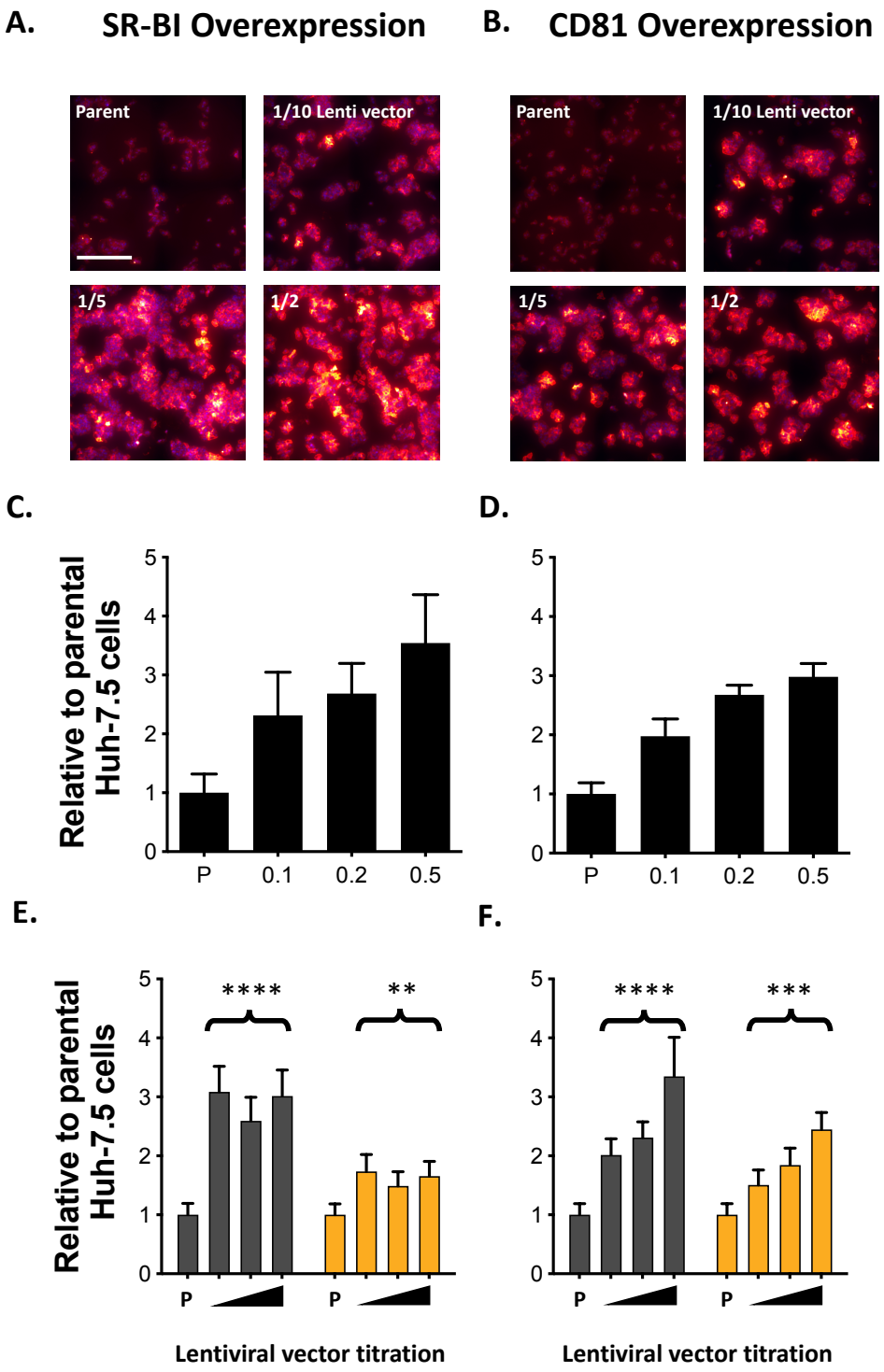

Figure 3.6. WT is hyperresponsive receptor overexpression. Huh-7.5 cells were transduced with a serial dilution of lentiviral vectors encoding SR-B1 or CD81 to increase receptor availability, prior to infection. Example fluorescent micrographs of (**A**) SR-B1 and (**B**) CD81 overexpressing cells. Scale bar = 50 μm. (**C**) SR-B1 and (**D**) CD81 overexpression was quantified using fluorescence microscopy. Bars represent mean values of three technical replicates and error bars indicate the standard error of the mean. Infection of (**E**) SR-B1 and (**F**) CD81 overexpressing cells by WT and I438V A524T HCVcc is expressed relative to infection of parental cells (P). Example data from one representative transduction is shown. Error bars indicate standard error of the mean, asterisks denote statistical significance ANOVA (GraphPad Prism).

3.6 Characterising HCV receptor dependency using soluble E2

To investigate the potential mechanism for the changes in SR-B1 dependent entry between WT and I438V A524T, we generated corresponding soluble forms of their E2 glycoproteins (sE2) and measured their binding to SR-B1 and CD81. Chinese hamster ovary (CHO) cells do not bind HCV sE2, however, binding can be conferred by the introduction of exogenous human SR-B1 or CD81. Thus, CHO cells were transduced with a lentiviral vector encoding one of the receptors, and GFP from a separate promoter (Fig 3.7 A). Antibody staining revealed high levels of receptor expression in GFP^{+ve} cells (Fig 3.7 B). Near saturation of binding was achieved at high concentrations of anti-receptor antibody (Fig 3.7 C). In parallel, transduced CHO cells were also incubated with a dilution of WT or I438V A524T sE2. Bound glycoprotein could then be measured by flow cytometry using an Alexa Fluor 647 conjugated antibody (see gating strategy, Fig 3.7 A). We found I438V A524T bound CHO cells expressing human SR-B1 at half the levels observed for WT sE2 (Fig 3.7 D & E). However, this observation was reversed in CHO cells expressing CD81, here we observed I438V A524T sE2 binding at >2 fold the levels of WT sE2. These data are consistent with the reduced dependency SR-B1 for I438V A524T entry (Fig 3.3 B), and with previous studies that found E1E2 in other HCV genotypes show enhanced CD81 binding after cell-culture adaptation (379). Notably, the reduction in SR-B1 binding by I438V A524T sE2 would suggest modulation of the SR-B1 binding site even though neither mutated resides maps to HVR-1.

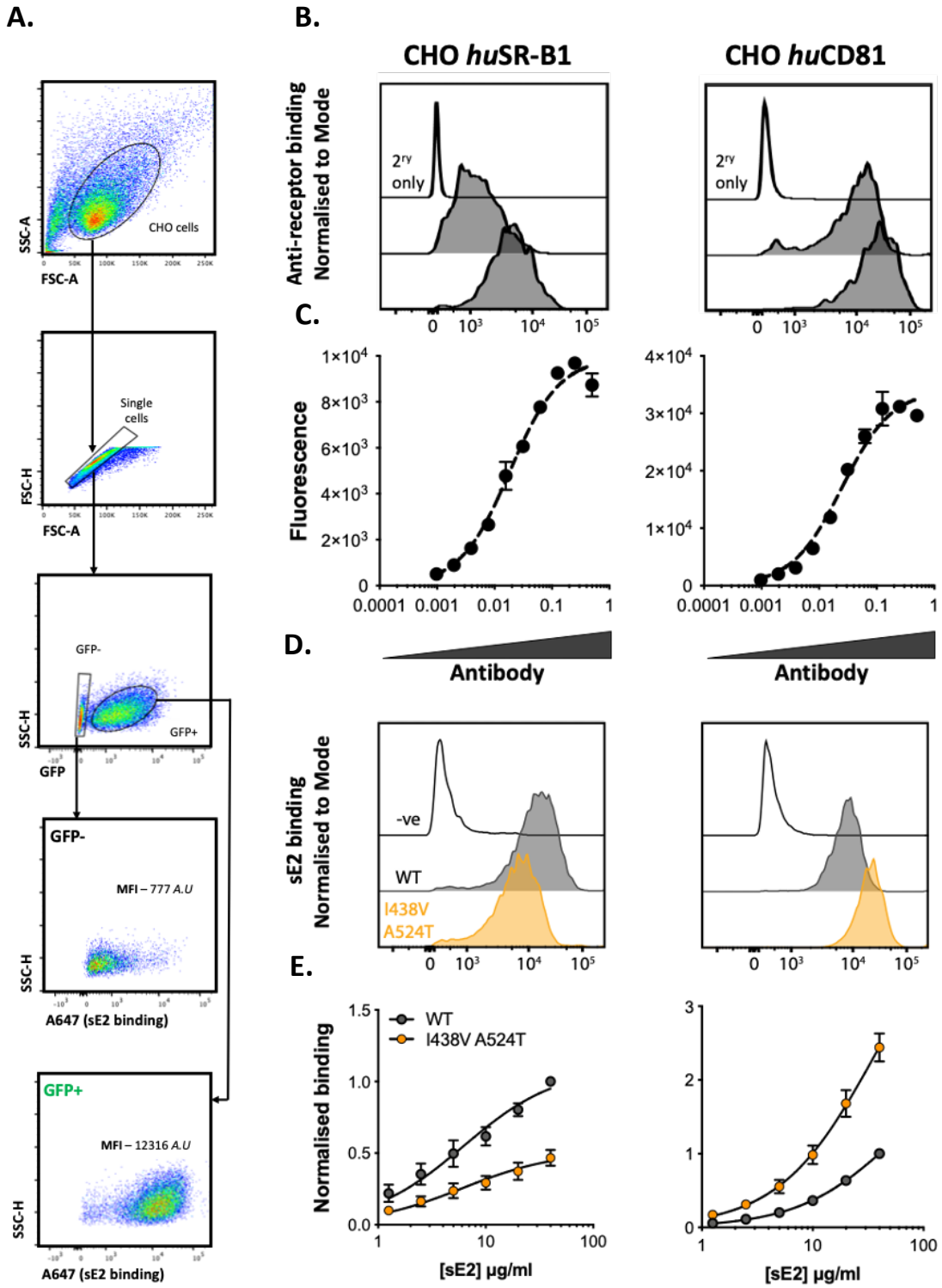

Figure 3.7. sE2 binding to CHO cells expressing human HCV receptors. CHO cells were transduced with lentiviral vectors expressing human SR-B1 or CD81 and then used in an sE2 binding assay. (**A**) Gating strategy to quantify sE2 or antibody binding to exogenously expressed human HCV receptors. Mean fluorescence intensity (MFI) was background corrected using MFI values from untransduced GFP^{-ve} cells, (i.e., bottom panel minus fourth panel MFI values). (**B**) Representative flow cytometry histograms of anti-SRB1 (left panel) or anti-CD81 (right panel) mAbs binding HCV receptor transduced CHO cells. (**C**) Transduced CHO cells were incubated with a serial dilution of anti-receptor antibody. Antibody binding was quantified by flow cytometry, high concentrations of antibody saturated available receptor. Continued on next page.

Figure 3.7 legend continued. Data from one representative experiment is shown, data points represent the mean of two technical replicates and the error bars indicate the standard error of the mean. (**D**) Representative flow cytometry histograms of 40 µg/ml WT or I438V A524T sE2 binding to CHO cells expressing SR-B1 (left panel) or CD81 (right panel). (**E**) Transduced CHO cells were incubated with a serial dilution of sE2. Data is normalised to 40 µg/ml WT sE2 binding to transduced CHO cells. Data are representative of the mean of three experiments and the error bars indicate the standard error of the mean. Data were fitted with hyperbola function and the curves compared by statistical testing to confirm significant difference (F-test, GraphPad Prism).

3.7 Inactivation of HCVcc particles at physiological temperature

As viral entry proteins are spring-loaded conformational machines, they are intrinsically unstable and tend to undergo spontaneous inactivation under certain environmental conditions including physiological temperature (311,324). Therefore, we compared the intrinsic stability of WT and I438V A524T particles at 37°C. We found that the mutant virus was > 3-fold less stable than WT virus (by comparison of half-life) (Fig 3.8), suggesting the I438V A524T mutations increase the propensity of HCV E1E2 to undergo spontaneous inactivation.

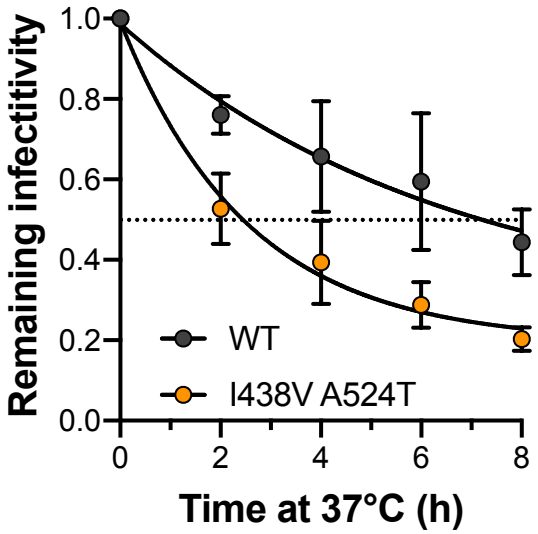

Figure 3.8. I438V A524T HCVcc is thermally unstable. WT and I438V A524T HCVcc were incubated for 0-8 hours at 37°C before infection of Huh-7.5 cells. Infectivity is expressed relative to that of the t=0 time point. Data points represent the mean of two independent experiments, data was fitted using an exponential decay function and the curves were determined to be statistically significant (F-test, GraphPad Prism), error bars indicate standard error of the mean.

3.8 Mathematical modelling of HCV entry

We recently developed a mathematical model to explore the mechanisms of HCV entry in collaboration with our colleagues in the Illingworth lab (219). As previously mentioned (see section 1.8), this work supports the notion that the early, post-attachment events of HCV entry can proceed via two routes. In route one, E1E2 acquires CD81 by first engaging SR-B1 which primes it for CD81 interactions. In the second route, E1E2 can intrinsically acquire CD81 without the need for prior SR-B1 engagement (Fig 3.9 A). The latter pathway accounts for residual infection of WT virus of SR-B1 KO cells (Fig 3.3 B). The Illingworth lab integrated the measurements of receptor blockade and overexpression and particle stability (Figs 3.5, 3.6 & 3.8) into the theoretical model, allowing us to compare the mathematical characteristics of WT and I438V A524T HCV. This analysis predicts that the I438V A524T mutant exists in a hyperreactive state, where its acquisition of CD81 is enhanced over WT, irrespective of the route of acquisition (parameter c_1 or c_2). SR-B1 mediated CD81 acquisition of the mutant is predicted to be particularly enhanced (Fig 3.9 B, parameter c_2), being ~1000 more efficient than WT. This may account for the mutant's ability to tolerate reductions in SR-B1 availability (Fig 3.5 E). Moreover, downstream events encompassing basolateral translocation, endocytosis and fusion, were predicted to occur at six times the rate of WT (Fig 3.8 B, parameter e).

The model also allows for exploration of HCV virion-CD81 interactions. To this end, fitting of WT and mutant data suggests the acquisition of just two CD81 molecules is sufficient to support an HCV particle through the entry programme (Fig 3.9 C). Lastly, we made estimations of WT and I438V A524T entry under varying availabilities of SR-B1 and CD81. As, expected the mutant exhibited increased entry efficiency over a greater range of receptor densities (Fig 3.9 D).

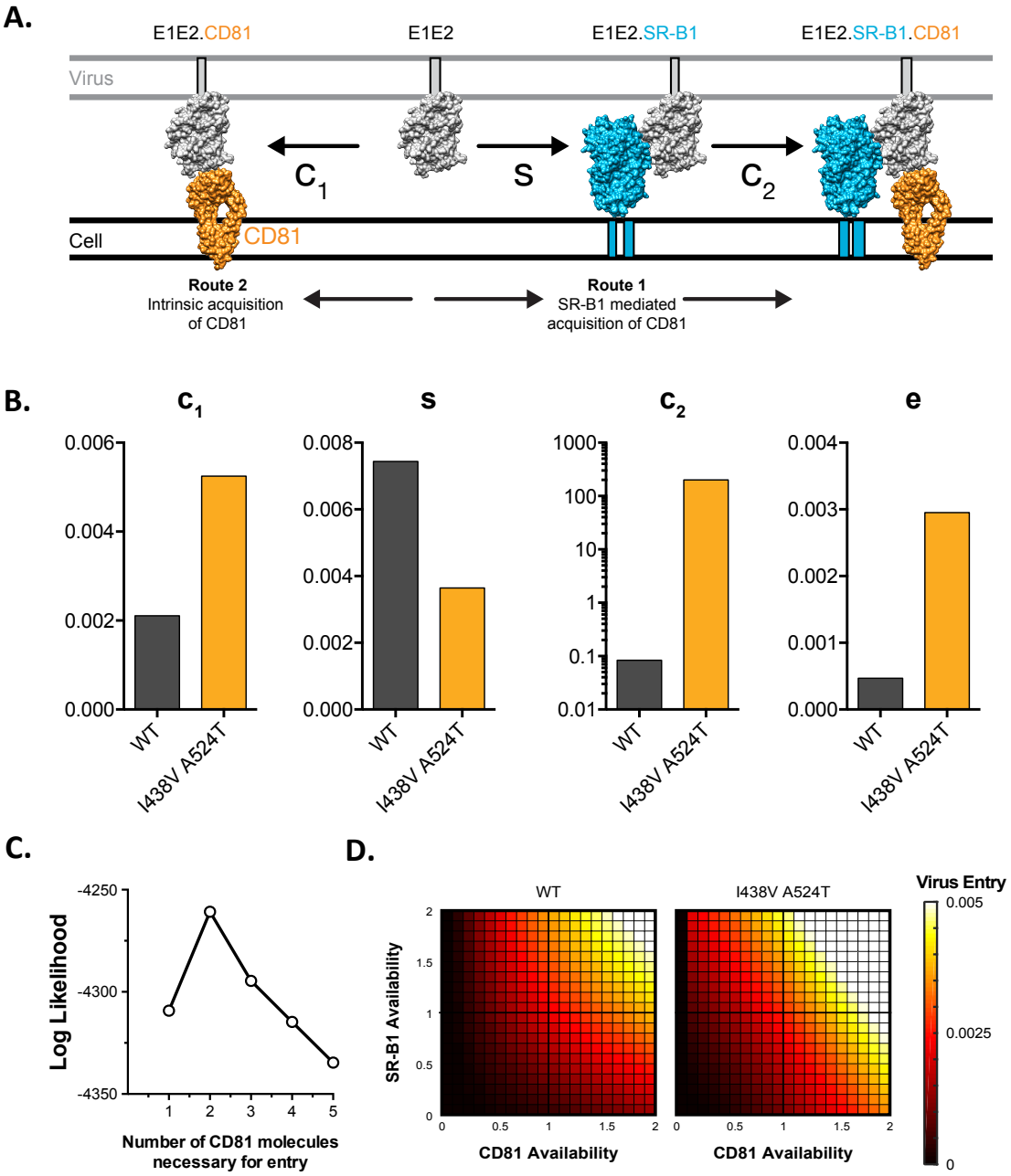

Figure 3.9. Mathematical modelling predicts I438V A524T HCV is hyperreactive. We previously developed a mathematical model to explore HCV receptor engagement and entry. (**A**) E1E2-receptor interactions at the cell surface, as recreated in our model. To achieve entry E1E2 must acquire CD81, this can occur via two routes. Route 1 SR-B1 mediated: prior binding to SR-B1 (at rate s), primes E1E2 for interaction with CD81 (at rate c2). Route 2 intrinsic binding: E1E2 interact with CD81 without prior engagement of SR-B1 (at rate c1). Once sufficient molecules of CD81 have been acquired the virus particle proceeds along the entry pathway (including endocytosis and fusion) at rate e. Molecular cartoons are based on previously published structures and are drawn to scale. (**B**) Receptor dependency data from WT and mutant HCVcc (Fig 3.4-3.6) was integrated into the mathematical model, as previously described, allowing estimation of the parameters defined above. Plots display WT and I438V A524T values for each rate constant. Continued on next page.

Figure 3.9 legend continued. (**C**) The model was used to explore the stoichiometry of CD81 engagement during HCV entry; the plot displays likelihood values for 1-5 molecules of CD81. Peak likelihood occurs at 2 molecules. (**D**) Mathematical modelling was used to explore the entry characteristics of WT and mutant HCVcc. The heat maps display the predicted probability of virus entry (as denoted in the key), for any given virus particle, upon varying availability of SR-B1 or CD81. Please note this data was generated and analysed by Chris Illingworth.

3.9 The entry kinetics of HCV

We employed the mathematical model to make predictions regarding the entry kinetics of WT and I438V A524T virus. The model predicted I438V A524T virus to have faster entry kinetics since the mutant exhibited greater entry efficiency over a wider range of receptor density (Fig 3.9 D, above). Specifically, the model predicted I438V A524T HCV enters cells >3 fold faster than WT (Fig 3.10 A).

Next, we sought to verify the prediction from the modelling with cell-culture experimentation. To appropriately measure single round infection kinetics, we made use of the HCVpp system. Here, biologically active HCV E1E2 glycoprotein complexes are presented on the surface of HIV-1 based reporter lentiviruses. Also, as viruses in suspension behave as colloidal matter, each particle's approach to the cell surface in solution is affected by diffusion rate, incubation time and mean distance to the cells (384–386). This results in asynchronous attachment and thus asynchronous initiation of infection. To overcome this, we appropriated an established experiment from HIV research and performed magnetoinfections (387). We preincubated HCVpp with magnetic nanoparticles for 15 min at room temperature before adding this mixture onto Huh-7.5 cells (Fig 3.10 B). We then applied a magnetic field by positioning a permanent magnet under the culture plate. After 15 min, the magnetic field was removed, the cells washed twice, and infection was allowed to proceed and an anti-CD81 antibody was added at regular intervals.

Following luciferase quantification, we found that mutant virus does indeed enter cells faster than WT. The experimentally determined values indicated the mutant virus completed entry ~3.6x the rate of WT ($T_{1/2}$, WT = 3.65 h, I438V A524T = 1.01 h) (Fig 3.10 C), which is in agreement with the estimate from the model. Thus, the experimental data as well as confirming I438V A524T as hyperreactive corroborates our modelling approach. Moreover, these data suggest that dependence on SR-B1 for HCV entry is a rate-limiting step in the HCV entry process.

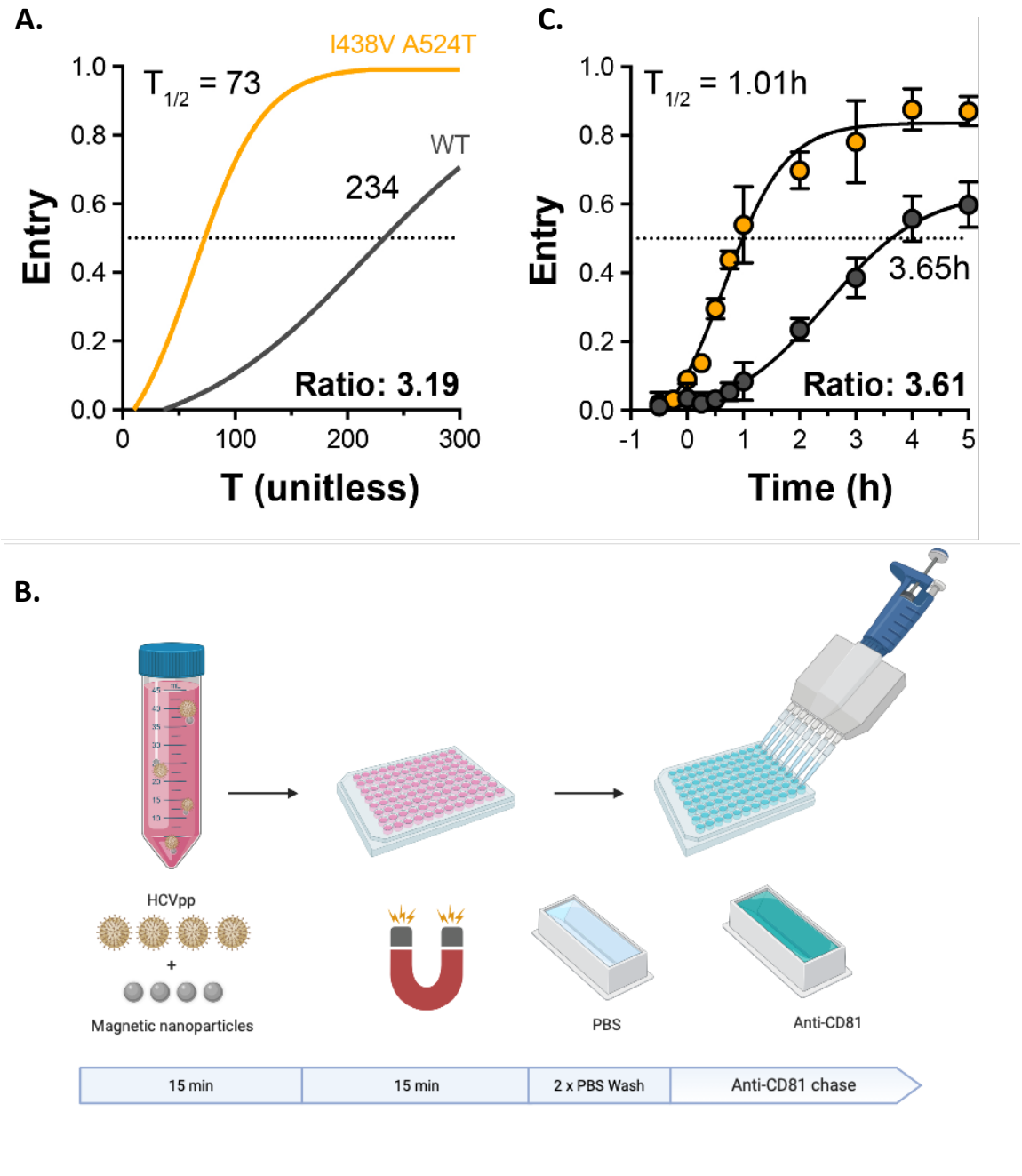

Figure 3.10. Entry optimisation results in faster HCV entry. (**A**) Kinetics of WT and mutant HCVcc entry, as predicted by mathematical modelling. The data is normalised to maximum entry. T represents uncalibrated time and, therefore, cannot be converted to real time (i.e., minutes and hours), but relative differences can be estimated. Data in subfigure was generated by Chris Illingworth. (**B**) Schematic strategy for achieving synchronous infection of Huh-7.5 cell using HCVpp. Diagram produced in BioRender. (**C**) Kinetics of WT and mutant HCV entry were experimentally measured by synchronised infection of Huh-7.5 cells by HCVpp, followed by a chase with a saturating inhibitory concentration of anti-CD81. Data points represent the mean of three independent experiments. The data was fitted with a sigmoid function, error bars indicate standard error of the mean.

3.10 The cell-to-cell spread kinetics of HCV

Seeing as I438V A524T HCVpp displayed faster entry kinetics we postulated it disseminates through confluent cell-culture faster than WT virus. To investigate this, we first electroporated Huh-7.5 cells with RNA of either virus, then when infection levels surpassed 90%, these cells were adoptively transferred into naïve uninfected cells to achieve 5% infection. To prevent cell-free spread, the cells were maintained in high concentrations of pooled antibodies isolated from the sera of two HCV$^+$ patients. At 24-hour intervals after mixing of donor and naïve cells, infection plates had their cells harvested and stained with anti-HCV NS5A to assess cell-to-cell spread by flow cytometry. In keeping with the kinetics data, hyperreactive I438V A524T exhibited greater cell spread than the WT virus from 48 hours onward (Fig 3.11 A & B). This data demonstrates that cell-culture adaptation improves the entry kinetics of HCV and consequently improves its ability to disseminate. Furthermore, these observations also reveal a potential mechanism by which the I438V lineage reached fixation and replaced WT virus by the latter stages of the adaptation experiment (Fig 3.1 B).

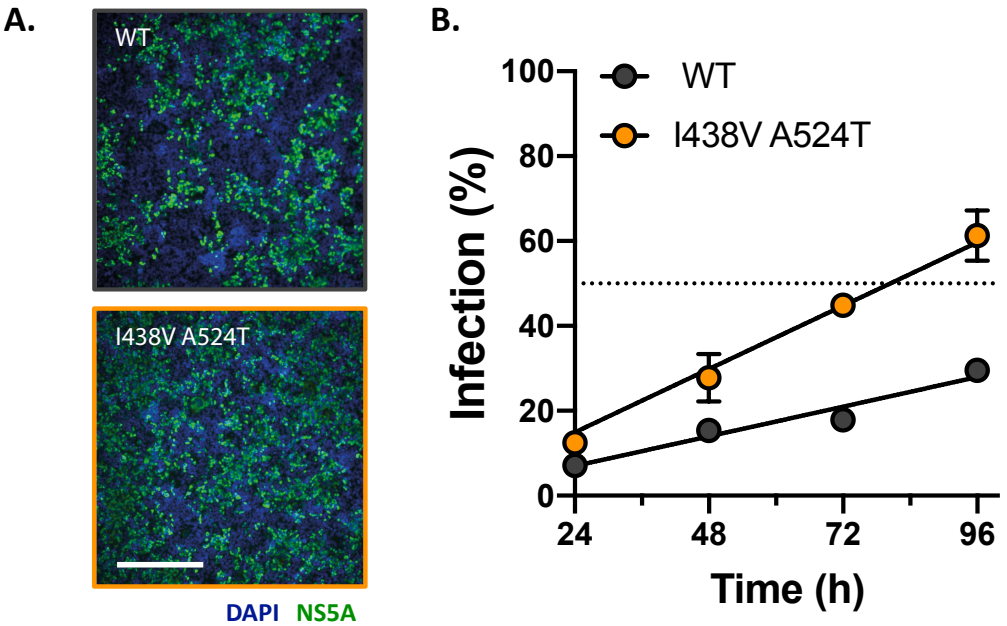

Figure 3.11. Entry optimised HCV spreads faster in cell culture. Previously infected cells were adoptively transferred into naïve uninfected cells so as to achieve 5% infected cells and cell-to-cell spread monitored by flow cytometry and fluorescence microscopy. (**A**) Example micrographs of infection levels 72 hours post adoptive transfer. Scale bar = 200 μm. (**B**) Percentage of infected (i.e., NS5A$^+$ cells) at the indicated time points as determined by flow cytometry. Data were fitted with hyperbola function and the curves compared by statistical testing to confirm significant difference (F-test, GraphPad Prism).

3.11 Entry optimised HCV is acutely sensitive to neutralisation

The majority HCV positive patients experience chronic life-long infection with persistently high viral loads. To achieve this, HCV must resist the E1E2-specific nAbs that arise in most individuals. Failure of HCV to evade and/or escape nAbs has been linked with viral clearance and understanding the molecular mechanisms of HCV antibody resistance is likely to inform ongoing HCV vaccine development (17,388,389). Several reports have found that cell-culture adapted strains of another genotype 2a HCV strain, JFH-1, exhibit increased sensitivity to nAbs compared to parental virus (382,390,391). Comparing the phenotypic features of WT J6, which is naturally resistant to neutralisation, with that of mutant with high sensitivity could aid to reveal the mechanism of HCV antibody resistance.

First, we evaluated the capacity of HCVcc to resist antibodies isolated and pooled from the sera of two chronic HCV^+ patients. WT HCV was highly resistant to patient nAbs with the neutralisation curve following a log-linear relationship, such that successive 10-fold increases in IgG concentration yielded only a modest increase in neutralisation (Fig 3.12 A). In stark contrast, the hyperreactive HCV I438V A524T mutant was acutely sensitive to patient IgG, reaching complete neutralisation even at low concentrations of nAb. We also assessed the ability of sCD81-LEL to neutralise HCVcc and observed I438V A524T was again more sensitive (Fig 3.12 B), consistent with the enhanced interaction of I438V A524T E2 with cell surface CD81 (Fig 3.7 D & E). We also observed that a monoclonal antibody isolated from an HIV^+ individual with no history of HCV infection showed no neutralising activity against either virus (Fig 3.12 C).

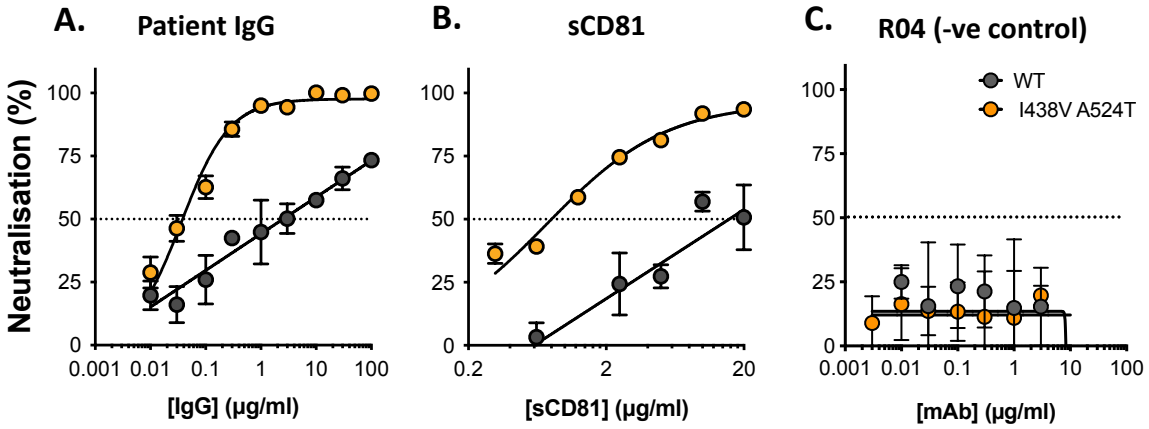

Figure 3.12. Neutralisation by pooled HCV⁺ IgG and the soluble CD81 long extracellular loop. (**A**) Neutralisation of WT and I438V A524T HCVcc by a serial dilution of HCV⁺ patient IgG. (**B**) Neutralisation of WT and I438V A524T HCVcc by a serial dilution of sCD81. (**C**) Neutralisation of WT and I438V A524T HCVcc by a serial dilution of R04, a mAb isolated from an HIV⁺ individual with no history of HCV infection. For all neutralisation curves, data points represent the mean of 3 independent experiments. I438V A524T data were best fitted by a hyperbola function, whereas WT data were best fitted by a semi-log function (GraphPad Prism).

Pooled patient IgG is polyclonal in nature and, therefore, likely targets multiple conformation-dependent epitopes. We sought to determine the sensitivity of WT and I438V A524T to monoclonal antibodies (mAbs) with defined epitopes in E2. Intense investigation of anti-HCV nAb responses by others has provided a detailed understanding of the major neutralising epitopes in E2 (322). Most HCV-E2 bNAbs map to the conserved but flexible CD81 binding site. The binding site is composed of three distinct regions which each targeted by bnAbs: antigenic site 412 (AS412) region (residues 412-423), the front layer (residues 424-459) and the CD81 binding loop (residues 519-535). The three regions occupy distinctive spaces on the tertiary structure of the E2 glycoprotein (Fig 3.13 A). We measured the sensitivity of WT and mutant HCV to a panel of mAbs targeting these defined epitopes.

We challenged the viruses with (i) J6.36, a J6 specific anti-HCV-E2 mAb whose epitope maps to HVR-1 (340), (ii) H77.39, a mouse anti-HCV-E2 bnAb whose epitope maps to the AS412 region (340), and (iii) AR3A, a patient-derived bnAb with epitopes structurally mapped to both the front layer and the CD81 binding loop (339). In all three cases, WT virus resisted mAb neutralisation, whereas I438V A524T was potently inhibited (Fig 3.13 B). To evaluate whether this apparent shift in nAb sensitivity reflected changes in antibody binding we measured nAb interactions with sE2 using

ELISA. Surprisingly, we observed near-identical binding curves for all each mAb, suggesting WT and I438V A524T are antigenically equivalent (Fig 3.13 C).

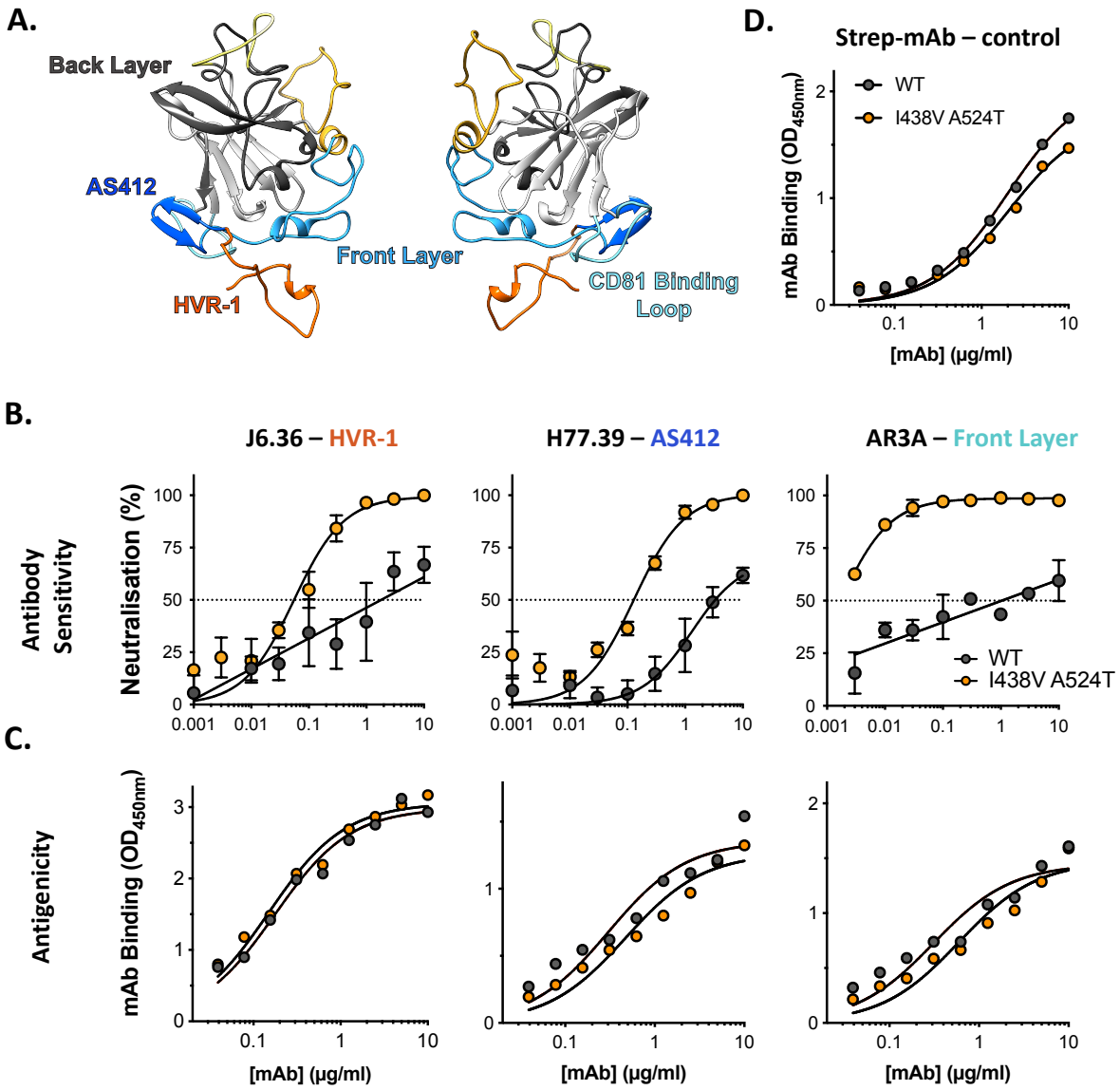

Figure 3.13. I438V A524T HCV is acutely sensitive to mAb neutralisation. (**A**) Molecular cartoon of the major antigenic sites targeted by nAbs. (**B**) Neutralisation curves for three representative mAbs targeting distinct epitopes, the mAb name and specific epitope are provided and colour coded to epitope-match **A**. (**C**) Binding of mAbs to WT and I438V A524T sE2 assessed by ELISA, mAbs are matched to the neutralisation data. (**D**) Binding of anti-Strep-II-tag mAb indicating ELISA plates were coated with equivalent amounts WT or I438V A524T sE2 for anti-E2 mAb binding determination. For all neutralisation curves, data points represent the mean of 3 independent experiments. I438V A524T data were best fitted by a hyperbola function, whereas WT data were best fitted by a semi-log function (except for H77.39) (GraphPad Prism). For ELISA data, one representative experiment is shown, with data fitted with a hyperbola function. In all plots error bars standard error of the mean.

The dramatic change in antibody sensitivity by the I438V A524T mutations is best illustrated by the change in IC_{50} values across a wider panel of nAbs (Fig 3.14 A).

Here the I438V A524T mutant exhibited at least a 10-fold increase in sensitivity of each mAb in the panel as indicated by the lowered IC_{50} value of mAb when challenged against WT virus. A summary of IC_{50} demonstrates an overall ~20-fold increase in nAb sensitivity for the mutant (Fig 3.14 B). Kd values were also obtained from the ELISA data and the results from the expanded panel were largely in keeping with the binding curves of the representative mAbs (Fig 3.13 C), with all mAbs except CBH-7 demonstrating no significant difference in binding to WT and I438V A524T sE2 (Fig 3.14 C). Moreover, a summary Kd plot corroborated there was no difference in the antigenicity of WT and I438V A524T E2 (Fig 3.14 D).

To summarise, the I438V A524T mutant exhibits acute sensitivity to antibody-mediated neutralisation without intrinsic changes to the antigenicity of E2. This would suggest that whilst nAb binding remains unaltered, the consequences of antibody binding are dramatically changed

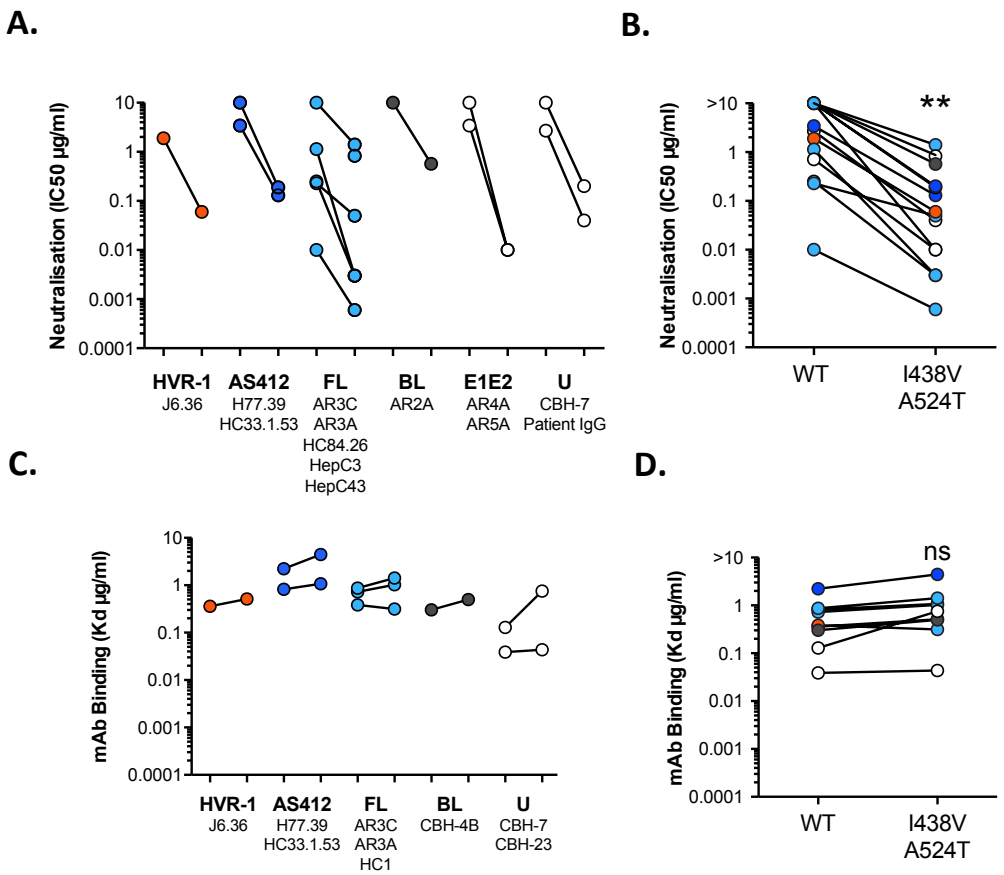

Figure 3.14. WT and I438V A524T HCV are differentially sensitive to mAb neutralisation despite possessing antigenically similar E2. (**A**) 50% inhibitory concentrations (IC_{50}) of mAbs separated according to antigenic targets. mAb names are provided for each target. FL and BL refer to Front Layer and Back Layer. Continued on next page.

Figure 3.14 legend continued. E1E2 mAbs bind to a discontinuous epitope comprising elements of both E1 and E2. U represents summary poorly defined epitopes. (**B**) A summary IC_{50} plot of the 14 mAbs in **A**, asterisks indicate statistical significance. (t-test, GraphPad Prism). (**C**) Estimated dissociation constants (Kd) of 9 mAbs separated according to antigenic targets. (**D**) A summary of the Kd values of the mAbs in **C**, there is no statistical difference between WT and I438V A524T (t-test, GraphPad Prism).

3.12 Differential rate of enzymatic processing of WT and mutant sE2

The antigenic similarity between WT and I438V A524T E2 would suggest there is no gross conformational change associated with the hyperreactive phenotype. Another way to gain insights into protein fold is by performing limited proteolysis (392). Therefore, we subjected WT and I438V A524T sE2 to Endoproteinase GluC processing; this serine proteinase preferentially cleaves peptide bonds C-terminal to glutamic acid (E) residues. We tracked the production of the N-terminal product by probing western blots with J6.36 (Fig 3.15 A), seeing as the first possible cleavage site in E2 is E446. The products following cleavage were identical between WT and the mutant sE2, however, there was a suggestion the two were processed at different rates. Quantification of the rate of production of the N-terminal fragment using ImageLab software revealed that I438V A524T underwent cleavage faster than WT sE2 (Fig 3.15 B). This suggests subtle structural differences may underpin hyperreactive phenotype.

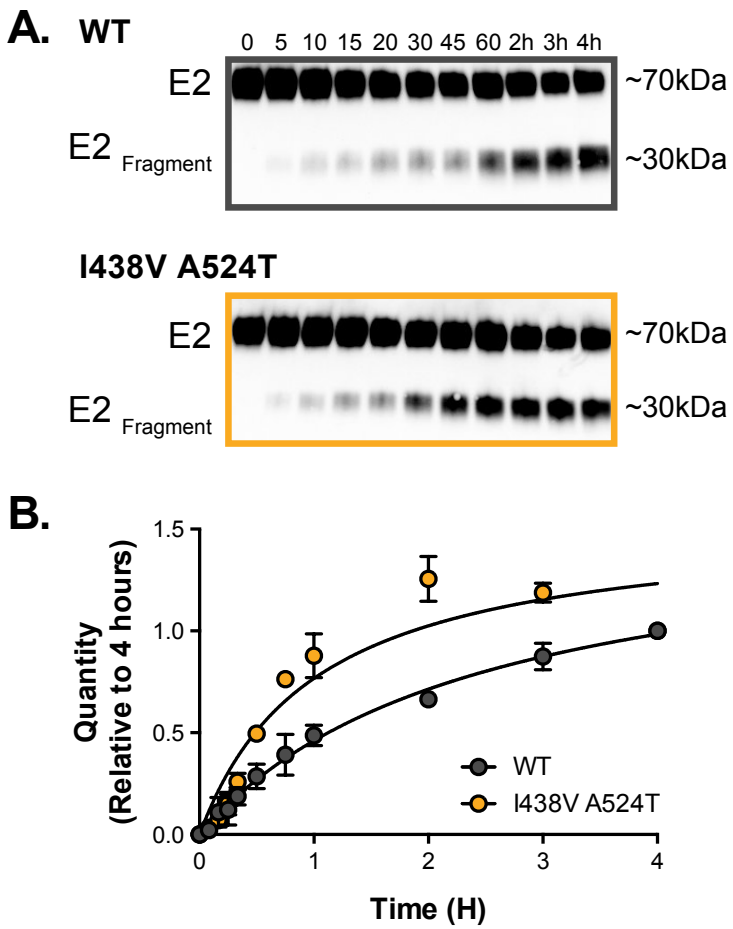

Figure 3.15. Limited proteolysis of Soluble E2. sE2 (WT or I438V A524T) was incubated at 37°C with Endoproteinase GluC for up to 4 hours. (**A**) Representative western blot images of digestion over time (minutes and hours as indicated); incubation with GluC gives rise to a ~30kda digest product (E2Fragment). (**B**) The kinetics of digestion was evaluation by measuring the quantity of E2Fragment; the data is expressed relative to the intensity of product at 4 hours, data points represent the mean of three independent experiments, error bars indicate standard error of the mean. Data were fitted with a hyperbola function and curves were compared to determine statistical significance (F-test, GraphPad Prism).

3.13 Pseudoparticles reproduce findings in authentic HCVcc

Previous work has suggested E1E2 mutations arising through cell-culture adaptation may alter the lipoprotein content of the virion (229). To remove all doubt that the hyperreactive phenotype of the I438V A524T is solely driven by E1E2 themselves, and does not require contributions from lipoproteins, we sought to replicate our findings in the pseudoparticle system (HCVpp), which are devoid of any lipoprotein components. To this end, I438V A524T HCVpp recapitulated the hyperreactive phenotype seen in HCVcc. First, we found that I438V A524T HCVpp was less

dependent on SR-B1 for entry, as indicated by enhanced infection of SR-B1 KO Huh-7 cells (Fig 3.16 A). The mutant HCVpp also underwent spontaneous inactivation more rapidly than WT virus (Fig 3.16 B). Lastly, the I438V A524T HCVpp was acutely sensitive to patient IgG (Fig 3.16 C). Taken together, these findings suggest that the contribution of virion-associated lipoprotein to the hyperreactive is negligible.

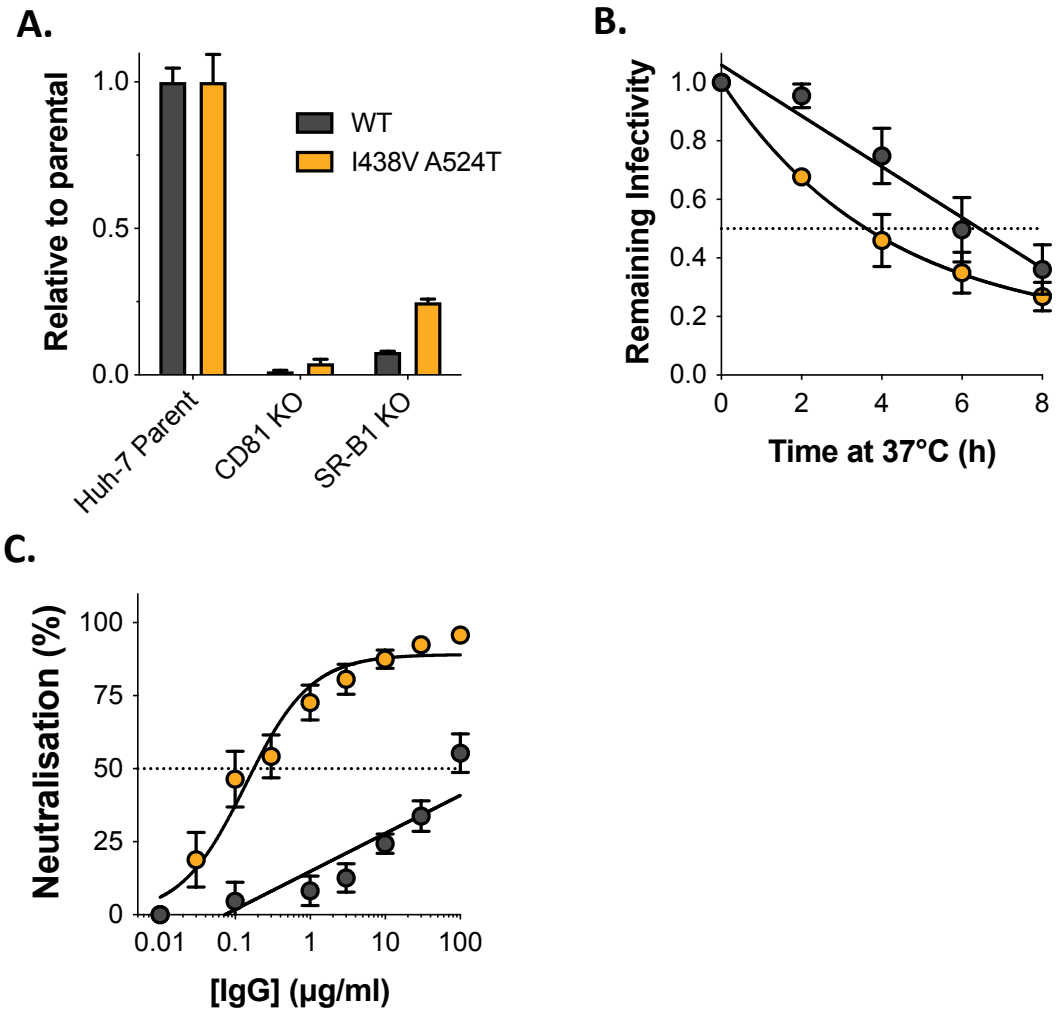

Figure 3.16. The hyperreactive phenotype is recapitulated in HCV pseudoparticles. We characterised WT and I438V A524T E1E2 in the context of HCV pseudoparticles. (**A**) HCVpp infection of parental or receptor knockout Huh-7, data is expressed relative to parental cells. (**B**) Stability of HCVpp at 37°C, data points represent the mean of three independent experiments, data was fitted using an exponential decay function. (**C**) Neutralisation of HCVpp by patient IgG, data points represent the mean of three independent experiments. Data was fitted with a hyperbola function (I438V A524T) or semilog function (WT). In each plot error bars indicate standard error of the mean; asterisks denote statistical significance (ANOVA, Graphpad prism); all curves determined to be statistically significant (F-test, Graphpad prism).

3.14 Discussion

In this chapter, we report that cell-culture adaptation of the J6 strain of HCV had pleiotropic effects on the viral infectivity, receptor interactions and nAb sensitivity. Comparison of the WT and I438V A524T E1E2 phenotypes indicate that there is an intrinsic link between the evolutionary selective pressures of efficient entry and nAb evasion. Notably, the data presented in this chapter suggests structural changes in E1E2 underpin the transition to hyperreactive HCV during cell-culture adaptation.

E1E2 acquisition of CD81 is a prerequisite for HCV entry, we previously demonstrated the viral glycoprotein can achieve this intrinsically or, more favourably, by first being primed by SR-B1 (219). Here we show SR-B1 dependency reduces HCV entry efficiency. This begs the question as to why HCV does not exist in a hyperreactive state akin to the I438V A524T mutant? The antibody challenge data indicate that, against an intact immune system, any gains in entry efficiency would be offset by reduced cell-free infections since hyperreactivity bestows increased nAb sensitivity. Therefore, it is likely HCV evolved to utilise SR-B1 during its evolutionary quest to resist the human humoral immune system. To this end, others have observed strong correlations between variant SR-B1 dependency and nAb resistance (346,393). Thus, the findings reported here add to this growing list of evidence indicating HCV SR-B1 dependency and nAb resistance are intrinsically linked.

Although direct evidence is lacking, it is widely presumed that the interaction with SR-B1 primes E1E2 for its acquisition of CD81 (222,346). Here, our entry kinetics data provides indirect but convincing evidence for this phenomenon. If one assumes that this dispensable stage of HCV entry is a rate-limiting step, then E1E2 that is hyperreactive to stimulation by SR-B1 or can bypass SR-B1 binding entirely should possess faster entry kinetics. Our data does indeed support this notion since hyperreactive mutant HCV completes entry much quicker than the SR-B1 dependent WT virus.

The contrasting stabilities of WT and I438V A524T virus mean we had to be cautious when interpreting the results obtained from the entry kinetics experiments. As I438V A524T E1E2 is three-fold less stable compared to WT, it is conceivable a large proportion of the mutant virus is already thermally inactivated by the time point we use for data normalisation. Therefore, the rapid saturation we see in the entry curve of the mutant virus could be reflective of a loss in infectivity rather than faster entry.

Nonetheless, the fact that the experimental data are in close agreement with the predictions from the mathematical model suggests our experiment tracked entry because the mathematical model integrated thermostability in addition to receptor dependency. It's important to note that the mathematical model does not capture HCV entry events when SR-B1 is entirely unavailable in the system. This is because WT and mutant virus were able to achieve infectivity of 30% and 75% (Fig 3.5 E), respectively, in cells that were treated with the highest concentration of anti-SR-B1 sera (Fig 3.5 C). These values are considerably higher than those observed in SR-B1 KO cells (Fig 3.3 B). High concentrations of a mAb would probably inhibit infection to a comparable extent as SR-B1 ablation; as was observed for CD81, where the complete inhibition observed in CD81 KO cells was recapitulated at saturating concentrations of anti-CD81 (Fig 3.5 D & F).

Acute sensitivity of the I438V A524T HCV to sCD81 and mAbs targeting the CD81 binding site suggest global structural changes. Intriguingly further assessment of the antigenic properties of the mutant by ELISA against a panel of mAbs suggests its E2 is antigenically equivalent to WT E2. This is consistent with Augestad et al who recently reported discrepancies in particle nAb sensitivity and E2 antigenicity measured by ELISA (346). A limitation of ELISA is that it is a solid-phase technique making it impossible to measure K_{off} rates and subsequently the true Kd. To this end, preliminary SPR experiments indicate that there is no difference in the K_{off} rate of WT and mutant E2 when bound to the large extracellular loop of CD81 (data not shown), thereby corroborating the results obtained by ELISA.

The antigenic similarity of WT and I438V A524T sE2 suggest SR-B1 engagement does not necessarily unmask E2 to expose critical epitopes as was previously suggested (335,394,395). However, it's important to note sE2 may not necessarily recapitulate epitope presentation on authentic virus particles. Still, the disparity in the processing rates of WT and mutant sE2 suggests there are subtle differences between the two. As the product of proteolytic cleavage appeared to be identical (see fragment bands in 3.14 A), the most likely reason for the faster processing of the mutant is that it has altered conformational dynamics. We recently reported that the HVR-1 of E2 bears the hallmarks of an intrinsically disordered protein region (330), which may allow it to regulate the conformational landscapes of distal E2 domains. Notably, SR-B1 binding is reduced in the mutant sE2, suggesting some intrinsic features of HVR-1, also the putative SR-B1 binding site, are altered to achieve

hyperreactivity. Thus, HVR-1 may be a structural linchpin governing both SR-B1 dependency and antibody resistance. A putative mechanism for this will be put forward and subsequently corroborated in the next chapter.

Viral evolution during cell-culture adaptation does not reflect, nor can it predict HCV evolution during natural patient infection. Indeed, given the acute nAb sensitivity of the mutant, it is highly improbable HCV would follow evolutionary pathways to become hyperreactive in the presence of an intact adaptive response. Nonetheless, polymorphisms at residue 438 have been observed in vivo, and are thought to control nAb escape and receptor dependency (17,396). Bailey and colleagues observed an L438I substitution in two HCV^{+} individuals who were under longitudinal clinical surveillance throughout their infection (17). Introducing this mutation into the transmitted/founder ancestor by reverse genetics led to a reduction in viral fitness and sE2-CD81 binding. Additionally, position 438 is often identified in predictive in-silico evolutionary modelling of E2 as a site that regulates escape from a broad number of bnAbs (393,397). Experimental work to validate the modelling in one of these studies found that an L438V mutation reduced binding to SR-B1 as well as increased the sensitivity of a genotype 1b strain of HCV to the non-overlapping bnAbs HC33.4 and AR4A (393). These observations highlight the relevance of using minimalist, in-vitro approaches such as cell-culture adaptation to study HCV evolution. In the next chapter, we again perform cell-culture adaptation but maintain infected cells in nAbs to emulate sustained immunological pressure.

In summary, we have demonstrated that HCV E1E2 evolves to optimise entry in the absence of adaptive immunity. Comprehensive phenotyping of a mutant from the successful lineage revealed evolution toward enhanced entry, achieved through a reduction in SR-B1 binding and a concomitant loss of nAb resistance. We also provide evidence for SR-B1 priming of E1E2-CD81 interactions via an experimentally verified mathematical model. Moreover, our data suggest that mutant, hyperreactive E2 has subtle structural differences with WT E2. In the next chapter, we compare the two glycoproteins using both in-vitro and in-silico methods to elucidate the physical properties governing SR-B1 dependency and nAb resistance, and how the two are necessarily mechanistically linked.

4 An entropic safety catch controls HCV entry and antibody resistance

4.1 Introduction

The findings in the preceding chapter suggest subtle structural differences, may underlie the hyperreactive, acute antibody sensitive phenotype of entry optimised HCV. The work described in this chapter builds upon work by Lenka Stejskal which characterised the hyperreactive mutant E2 glycoprotein computationally and biophysically. An overview of her findings is described as part of the introduction.

Previous work by ourselves and others has indicated that flexibility and disorder are conserved features of E2 (323,330,355,358). Efforts to study E1E2 protein dynamics on native virions, as performed with HIV-Env and SARS-CoV-2 spike (325,398), are hampered by the heterodimer's small size, and the fact the oligomeric arrangement relevant for infection is yet to be solved. So, we instead performed molecular dynamics (MD) to study the conformational landscape of monomeric hyperreactive E2. MD is an in-silico method employed to simulate the motions of atoms in space (399) by the numerical solution of classical Newtonian dynamic equations. Therefore, MD can be used to model the conformational ensemble of a given protein.

In our previous work, we first modelled the complete structure of the J6 (WT) E2 ectodomain and performed five independent 1 μs MD simulations (330). We again employed a similar strategy to compare WT E2 and I438V A524T E2. We found that the overall motion of the two was similar, as reflected by their root mean square fluctuation profiles. However, HVR-1 in I438V A524T was consistently stabilised compared to that of WT E2, which, as previously reported, is highly dynamic (Fig 4.1 C). This stabilisation is best illustrated by comparing mutant and WT HVR-1 root mean squared deviation (Fig 4.1 A & B), which captures motion over time. This result is interesting considering the two mutations do not map to HVR-1. Indeed, this result offers a coherent explanation as to how cell-culture adapted HCV strains exhibit reduced SR-B1 dependency despite HVR-1 remaining genetically unchanged (248,379,380,390).

Interestingly, HCV virions genetically deleted of HVR-1 remain infectious. Notably, ΔHVR-1 HCVcc strains exhibit acute sensitivity to nAbs, akin to I438V A524T, and they intrinsically have to traverse route 2 (SR-B1 independent route) for entry (Fig 1.23) (219,310,311,400). We, therefore, reasoned that ΔHVR-1 and I438V A524T E2 may share biophysical properties. We first analysed sE2 by circular dichroism (CD), which gives a low-resolution ensemble measurement of protein structure. Here I438V

A524T and ΔHVR-1 were physically indistinguishable from one another but distinct to WT E2 (Fig 4.1 D). Of note, estimations of their structural composition indicated I438V A524T and ΔHVR-1 E2 exhibited a significant reduction in unordered components, consistent with the MD experiments. We also analysed E2 by differential scanning fluorimetry (DSF). DSF tracks the changes in intrinsic protein fluorescence upon solvent exposure of tryptophan residues, thereby providing a surrogate measure of protein folding. At physiological temperature, the intrinsic fluorescence ratio of I438V A524T and ΔHVR-1 E2 were higher than WT, consistent with the two adopting an alternative fold to WT (Fig 4.1 E).

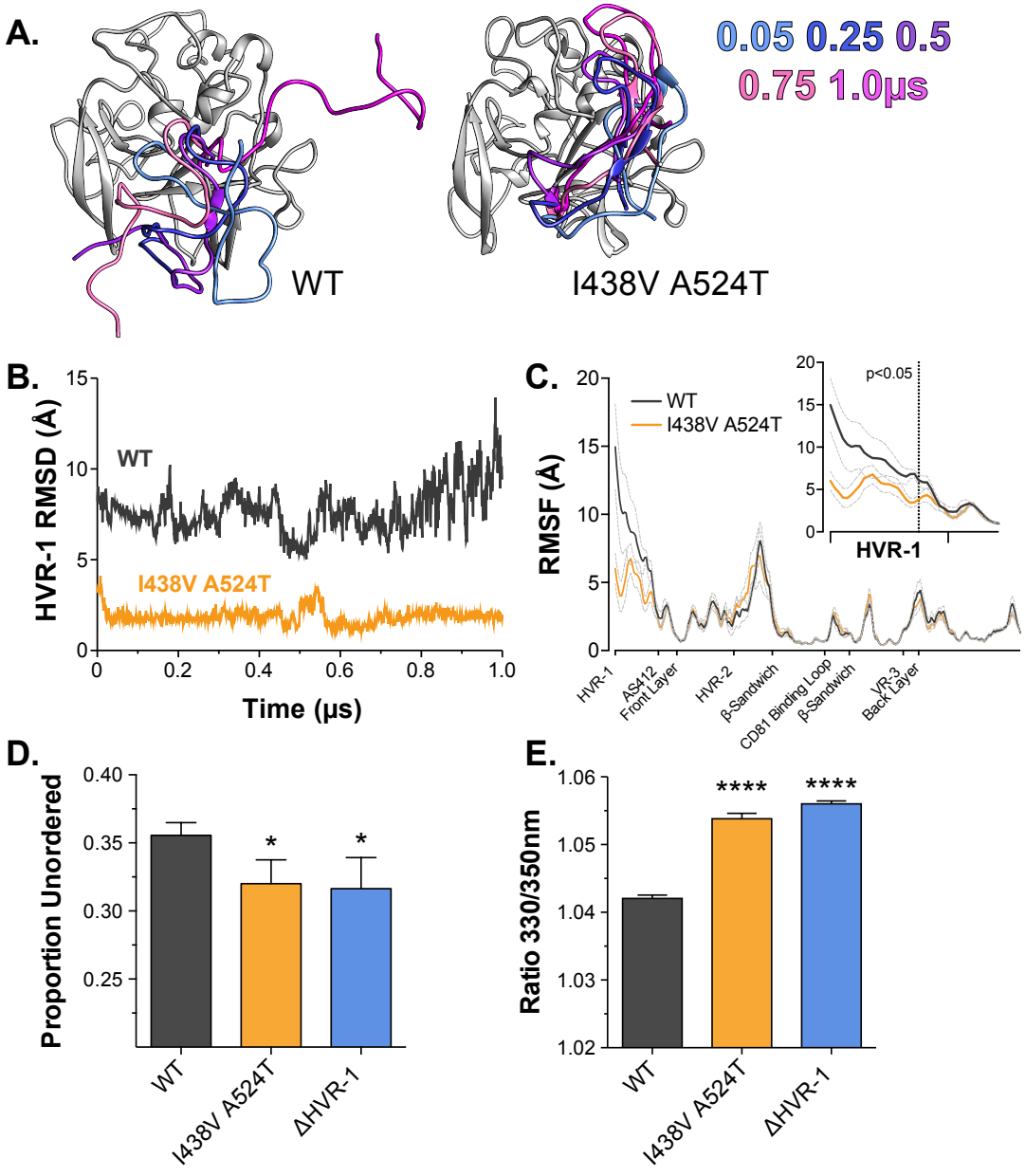

Figure 4.1. I438V A524T E2 exhibits stabilisation of HVR-1. The conformational dynamics of WT and I438V A524T E2 ectodomain were explored by MD simulations. (**A**) Images summarising two representative simulations; HVR-1 is colour coded according to time (as shown in key), the remainder of E2 is shown in grey for the t=0.05μs frame only. (**B**) Root mean square deviation (RMSD) of HVR-1 for the simulations shown in **A**. (**C**) Mean root mean square fluctuation for WT and I438V A524T E2, from five independent experiments, error bars indicate standard error of the mean. X-axis displays regions of E2. Inset provides a zoom of the data for HVR-1, RMSF values to the left of the dashed line reach statistical significance (ANOVA, GraphPad Prism). (**D**) Estimation of unordered protein content, by circular dichroism spectroscopy, for WT, I438V A524T and ΔHVR-1 soluble E2. Data represent the mean of three independent measurements. (**E**) Intrinsic fluorescence ratio (330nm and 350nm) measured by nanoscale differential scanning fluorimetry, for WT, I438V A524T and ΔHVR-1 soluble E2 at 37°C. Data represent the mean of three independent measurements. Asterisks denote statistical significance (ANOVA, GraphPad Prism). Data generated by Lenka Stejskal.

The MD simulations suggest that E1E2 hyperreactivity is achieved through tuning of HVR-1 dynamics, a notion supported by the biophysical similarity of I438V A524T and ΔHVR-1 E2. Thus HVR-1 dynamics provide a potential mechanism that links SR-B1 dependency, entry efficiency and nAb sensitivity. We propose a molecular model of the early events of HCV entry: on circulating particles HVR-1 exhibits high conformational entropy, constantly sampling different disordered states (Fig 4.2). However, during virus entry, engagement of SR-B1 constrains HVR-1 motion, this will, necessarily, reduce conformational entropy (401). The requirement for SR-B1-mediated stabilisation of HVR-1 creates an energy barrier to subsequent events in HCV entry, including CD81 engagement and fusion. In this way, HVR-1 acts as a safety catch that prevents premature triggering of E1E2. In the hyperreactive I438V A524T mutant, pre-stabilisation of HVR-1 overcomes (or lowers) the energy barrier, thereby releasing the safety catch, reducing the dependency for SR-B1 and enhancing entry efficiency, but rendering E1E2 more prone to spontaneous triggering and inactivation.

The work presented in this chapter sets out to validate the entropic safety model using cell-culture systems. Firstly, we examined ΔHVR-1 (in HCVcc and sE2 systems) to see if it is phenotypically like I438V A524T, as the two appear biophysically similar (Fig 4.1 D & E). Indeed, the entropic safety catch should theoretically be entirely abolished in the ΔHVR-1 virus meaning its reactivity may exceed that of I438V A524T. Next, we performed a second cell-culture adaptation experiment, this time maintaining WT HCV infected cells in the absence or presence of HCV^+ patient IgG to recapitulate

nAb-exerted immune pressure on E1E2. In this experimental set-up, come the end of the adaptation, virus maintained in patient IgG should retain the entropic safety catch if it is indeed a mechanism for HCV to resist the humoral immunity. As before, we assessed any mutants observed for their impact on HCV infectivity, receptor dependency and antibody sensitivity.

The specific aims were to:

1. Compare the phenotypes of the hyperreactive mutant to ΔHVR-1 HCV.
2. Track HCV E1E2 evolution when cultured under the selective pressure of nAbs.
3. Determine the cell entry properties and nAb sensitivity of any E1E2 polymorphisms arising in the adaptation experiment.

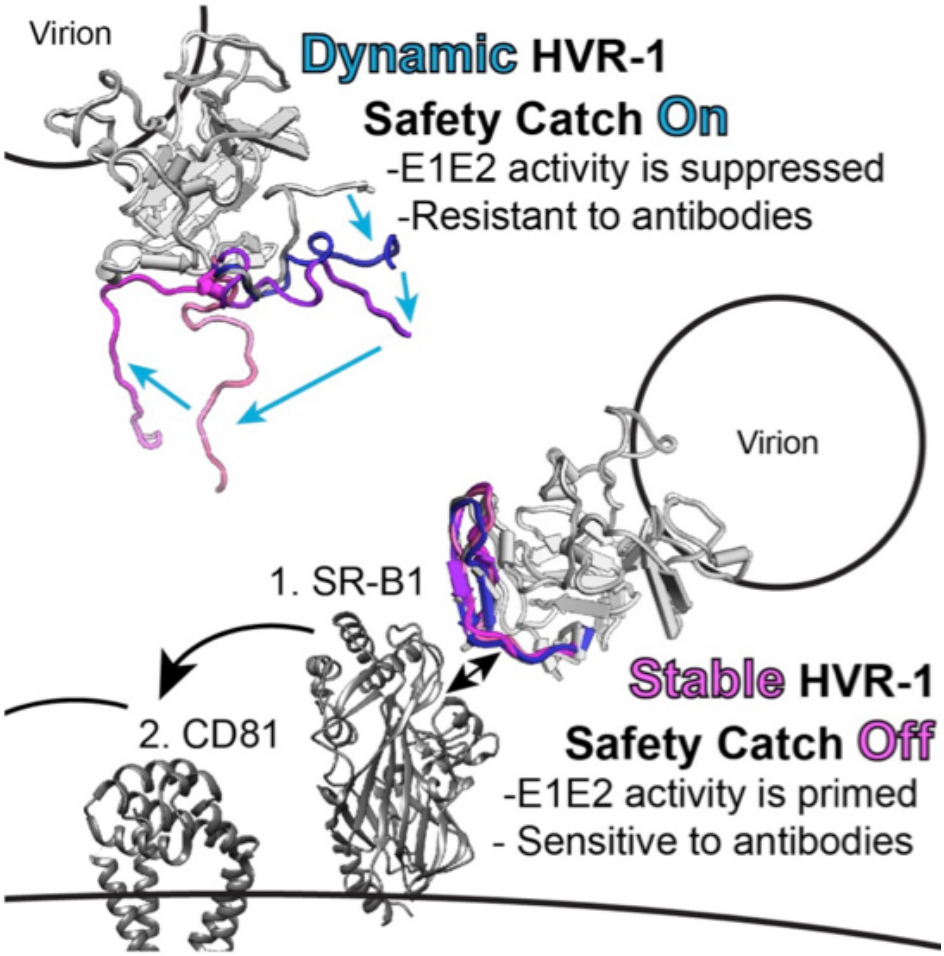

Figure 4.2. HVR-1 is an entropic safety catch that controls HCV entry and nAb resistance. On free virions HVR-1 is dynamic and disordered. In this state, it exerts an autoinhibitory function and suppresses E1E2 activity while maintaining nAb resistance. When HVR-1 is stabilised by interaction with SR-B1 (1., bottom) autoinhibition is turned off, thereby priming E1E2 for downstream events, including subsequent engagement to CD81 (2.). Therefore, HVR-1 function is analogous to that of a safety catch on a firearm, turning it off it the first step to fusion. Mutations that pre-stabilise HVR-1 also turn off the safety catch to prime entry but render E1E2 acutely sensitive to nAbs. The dynamics of HVR-1 are illustrated with snapshots from MD simulations of WT E2 (top) and an HVR-1 stabilised mutant (I438V A524T, bottom). HVR-1 is colour-coded by time, each colour representing a 50 ns snapshot in time. Models not in scale.

4.2 HVR-1 deleted HCV is hyperreactive

Based on our previous work, HVR-1 has the hallmarks of an intrinsically disordered protein region (IDPR). Regulation of protein function by IDPRs has been described in other systems. For example, the entropic force generated by an IDPR in the enzyme UGDH (UDP-α-D-glucose-6-dehydrogenase) was shown to shift the conformational ensemble of the protein toward a substrate with a high affinity for an allosteric inhibitor.

Drawing from this, we further analysed our MD data using dynamic cross-correlation (DCC), which provides a measure of coordinated/correlated motion within MD simulations. DCC analysis of WT E2 suggests that motions in HVR-1 generate force that is transmitted throughout the protein (Fig 4.3). Conversely, correlated motions were absent in simulations of I438V A524T E2, where HVR-1 is stabilised. This result suggests the absence of an entropic force in the mutant and provides a potential mechanism by which disorder in HVR-1 can influence the entire protein.

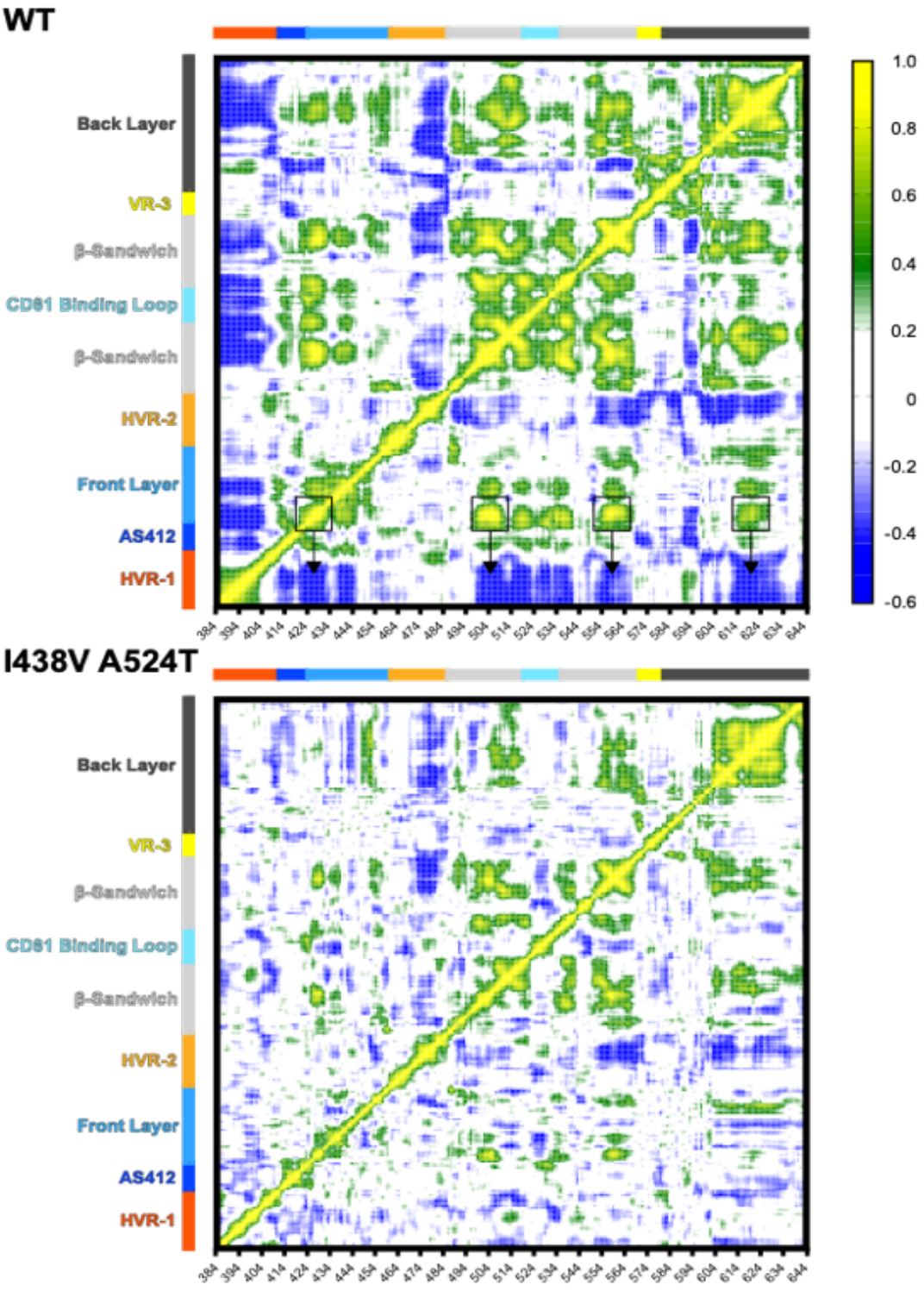

Figure 4.3. Dynamic cross-corelation analysis of E2 MD simulations. Dynamic cross correlation provides a residue-by-residue pairwise comparison of motion in MD trajectories to reveal correlations/anti-correlations in protein movement. Average DCC matrices for WT and I438V A524T E2 MD simulations are provided. As depicted in the key, yellow/green indicate positive correlations; blue indicates negative correlations; white indicates lack of correlation. The black boxes indicate hotspots of correlation at disulphide bonds; these correspond to areas in which HVR-1 motions are felt most strongly (arrows).

Drawing from the DCC analysis, we postulated that genetic removal of HVR-1 would overcome the energy barrier and release the entropic catch, and thereby generate hyperreactive HCV. We first analysed the entry properties of WT, I438V A524T and ΔHVR-1 HCVcc. As before, the I438V A524T mutant had a higher infectious titre and was less dependent on SR-B1 compared to WT (Fig 4.4 A & B). However, ΔHVR-1 virus exceeded the mutant in both criteria, particularly in terms of infectivity, where we witnessed two-fold the level seen in the mutant.

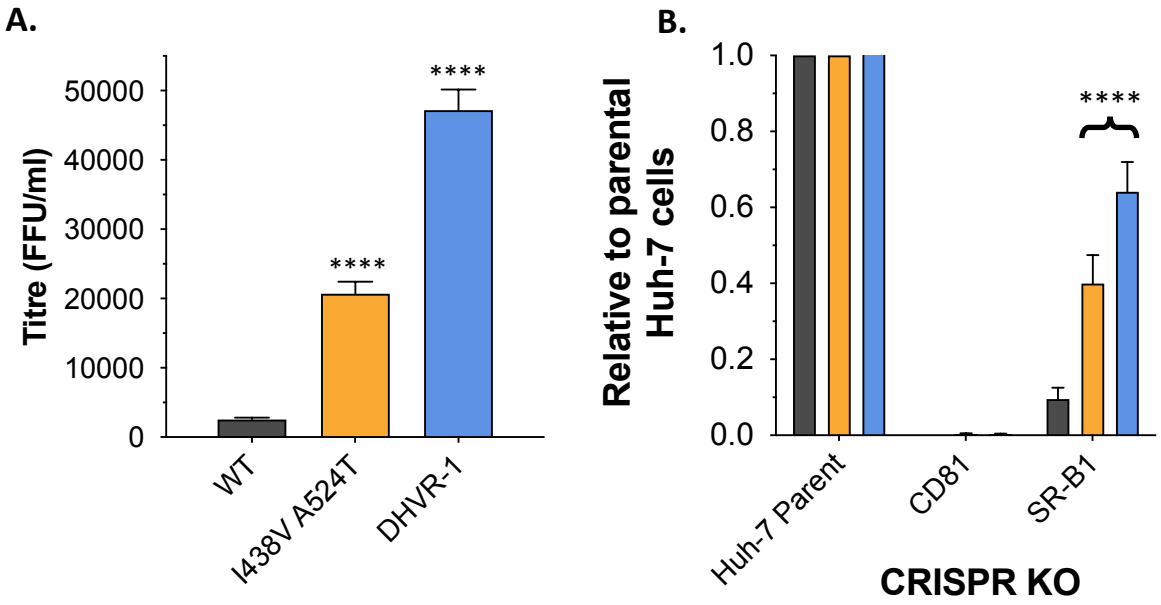

Figure 4.4. HVR-1 deletion renders HCV hyperreactive. (**A**) The mean infectivity of WT, I438V A524T and ΔHVR-1 HCVcc; foci forming units are corrected for input HCVcc copy numbers (**B**) HCVcc infection of parental Huh-7 cells or those CRISPR/Cas9 edited to prevent expression of CD81 or SR-B1. Data is expressed relative to parental cells, mean of three independent experiments. In each plot error bars indicate standard error of the mean; asterisks denote statistical significance (ANOVA, GraphPad Prism).

Next, we compared the intrinsic stability and neutralisation sensitivities of the three viruses. We found that ΔHVR-1 HCV exhibited a hyperreactive phenotype that far exceeded the I438V A524T mutant: ΔHVR-1 particles were >2-fold less stable and

>10-fold more sensitive to patient IgG compared to WT. Collectively, these data agree with the safety catch model. Furthermore, as the safety catch mechanism is regulated by HVR-1 conformational dynamics, then it may be expected that its removal would render HCV more reactive than its stabilisation, as our data shows. Indeed, MD simulations show that, though it is stabilised relative to WT, HVR-1 in the I438V A524T mutant still possess appreciable motility (Fig 4.1 A).

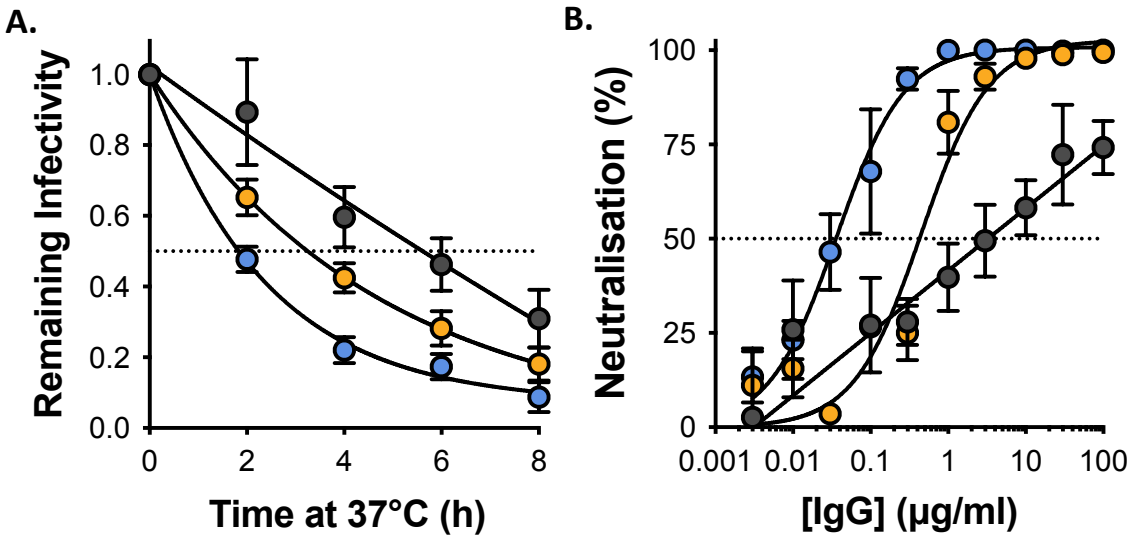

Figure 4.5. HVR-1 HCVcc is acutely sensitive to antibodies. (**A**) Stability of HCVcc at 37°C, data points represent the mean of three independent experiments, data was fitted using an exponential decay function. (**B**) Neutralisation of HCVcc by patient IgG, data points represent the mean of three independent experiments. Data was fitted with a hyperbola function (I438V A524T and ΔHVR-1) or semilog function (WT). In each plot error bars indicate standard error of the mean. All curves determined to be significant different to one another (F-test, GraphPad Prism).

4.3 ΔHVR-1 soluble E2 does not exhibit enhanced CD81 binding

Next, seeing as ΔHVR-1 virus displayed all the hallmarks of hyperreactivity, we reasoned it would also exhibit superior binding to CD81, akin to the I438V A524T mutant. We therefore again employed cell-binding assays to measure sE2 binding to CHO cells transduced to express the human HCV binding receptors (see Fig 3.6). As expected, ΔHVR-1 E2 did not bind SR-B1 expressing cells since HVR-1 contains the putative SR-B1 binding site (Fig 4.6 A, left panel). Curiously, we observed that ΔHVR-1 E2 bound CD81 to the same degree as WT E2 whereas I438V A524T E2 binding was enhanced three-fold (Fig 4.6 A & B). As our DCC analysis suggests HVR-1 dynamics are communicated throughout E2, this unexpected result may be a consequence of a loss in the conformational flexibility in the CD81 binding site

(specifically the front layer) following HVR-1 removal (322,363). This potentially limits the access of ΔHVR-1 E2 to conformational ensembles most preferable for direct CD81 engagement. Alternatively, the mutations in I438V A524T may have a direct effect on CD81 engagement (see discussion).

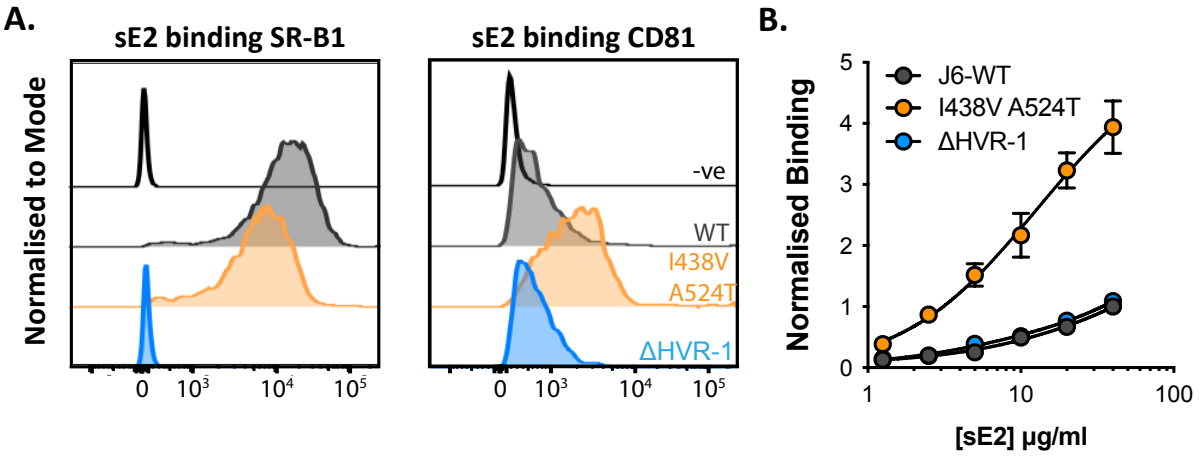

Figure 4.6. ΔHVR-1 sE2 binding to CHO cells expressing human HCV receptors. CHO cells were transduced with lentiviral vectors expressing human SR-B1 or CD81 and then used in an sE2 binding assay. (**A**) Representative flow cytometry histograms of 40 µg/ml WT, I438V A524T or ΔHVR-1 sE2 binding to CHO cells expressing SR-B1 (left panel) or CD81 (right panel). (**B**) Transduced CHO cells were incubated with a serial dilution of sE2. Data is normalised to 40 µg/ml WT sE2 binding to transduced CHO cells. Data are representative of the mean of three experiments and the error bars indicate the standard error of the mean. Data were fitted with hyperbola function and the curves compared by statistical testing to confirm significant difference (F-test, GraphPad Prism).

We also noticed that the margin of CD81 binding between WT and I438V A524T E2 was dependent on the anti-sE2 primary antibody used for detection. CD81 binding signals were more prominent when detected using J6.36, an HVR-1 specific mAb (Fig 4.7 A & B). However, detection using an anti-Strep-II tag increased I438V A524T CD81 binding from >2-fold (as determined via J6.36) to nearly ~4-fold (Fig 4.7 C). This disparity in fold binding may again be a consequence of restricted access to conformational ensembles due to the stabilisation of a distal epitope. In this instance, induced fitting of the CD81 binding surface of E2 (front layer and AS412) into the apposed CD81 surface may restrict HVR-1 fold to that with reduced J6.36 accessibility in the mutant. Indeed, J6.36 engagement may stabilise HVR-1, mimicking SR-B1 in the safety catch model, thereby promoting interaction with CD81. If the safety catch model faithfully recaptures authentic E1E2 receptor-binding events, one may expect

HVR-1 stabilisation to benefit WT sE2 binding to CD81 more so than the mutant, where HVR-1 is inherently stabilised (Fig 4.1 A-C). Therefore, the differential in I438V A524T CD81 binding as detected by Strep-mAb and J6.36 may reflect the mutant's intrinsic binding to said receptor and a subpopulation of mutant E1E2 that still requires SR-B1 priming to acquire CD81 (Fig 4.4 B)

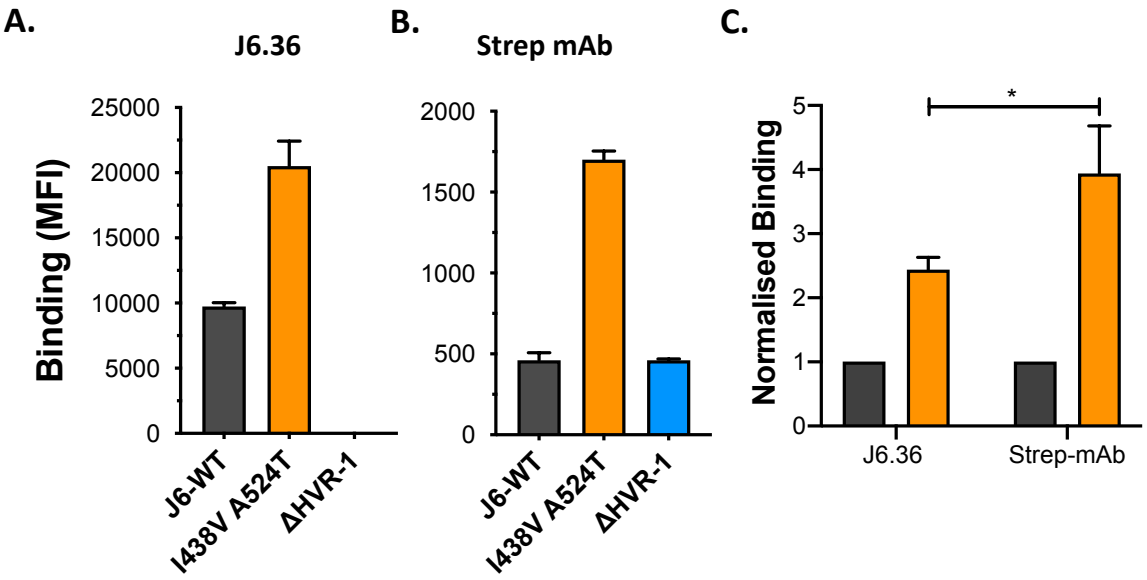

Figure 4.7. ΔHVR-1 sE2 binding to CHO cells expressing human HCV receptors. CHO cells were transduced with lentiviral vectors expressing human SR-B1 or CD81 and then used in an sE2 binding assay. Raw mean fluorescence intensity (MFI) values of 40 µg/ml of indicated sE2 binding to CD81 detected by (**A**) J6.36 and (**B**) strep-mAb. Of note, ΔHVR-1 sE2 binding is not detected by J6.36 since HVR-1 contains the J6.36 epitope. (**C**) Normalised binding of 40 µg/ml WT and I438V A524T sE2 as detected by stated primary mAb. Data is normalised to 40 µg/ml WT sE2 binding to transduced CHO cells. Data are representative of the mean of three experiments and the error bars indicate the standard error of the mean. Asterisks indicate statistical significance. (t-test, GraphPad Prism)

4.4 Culture adaptation of HCV in the presence of nAbs

Our analysis of representative sequences from HCV genotypes 1-6 predicts that intrinsic disorder within HVR-1 is conserved, therefore the safety catch mechanism may be ubiquitous to all HCV strains (330). Given the advantages of increased infectivity and improved entry efficiency, we questioned why HCV would not evolve exist in a hyperreactive state. Considering the acute sensitivity of hyperreactive HCV, it's likely that the development of a nAb response during natural infection prevents the emergence of hyperreactive strains. To test this, we performed new culture adaptations. We propagated WT HCV in the presence or absence of pooled patient

IgG. A serial passage strategy was employed, with the concentration of IgG increased at each round of selection (Fig 4.8 A). By the fourth round, we observed that virus in the unselected culture exhibited enhanced spread and superior infectivity compared to virus maintained under antibody selection (Fig 4.8 B and C). When we challenged the viral harvests from this round of selection, we saw that virus under patient IgG selection retained high resistance to neutralisation whereas unselected virus was acutely sensitive (Fig 4.9 A). Furthermore, sensitivity to neutralisation of unselected virus isolated from round six of the adaptation was even more pronounced (Fig 4.9 B). Altogether, these data suggest that antibody selection does indeed prevent the emergence of hyperreactive HCV and provide another demonstration that in the absence of immune selection, HCV will evolve to become increasingly hyperreactive.

A.

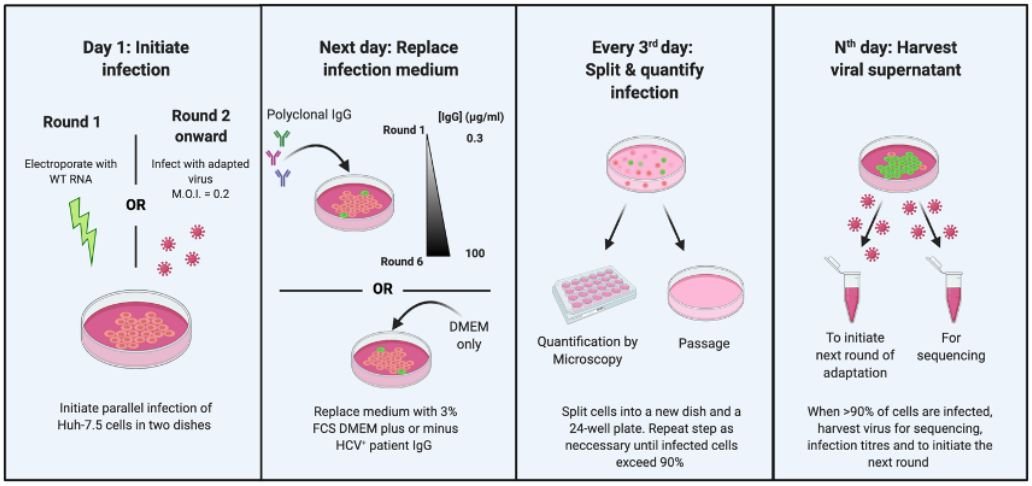

B.

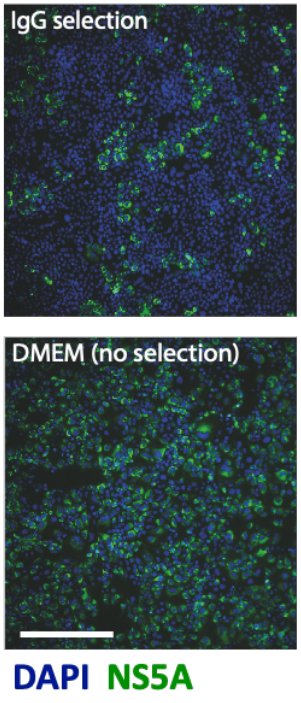

C.

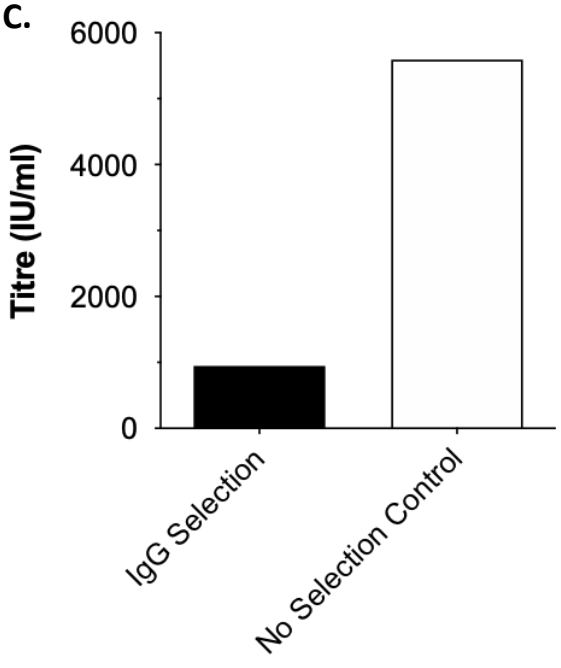

Figure 4.8. Culture adaptation of HCV under patient antibody selection. J6/JFH-1 HCVcc was propagated in Huh-7.5 cells with or without antibody selection by pooled HCV$^+$ patient IgG. (**A**) Schematic cartoon of the selection experiment. Diagram produced in BioRender. (**B**) Micrographs of infection levels 72 hours post initiation of round four of the selection experiment. Scale bar = 200 μm. (**C**) Infectious titre of HCVcc cultured with or without patient IgG. Data represent the mean of three technical replicates.

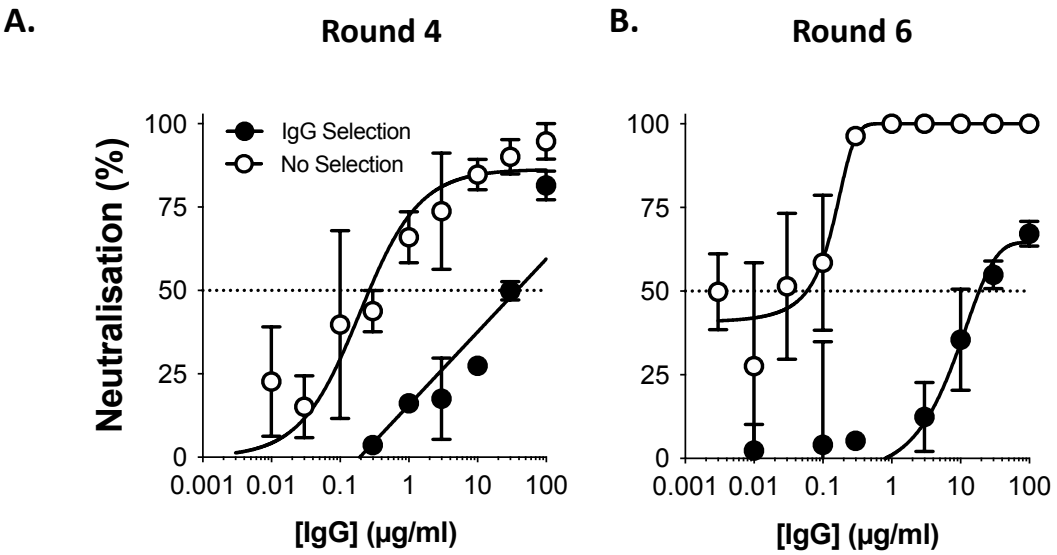

Figure 4.9. Neutralisation of culture adapted HCV. Patient IgG Neutralisation sensitivity of HCVcc adapted with or without antibody section from (**A**) round 4 and (**B**) of the adaptation experiment. Data points represent the mean of three technical replicates.

4.5 Antibodies prevent the selection of hyperreactive mutants

We next performed NGS on supernatant harvests from rounds four and six of the adaptation. Analysis of the antibody-maintained culture at round 4 revealed a mixture of WT and four polymorphisms with a relative frequency > 0.1 (Fig 4.10 A, right panel). However, by the sixth round, all four mutations were no longer detectable, and we instead noticed three new polymorphisms present at very low frequencies, indicative of a reversion to WT. The loss of the four mutations is consistent with the increased concentration of patient IgG selecting for neutralisation resistant virus (i.e., WT).

Analysis of the unselected culture at round four also revealed several mutations, including an S449P substitution (Fig 4.10 A, left panel), which was also identified in the early time points of the original culture adaption experiment (Figs S1 & 3.1) and has previously shown to regulate SR-B1 dependency (402). We therefore used reverse genetics to introduce this single mutation and comprehensively characterised its E1E2 activity. In every respect, S449P HCVcc exhibited a

hyperreactive phenotype practically indistinguishable from I438V A524T virus: with enhanced infectivity over WT virus, reduced SR-B1 dependency, high thermal instability, and acute sensitivity to nAbs (Fig 4.11 A-D).

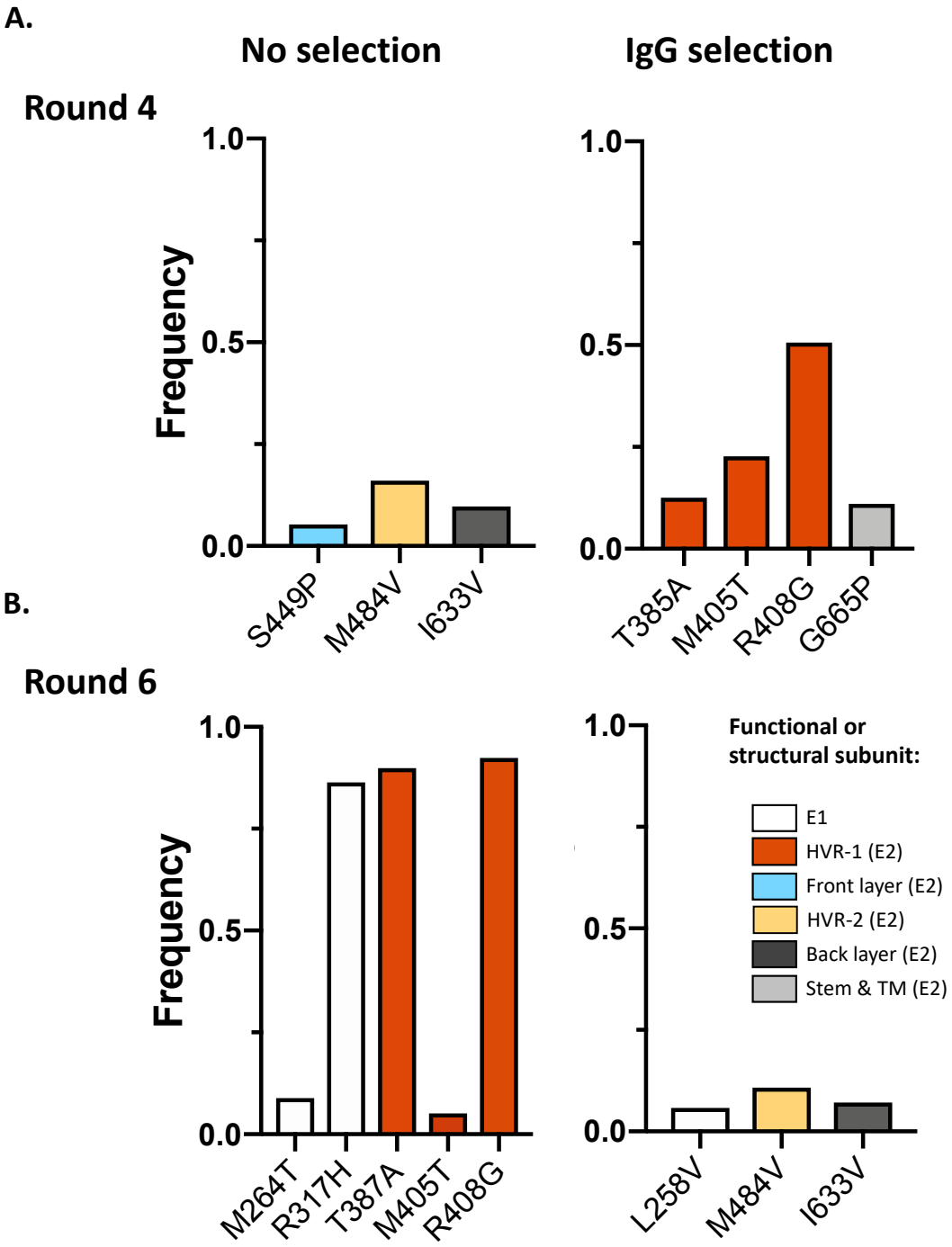

Figure 4.10. Antibody neutralisation prevents the selection of hyperreactive mutants during culture adaptation. We performed NGS on supernatant harvests from rounds four and six of the serial passage adaptation. The frequency of E1E2 substitutions that were present at >5% in the population at the end of (**A**) round four and (**B**) round six of serial passage culture adaptation. Graphs on the left represent polymorphisms observed in virus maintained without antibody selection and those on the right virus that underwent antibody selection. The bars are coloured according to the functional/structural subunit locale of the substitution.

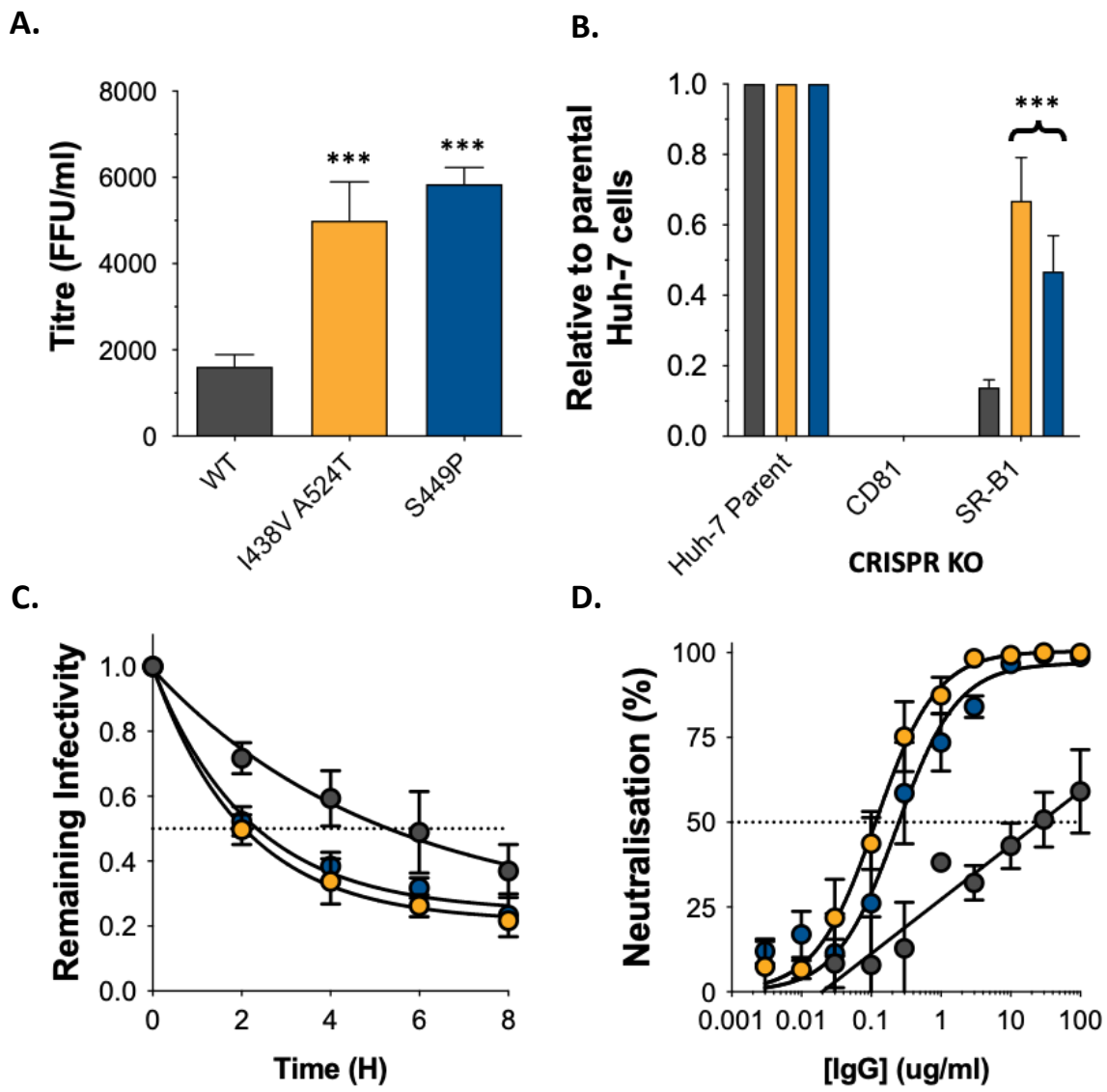

Figure 4.11. S449P HCVcc is hyperreactive. We comprehensively phenotyped the S449P mutant seen at round four of the culture adaptation. (**A**) Infectivity of WT, I438V A524T and S449P HCVcc, expressed as foci forming units per ml, values were normalised for in input particle numbers (RNA genomes). (**B**) Receptor dependency of HCVcc, infection values have been expressed relative to that observed in parental Huh-7 cells**.** (**C**) Stability of HCVcc at 37°C, data was fitted using an exponential decay function. (**D**) Neutralisation sensitivity of HCVcc. Data was fitted with a hyperbola function (I438V A524T and ΔHVR-1) or semilog function (WT). In each plot error bars indicate standard error of the mean. Asterisks denote statistical significance (ANOVA, GraphPad prism). All curves determined to be significant different to one another (F-test, GraphPad prism).

NGS analysis of the unselected culture at round six revealed three polymorphisms (R317H [in E1], T387A and R408G) that had very nearly reached fixation (Fig 4.10 B, left panel). We subsequently introduced all three mutations together into E1E2 and determined the receptor usage and antibody sensitivity of the triple mutant in using the pseudoparticle system. Just as the S449P HCVcc from round

four, triple mutant HCVpp exhibited a hyperreactive phenotype. Of note, the reactivity of triple mutant E1E2 appeared to surpass that of I438V A524T since the triple mutant is less dependent on SR-B1 and >5 fold more sensitive to patient IgG (Fig 4.12 A & B). This would explain why the S449P polymorphism was lost by round six. As the triple mutant HCV is more reactive I438V A524T virus (the phenotypic equal to S449P), it is likely the triple mutant disseminates in culture faster (see Fig 3.10).

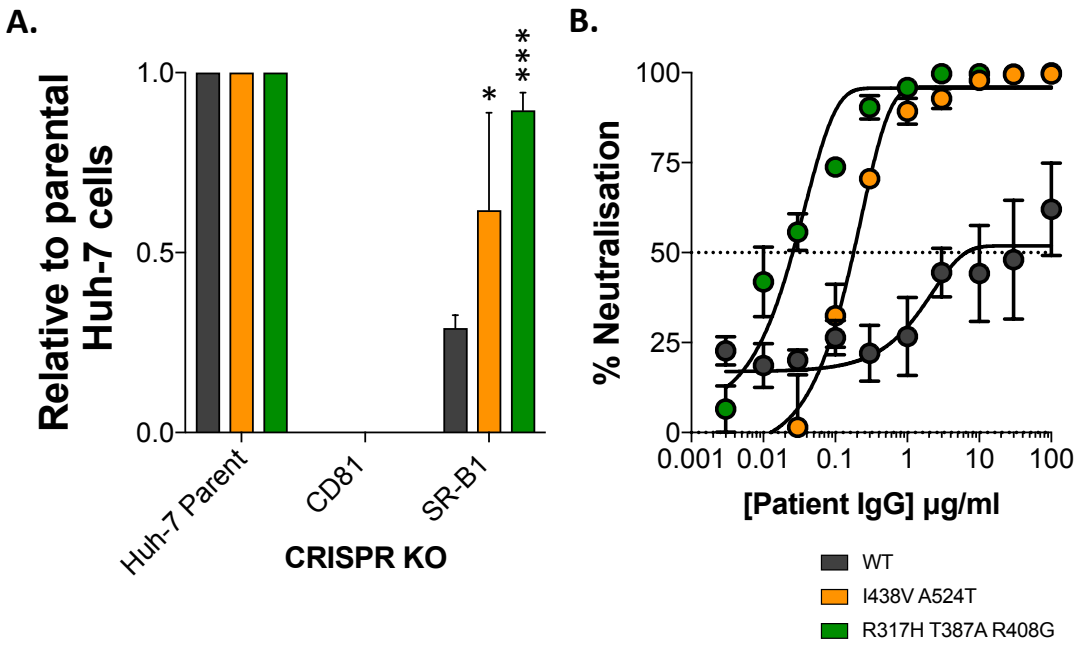

Figure 4.12. R317H triple mutant pseudoparticles are hyperreactive. We characterised WT, I438V A524T and R317H T387A R408G E1E2 in the context of HCV pseudoparticles. (**A**) HCVpp infection of parental or receptor knockout Huh-7, data is expressed relative to parental cells. (**B**) Neutralisation of HCVpp by patient IgG, data points represent the mean of three independent experiments. Data was fitted with a sigmoidal function. In each plot, error bars indicate standard error of the mean; asterisks denote statistical significance (ANOVA, GraphPad Prism); all curves determined to be statistically significant (F-test, GraphPad Prism).

4.6 S449P HVR-1 is stabilised in MD simulations

Given its likeness to I438V A524T, we reasoned that S449P would also exhibit HVR-1 stabilisation. MD simulations revealed that HVR-1 in S449P E2 was stabilised to the same extent as in I438V A524T (Fig 4.13 B & C). Conversely, HVR-1 in WT E2 was highly dynamic even though the overall motion of all three E2 was similar (Fig 4.13 A), in keeping with our previous simulations (Fig 4.1 A-C). Taken together with the results from S449P HCVcc phenotyping (Fig 4.11), the MD data strongly supports the safety catch model and suggest that hyperreactive HCV can only emerge in the absence of

antibody selection. Moreover, the safety catch appears to be an important mechanism for maintaining HCV resistance to neutralising antibodies.

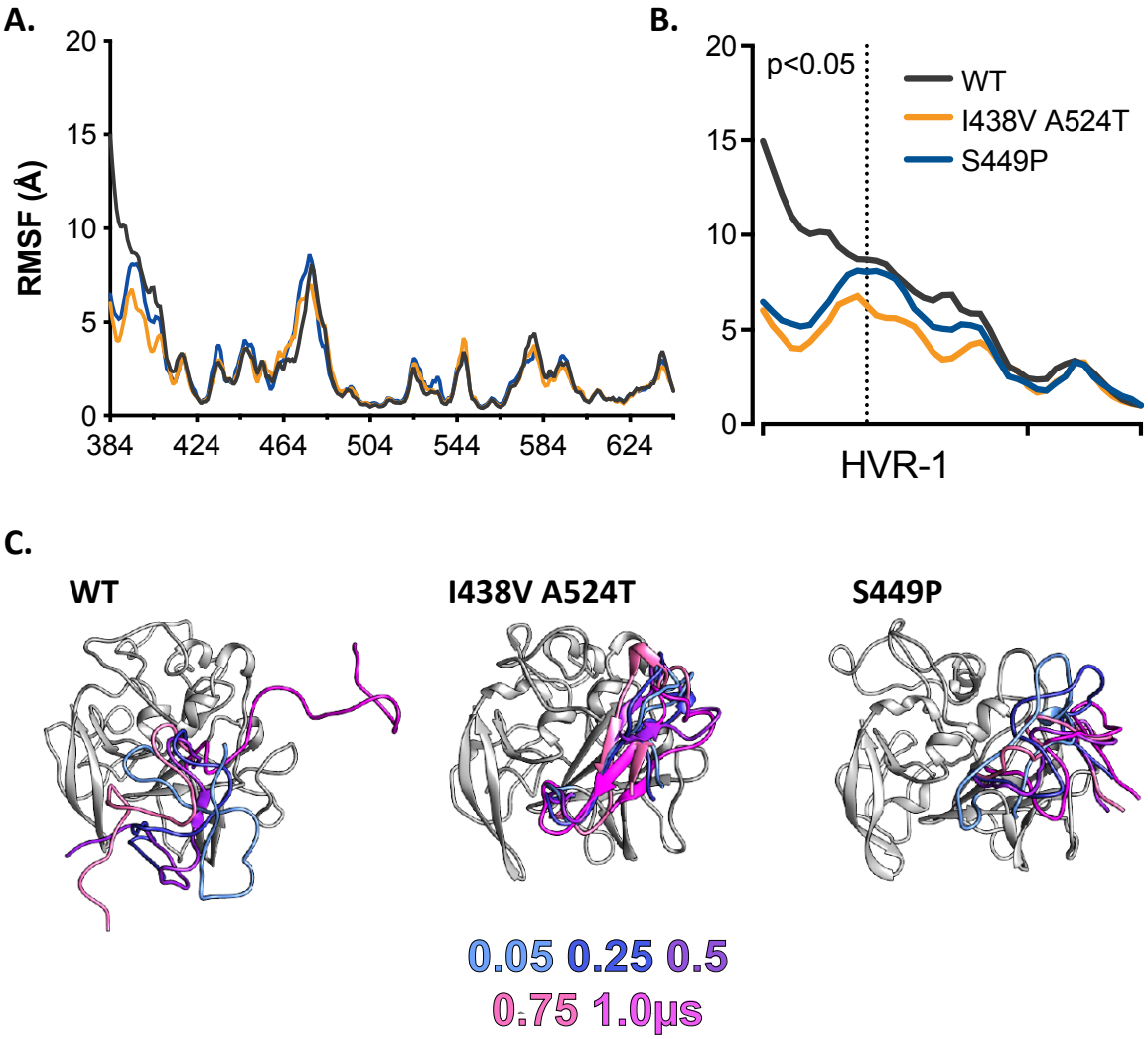

Figure 4.13. HVR-1 is stabilised in S449P E2. The conformational dynamics of WT, I438V A524T and S449P E2 ectodomains were explored by MD simulations. (**A**) Root mean square fluctuation (RMSF) of the three E2, from five independent experiments, error bars indicate standard error of the mean. (**B**) Average RMSF of WT I438V A524T and S449P HVR-1. (**C**) Images summarising representative MD simulations of three E2. HVR-1 is colour coded according to time (as shown in key), the remainder of E2 is shown in grey for the t=0.05 µs frame only

4.7 Discussion

In this chapter, we propose that HVR-1 of HCV E2 possesses an entropic safety catch that regulates E1E2 reactivity, entry efficiency and antibody resistance. Our model suggests that, by constraining HVR-1, E2-SR-B1 interactions release the safety catch at the cell surface. Alternatively, HCV can evolve to pre-constrain HVR-1, therefore

de-suppressing E1E2 reactivity, however, this evolutionary pathway is blocked by neutralising antibody selection.

The safety catch model we are proposing is supported by over a decade of research into HCV entry. It has long been established that HVR-1 deletion renders HCV sensitive to neutralising antibodies (306,310,311,403,404). This originally led to the hypothesis that HVR-1 acts as a shield to occlude neutralising epitopes and the CD81 binding site. However, it has since become clear that the breadth in nAb sensitisation is not easily explained by a simple shielding model (311,346). Moreover, many studies have noted that polymorphisms arising during cell-culture adaptation confer altered SR-B1 dependency and sensitivity to neutralisation (205,379,405,406). Finally, data presented in chapter three and that from other studies strongly indicates that initial interactions with SR-B1 may act to prime subsequent events in HCV entry (219,400). The HVR-1 safety catch model sufficiently explains all the above observations. As such, this work likely provides some insights regarding the order and functional consequences of early E1E2-receptor binding events.

Curiously, HVR-1 deletion did not confer complete independence from SR-B1 mediated entry, even though E2-SR-B1 interactions are not possible in this virus (211). Considering SR-B1 is a lipoprotein receptor and HCVcc particles high LDL and VLDL content, it is very likely virion-associated lipoproteins contribute to cell surface attachment. Therefore, the residual SR-B1 dependency of ΔHVR-1 virus may reflect the lack of particle tethering through SR-B1-apolipoprotein interactions. It was previously suggested LDL-R and SR-B1 play a redundant role in HCV entry (218). Nonetheless, we did not consider the contribution of LDL-R in our investigations as LDL-R does not interact directly with E1E2. Furthermore, the hyperreactive phenotype was recapitulated in HCV pseudoparticles, a system where LDL-R dependent virion tethering through apolipoprotein interactions is impossible.

Our model implies that HCV entry efficiency and nAb resistance are opposing selection pressures that are balanced via tuning of HVR-1 dynamics. Consistent with changes in E1E2 reactivity, various studies have identified E2 polymorphisms in patients that alter antibody sensitivity, receptor usage and infectivity when evaluated in cell culture (205,393,407). This would suggest that HCV responds to emergent nAb responses by trading reductions in entry efficiency for increases in nAb resistance. Therefore, the HVR-1 safety catch likely represents an adaptation to the ongoing immune assault in chronic infection. Indeed, sequence alignment with E2 from closely

related hepaciviruses (e.g., equine hepacivirus) suggest that HVR-1 was acquired at, or before, HCV's emergence as a human virus. Fittingly, unlike HCV, equine hepacivirus (EqHV) has an acute resolving course and immune protection lasts at least a year and attenuates subsequent infections (408). This highlights HVR-1 not only as a feature by which HCV can resist immune assault but also one that contributes significantly to the virus' ability to establish chronicity.

HVR-1 is an immunodominant target for antibodies, but as HVR-1 is also highly unstable at the genetic level, it can quickly accumulate mutations to escape nAb responses during infection (400,409). Polymorphisms here not only permit for the evasion of HVR-1 specific responses, they can also protect the virus from antibodies targeting distal epitopes, including the front layer (346). Our model would suggest that disorder and conformational entropy are critical for HVR-1 function. This feature likely underpins its ability to tolerate such extensive variation. Whereas antigenic variation driven by nAb selection is detrimental to other functionally important E2 regions (17), it's that likely continuous antigenic drift ensures that the disorder of HVR-1 is maintained as the disease progresses. This provides a potential feedback system where positive selection by HVR-1 specific antibodies promotes its conformational entropy, thus sustaining the safety catch mechanism.

Unlike the I438V A524T mutations, deletion of HVR-1 did not improve binding to CD81, which was surprising given the reactivity of ΔHVR-1 HCV exceeds that of the double mutant. This suggests that although CD81 binding is enhanced for I438V A524T HCV, it is the reduction in SR-B1 dependency that underpins hyperreactivity and speeds up entry kinetics (Fig 3.9). Indeed, it appears E1E2 hyperreactivity is not naturally accompanied by improved engagement to CD81. Enhanced CD81 binding is reflective of where the two mutations map to, the front layer (I438V) and CD81 binding loop (A534T). Still, the epitopes encompassing the CD81 binding site are flexible despite consisting of highly conserved residues (322,323,363). Thus, it is possible that HVR-1 configurations regulate the conformational landscape of the CD81 binding site, and that these states may have different affinities for the receptor. As such, the fold with enhanced CD81 affinity may be inaccessible in the absence of HVR-1.

A better understanding of the structure-to-function relationship of E1E2 will inform rational vaccine design. Our work highlights the importance of HVR-1 in regulating E1E2 reactivity and warrants its inclusion in B cell immunogens. Guided by the notion that HVR-1 acts as an epitope shield, Law et al immunised mice with ΔHVR-

1 E1E2 and found it to be inferior to WT E1E2 (410). This reduction in immunogenicity may reflect the transition of E1E2 to a non-functional state. Our data suggest that it will spontaneously inactivate without the constraint of the HVR-1 safety catch mechanism. Furthermore, ΔHVR-1 E1E2 immunisation induced dampened cross-genotype protection in the same study. This again provides evidence for HVR-1 regulating the folding states of CD81 binding epitopes since cross neutralising responses are principally directed toward the front layer and the CD81 binding loop. Vaccine development studies for other viruses suggest that locking entry proteins in a prefusion state elicits potent nAb responses (252,411–413). Thus, engineering the HVR-1 safety catch to improve E1E2 stability may be a viable strategy for HCV immunogen design.

To summarise, we report that HCV has a safety catch in place to regulate E1E2 reactivity. This feat allows it to balance the opposing selective pressures of efficient entry and nAb resistance. Although intrinsically disordered protein tails that regulate protein function have been observed in eukaryotes (414,415), this is the first account of one regulating viral entry/fusion events. Further afield, it is possible convergent evolution may have led other viral entry proteins to acquire safety catches as a way to resist nAbs (416). Overall, this work puts forward a novel mechanism with regards to the early steps of HCV entry. However, there are many gaps yet to fill regarding the molecular description of E1E2 function, from receptor binding to fusion pore formation. Filling these will not only inform rational vaccine development but also likely reveal a novel fusion mechanism.

5 Optimising cell systems for the investigation of E1E2 glycoproteins.

5.1 Introduction

Since viruses are genetically diverse it is imperative that experimental systems have the capacity to include many isolates allowing for comprehensive assessment of the effectiveness of therapeutic and prophylactic interventions (417–419). There are two major systems to assess HCV infection in vitro: HCV pseudoparticles (HCVpp) and cell-culture derived HCV (HCVcc). HCVpp are based on a disabled retroviral construct, which encodes a reporter gene and incorporates the HCV glycoproteins E1 and E2 in their lipid envelope (281,420). HCVcc are full-length replicative viruses generated by the introduction of in vitro transcribed RNA genome in to permissive cells; HCVcc are typically based on the JFH-1 clone or chimeras consisting of the JFH-1 replicase genes NS3-NS5B and Core-NS2 regions of alternative HCV genomes (282,283,421).

The HCVcc system represents a more physiological model of infection and allows for a broader study of the HCV life cycle (422). However, this system still largely depends on JFH-1 chimeras, which often rely on culture adaptation for optimal infectivity, and has challenging production and handling protocols given its biosafety level III designation in most regions (423). In contrast, producing HCVpp is a relatively simple task and the ease of handling allows for the simultaneous generation of a multitude of clones if one requires (424). The major disadvantage of HCVpp is that their application is limited to studying viral entry. Regardless, due to its flexibility, the HCVpp system is preferred for characterising neutralising antibody breadth, an essential component for screening HCV vaccine candidates. To this end, Wasilewski and colleagues recently observed a very strong positive correlation between the relative neutralisation resistance of E1E2-matched HCVcc and HCVpp variants indicating that either system can be used to phenotype neutralising antibodies (425). Furthermore, diverse HCVpp panels were key in identifying the relationship between the development of broadly neutralising antibodies (bNAbs) and spontaneous clearance of HCV infection (16–18).

Another important tool for studying HCV entry and vaccine development is a soluble form of its glycoprotein E2 (sE2), which is devoid of its transmembrane region and is expressed in the absence of E1. Screenings based on sE2 binding to human hepatoma cell lines identified the first two HCV entry receptors as being the tetraspanin CD81 and scavenger receptor class type B 1 (SR-B1) (211,381). sE2

retains proper folding as evidenced by its ability to recapitulate HCV binding to CD81 and SR-B1, block HCVcc infection and bind various antibodies (301), thereby allowing for functional, structural and biophysical characterisation of E2.

HEK 293-derived cell lines are extensively used to produce many recombinant proteins and pseudoviruses, including sE2 and HCVpp. HEK 293 cells express CD81 (222,223), therefore it is possible that it may affect the functionality and antigenicity of pseudovirus and/or sE2 by interacting with E2 in the cytoplasm during production. Here, we generate a novel 293T cell line knocked out for CD81 expression ($293T^{CD81KO}$). Producing HCVpp in this cell line significantly improved or rescued the infectivity of the majority of clinical isolates screened (15) without altering particle antigenicity. Finally, we show that while sE2 molecules produced in $293T^{CD81KO}$ and 293T cells are very similar, they show enhanced binding to anti-E2 antibodies when compared to sE2 produced in Freestyle 293-F cells (293-F); another 293-derived cell line preferred for the large-scale production of viral glycoproteins (426–428).

5.2 293T cells produce substantial quantities of extracellular CD81

Our study was initiated following an observation we made during routine experiments: conditioned media taken from 293T cells contains a high level of CD81. Figure 5.1 displays extracellular CD81 in filtered conditioned cell-culture supernatant from two cell lines extensively used in HCV research (the Huh-7 and 293T cell lines). We detected CD81 in both 293T and Huh-7 conditioned supernatant, although the former contained considerably more (Fig 5.1). The extracellular source of CD81 is likely to be exosomes: small extracellular vesicles formed by the inward budding of the late endosomal membrane. They measure 30-120 nm in size and are composed of proteins, lipids, nucleic acids and other metabolites. Notably, their surfaces are highly enriched in tetraspanins such as CD81, which consequently serves as an exosome biomarker.

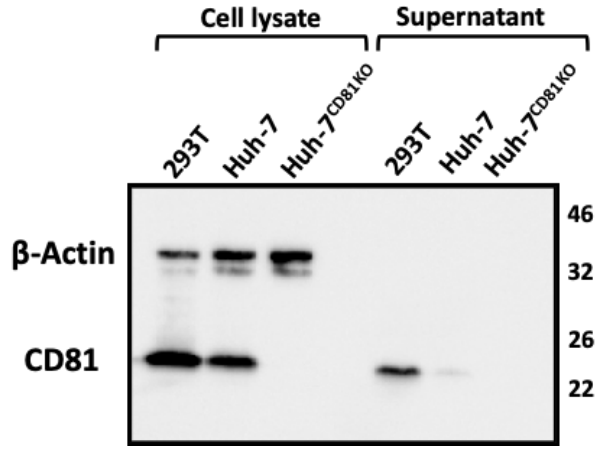

Figure 5.1. Detecting CD81 in culture conditioned supernatant. Cell lysates and unconcentrated conditioned supernatant of cell lines involved in HCV research were analysed by SDS-PAGE and Western blot with a specific anti-CD81 antibody (note: a CD81 knockout Huh-7 line is included as a negative control).

We next sought to determine if the extracellular source of CD81 was exosomes. First, we subjected 293T conditioned supernatant to incremental ultracentrifugation, thereby separating extracellular vehicles (EV) according to physical properties, including mass and size. The final pellet was then resuspended in PBS and probed for exosomal markers by western blot. We detected CD81 in the pellet along with four other markers: EpCaM, CD9, Flotilin-1 and Alix (Fig 5.2 A). We also examined the EV pellet for CD81 levels by fluorescence microscopy and found it was abundant with the tetraspanin (Fig 5.2 B). These data indicate 293T cells secrete extracellular CD81 and that this is likely in the context of exosomes.

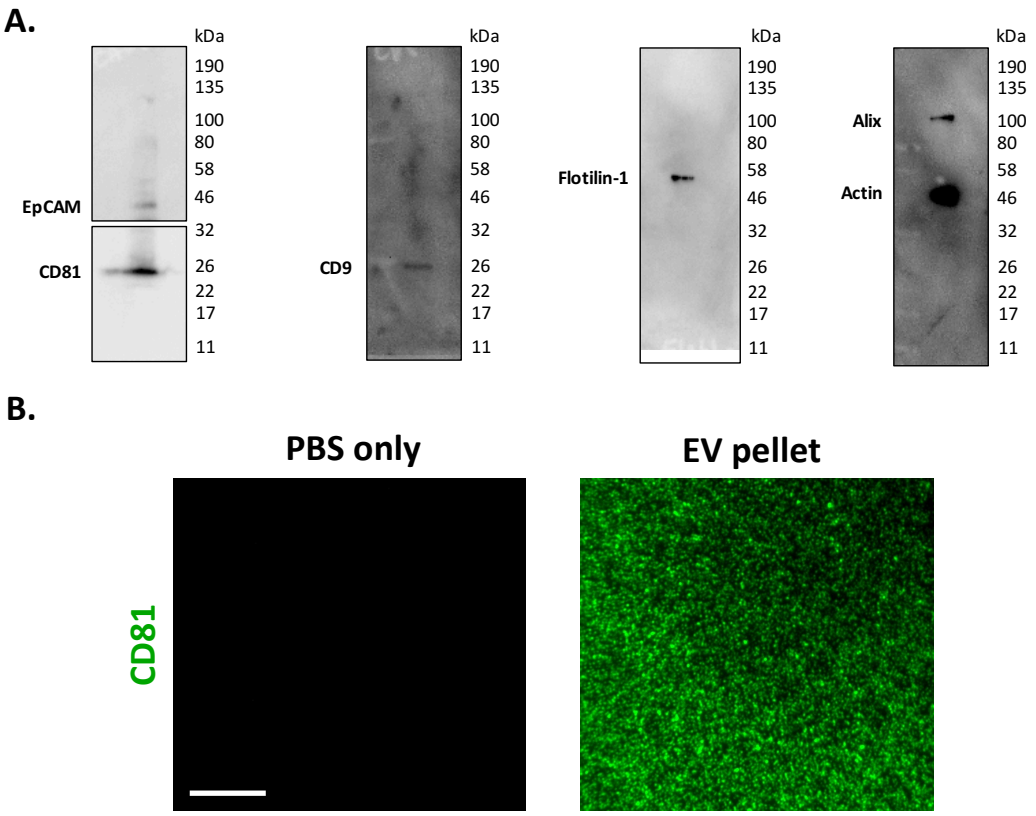

Figure 5.2. 293T conditioned supernatant contains exosomes. Conditioned supernatant was centrifuged sequentially at 300xg, 2000xg, 10,000xg and 100,000xg. The final pellet was resuspended in PBS and probed for exosomal marker expression. (**A**) The resuspended pellet was analysed by SDS-PAGE and Western blot. Blot were probed using a commercial exosome marker kit. (**B**) Micrographs of slides incubated with PBS or resuspended EV pellets and stained for CD81. Scale bar = 5 μm.

5.3 HCVpp made in CD81 knock-down 293Ts show enhanced infectivity

Having confirmed 293Ts produce exosomes, we theorised that they may complex extracellularly with HCV particles through interactions between CD81 and E2, and that this may be detrimental for HCVpp infectivity. To test this, we screened the infectivity of a panel of HCVpp produced in 293T cells treated with siRNA targeting CD81 (Fig 5.3 A). We consistently observed greater infection of Huh-7 cells for HCVpp produced in CD81 knockdown 293T cells (CD81-2) compared to their E1E2 matched equivalents produced in non-targeted pool siRNA (NTP-2) treated 293T cells (Fig 5.3 B). Collectively, CD81 knock-down led to a two-fold increase in infection for viruses in the panel (Fig 5.3 C) indicating that the expression of CD81 in 293T cells affects HCVpp production.

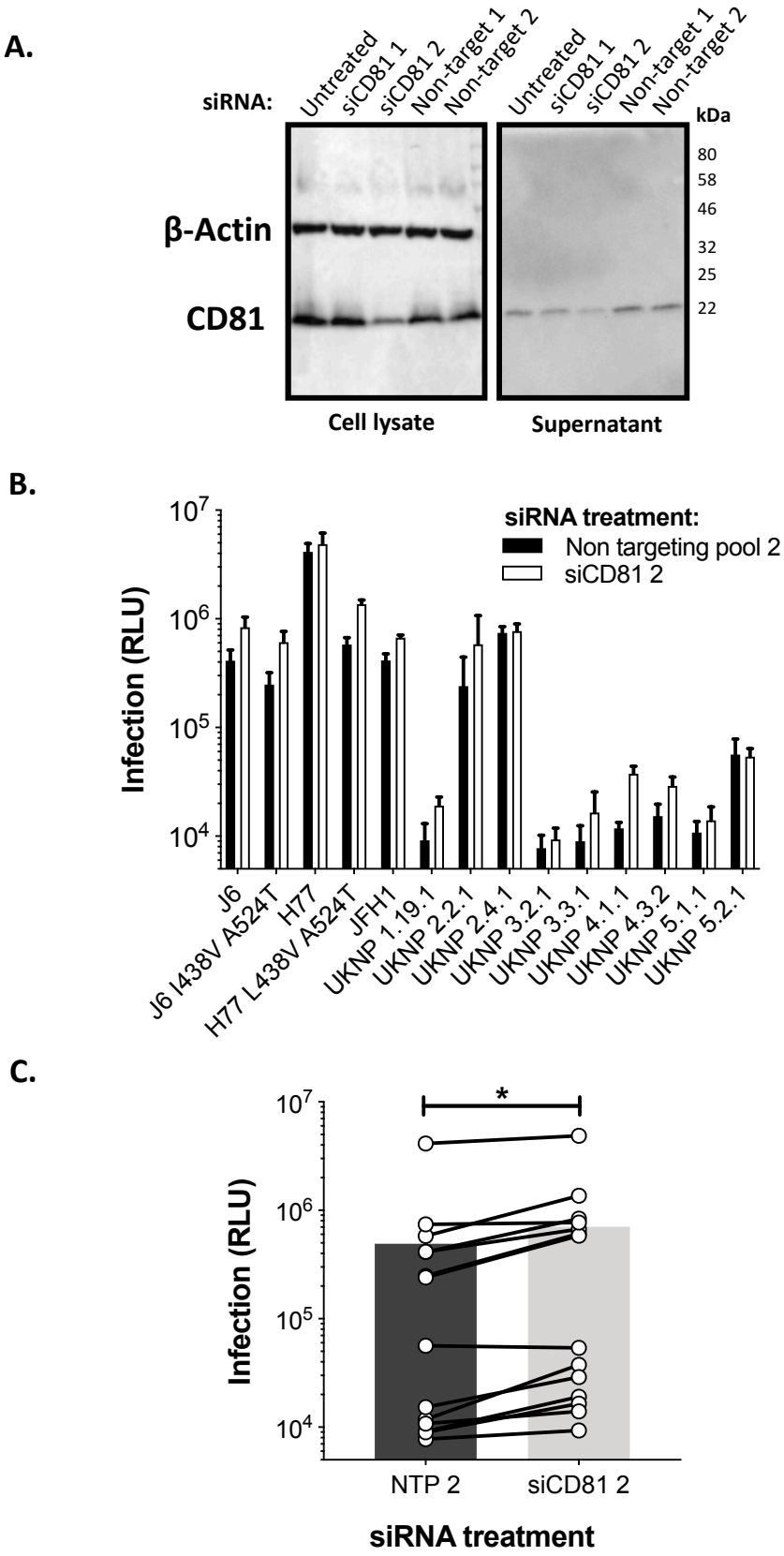

Figure 5.3 Knockdown of CD81 in producer 293T cells increases HCVpp infectivity. (**A**) Cell lysates and unconcentrated conditioned supernatant of 293T cells transfected with either a CD81 targeting pool or a non-targeting pool (NTP) of siRNA were analysed by SDS-PAGE and Western blot. Molecular mass markers are indicated on the right (kDa). Continued on next page.

Figure 5.3 legend continued. (**B**) Huh-7 cells were infected with an HCVpp panel consisting of 14 E1E2 clones produced in 293T cells exhibiting appreciable CD81 knockdown (white bars) or 293T cells treated with a non-targeting siRNA pool (NTP-2) (black bars). Data are represented as raw luciferase units (RLU) and are from a single experiment performed in triplicate. Error bars indicate the standard deviations between three replicate wells. (**C**) A compiled summary of the data shown in **B**, connected points indicate a single E1E2 clone and the grey bars represent the mean RLU of all clones. Paired t-test, asterisks denote statistical significance.

5.4 Generation of CD81 knock-out HEK 293T cells

Following the above observations, we decided to generate stable cell lines ablated of CD81 expression as they could be a useful resource for the production of HCVpp (15,429). To delete CD81, we engineered 293T cells with the CRISPR-Cas9 gene-editing system. We were able to sort edited cells by flow cytometry to obtain pure CD81 negative populations (coloured boxes in Fig 5.4 A) since it is a cell surface receptor. Sorted cells were then diluted to obtain single-cell clones and expanded (Fig 5.4 B) until we obtained two stable cell lines: $293T^{CD81KO}$ guide 1 and guide 3 (g1 and g3) (Fig 5.4 C). In addition to producing HCVpp, conditioned supernatant from these cells could help us establish if HCVpp and $CD81^{+}$ exosomes interactions neutralise particle infectivity.

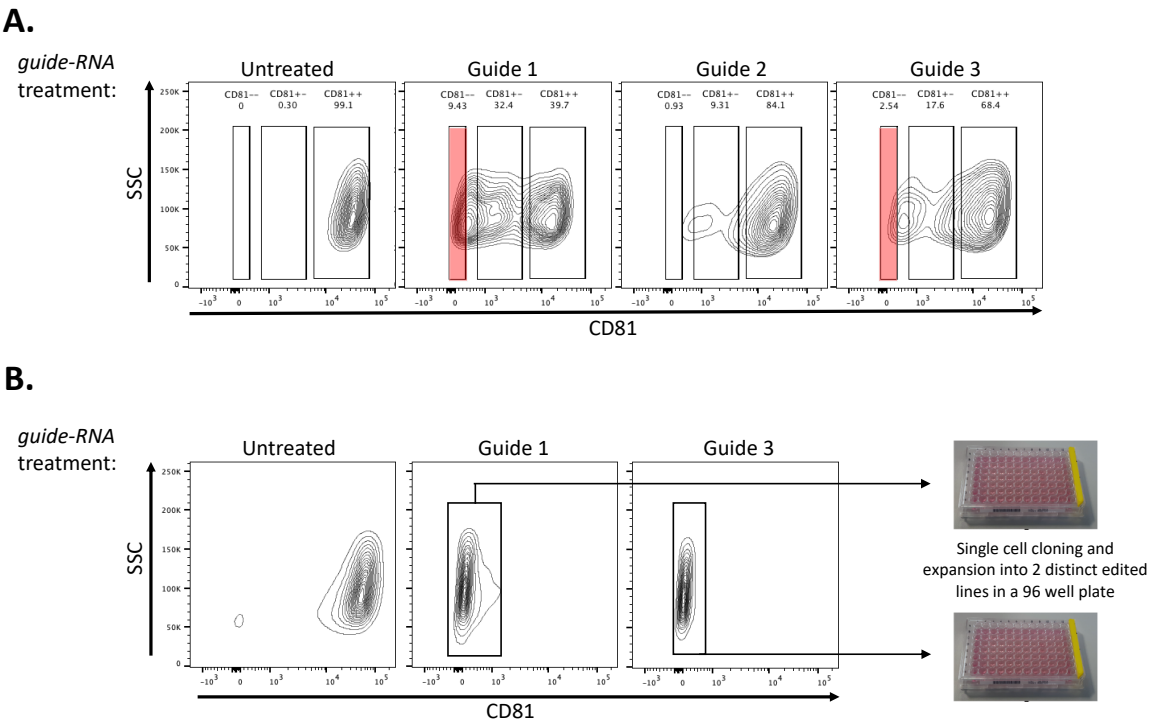

Figure 5.4. Generation of CD81 knock-out 293T cells using CRISPR. 293T cells were transfected with CRISPR Cas9 gene-editing components along with one of three guide RNAs (sgRNA) targeting the CD81 exon. **(A)** 72 hours later cells were sorted using flow cytometry to obtain CD81 double negative populations (CD81-/-) (red coloured boxes). **(B)** Cells that received sgRNAs guides 1 and 3 were then expanded for 48 hours before dilution for single cell cloning and expansion in a 96 well plate. (**C**) CD81 ablation was confirmed by SDS-PAGE and Western blot analysis.

5.5 Deletion of CD81 in 293T cells enhances or rescues infectivity of patient-derived HCVpp

To comprehensively determine whether CD81 deletion enhanced HCVpp infection, three independent labs screened the infectivities of HCVpp produced in parental 293Ts and CD81 knock-out cell lines. Firstly, a panel consisting of both prototypical strains (e.g., J6 and H77) and clinical isolates was made in the aforementioned cell

lines. We consistently observed higher infection across the panel for HCVpp harvested from both 293T^{CD81KO} lines (g1 and g3) compared to matched viruses made in parental cells (Fig 5.5 A-C). As the infectivities of HCVpp recovered from the two 293T^{CD81KO} cell lines were very similar (Fig 5.5 B), we chose the g3 CD81 knock-out lineage for subsequent experiments because it exhibited a more homogenous CD81$^{-/-}$ population after FACS sorting (see gating in Fig 5.4 B). These cells are, henceforth, referred to as 293T^{CD81KO}.

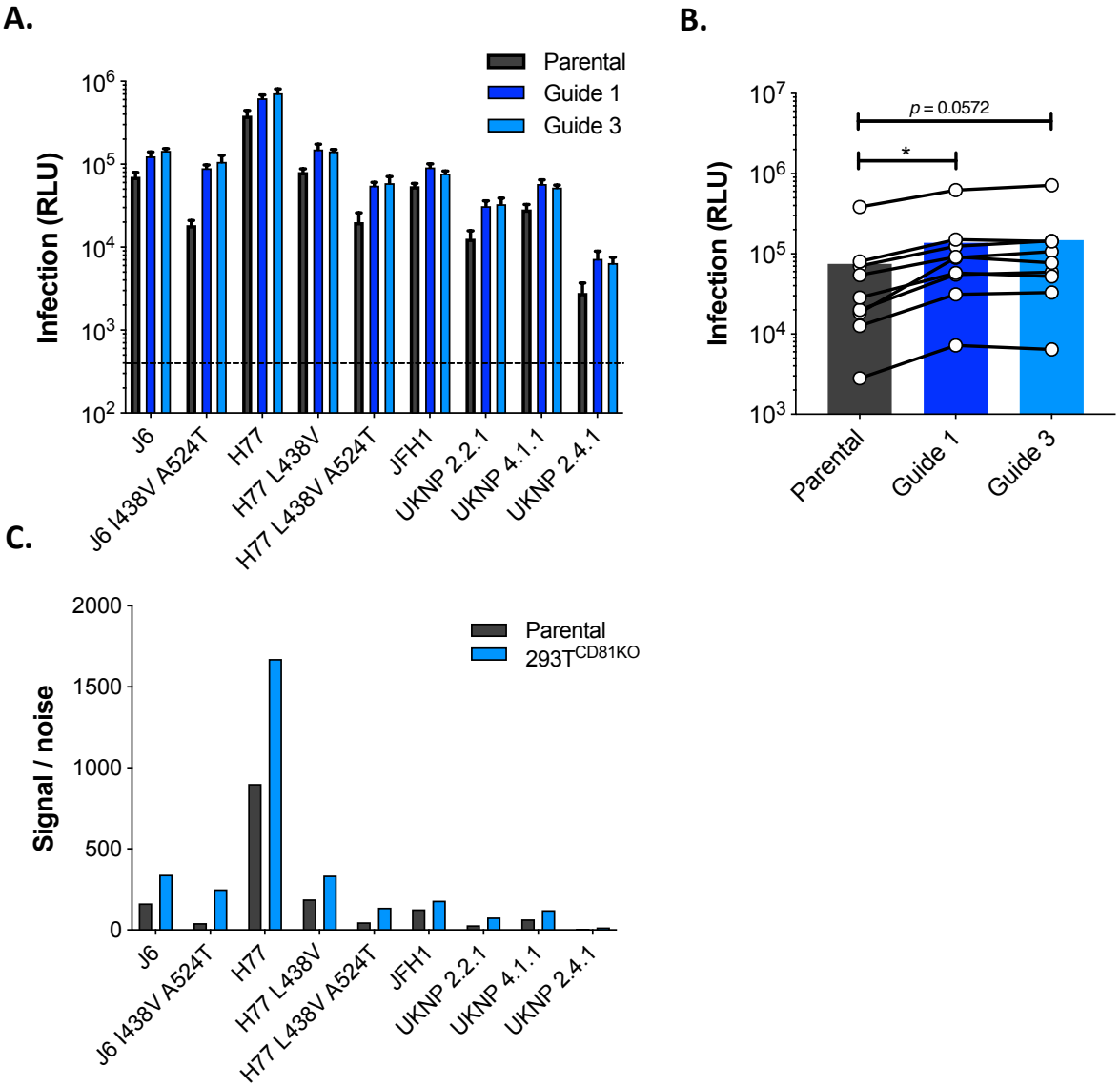

Figure 5.5. HCVpp made in CD81 knock-out 293T cells exhibit enhanced infectivity. Huh-7 cells were infected with HCVpp produced in parental or 293T^{CD81KO} cell lines. **(A)** The infection levels for each clone in the UCL panel which consists of prototypical, lab observed and clinical isolates. (**B**) A compiled summary of the infection levels for the UCL HCVpp panel. Connected points indicate a single E1E2 clone and the coloured bars represent the mean value. Paired t-test with virus produced in parental 293Ts, asterisks denote statistical significance. **(C)** Calculated signal-to-noise ratio (S/N) for the panel. Note, only S/N of virus made in 293T^{CD81KO} g3 cells is included.

The next screen was of a panel of HCVpp expressing patient-derived E1E2 observed in patient cohorts from hospitals in Amsterdam (32 and unpublished) or Nottingham (431). Here, the improvement in infection for HCVpp produced in 293T^{CD81KO} cells compared to their equivalents made in parental cells was more apparent (Fig 5.6 A & B). We observed a five-fold increase in infectivity for four of the tested clones, and this effect reached ten-fold for the UKNP 5.2.1 clone. The enhancement of infectivity is best demonstrated in the summary of the signal-to-noise ratio, where a three-fold increase in S/N is observed for the panel collectively (Fig 5.6 D).

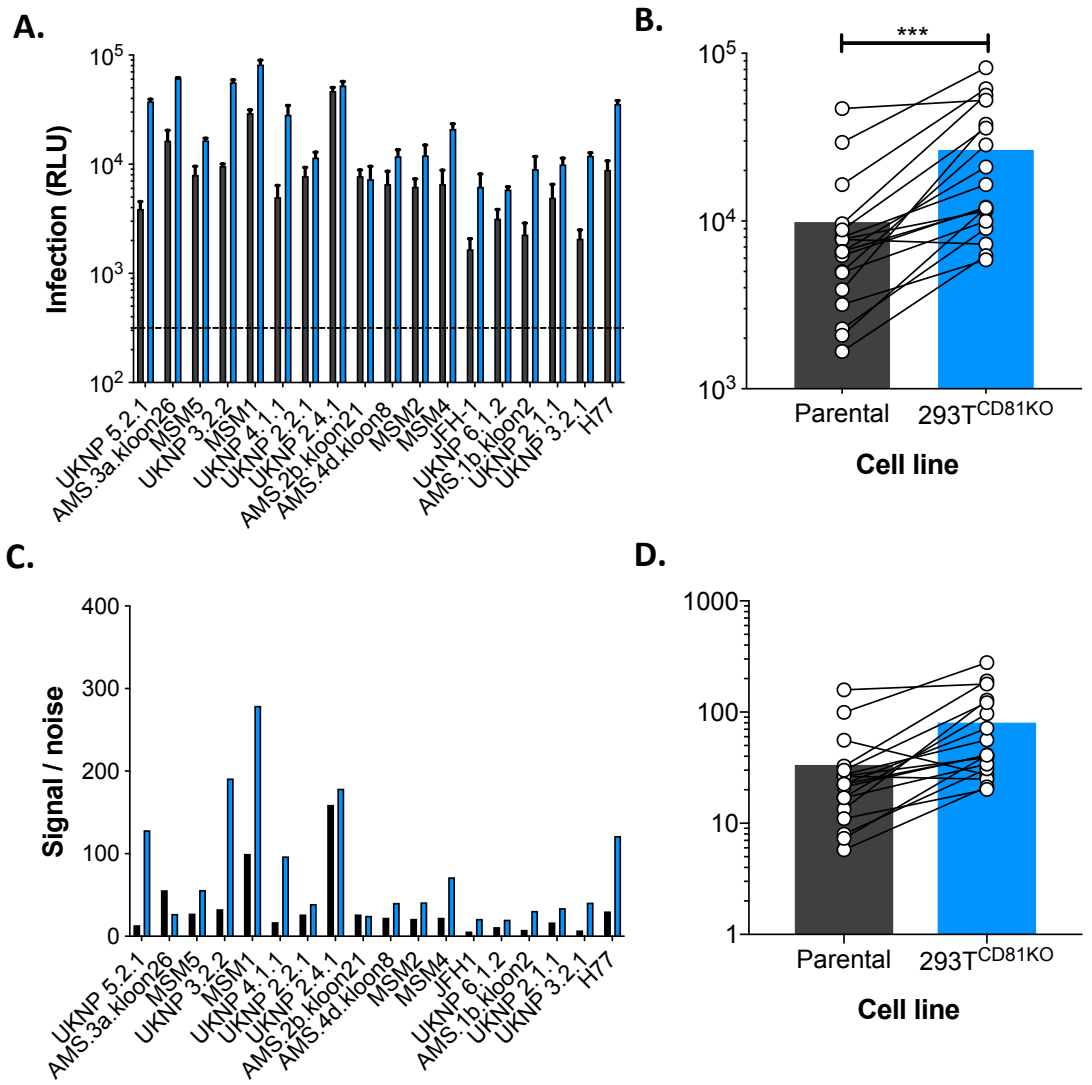

Figure 5.6. HCVpp made in CD81 knock-out 293T cells exhibit enhanced infectivity. Huh-7 cells were infected with HCVpp produced in parental or 293T^{CD81KO} cell lines. **(A)** The infection levels for each clone in the AMS panel which consists of prototypical and clinical isolates. (**B**) A compiled summary of the infection levels for the AMS panel. Paired t-test with virus produced in parental 293Ts, asterisks denote statistical significance. **(C)** Calculated S/N for each clone in the panel. (**D**) A collective summary of the S/N for AMS panel. Connected points indicate a single E1E2 clone and the coloured bars represent the mean value. AMS data generated by Ana Chumbe.

Lastly, we made a panel of HCVpp expressing E1E2 observed in HCV^{+} individuals from the Australian Hepatitis C Incidence and Transmission Studies in prisons (HITS-p) cohort in the 293T^{CD81KO} cells (432). Following infection read-out, we used the signal observed in cells infected with a non-enveloped control to calculate S/N for each clone in the panel and compared it to a value previously obtained from when the clone was produced in parental 293Ts (Table S1). We saw an increase in the S/N for most clones when made in 293T^{CD81KO} cells. Strikingly, 5 of the 22 screened clones previously found to be non-infectious (15) were now infectious (S/N ≥ 5) and a further 8 of the 22 screened clones exhibited at least a five-fold increase in S/N (Table S1 and Fig 5.7 A). Finally, a comparison of calculated S/N for all screened clones from all three panels generally demonstrated an upward trend in infectivity for HCVpp following production in 293T^{CD81KO} cells (Fig 5.7 B). Taken together, the data in this section suggest the 293T^{CD81KO} cells we have produced could be a useful resource for HCV research.

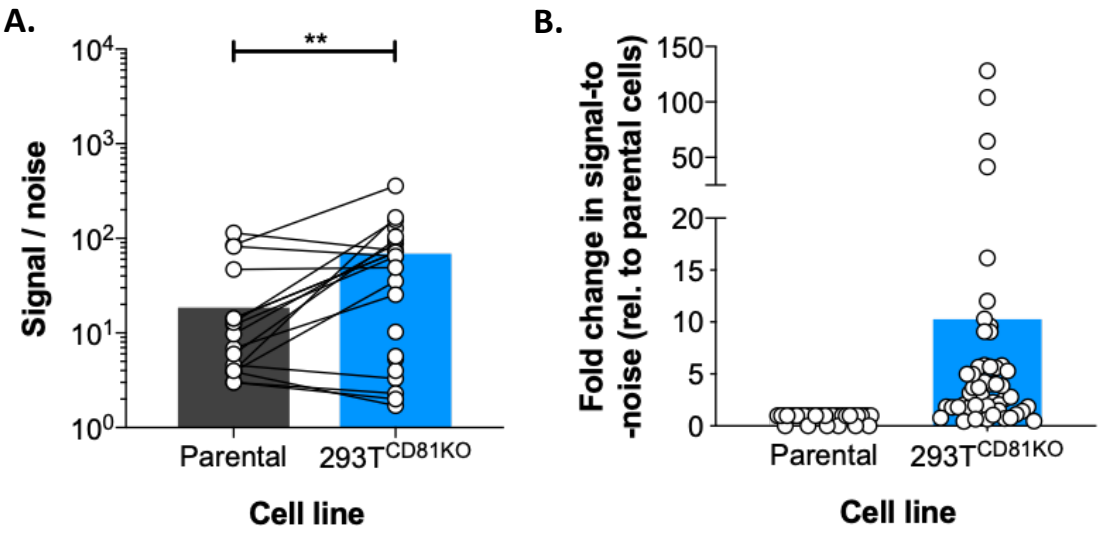

Figure 5.7. HCVpp made in CD81 knock-out 293T cells exhibit enhanced infectivity. Huh-7 cells were infected with HCVpp expressing produced in parental or 293T^{CD81KO} cell lines. (**A**) A compiled summary of the S/N of the HITS-p panel. Paired t-test with virus produced in parental 293Ts, asterisks denote statistical significance. Connected points indicate a single E1E2 clone and the coloured bars represent the mean value. **(B)** A compiled summary of the S/N for all screened clones, fold values are relative to virus produced in parental 293T cells. HITS-p data generated by Alexander Underwood.

5.6 Production of HCVpp in CD81 knock out cells does not affect virion entry pathway

Next, we sought to ensure deletion of CD81 in producer 293T cells did not affect the entry pathway of HCVpp. The E1 and E2 glycoproteins mediate the virus' intricate entry pathway. The E1 and E2 genes display the greatest diversity in the HCV genome, yet receptor interactions remain highly conserved across distinct genotypes and entry is widely understood to involve the essential receptors CD81, SR-B1, Claudin and Occludin (142,225). We infected Huh-7 cells ablated for these proteins (218) with HCVpp produced in parental or 293T^{CD81KO} cells. Whilst ablation of CD81, Claudin-1 and Occludin abolished infection for all four tested strains, a proportion of all strains was still able to infect SR-B1 knock-out cells (Fig 5.8). These data are consistent with previous findings for both HCVcc and HCVpp particles (218,219,433) and indicate pseudoparticles made in 293T^{CD81KO} cells follow the correct HCV entry pathway.

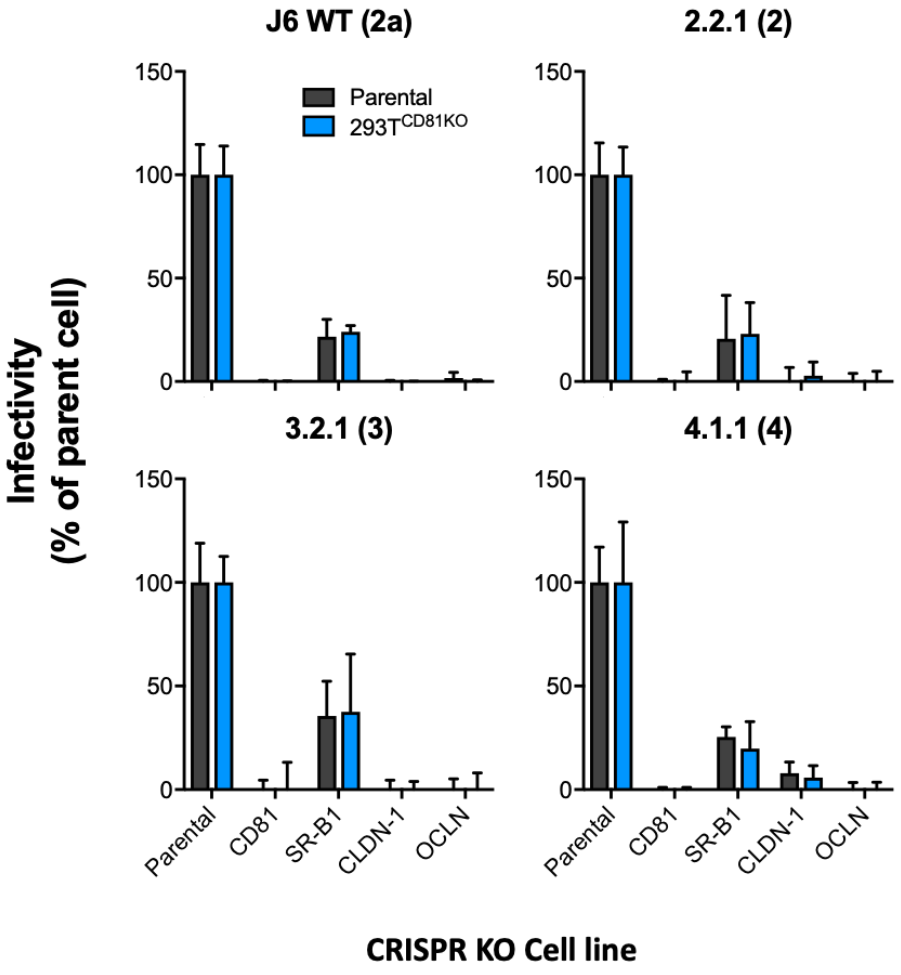

Figure 5.8. Receptor dependency of 293T^{CD81KO} produced HCVpp. Huh-7 cell lines CRISPR/Cas9 engineered to not express one HCV receptor were infected with HCVpp produced in parental or 293T^{CD81KO} cell lines. Data are expressed as a percentage of the infection observed in parental Huh-7 cells. Error bars indicate the standard deviations between replicate wells. Data are representative of two independent experiments performed in quadruplicate.

5.7 Exosomal CD81 does not affect HCVpp infectivity

The enhancement of infection following production in 293T^{CD81KO} cells suggests that E2 and CD81 interact at some point during the process of HCVpp production. One possibility is that exosomal CD81 neutralises HCVpp while in culture medium prior to viral harvest. To test this, we first preincubated a panel of HCVpp variants with centrifugally concentrated conditioned supernatant from parental or CD81KO 293T cells, which is CD81^{+ve} and CD81^{-ve}, respectively. We observed that all four strains were similarly affected following incubation with either CD81^{+ve} and CD81^{-ve} supernatant, irrespective of the cell line of production (Fig 5.9 A). Next, we challenged an acutely CD81 sensitive strain, J6 I438V A524T, produced in 293T^{CD81KO} cells, with a serial dilution of conditioned supernatant. Again, the pseudoparticles were similarly sensitive to CD81^{+ve} and CD81^{-ve} supernatant. These data suggest exosomal CD81 does not affect HCVpp infectivity. Therefore, enhancement of HCVpp infectivity following production in 293T^{CD81KO} cells may not be due to the elimination of neutralising extracellular CD81. In actuality, CD81 may affect HCVpp production intracellularly or during viral egress (see discussion).

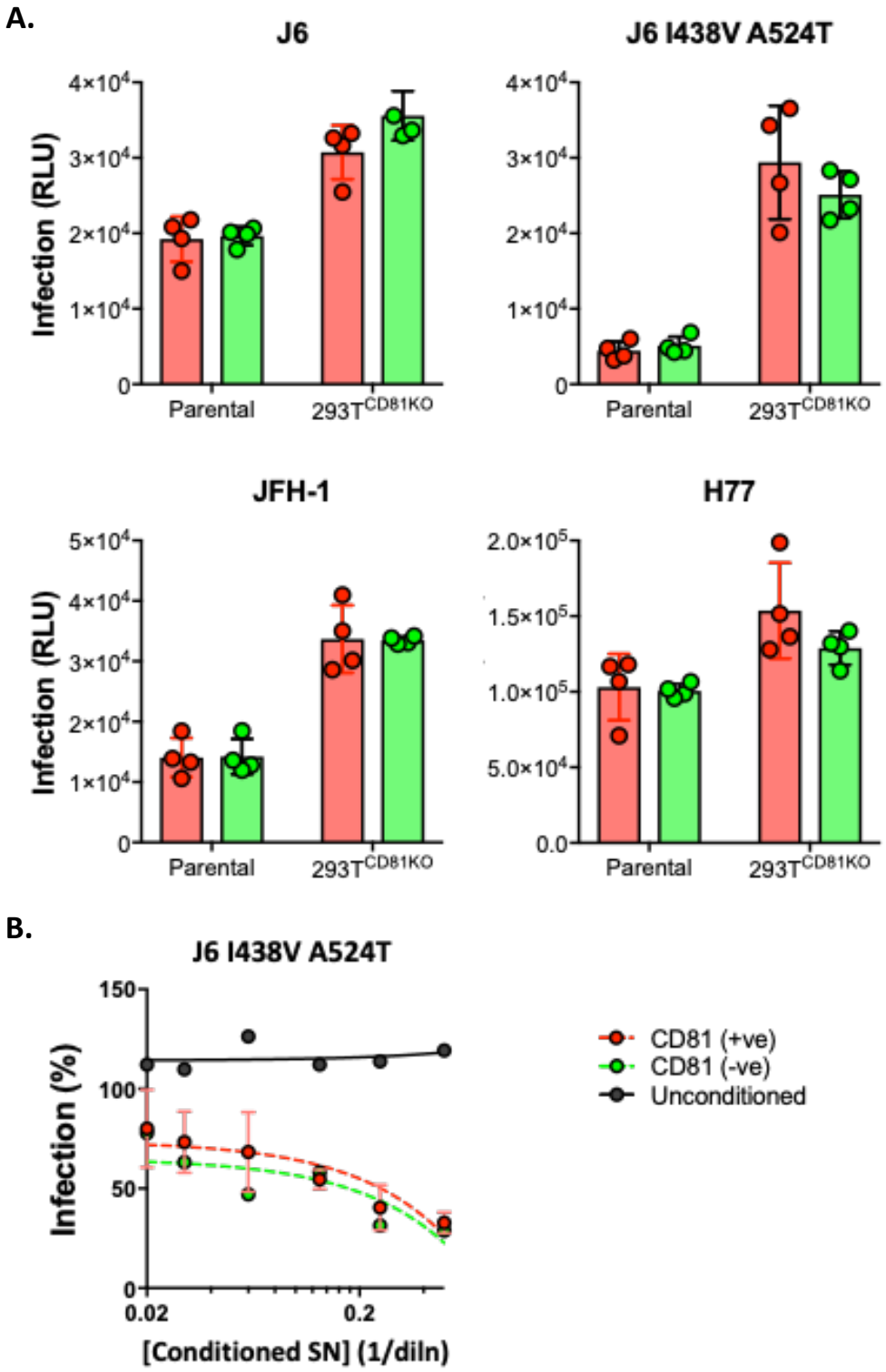

Figure 5.9. Conditioned supernatant from CD81^{+ve} cells does not neutralise HCVpp. HCVpp were preincubated with conditioned supernatant (SN) from CD81^{+ve} parental 293Ts or CD81^{-ve} 293T^{CD81KO} cells for 2 hours before infection of Huh-7 cells and infection levels were read 72 hours later. **(A)** A panel of HCVpp variants was preincubated with conditioned SN at 1/2 dilution. Data are represented as raw luciferase units (RLU) and the error bars indicate the standard error of the mean between four replicate wells. (**B**) J6 I438V A524T, a lab adapted strain shown to be acutely sensitive to soluble CD81, was challenged with a seral dilution of conditioned SN.

5.8 CD81 deletion in producer cells also improves SARS-CoV-1/2 pseudoparticle infectivity

To determine whether CD81 deletion in producer 293T cells specifically affects the infectivity of HCV, we produced lentiviral packaged pseudoparticles bearing the glycoproteins of Indiana vesiculovirus (VSV), Middle East respiratory syndrome-related coronavirus (MERS) and severe acute respiratory syndrome coronaviruses 1 and 2 (SARS-CoV 1 and SARS-CoV 2) glycoproteins in parental 293Ts or 293T^{CD81KO} cells. Following infection of the appropriate cell line, we observed no difference in the infectivity of VSV or MERS pseudoparticles when produced in 293T^{CD81KO} cells whereas the two HCV J6 strain viruses tested exhibited an improvement in infectivity, as expected (Fig 5.10). Remarkably, we also observed an increase in infectivity for both SARS-CoV 1 and 2 (Fig 5.10, bottom panels). These data indicate that whilst CD81 ablation in producer 293Ts does not improve the infectivity of all pseudoparticles, enhanced infection is not limited to HCVpp. However, it is difficult to speculate on the mechanism(s) of enhancement without further investigation.

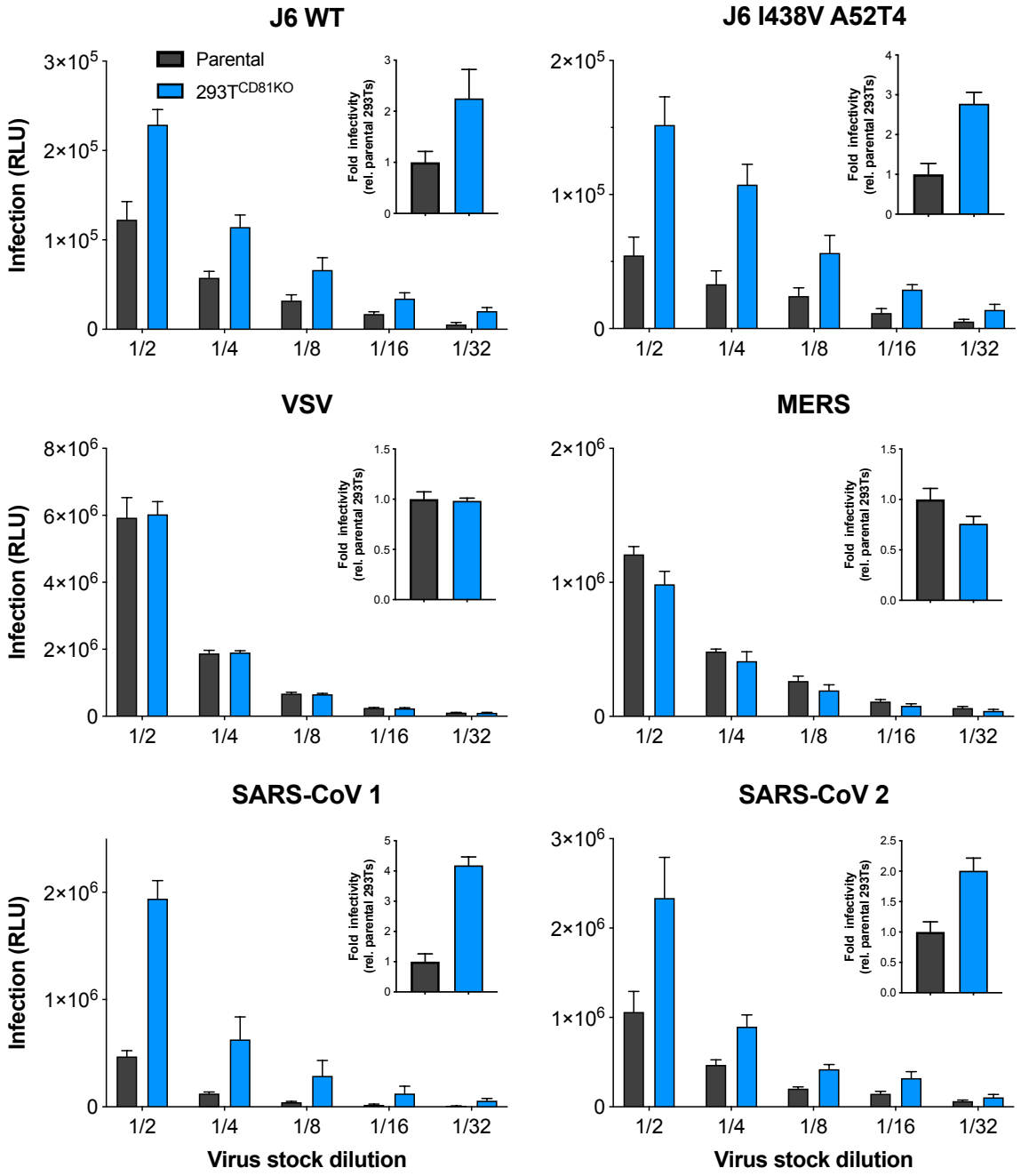

Figure 5.10. Effect of CD81 knockout on lentiviral-based pseudovirus infectivity. Huh-7 (HCV J6 and VSV), Caco-2 (MERS) and HeLa-Ace2 (SARS-CoVs) cell lines were infected with a two-fold serial dilution of viral pseudoparticles produced in parental or 293T^{CD81KO} cell lines. Data are represented as raw luciferase units (RLU) and the error bars indicate the standard deviations between five replicate wells. Insert graphs show the overall fold infectivity of pseudoparticles across all five concentrations used, data are presented relative to virus produced in parental 293Ts. Data are representative of two independent experiments.

5.9 Production in CD81 knock-out 293T cells does not alter HCVpp antibody sensitivity

HCVpp are widely used to examine the neutralising breadth and potency of monoclonal antibodies (mAbs) and polyclonal sera from humans and immunised animals (15,17). Before we could propose the routine adoption of 293T^{CD81KO} cells in said screens, it was imperative to ensure that HCVpp produced in these cells are antigenically similar to those produced in parental cells. First, we challenged H77 and UKNP 5.2.1 pseudoparticles with a serial dilution of AR3B, a bNAb that targets the CD81 binding site (CD81-bs) (339). We observed similar neutralisation for each clone irrespective of the cell line of production; indeed, the hyperbola curves generated for the H77 pair overlapped and, accordingly, their calculated IC_{50} was identical (Fig 5.11 A & B). We also challenged H77 and UKNP 5.2.1 pseudoparticles with a serial dilution of a soluble form of the large extracellular loop of CD81 (sCD81). As with AR3B, the IC_{50} of sCD81 toward H77 was indistinguishable regardless of the cellular source of the HCVpp (Fig 5.11 C). The IC_{50} of sCD81 toward the matched UKNP 5.2.1 HCVpp pair was also similar (Fig 5.11 D).

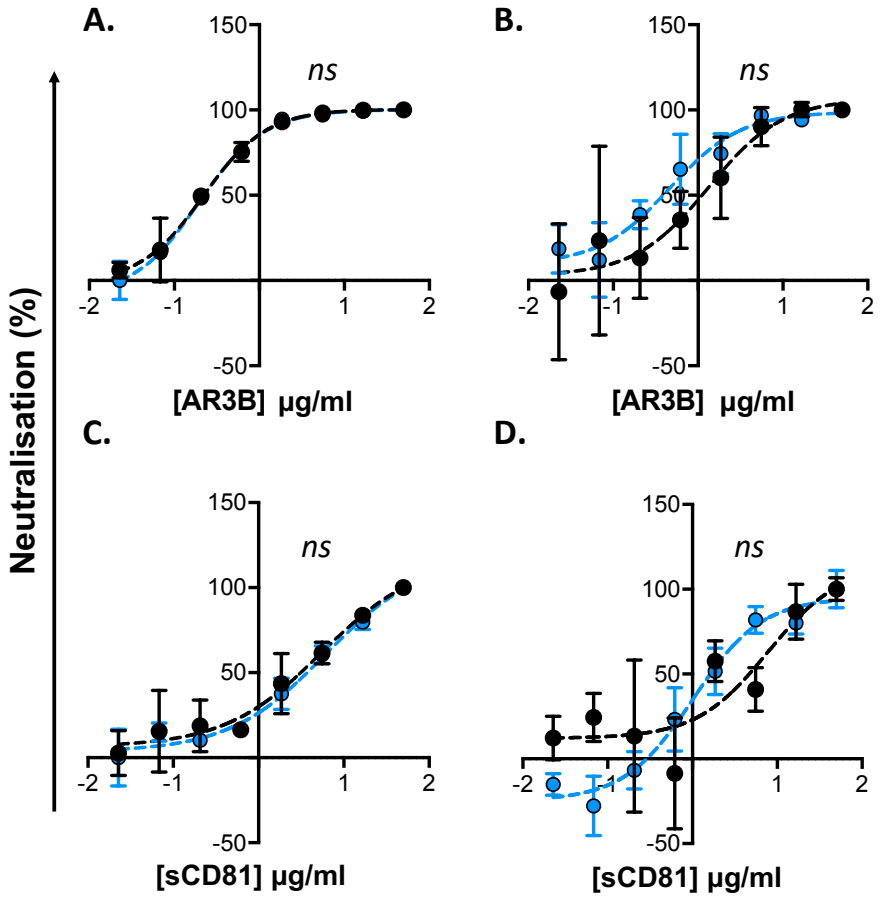

Figure 5.11. Absence of CD81 in producer 293T cells does not affect antibody and CD81 sensitivity of HCVpp. The prototypical lab strain (**A**) H77 and the clinical isolate (**B**) UKNP 5.2.1 were incubated with a serial dilution of the mAb AR3B prior to infection. The prototypical lab strain (**C**) H77 and the clinical isolate (**D**) UKNP 5.2.1 were incubated with a serial dilution of the sCD81 prior to infection. Data are expressed as percent neutralisation relative to wells not preincubated with antibody or receptor molecules and each point is the mean of three replicate values. The black and sky blue points are representative of parental and 293T^{CD81KO} cells, respesctively. Error bars indicate the standard deviations between replicate wells. Data were fitted using the log (inhibitor) vs. response (four parameters) function on GraphPad Prism. *ns* indicates best fit curves do not differ significantly, F-test.

Next, we compared the neutralisation of an HCVpp panel following incubation with a fixed concentration of AR3B. We found the infectivity of most clones was similar irrespective of the cell line of production and saw no significant difference for the panel as a whole (Fig 5.12 A). This experiment was conducted for an additional four mAbs: (i) AR4A, which targets an epitope composed of both E1 and E2 residues, (ii) AT-12009 (front layer), (iii) HC84.26 (front layer) and (iv) IgH505, which targets a discontinuous epitope in E1 (residues 313-327) (337,339,430,434). We saw no significant difference in the neutralisation levels of the panel against all four mAbs irrespective of the cell line of production (Fig 5.12 A). Similar observations were also made when pseudoparticles were pre-incubated with sCD81 (Fig 5.12 A). Finally, a scatter plot for data shown in figure 5.11 A revealed a very strong correlation for neutralisation sensitivity between HCVpp produced in 293T^{CD81KO} cells and HCVpp made in parental 293T cells (Fig 5.12 B). These data indicate ablation of CD81 in producer 293T cells does not change the sensitivity of pseudoparticles to neutralisation by sCD81 or mAbs. However, we did find a significant positive correlation (r = 0.58, p = 0.0092) between the sensitivity of HCVpp to sCD81 neutralisation and their fold increase in infectivity following production in 293T^{CD81KO} cells (Fig 5.12 C). This suggests that HCVpp that are sensitive to CD81 neutralisation benefit more from production in 293T^{CD81KO} cells. In summary, the data demonstrate that producing HCVpp in 293T^{CD81KO} cells does not alter their antigenicity or sensitivity to mAbs. These findings considered along with their ability to improve virus infectivity suggest that the 293T^{CD81KO} cell line is a superior system for assessing the functionality and neutralisation of diverse HCVpp.

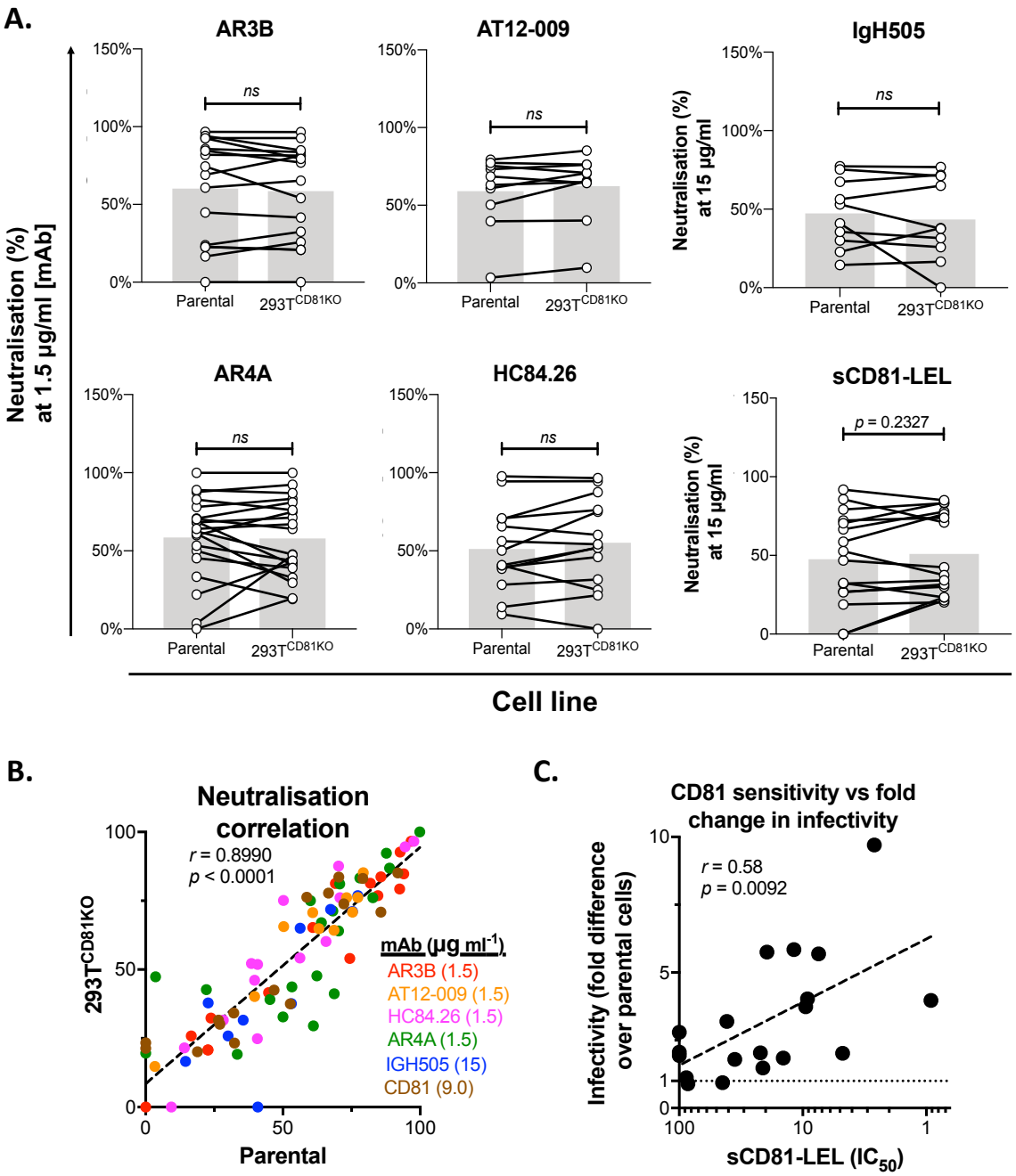

Figure 5.12. Absence of CD81 in producer 293T cells does not affect antibody and CD81 sensitivity of HCVpp. (**A**) Compiled summaries of the neutralisation of HCVpp panels when challenged with a single concentration of the indicated mAb or soluble protein prior to infection. Connected points indicate a single E1E2 clone and the grey bars represent the mean value. Paired t-test, no significance (ns). (**B**) A scatter plot of the percentage neutralisation for a panel of HCVpp clones produced in parental 293T cells (x-axis) vs when produced in 293T^{CD81KO} cells (y-axis) after challenge with a single concentration of indicated mAb or sCD81. (**C**) A scatter plot of HCVpp CD81 sensitivity (sCD81 IC_{50}) (x-axis) and fold change in infectivity following production in 293T^{CD81KO} cells (y-axis). Each point in **B** and **C** represents a lone HCV isolate. Spearman correlation (*r*) and *p* values were computed on GraphPad Prism. All data are from lone experiments performed in triplicate. Data generated by Ana Chumbe.

5.10 Soluble E2 made in 293Ts displays a mixture high-mannose and complex-type glycans

HEK 293T cells are commonly used for the production of sE2. Consequently, we examined whether 293T^{CD81KO} cells improve sE2 production, as they did HCVpp production, without altering the properties of the resultant protein. To do this, we first adapted the 293T^{CD81KO} and parental 293T cell lines to grow in suspension, which makes the cells more suitable for large-scale protein production. We refer to these cell lines as susp-293T and susp-293T^{CD81KO} cells. We used conventional transient transfection to produce sE2 in these two cell lines. In parallel, we also compared these to sE2 generated in the 293-F cells. Although this cell line is also derived from HEK 293 cells, and grows in suspension, it is preferred for the production of recombinant viral glycoproteins, including those of HIV-1, influenza and HCV, because of the high production yields (426,427,435). We isolated sE2 monomers from harvested supernatants using affinity purification followed by size exclusion chromatography (SEC). Very similar yields of sE2 were obtained following purification of harvested susp-293T^{CD81KO}, susp-293T (both ~14 mg/L) and 293-F (12 mg/L) supernatant, although relatively more aggregates were observed in sE2 from the susp-293T lineages. Furthermore, the retention volumes for monomeric sE2 made in susp-293T^{CD81KO} and susp-293T cells were practically identical (~13.1 ml) yet monomeric sE2 produced in 293-F cells eluted at a lower volume (~12.3 ml) suggesting it is larger than that produced in the susp-293T cell lines (Fig 5.13 A). Indeed, SDS-PAGE analysis of unfractionated sE2 and their monomeric peak fractions, under both reducing and non-reducing conditions, revealed sE2 made in 293-F cells migrated more slowly than sE2 from the two susp-293T lines (Fig 5.13 B). These data suggest that sE2 undergoes distinct post-translational modifications in 293-F and 293T cells.

Up to 11 Asn-linked glycosylation sites can be detected in most E2 sequences and fully processed E2, in both its soluble form or in the context of viral particles, is heavily glycosylated and displays a mixture of high-mannose and complex-type glycans (153,435). As a result, the molecular mass of E2 is significantly influenced by glycans. To test whether differences in glycosylation account for the disparate molecular weight between sE2 from 293T and 293-F cells, we treated purified monomeric sE2 with PNGase F or EndoH deglycosylation enzymes. PNGase F cleaves both high-mannose and complex-type glycans yielding a mostly

deglycosylated protein whereas Endo H specifically cleaves high-mannose and some hybrid glycans.

We compared sE2 produced in 293-F cells to susp-293T^{CD81KO}-derived sE2 (glycoprotein produced in either the edited or parental 293T cells migrated identically suggesting their glycosylation status is similar, Fig 5.13 B). As expected, PNGase F treatment confirmed sE2 made in both susp-293T^{CD81KO} cells and 293-F cells to be heavily glycosylated. Undigested sE2 migrated to around ~65 kDa and its deglycosylated form migrated to ~35 kDa irrespective of the cell line of production (Fig 5.13 C). Strikingly, the sensitivity of sE2 from 293-F and susp-293T^{CD81KO} cells to EndoH treatment was different. sE2 made in 293-F cells was mostly unaffected by EndoH treatment as evidenced by the similar migration observed for the untreated and EndoH digested samples (Fig 5.13 C). This suggests that 293-F-produced sE2 is composed of mostly complex-type glycans, a hallmark of maturation through the Golgi apparatus. On the other hand, sE2 from susp-293T^{CD81KO} was sensitive to EndoH as evidenced by the faster migrating smear on SDS-PAGE after treatment. Furthermore, the smear length indicates glycans on 293T^{CD81KO}-produced sE2 ranged from fully EndoH resistant to almost completely EndoH sensitive. This suggests that susp-293T^{CD81KO} cells produce a heterogeneous population of sE2 molecules in terms of glycosylation and that some sE2 molecules are only partially matured as some remain high-mannose type, while others have been heavily modified by Golgi enzymes (Fig 5.13 C & D). As an aside, we noted an unexpected loss of AP33 binding upon PNGase F treatment in the western blot (Fig 5.13 D). AP33 binding is not dependent on glycosylation, however, its contact residues are proximal to Asn-417 and enzymatic removal of the glycan at this position may have affected the AP33 epitope (354). Notably, heterogeneity in the glycosylation status of E2 has also been observed in HCVcc-associated E2 (153). This implies that the processing of sE2 through the Golgi apparatus of susp-293T^{CD81KO} cells more closely resembles that of E2 destined to be incorporated in authentic HCV virions than sE2 from 293-F cells. In summary, these data demonstrate compositional differences in the glycans of sE2 produced in susp-293T^{CD81KO} and 293-F, based on previous findings it is likely that susp-293T produced sE2 is more representative of E2 on HCVcc particles.

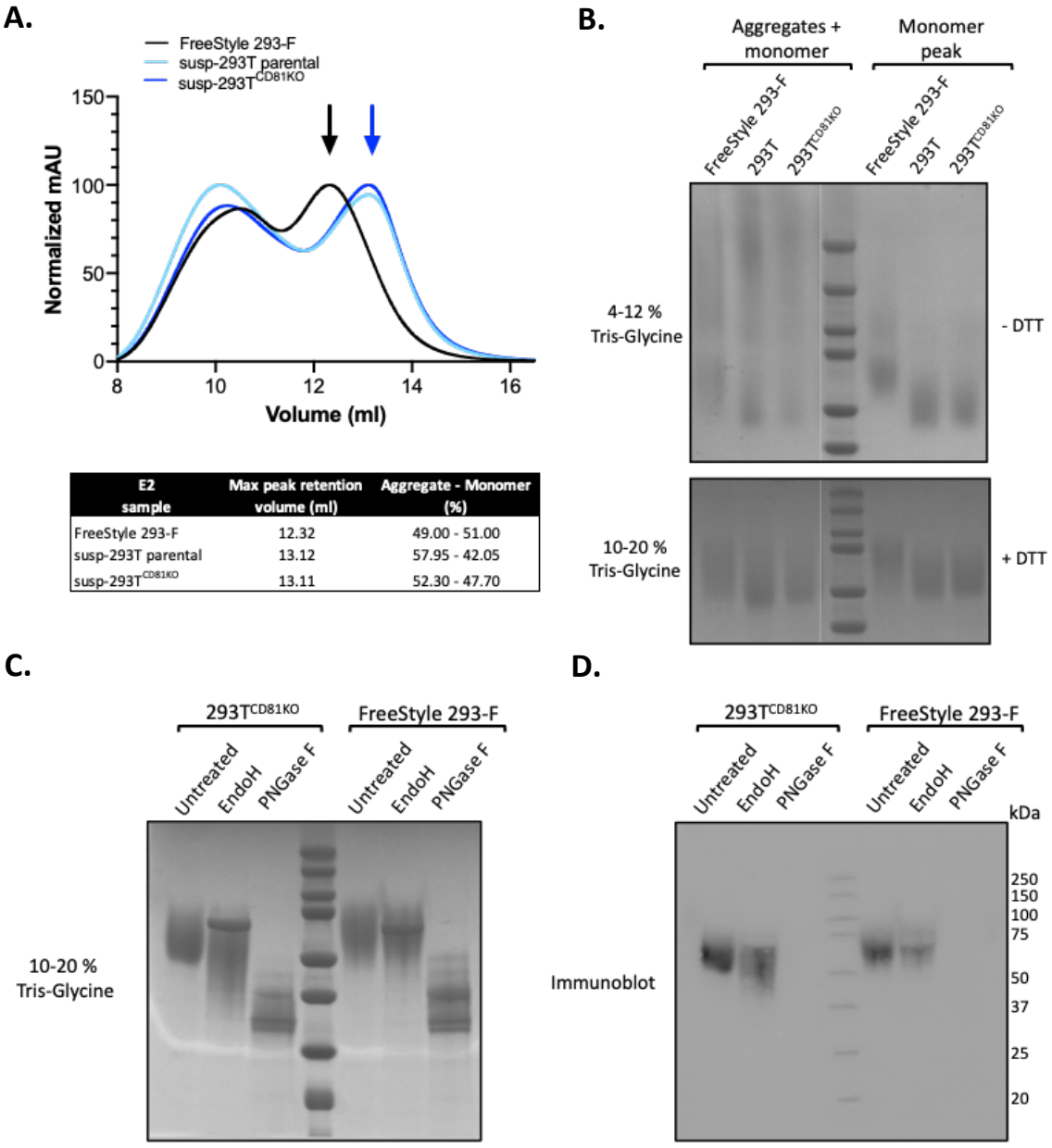

E2 sample	Max peak retention volume (ml)	Aggregate - Monomer (%)
FreeStyle 293-F	12.32	49.00 - 51.00
susp-293T parental	13.12	57.95 - 42.05
susp-293T^{CD81KO}	13.11	52.30 - 47.70

Figure 5.13. **Soluble E2 is differentially glycosylated in susp-293T and 293-F cells.** (**A**) Superdex 200 size-exclusion chromatography profile of susp-293T- (turquoise), susp-293T^{CD81KO}-(blue) and 293-F- (black) derived sE2 following Strep-II-tag affinity chromatography. Blue arrow corresponds to the peak fraction of monomeric sE2 from susp-293T and susp-293T^{CD81KO} cells and the black arrow corresponds to monomeric sE2 from 293-F cells. mAU, milliabsorbance units. (**B**) Nonreducing BN-PAGE gel (top panel) and reducing SDS-PAGE gel (bottom panel) of the purified sE2 derived from the aforementioned cell lines (Coomassie Brilliant Blue G-250 staining). (**C**) Reducing SDS-PAGE gel of monomeric susp-293T^{CD81KO}- and 293-F- derived sE2 after treatment with PNGase F or EndoH (Coomassie Brilliant Blue G-250 staining). (**D**) Western blot of SDS-PAGE gel shown in c. Please note, we failed to detect PNGase F treated E2 with AP33 on the western blot on multiple attempts. Molecular mass markers are indicated on the right (kDa). Data is from a single experiment and was generated by Joan Capella-Pujol.

5.11 Soluble E2 made in 293Ts displays a mixture high-mannose and complex-type glycans

To investigate whether producing sE2 in cells lacking CD81 altered its antigenicity, we first tracked the binding of immobilised sE2 monomers from susp-293T, susp-293T^{CD81KO} and 293-F cells to serially diluted mAbs and human Fc-tagged sCD81 (sCD81) by enzyme-linked immunosorbent assay (ELISA). The mAb panel included the AS412 targeting AP33, AR3B and AT12-009 which target the front layer and binding loop of the CD81 binding site, HC84.26 (front layer) and CBH-4B (domain A) (339,430,434,436). All tested antibodies and sCD81 bound equally well to sE2 produced in susp-293T^{CD81KO} or parental susp-293T cells, suggesting that the expression of CD81 in 293T cells does not affect the antigenicity of sE2 (Fig 5.14 A). sE2 produced in 293-F cells exhibited reduced binding to conformational antibodies, with equivalent binding observed only for AP33, which targets a continuous epitope (AS412). These results suggest there is a difference in epitope accessibility between the two forms of sE2. This difference was even more apparent when comparing the binding of sCD81 to the different sE2 types (Fig 5.14 B).

The binding of the three types of sE2 to the mAb panel and -sCD81 was further characterised by biolayer interferometry (BLI) (Fig 5.15). Antibodies and sCD81 were immobilised on a protein A biosensor and incubated with the same concentration of sE2. Consistent with the ELISA data, near-identical binding profiles were observed for sE2 made in susp-293T^{CD81KO} and parental susp-293T cells; again, besides AP33, sE2 made in 293-F exhibited lower binding to all mAbs and sCD81. Together, the BLI and ELISA data reveal a previously unappreciated difference between the antigenicity of sE2 produced in 293-F and 293T cells. This may have implications for functional/structural studies of sE2 and/or future immunogen production.

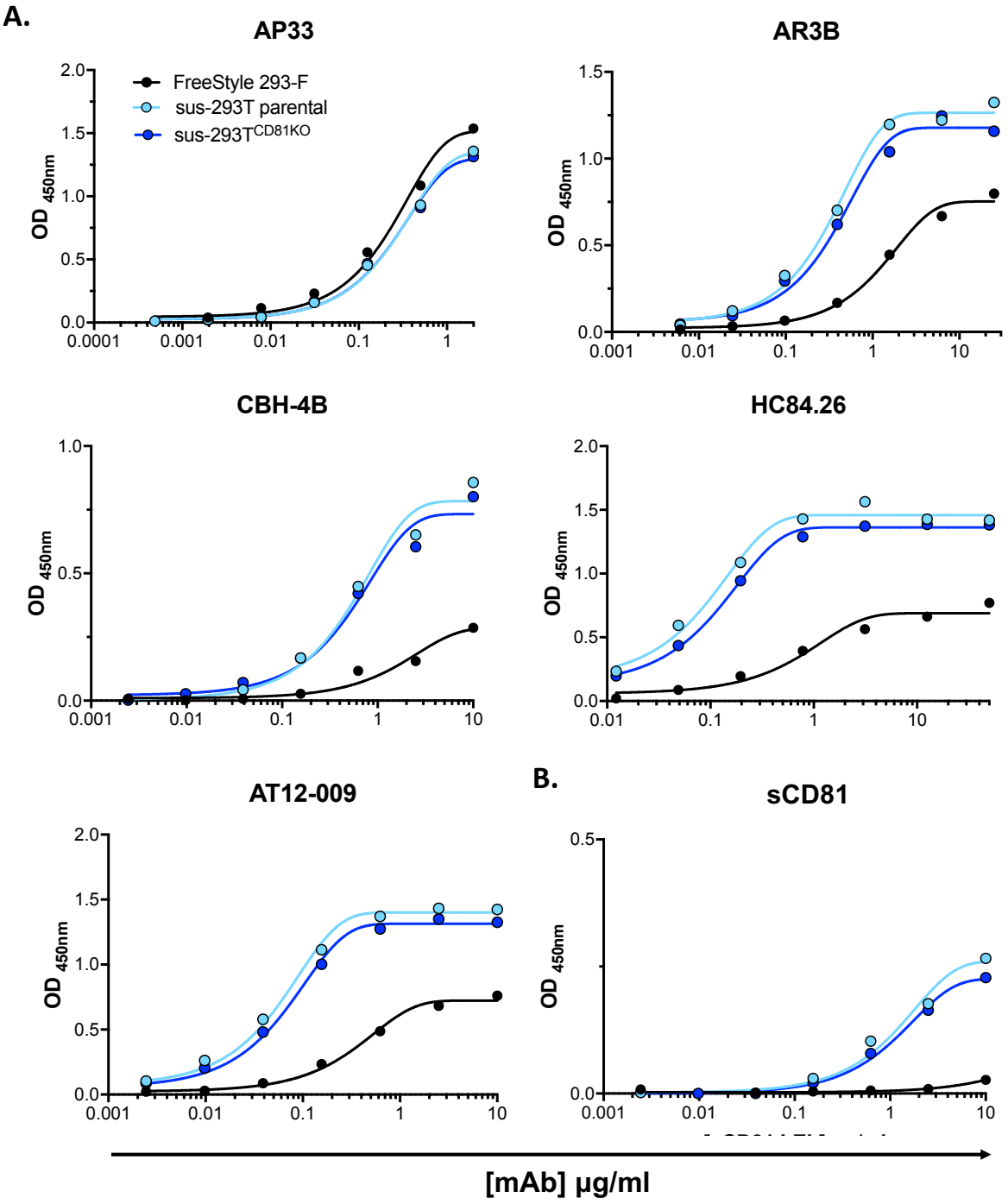

Figure 5.14. ELISA analysis of antibody and CD81 binding to sE2 form susp-293T, susp-293T^{CD81KO} and 293-F cells. sE2 was immobilised to Strep-TactinXT coated microplates and incubated with a serial dilution of the indicated (**A**) mAb or (**B**) sCD81. Each point represents a single value from a lone experiment. Data were fitted using a sigmoidal curve in GraphPad Prism). Data is from a single experiment and was generated by Joan Capella-Pujol.

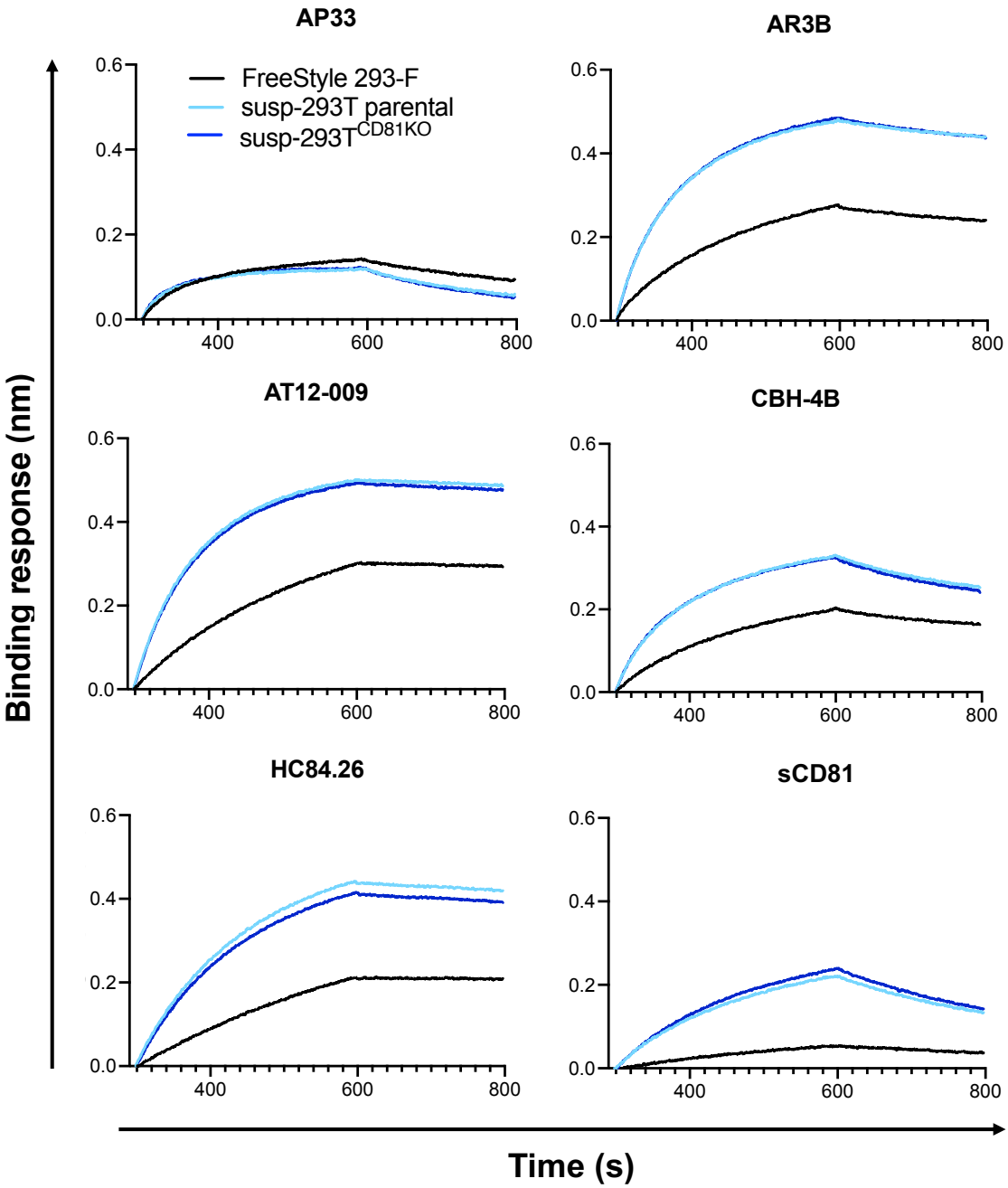

Figure 5.15. BLI analysis of antibody and CD81 binding to sE2 form susp-293T, susp-293T^{CD81KO} and 293-F cells. CD81-LEL-hFc and the indicated mAbs were immobilised onto protein A biosensors and incubated with a single concentration of sE2. Sensorgrams were obtained from an Octet K2 instrument. Data is from a single experiment). Data is from a single experiment and was generated by Joan Capella-Pujol.

5.12 Discussion

The HCV pseudoparticle system is a flexible platform for evaluating the phenotypes of clinical isolates and has proven to be a crucial tool for defining the sequence of virion and receptor interactions occurring during HCV entry; it is likely to be an important component for the assessment of future HCV vaccine candidates (222,223,424). Nonetheless, producing infectious viruses from polymorphic HCV populations circulating in patients has repeatedly proved challenging (431,437,438). This is problematic for vaccine screens and antibody neutralising breadth studies, as only strains which recover workable infectivity are included in such analyses and they may not necessarily be representative of the diversity circulating in the population. Moreover, some infectious strains give low yields which fail to reach a signal to noise threshold sufficient for neutralisation analysis, a signal at least 10-fold above background is favoured but can be lowered to a minimum of 5 for clinical isolates (15,439). Perhaps owing to its flexibility, several studies have demonstrated the HCVpp system is amenable to optimisation. Urbanowicz, Tarr and colleagues have shown infectivity for some strains in the HCVpp system partly depends on the choice of retroviral background and the stoichiometry of transfected plasmids (429). More recently, it has been shown that the cellular co-expression of the HCV p7NS2 open reading frame in producer cells enhances pseudoparticle infectivity for the H77 strain (440). Others have also proposed that the inclusion of an intact HCV Core at the N-terminal of the glycoprotein plasmid is required for efficient pseudoparticle morphogenesis for some strains (441). Nonetheless, it is now generally recognised that the inclusion of the last 21 residues of the Core/E1 peptide is sufficient for the vast majority of clones. Here, we disclose that a 293T cell lineage genetically edited to not express CD81 improves or rescues the infectivity of a wide range of HCVpp strains.

Producing HCVpp in $293T^{CD81KO}$ cells is a facile method for improving HCVpp infectivity as it does not require empirical optimization of the plasmid ratios or co-expression of additional HCV genome elements. Unlike Soares and colleagues, we demonstrate an increase for the infectivities of a broad range of strains representing multiple genotypes (440). Furthermore, producing HCVpp in $293T^{CD81KO}$ cells had a more dramatic effect on viral infectivity compared to plasmid ratio optimization (429). Moreover, none of the 45 clones became non-infectious after production in $293T^{CD81KO}$

cells (see Table S1). Therefore, we would recommend the routine adoption of this cell system for the generation of HCVpp.

We are yet to uncover the mechanism by which the presence of CD81 in the 293T cells influences the infectivity of HCV. However, the correlation between HCVpp sCD81 neutralisation sensitivity and the fold increase in infectivity following production $293T^{CD81KO}$ cells (Fig 5.11 B) suggests that there is a direct interaction between CD81 produced by regular 293T cells and HCVpp. There are several points during HCVpp production where E2 could encounter its cognate binding partner. The E1E2 glycoprotein and CD81 undergo glycosylation and palmitoylation in the Golgi compartment, respectively. When co-transfected, CD81 associates with E1E2 in the endoplasmic reticulum (ER) and influences the glycoprotein's maturation through the Golgi membranes (442). This association redirects the glycoprotein toward the endocytic pathway culminating in its incorporation into exosomes possibly reducing the amount of E1E2 available at the cell surface, where retroviral budding occurs. CD81 is also incorporated into retroviral pseudoparticles and its deletion possibly reduces protein density in lipid rafts at the cell membrane thereby permitting for increased E1E2 incorporation into budding HCVpp. However, glycoprotein incorporation is a poor predictor of HCVpp infectivity as others have shown that the majority of E2 in the supernatant of cells producing pseudoparticles does not sediment with infectious particles (443). Additionally, as released virions in suspension will behave as colloidal matter (385) it is highly probable that many particles contact the cell surface and are retained or fated to non-productive uptake since 293T cells do not express the additional HCV entry factor claudin (222,223).

Our findings somewhat contrast a recent report by Soares and colleagues who concluded that CD81 was required to generate HCVpp (444). This is likely because Soares et al. did not perform infections with the HCVpp they generated from cells silenced for CD81 expression and instead relied on the quantities of E2 in viral harvests as their gauge. Furthermore, as mentioned above, E2 incorporation is a poor predictor of HCVpp infectivity (443) and the observed decrease in E2 in their HCVpp harvests following CD81 silencing is more likely a reflection of reduced E2 incorporation into exosomes since CD81 chaperons E2 into the endocytic pathway, from where exosomes are biosynthesised (442).

The infectivities of VSV and MERS pseudoparticles were unaltered when made in 293T^{CD81KO} cells, ruling out a general enhancement of pseudoparticle production; however, SARS-CoV-1/2pp infection was increased by ablation of CD81. A role for CD81 in the life cycles of the SARS-CoVs is yet to be identified, nonetheless, the related tetraspanin CD9 influences MERS entry by scaffolding dipeptidyl peptidase 4 (DPP4) and type II transmembrane serine protease (TTSP), the cell receptor and CoV activating protease used by MERS, respectively (194,445). CD81 may play an analogous role during SARS-CoV 1 and 2 entry by scaffolding their receptor angiotensin-converting enzyme 2 (ACE2) (446,447). Thus, CD81 deletion may reduce 293T-surface ACE2 or host CoV protease which, in turn, may reduce both pseudoparticle retention and non-productive uptake, as discussed for HCVpp above. Work to ensure SARS-CoV-1/2pp produced in 293T^{CD81KO} cells are similar to their counterparts made in parental 293Ts and the authentic full-length virus is ongoing.

Considering CD81 ablation evidently improves the production of HCVpp, it is surprising we did not observe an increase in the amount sE2 recovered from susp-293T^{CD81KO}. This may be due to the absence of the signal peptide at the intersection of core and E1, which retains E1E2 in the ER lumen, where virion morphogenesis would normally commence in full-length virus (448). Therefore, it is plausible that, unlike the E1E2 heterodimer, sE2 has reduced opportunity for interaction with CD81 as it matures through the Golgi membranes.

The observation that sE2 made in susp-293T and 293-F cells is differentially glycosylated was unexpected and requires further scrutiny. EndoH digestion indicated that some E2 glycans remain shielded from Golgi glycosidases and glycosyltransferases in 293Ts, whereas a much higher proportion of total sE2 efficiently matured through the Golgi apparatus when produced in 293-Fs. Differential glycosylation patterns for the same viral glycoprotein have been demonstrated in cell lines from different species but not in cell lines sharing an immediate predecessor, as 293Ts and 293-Fs do (71,428,435). There are likely many differences between the two lines; however, the most obvious are that 293-Fs are usually grown in suspension and do not express Simian virus large T 40 antigen. We adapted the 293T^{CD81KO} to suspension thus this cannot explain the difference in glycosylation. The SV40 origin of replication is present on the H77 sE2 expression vector (pPPI4) we used (449); however, it is highly improbable that an improvement in plasmid stability would affect the distal process of sE2 glycosylation. A recent omics study of the HEK 293 line and

its progeny not only revealed transcriptome profile differences between adherent 293T cells and 293-F cells but also between 293H cells adapted to suspension and 293-F cells (450). This indicates genes other than those involved in the adherent to suspension transition are also differentially expressed in 293 progeny cell lines. Hence, we suspect that some genetic difference(s) between 293-F and 293T cells ultimately underlies our observation.

The observed disparity in the antigenicity between 293T- and 293-F- produced sE2 is probably a direct result of the difference in glycosylation pattern between the two. Glycans, directly and indirectly, influence E1E2 folding through their interactions with ER chaperones such as calnexin (279,315). Several E2 glycans have been shown to play an important role in folding and E1 and E2 heterodimerization (318). Furthermore, it is well documented that glycans protect conserved viral glycoprotein epitopes, including those on E1E2, from recognition by neutralising antibodies through a phenomenon termed glycan shielding (278,279,321). Our deglycosylation experiments indicate that 293-F-produced sE2 molecules harbour mostly complex glycans, while susp-293T^{CD81KO}-produced sE2 also contain high-mannose or hybrid glycans. Complex glycans are usually larger and this could explain why some epitopes on 293-F-produced E2 seem to be less accessible for most mAbs and CD81 as measured by ELISA and BLI (Fig 5.13 & 5.14). Our results suggest that apparently highly similar 293-derived cell lines can produce glycoproteins with different glycan species. Site-specific glycan analysis (435,451) is needed to more thoroughly compare the difference in glycosylation between two lines and its effect on antigenicity.

Deleting one of the main receptors of HCV from producer cells significantly increased HCVpp infectivity. It is plausible that similar receptor-deleting strategies could be applied to increase the recovered infectious titres of other pseudotyped viruses. However, one should always carefully consider the biological role of these receptors. For example, integrins and lipoprotein receptors are targeted by a range of viruses, but integrins also play a significant role in maintaining cell integrity and cell cycle progression, while many lipoprotein receptors are essential for proper cholesterol homeostasis (452,453). Disruption of either cellular process would likely reduce infectious titres. Therefore, yielded viruses must be phenotyped for cell entry pathway and antibody sensitivity to ensure there are no disparities with pseudoparticles obtained from the parental lineage, as we have done here.

6 General discussion

6.1 Introduction

HCV remains a significant health and economic burden in both developing and developed countries. In 2019, the cost of a single pill of the DAA Sofosbuvir in North America was $1000, with the full cost of a 12-week regimen costing $84000 (454). The cost of treating HCV-related disease on the continent was over $4 billion, with projections indicating that this figure stands to increase in the coming years as the opioid epidemic sweeps the US. Once adjusted as a ratio to national GDP, the cost of treatment per patient is even higher in developing countries such as Egypt due to increased historical caseloads (455). This is despite brand DAAs costing 1% of their US prices and the availability of locally manufactured generic DAAs with comparable safety and efficacy to branded drugs. The high cost of DAAs, the risk of reinfection following therapeutic cure or spontaneous clearance and the low screening of high-risk groups necessitate the development of a prophylactic HCV vaccine.

The high economic burden of DAA therapy presents a significant obstacle to achieving WHO HCV elimination targets: i.e., 80% reduction in new chronic infections and a 65% reduction in mortality from their 2015 levels by 2030 (4,456). To reach these targets and eliminate HCV as a public health threat, the WHO recommends its members deploy the extensive use of DAAs, boost care and treatment services. It also recommends developing evidence-based policy and increasing preventative measures, such as raising awareness, expanding blood screening in developing countries and preserving needle and syringe programmes for PWIDs. The development of a safe and effective vaccine would inarguably aid in reaching these ambitious WHO goals through the prevention of new infections.

In addition to providing some molecular insights into the quandary that is HCV entry, the results presented in this thesis potentially also have implications for vaccine development. A catalogue of promising B- and T-cell based vaccines have reached phase II clinical trials only to fail to elicit protection to chronic HCV infection (457–461). The most recent trial followed a prime-boost strategy using a recombinant chimpanzee adenoviral vector followed by modified vaccinia Ankara; both vaccines encoded HCV NS proteins (460). Although the strategy produced HCV-specific T-cell responses and lowered peak HCV RNA levels, unfortunately, it still failed to prevent chronic HCV infection. The current consensus is that an effective HCV vaccination regimen will need to generate both humoral and cellular immune responses. Achieving these goals

will require identifying the combination of NS proteins that generates the most robust cellular response and designing an E1E2 immunogen that elicits broadly reactive antibodies. In addition to guiding rational vaccine design, an improved understanding of E1E2 function could inform the development of pangenotypic HCV entry inhibitors for use in combination with DAA therapy.

6.2 Defining the early post-attachment events of HCV entry

The entry of a large proportion of enveloped viruses involves engaging a series of co-receptors that direct particle entry into permissive cells in a spatial-temporal manner. In many cases, the viral entry proteins interact with a sequence of receptors, with each interaction facilitating the next (193,462–464). Viral entry is also reliant on proteins that do not directly associate with the viral entry proteins but are involved in processes such as actin remodelling. Since the turn of the century, as more investigative tools have become available, HCV has revealed itself to possess one of the more intricate entry pathways in the virosphere, requiring at least five cell membrane proteins (221). The work in this thesis focused on the cell membrane proteins with proven interactions with the HCV entry proteins: CD81 and SR-B1. This section discusses our work in the context of the current conventional model of HCV entry (see Fig 1.10).

The spatial distribution of the HCV entry receptors /cofactors predicts the point at which they become involved in the entry process (223). Due to the topology of the liver, HCV encounters the basolateral surface of hepatocytes first, here SR-B1 and CD81 associate with the virion soon after attachment, whereas CLDN1 and OCLN only colocalise with the virion at or during translocation to the tight junction (225). It's currently accepted that E1E2 interactions with SR-B1 and, perhaps more significantly, CD81 lead to the recruitment of signalling proteins that drive virion basolateral translocation to the tight junctions. Thus, post-attachment steps of HCV entry can be separated into the early and late steps.

In the early steps, E1E2 binds its cognate receptors and, in doing so, triggers irreversible conformational changes that help prime the virus for the subsequent events in the entry process, culminating in low pH-dependent fusion with host endosomes. The E1E2-CD81 interaction is predicted to be the binding event that primes the fusogenic activities of the glycoprotein seeing as SR-B1 is dispensable for

HCV entry (218,219,241). As such, the importance of the E1E2-SR-B1 interaction during HCV entry has remained unclear.

The authentic HCV particle has unusually high cholesterol and apolipoprotein content compared to other viral particles (116). Unsurprisingly, because of this, many cell surface proteins involved in cholesterol uptake and homeostasis have been implicated in HCV entry (218,229,230,465). Due largely to the comparable falls in HCV infectivity following their genetic abrogation SR-B1, LDL-R and VLDL-R were inappropriately concluded to play a redundant role during HCV entry (218). To this end, although all three proteins can function as attachment factors by tethering VLPs through interactions with apolipoproteins, only SR-B1 binds the HCV entry machinery. Indeed, we found little evidence that the role of SR-B1 during viral entry was defined by anything other specified receptor-viral particle interactions. Our current work, along with that of others, indicates that SR-B1 dependent entry is a mechanism HCV evolved to evade humoral immunity (311,346,393). Here we propose a mechanism in which, by binding and stabilising HVR-1, SR-B1 switches off the entropic safety catch mechanism, making E1E2-CD81 interactions more favourable. Additionally, there is evidence that the lipid transfer activity of SR-B1 may be a driving force during virus internalisation (216). Moving forward, it's vital SR-B1 is considered in investigations not simply as an HCV VLP-tethering cholesterol receptor but rather a bonafide, multifaceted HCV receptor.

Our study was built around a model of HCV entry wherein the virus sequentially engages its receptors to achieve entry. Several studies have assessed HCV entry kinetics by employing time of addition with entry inhibitors and found SR-B1 functions immediately after viral attachment and likely precedes CD81 engagement (216,466,467). Thus, our working model of entry assumes HCV first engages SR-B1 before it acquires CD81 (219). Since HCV infectivity is severely affected following SR-B1 ablation in Huh-7 cells (with all other receptors left intact), we hypothesised that SR-B1 primes E1E2-CD81 interactions, hence the requirement for sequential receptor engagement. The comparison of the entry kinetics of WT and I438V A524T viruses in this thesis provides indirect evidence for the said hypothesis. This theory is further upheld by our mathematical modelling as it accurately predicted the ratio at which the rates of WT and I438V A524T entry would proceed via route 1 (SR-B1 mediated acquisition of CD81). As such, this work offers compelling mathematical and experimental evidence for SR-B1 mediated priming of E1E2.

The acquisition of CD81 is the defining step of HCV entry. While the E1E2-CD81 binding event induces conformational changes in the glycoprotein, it also induces signalling events in the target cell that promote viral entry. For example, the binding of sE2 triggers Rho family GTPases, leading to the rearrangement of the actin cytoskeleton, which drives basolateral translocation of CD81-HCV complexes (468). Additionally, the HCV-CD81 association induces EGFR activation, which is required for viral endocytosis (235,243). CD81 also forms associations with CLDN1 and EGFR independent of HCV binding. Thus, CD81 acts as the anchor in a receptor/cofactor platform by crosslinking the other entry factors in the plasma membrane.

The mathematical model predicts the acquisition of just two CD81 molecules is sufficient to support an HCV particle through the entry programme. This value is lower and more decisive compared to our previous estimate and that of others (219,469). This is probably because we included two strains and subsequently fitted the model with more data than we did previously, and our model assumes the stepwise acquisition of receptors, unlike Dixit and colleagues (469). It's important to note a major limitation of the model; it assumes that the HCV glycoproteins and the receptors on any given virion or cell, respectively, are distributed homogeneously. However, this is certainly not the case for HCV particles because their association with host lipoproteins guarantees their heterogeneity.

We have previously shown that HCV can acquire CD81 independent of SR-B1 and that this route of entry is only accessible to a minority of the WT population (219). Here we show that HCV particles that arrive at the cell surface in a hyperreactive state, primed for entry exhibit superior passage through the SR-B1 independent route of entry. Interestingly, the probability that WT and I438V A524T virus could successfully infect SR-B1 KO cells (Fig 3.8 B, parameter c_1) mirrored sE2 binding CHO-CD81 data (Fig 3.6 E), with the mutant performing twice as well in either instance. Again, this strongly supports a model of entry where CD81 function immediately succeeds SR-B1 binding. Our mathematical model also suggests that hyperreactive HCV, specifically I438V A524T the double mutant, is 1000-fold better at acquiring CD81 via the SR-B1 mediated route (Fig 3.8 B, parameter c_2) despite demonstrating reduced binding to the lipoprotein receptor. To this end, SR-B1 both protrudes further from the cell membrane and binds E1E2 with a higher affinity compared to CD81. So, post-SR-B1 engagement, hyperreactive E1E2 is likely more rapidly liberated to acquire CD81 as its safety-catch mechanism is already (or near) inactive.

6.3 Peptide tail entropy, a new frontier in immune evasion?

The role of HVR-1 in protecting epitopes composing the CD81 binding site has long been appreciated (213,306,400); it was initially thought that HVR-1 shields the CD81-bs, and given its size and location (Fig 1.16), this rationale was certainly reasonable (403,470). However, we now know that the E2 epitopes protected by HVR-1 extend to the back layer, and some are only realised in the context of an E1E2 dimer. Consequently, HVR-1 is too small to shield the protected surface area. This thesis proposes an attractive, coherent mechanism through which a small peptide tail such as the HVR-1 could influence global protein antigenicity. Here, our findings suggest that motions in the highly dynamic HVR-1 are communicated throughout E1E2. We reason that by existing in an entropically dynamic state, HVR-1 continuously alters the antigenic landscape of the tethered glycoprotein. To this end, the structural studies indicating the CD81-bs and back layer surfaces to be conformationally dynamic certainly lend weight to the safety catch model (see section 1.6.2 and review (322)).

Given HCV is a member of the *Flaviviridae* family and is sensitive to inactivation at higher temperatures, it has been suggested E1E2 undergoes a phenomenon termed ‘envelope breathing’ (311,471). The line of thought here is that the viral envelope exists in a dynamic equilibrium between open and closed conformational states, wherein the open conformation is more sensitive to neutralisation (i.e., antigen exposed). With regards to HCV, it’s possible motions within HVR-1 propel global E1E2 breathing. Certainly, the feasibility that SR-B1 triggers conformational opening of E1E2, exposing critical CD81 binding epitopes, makes it an attractive mechanism for HCV nAb evasion (346). However, the entry machinery of HCV is not class II like the members of the *flavivirus* genus (DENV & ZIKV), where the term ‘envelope breathing’ has been frequently adopted (324,472–475).

The breathing of Flaviviral E proteins is made practical by their arrangement into rigid long rods which pack closely to create a lattice on the virion surface (Fig 1.13) (252,476,477). In contrast, HCV E2, analogous to flavivirus E based on genomic organisation, is globular with several disordered regions (280,293). Furthermore, infection with a flavivirus is acutely resolved and elicits protective antibodies, unlike HCV. However, the lipoprotein content and greater diversity of HCV may explain its slower resolution and poorer protection from reinfection. Nonetheless, existing structural evidence and the comparable antigenicity we saw for WT and I438V A524T

sE2 are inconsistent with binary E1E2 states. Indeed, the entropic safety catch integrates theoretical open and closed states. The folding of E1E2 following HVR-1 stabilisation is consistent with the open state as it's primed to engage CD81 and is nAb sensitive. Whereas the closed state is reconciled with the dynamic folds E1E2 adopts when the safety catch is on to maintain nAb resistance.

Might HCV E1E2 represent a zenith among the known viral envelope proteins in terms of nAb escape mechanisms? Arguably so, particularly when you consider that of the human viruses recognised to establish truly chronic (life-long) infections, HCV is unique in that it does not undergo dormancy (HBV, herpesviruses) or integrate into the host genome (HBV, retroviruses) (478,479). As such, E1E2 are under constant immune pressure as the virus actively replicates throughout infection. To evade nAbs, E1E2 are heavily glycosylated, exhibit antigenic variation and conformationally protect critical CD81 epitopes. All three tactics are common in the virosphere. However, the mechanism by which we propose E1E2 conformationally protects the nAb epitopes, HVR-1 disorder, or the 'entropic safety catch' as we coin here, is currently unique to HCV. Classical conformational protection constitutes the physical occlusion of critical epitopes (480–483). These epitopes are exposed only following dramatic structural changes cued after specific triggers such as receptor engagement (e.g., HIV Env-CD4). Regarding the safety catch, the acquisition of HVR-1 appears to have enhanced HCV nAb escape beyond that of its close relatives. Infection with EqHV (hepacivirus) and BVDV elicits protective humoral responses in horses and bovines (408), respectively; there are even multiple vaccines available for the latter (484)! Indeed, if the entropic safety catch mechanism is accurate, then the physical and genetic properties of HVR-1 must truly represent a feat in viral genetic economy. HVR-1 protrudes relative to the rest of E1E2, allowing it to divert immune responses away from the neutralising face. HVR-1 can itself tolerate extensive immune assault due to its genetic flexibility. In turn, targeted responses may drive a feedback system where positive selection by HVR-1-specific antibodies promotes its entropy, thus maintaining the safety catch. In essence, HCV has managed to condense into ~27 residues an immunodominant decoy that continually drifts antigenically, whose motions effectively make the E1E2 landscape so dynamic that it resists antibody engagement.

6.4 Implications for HCV vaccine development

HCV shares common mechanisms to evade humoral immunity, discussed above, with other highly diverse viruses, namely HIV and influenza virus. Although seasonal influenza vaccines exist, an effective pan-genotypic vaccine is yet to be developed for any of the three. The envelope protein of each of these viruses presents researchers with a unique set of challenges for immunogen design. However, the HCV field is particularly handicapped by the lack of virion-associated E1E2 crystal structure, which also means their oligomeric arrangement remains unknown. Consequently, most B-cell immunogens designed and tested to date are constructs encompassing complete E1E2 or sE2. Nonetheless, these constructs have provided some insights regarding the properties that future B cells immunogens must possess.

When the protective function of HVR-1 was first described, it was expected HVR-1 deletion would make E1E2 or sE2 better immunogens. Instead, a wide body of work now demonstrates that ΔHVR-1 glycoprotein constructs elicit similar, or sometimes poorer, antibody responses in vaccinated animals and patients. The data in chapter two provides two plausible mechanisms to how ΔHVR-1 constructs might elicit poorer responses. Firstly, the safety catch mechanism appears to protect HCV from spontaneous inactivation at physiological temperature (Fig 4.5). As such, it's likely the duration for which E1E2 is presented to the immune system in their prefusion fold reduced, thereby reducing their immunogenicity. Secondly, HVR-1 stabilisation rather than deletion conferred improved sE2 binding to CD81 in a CHO cell-binding assay (Fig 4.6). This suggests that some CD81-bs conformations are attainable only under certain HVR-1 configurations and these CD81-bs folds may be particularly adept at inducing bnAb responses.

Based on the above observations, it seems possible that E1E2 or sE2 constructs where HVR-1 is stabilised (e.g., I438V A524T) might make superior immunogens to their WT and ΔHVR-1 counterparts. Here, any losses in E1E2 thermal stability compared to WT constructs may be offset by the CD81-bs existing in conformations primed for receptor binding, which theoretically favours bnAb induction (322). Irrespective of the tactics used, HVR-1 is a tricky customer to account for in the rational design of HCV immunogens, so it may be necessary to invoke the safety catch mechanism without it. Nonetheless, the fact patients readily develop bnAbs to virus

that always comprises HVR-1 during natural infection offers reasons to be optimistic that a vaccine is achievable.

Nowadays, a two-pronged approach is often employed to elucidate the mechanisms behind bnAb development (485). Firstly, structural characterisation of viral envelope-bnAb complexes to infer how the immune system recognises the virus to achieve neutralisation. Secondly, the thorough study of the bnAbs themselves from identifying the germline genes encoding them to the kinetics of their appearance. The second method considers the diversity of in-host responses to identify amenable B cell evolutionary pathways to exploit for the design of broadly effective vaccines.

The abovementioned approach has found that some bnAbs against particular epitopes share a restricted set of IgG heavy chain variable (V_H) genes and are often similar in structure. Notably, *V_H1-69* encode bnAbs that are dominantly found in protective responses to viral pathogens. Epitopes targeted by these bnAbs include the HA stem of influenza, multiple sites on HIV-Env, including the heptad repeat 1 of gp41 and CD81-bs on HCV E2 (486). The genetic and structural characteristics of V_H1-69 bnAbs make them appealing candidates for rational vaccine. Despite great inter-host diversity in both immune responses and virus sequence, V_H1-69 antibodies targeting largely overlapping epitopes but isolated from different patients often employ a conserved mode of recognition to engage their antigen. Additionally, longitudinal NGS indicates these antibodies require low-to-medium rates of somatic hypermutation (SHM), which should be achievable through vaccination. It is hoped that studies to design immunogens that engage a specific B cell lineage to a highly conserved epitope will provide a means to achieve cross-protection for these viruses.

To date, V_H1-69 bnAbs to HCV have only been isolated from infected patients (309), suggesting an intact HVR-1 is necessary for their development. While the isolation of this class of antibodies from patients with chronic HCV might intuitively suggest that they were ineffective in counteracting the virus (339), it is becoming ever more apparent that the kinetics of the appearance of their germline precursors influences disease outcome (15,17,18,487,488). Mechanistically, Flyak et al found that the CDRH3 motif utilised by some V_H1-69 bnAbs was, in fact, imprinted early in the germline, with bnAb precursors recognising E2 of several circulating HCV variants (280). Although kinetics in this sense should be of less importance in the context of vaccination, it is still favourable that vaccine candidates mimic the quick induction of germline antibodies binding the CD81-bs on E2.

While the results from characterising B-cell ontogeny with regards to HCV are very promising, ensuring immunogens are capable of eliciting responses across diverse human populations against diverse virus will still prove challenging. Once said immunogens are at the point of preclinical and clinical testing it is that imperative that experimental systems have the capacity to include broad and representative isolates. To this end, the cell line we developed in chapter five permits for the inclusion of circulating isolates previously deemed unworkable in the HCVpp system (375). This will improve diversity within the vaccine panel screens and allow for more thorough characterisation of prophylactic candidates.

6.5 Study limitations

A major limitation of the entry mechanism aspect of the study (results chapters one and two) is that we employed a single prototypical lab strain, J6, for all experimentation. Therefore, it's possible our findings are not representative of HCV in general and that our conclusions do not apply to the diverse virus circulating in the population. Nonetheless, we reasoned early on that it would be wiser to deduce a compelling mechanism from a rich, comprehensive dataset generated via a multidisciplinary approach on a single strain. Indeed, this has allowed us to develop and refine methodologies, thusly creating both physical and computational pipelines for the study of HCV entry. In this way, the current body of work forms a springboard from which we can launch to experimentally explore diverse HCV strains with the aim of further refining the mechanistic details concerning HCV entry and nAb evasion.

The entropic safety catch model, though upheld by the in vitro and cell culture experiments, is founded on our computational modelling of E2 ectodomain dynamics. It remains unknown to what extent E2 dynamics *in silico* remain faithful to its virion-associated form and in the context of an E1E2 heterodimer. Given the heterogeneity of HCVcc particles, HCV envelope proteins in their purified soluble form or on HCVpp offer more tractable systems in which to focus attempts to observe the safety catch mechanism. Here E1E2 conformational dynamics could theoretically be captured by single-molecule fluorescence resonance transfer (smFRET), as seen for HIV-Env and SARS-CoV-2 spike (325,398). However, as it currently stands, the field is yet to develop correctly folded HCV envelope ectodomains that are within the detection limits of smFRET. For the determination of HVR-1 stabilisation, nuclear magnetic resonance

(NMR) spectroscopy could suffice (489). Here, comparing the spectra of WT HVR-1/AS412 peptides to those carrying putative hyperreactive mutations such as I414T (in JFH-1) (390,391) and G406S, identified in the first adaptation experiment (Fig S1) with preliminary screening indicating it to be hyperreactive, could be informative. All in all, direct measurement of E1E2 dynamics will aid determine its transitional states following receptor engagement and inform us on the consequence of nAb engagement; providing answers as to how antibodies can bind WT and I438V A524T sE2 equally, yet only the mutant virus is proficiently neutralised.

One significant oversight of the work presented here is the absence of isotype controls for the primary antibodies used for fluorescence microscopy and flow cytometry. The antibodies used here were kind gifts from other labs or purchased from a vendor who assessed their binding specificity and affinity, and the published results assured us of their function (see table 2.1). Nonetheless, for certainty, isotype controls should have been included; we, however, did not have these materials during this research period. Another control the work is missing is total IgG isolated from an HCV seronegative individual to match the HCV^{+} patient IgG. This would have been a particularly valuable control in the second adaptation experiment. In theory, HCV adapted to Huh-7.5 cells in the presence of IgG from a seronegative individual should evolve to be hyperreactive as there would be no selective pressure on E1E2 from HCV specific antibodies in the experiment. Moving forward, IgG will be isolated from the sera of seronegative individuals and be included in the future work of the lab.

6.6 Closing remarks

It has been over thirty years since Houghton and colleagues isolated HCV and determined it to be a major etiological agent of viral hepatitis, yet for much of this time, the functional mechanisms of E1E2 remained unknown. In a comparable timeframe, significantly more detail surrounding HIV entry events and nAb recognition of HIV-Env was uncovered. This is not a reflection of lesser efforts by the HCV field but rather a combination of several factors: including but not limited to difficulties in imaging and propagating proficient HCV virions, E1E2's unique structural organisation and manner of function, and lopsided funding awarded toward HIV research. The astonishing pace at which B-cell vaccines toward SARS-CoV-2 spike have been developed has illuminated the power of well-funded, multidisciplinary research (490,491).

As we emerge from the COVID pandemic, it's imperative governments and funding bodies do not scale back the funding for virology research. Rather they must redistribute COVID funds to incite a wave of collaborative research for other viral pathogens to be conducted with the same vigour observed for SARS-CoV-2. Indeed, in the last decade, adopting multidisciplinary approaches in HCV has accelerated our understanding of the E2 structure (492) and brought to light the type of antibodies an effective vaccine will need to induce. Certainly, improved collaborative networks and the appropriation of the new cutting-edge tools developed for COVID research would serve to accelerate the development of HCV vaccine candidates, bringing us closer to the WHO target of HCV elimination.

In the current study, by combining basic virology with mathematical and computational modelling approaches, we have provided novel insights into the structure-to-function relationship of E1E2. We propose that the intrinsic disorder of HVR-1 drives HCV nAb evasion and coin this mechanism 'the entropic safety catch'. We provide evidence that SR-B1 engagement stabilises HVR-1, thereby turning off the safety catch mechanism and primes E1E2 for downstream entry events, this is one of the first coherent proposals of a functional consequence for this binding event. Although further validation of the 'entropic safety catch' is needed, our findings along with analyses of ΔHVR-1 immunogens (312,400) suggest the inclusion of HVR-1 is a prerequisite in the design of effective B cell immunogens.

7 Appendix

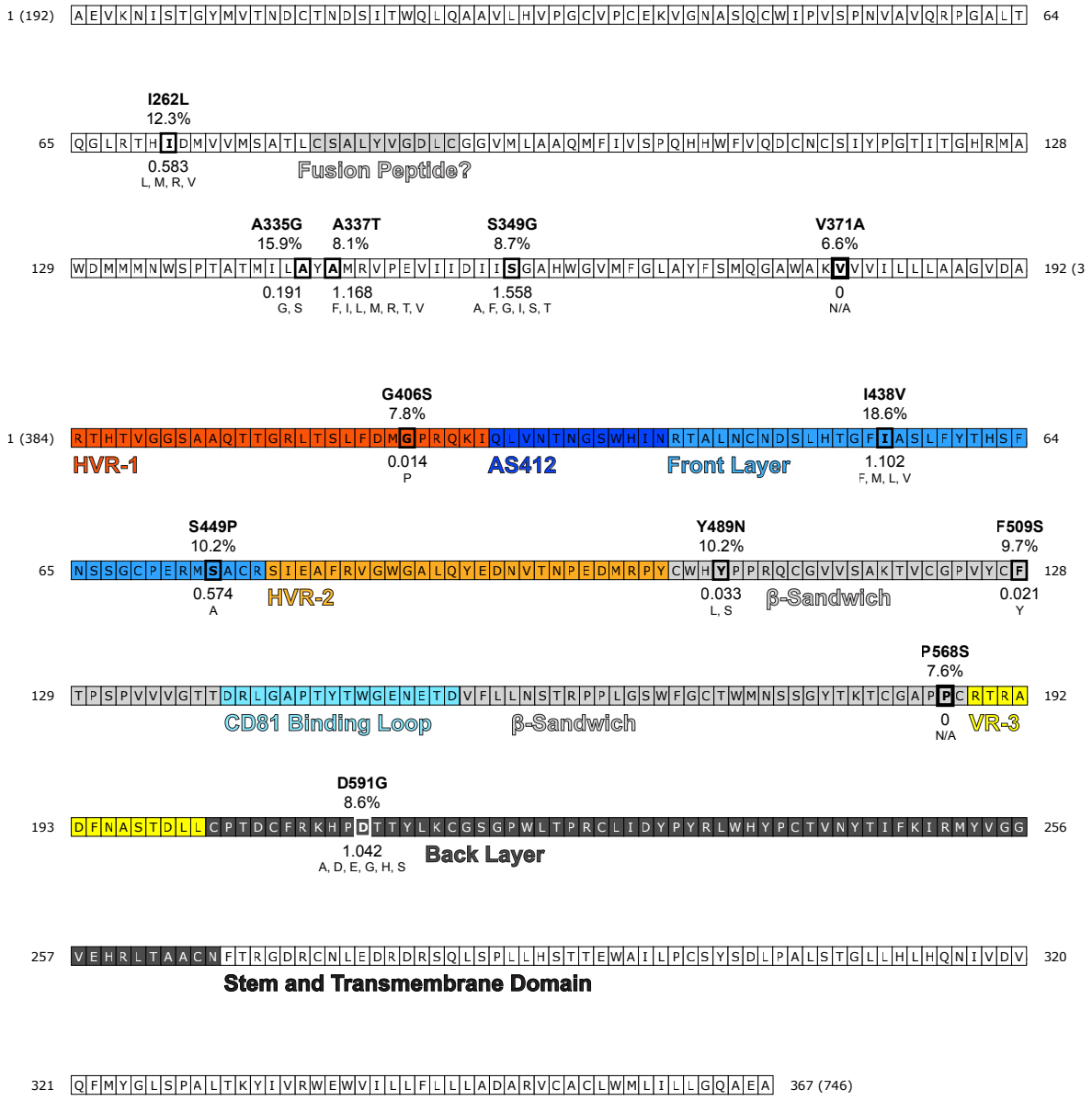

Supplementary Figure 1. Location and frequency of non-synonymous substitutions. Non-synonymous substitutions mapped onto linear representations of the E1 and E2 protein sequences. Functional and structural features are highlighted (e.g., the putative fusion peptide). The E2 sequence is color-coded by region, as denoted on the three-dimensional model.

Supplementary Table 1. Signal-to-noise ratio (S/N) for all HCV strains tested in the study

HCVpp [a]	Core [b]	Genotype	293T line of HCVpp production		Fold change in S/N [c]
			Parental	293T^{CD81KO}	
H77	Lentiviral	1a	901.34	1673.03	1.86
H77 L438V ✤	Lentiviral	1a	188.55	335.28	1.78
H77 L438V A524T ✤	Lentiviral	1a	47.04	138.06	2.94
J6	Lentiviral	2a	164.88	340.21	2.06
J6 I438V A524T ◆	Lentiviral	2a	43.05	250.15	5.81
JFH1	Lentiviral	2a	127.48	181.22	1.42
UKNP 2.2.1	Lentiviral	2	29.57	77.21	2.61
UKNP 2.4.1	Lentiviral	2	6.57	15.02	2.29
UKNP 4.1.1	Lentiviral	4	66.53	122.53	1.84
AMS.1b.kloon2	Retroviral	1b	7.96	30.86	3.88
AMS.2b.kloon21	Retroviral	2b	26.45	24.91	0.94
AMS.3a.kloon26	Retroviral	3a	55.90	27.27	0.49
AMS.4d.kloon8	Retroviral	4d	22.47	40.43	1.80
h77	Retroviral	1a	30.11	121.48	4.03
jfh1	Retroviral	2a	5.79	21.29	3.68
msm1	Retroviral	1	99.77	279.03	2.80
msm2	Retroviral	2	21.22	41.13	1.94
msm4	Retroviral	4	22.46	71.53	3.19
msm5	Retroviral	5	27.34	56.30	2.06
uknp 2.1.1	Retroviral	3	26.61	39.23	1.47
uknp 2.2.1	Retroviral	2	159.01	178.74	1.12
uknp 2.4.1	Retroviral	2	16.94	34.02	2.01
uknp 3.2.1	Retroviral	3	7.30	40.99	5.62
uknp 3.2.2	Retroviral	3	32.75	191.18	5.84
uknp 4.1.1	Retroviral	4	17.11	96.81	5.66
uknp 5.2.1	Retroviral	5	13.38	128.37	9.59
uknp 6.1.2	Retroviral	6	11.04	20.17	1.83
168_Cl T/F	Retroviral	1b	85.14	360.00	4.23
277_Cl T/F	Retroviral	3a	4.60	3.30	0.72
360_Cl T/F	Retroviral	1a/2b	3.90	35.30	9.05
686_Cl T/F	Retroviral	1a	6.90	25.50	3.70
4032_Cl T/F	Retroviral	3a	3.90	1.70	0.44
4087_Cl T/F	Retroviral	1b	0.00	128.00	128.00
023_Ch T/F1	Retroviral	1a	12.13	64.50	5.32
023_Ch T/F2	Retroviral	1a	0.00	10.30	10.30
023_197DPI	Retroviral	1a	0.00	5.30	5.30
240_Ch T/F	Retroviral	3a	3.00	2.30	0.77
256_Ch V1	Retroviral	1a	9.70	88.00	9.07
256_Ch V2	Retroviral	3a	6.00	97.00	16.17
256_79DPI 1	Retroviral	3a	0.00	4.00	4.00
256_287DPI	Retroviral	3a	3.00	2.00	0.67
HOK_Ch T/F	Retroviral	1b	12.90	155.00	12.02
HOK_30DPI	Retroviral	1b	4.00	166.00	41.50
HOK_233DPI	Retroviral	1b	0.00	5.70	5.70
THD T/F	Retroviral	1a	14.30	71.30	4.99
THD_109DPI	Retroviral	1a	114.30	74.50	0.65
THD_198DPI	Retroviral	1a	0.00	104.00	104.00
THG_Ch T/F	Retroviral	1a	14.30	71.30	4.99
THG_58DPI	Retroviral	1a	82.50	64.80	0.79
THG_184DPI	Retroviral	1a	47.00	49.00	1.04

[a] E1E2 identification, [b] gag-pol genes origins: Lentiviral (HIV) and Retroviral (MLV), [c] fold change in HCVpp S/N (relative to S/N of parental 293T produced HCVpp), T/F:

Transmission founder, ❖ E1E2 sequence of H77 mutants generated via site-directed mutagenesis, ◆ E1E2 sequence of an unpublished full-length cell-culture adapted J6/JFH chimeric strain.

8 Bibliography

1. Lanford RE, Bigger C, Bassett S, Klimpel G. The chimpanzee model of hepatitis C virus infections. ILAR J. 2001;
2. Choo QL, Kuo G, Weiner AJ, Overby LR, Bradley DW, Houghton M. Isolation of a cDNA clone derived from a blood-borne non-A, non-B viral hepatitis genome. Science (80-). 1989;
3. Bhamidimarri KR, Satapathy SK, Martin P. Hepatitis C virus and liver transplantation. Gastroenterol Hepatol. 2017;
4. Gelson W, Alexander G. Is elimination of hepatitis C from the UK by 2030 a realistic goal? British Medical Bulletin. 2017.
5. Millman AJ, Nelson NP, Vellozzi C. Hepatitis C: Review of the Epidemiology, Clinical Care, and Continued Challenges in the Direct-Acting Antiviral Era. Curr Epidemiol Reports. 2017;
6. Ding Q, von Schaewen M, Ploss A. The impact of hepatitis C virus entry on viral tropism. Cell Host Microbe. 2014;16(5):562–8.
7. Lavanchy D. The global burden of hepatitis C. In: Liver International. 2009. p. 74–81.
8. Micallef JM, Kaldor JM, Dore GJ. Spontaneous viral clearance following acute hepatitis C infection: A systematic review of longitudinal studies. Journal of Viral Hepatitis. 2006.
9. Seeff LB. Natural history of chronic hepatitis C. In: Hepatology. 2002.
10. Hoofnagle JH. Course and outcome of hepatitis C. Hepatology. 2002;
11. Spengler U, Nattermann J. Immunopathogenesis in hepatitis C virus cirrhosis. Clinical Science. 2007.
12. Hotchkiss RS, Dunne WM, Swanson PE, Davis CG, Tinsley KW, Chang KC, et al. Role of apoptosis in Pseudomonas aeruginosa pneumonia. Science. 2001;294(5548):1783.
13. Chang KM, Thimme R, Melpolder JJ, Oldach D, Pemberton J, Moorhead-Loudis J, et al. Differential CD4+ and CD8+ T-cell responsiveness in hepatitis C virus infection. Hepatology. 2001;
14. Grakoui A, Shoukry NH, Woollard DJ, Han JH, Hanson HL, Ghrayeb J, et al.

HCV Persistence and Immune Evasion in the Absence of Memory T Cell Help. Science (80-). 2003;

15. Walker MR, Leung P, Eltahla AA, Underwood A, Abayasingam A, Brasher NA, et al. Clearance of hepatitis C virus is associated with early and potent but narrowly-directed, Envelope-specific antibodies. Sci Rep. 2019 Dec 16;9(1):13300.
16. Merat SJ, Bru C, van de Berg D, Molenkamp R, Tarr AW, Koekkoek S, et al. Cross-genotype AR3-specific neutralizing antibodies confer long-term protection in injecting drug users after HCV clearance. J Hepatol. 2019 Jul;71(1):14–24.
17. Kinchen VJ, Zahid MN, Flyak AI, Soliman MG, Learn GH, Wang S, et al. Broadly Neutralizing Antibody Mediated Clearance of Human Hepatitis C Virus Infection. Cell Host Microbe. 2018;
18. Osburn WO, Snider AE, Wells BL, Latanich R, Bailey JR, Thomas DL, et al. Clearance of hepatitis C infection is associated with the early appearance of broad neutralizing antibody responses. Hepatology. 2014;
19. Timm J, Lauer GM, Kavanagh DG, Sheridan I, Kim AY, Lucas M, et al. CD8 epitope escape and reversion in acute HCV infection. J Exp Med. 2004;
20. von Hahn T, Yoon JC, Alter H, Rice CM, Rehermann B, Balfe P, et al. Hepatitis C Virus Continuously Escapes From Neutralizing Antibody and T-Cell Responses During Chronic Infection In Vivo. Gastroenterology. 2007;
21. Dowd KA, Netski DM, Wang XH, Cox AL, Ray SC. Selection Pressure From Neutralizing Antibodies Drives Sequence Evolution During Acute Infection With Hepatitis C Virus. Gastroenterology. 2009;
22. Farci P, Shimoda A, Coiana A, Diaz G, Peddis G, Melpolder JC, et al. The outcome of acute hepatitis C predicted by the evolution of the viral quasispecies. Science (80-). 2000;
23. Kelly C, Swadling L, Capone S, Brown A, Richardson R, Halliday J, et al. Chronic hepatitis C viral infection subverts vaccine-induced T-cell immunity in humans. Hepatology. 2016;
24. Simmonds P, Becher P, Bukh J, Gould EA, Meyers G, Monath T, et al. ICTV virus taxonomy profile: Flaviviridae. J Gen Virol. 2017;
25. Smith DB, Becher P, Bukh J, Gould EA, Meyers G, Monath T, et al. Proposed update to the taxonomy of the genera Hepacivirus and Pegivirus within the

Flaviviridae family. J Gen Virol. 2016;

26. Drexler JF, Corman VM, Drosten C. Ecology, evolution and classification of bat coronaviruses in the aftermath of SARS. Antiviral Research. 2014.
27. Deinhardt F, Holmes AW, Capps RB, Popper H. Studies on the transmission of human viral hepatitis to marmoset monkeys. I. Transmission of disease, serial passages, and description of liver lesions. J Exp Med. 1967;
28. Hartlage AS, Cullen JM, Kapoor A. The Strange, Expanding World of Animal Hepaciviruses. Annual Review of Virology. 2016.
29. Shi M, Lin X-D, Vasilakis N, Tian J-H, Li C-X, Chen L-J, et al. Divergent Viruses Discovered in Arthropods and Vertebrates Revise the Evolutionary History of the Flaviviridae and Related Viruses. J Virol. 2016;
30. Porter AF, Pettersson JHO, Chang WS, Harvey E, Rose K, Shi M, et al. Metagenomic identification of diverse animal hepaciviruses and pegiviruses. bioRxiv. 2020.
31. Scheel TKH, Simmonds P, Kapoor A. Surveying the global virome: Identification and characterization of HCV-related animal hepaciviruses. Antiviral Research. 2015.
32. Simmonds P. The origin of hepatitis C virus. Curr Top Microbiol Immunol. 2013;
33. Schroder K, Hertzog PJ, Ravasi T, Hume DA. Interferon- y : an overview of signals , mechanisms and functions. J Leukoc Biol. 2004;75(February):163–89.
34. Pfaender S, Cavalleri JMV, Walter S, Doerrbecker J, Campana B, Brown RJP, et al. Clinical course of infection and viral tissue tropism of hepatitis C virus-like nonprimate hepaciviruses in horses. Hepatology. 2015;
35. Thézé J, Lowes S, Parker J, Pybus OG. Evolutionary and phylogenetic analysis of the hepaciviruses and pegiviruses. Genome Biol Evol. 2015;
36. Borgia SM, Hedskog C, Parhy B, Hyland RH, Stamm LM, Brainard DM, et al. Identification of a novel hepatitis C virus genotype from Punjab, India: Expanding classification of hepatitis C virus into 8 genotypes. J Infect Dis. 2018;
37. Bukh J. The history of hepatitis C virus (HCV): Basic research reveals unique features in phylogeny, evolution and the viral life cycle with new perspectives for epidemic control. Journal of Hepatology. 2016.

38. Simmonds P, Holmes EC, Cha TA, Chan SW, McOmish F, Irvine B, et al. Classification of hepatitis C virus into six major genotypes and a series of subtypes by phylogenetic analysis of the NS-5 region. J Gen Virol. 1993;
39. Smith DB, Bukh J, Kuiken C, Muerhoff AS, Rice CM, Stapleton JT, et al. Expanded classification of hepatitis C virus into 7 genotypes and 67 subtypes: Updated criteria and genotype assignment web resource. Hepatology. 2014;
40. Okamoto H, Kurai K, Okada SI, Yamamoto K, Lizuka H, Tanaka T, et al. Full-length sequence of a hepatitis C virus genome having poor homology to reported isolates: Comparative study of four distinct genotypes. Virology. 1992;
41. Simmonds P, Bukh J, Combet C, Deléage G, Enomoto N, Feinstone S, et al. Consensus proposals for a unified system of nomenclature of hepatitis C virus genotypes. Hepatology. 2005.
42. Echeverría N, Moratorio G, Cristina J, Moreno P. Hepatitis C virus genetic variability and evolution. World J Hepatol. 2015;
43. Bukh J, Purcell RH, Miller RH. Sequence analysis of the 5' noncoding region of hepatitis C virus. Proc Natl Acad Sci U S A. 1992;
44. Piñeiro D, Martinez-Salas E. RNA structural elements of hepatitis C virus controlling viral RNA translation and the implications for viral pathogenesis. Viruses. 2012.
45. Argentini C, Genovese D, Dettori S, Rapicetta M. HCV genetic variability: From quasispecies evolution to genotype classification. Future Microbiology. 2009.
46. Guillou-guillemette H Le, Vallet S, Payan C, Pivert A, Goudeau A. Genetic diversity of the hepatitis C virus and antiviral therapy. World J Gastroenterol. 2007;
47. Domingo E, Gomez J. Quasispecies and its impact on viral hepatitis. Virus Res. 2007;
48. Martell M, Esteban JI, Quer J, Genescà J, Weiner A, Esteban R, et al. Hepatitis C virus (HCV) circulates as a population of different but closely related genomes: quasispecies nature of HCV genome distribution. J Virol. 1992;
49. Alter HJ, Conry-Cantilena C, Melpolder J, Tan D, Van Raden M, Herion D, et al. Hepatitis C in asymptomatic blood donors. Hepatology. 1997;
50. Grebely J, Page K, Sacks-Davis R, van der Loeff MS, Rice TM, Bruneau J, et al. The effects of female sex, viral genotype, and IL28B genotype on

spontaneous clearance of acute hepatitis C virus infection. Hepatology. 2014;
51. van den Berg CHBS, Grady BPX, Schinkel J, van de Laar T, Molenkamp R, van Houdt R, et al. Female sex and IL28b, a synergism for spontaneous viral clearance in hepatitis c virus (HCV) seroconverters from a community-based cohort. PLoS One. 2011;
52. J. GG, K. P, M. H, G.V. M, V. S, T. A, et al. Potential role for interleukin-28B genotype in treatment decision-making in recent hepatitis C virus infection. Hepatology. 2010;
53. H.L. T, A.J. T, K. P, M. W, H. T, H.D. N, et al. A polymorphism near IL28B is associated with spontaneous clearance of acute hepatitis C virus and jaundice. Gastroenterology. 2010;
54. Swann RE, Mandalou P, Robinson MW, Ow MM, Foung SKH, McLauchlan J, et al. Anti-envelope antibody responses in individuals at high risk of hepatitis C virus who resist infection. J Viral Hepat. 2016;
55. Dustin LB. Innate and Adaptive Immune Responses in Chronic HCV Infection. Curr Drug Targets. 2015;
56. Diepolder HM, Gerlach JT, Zachoval R, Hoffmann RM, Jung MC, Wierenga EA, et al. Immunodominant CD4+ T-cell epitope within nonstructural protein 3 in acute hepatitis C virus infection. J Virol. 1997;
57. Missale G, Bertoni R, Lamonaca V, Valli A, Massari M, Mori C, et al. Different clinical behaviors of acute hepatitis C virus infection are associated with different vigor of the anti-viral cell-mediated immune response. J Clin Invest. 1996;
58. Lechner F, Wong DKH, Dunbar PR, Chapman R, Chung RT, Dohrenwend P, et al. Analysis of successful immune responses in persons infected with hepatitis C virus. J Exp Med. 2000;
59. Walker MR, Li H, Teutsch S, Betz-Stablein B, Luciani F, Lloyd AR, et al. Incident hepatitis c virus genotype distribution and multiple infection in australian prisons. J Clin Microbiol. 2016;
60. Swann RE, Cowton VM, Robinson MW, Cole SJ, Barclay ST, Mills PR, et al. Broad Anti-Hepatitis C Virus (HCV) Antibody Responses Are Associated with Improved Clinical Disease Parameters in Chronic HCV Infection. J Virol. 2016;
61. Krugman S, Giles JP, Hammond J. Infectious Hepatitis: Evidence for Two Distinctive Clinical, Epidemiological, and Immunological Types of Infection.

JAMA J Am Med Assoc. 1967;

62. Blumberg BS, Alter HJ, Visnich S. A “New” Antigen in Leukemia Sera. JAMA J Am Med Assoc. 1965;
63. Crofts N, Hopper JL, Milner R, Breschkin AM, Bowden DS, Locarnini SA. Blood-borne virus infections among Australian injecting drug users: Implications for spread of HIV. Eur J Epidemiol. 1994;
64. Petruzziello A, Coppola N, Loquercio G, Marigliano S, Giordano M, Azzaro R, et al. Distribution pattern of hepatitis C Virus genotypes and correlation with viral load and risk factors in chronic positive patients. Intervirology. 2014;
65. ROY K, HAY G, ANDRAGETTI R, TAYLOR A, GOLDBERG D, WIESSING L. Monitoring hepatitis C virus infection among injecting drug users in the European Union: a review of the literature. Epidemiol Infect. 2002;
66. Scheinmann R, Hagan H, Lelutiu-Weinberger C, Stern R, Jarlais DCD, Flom PL, et al. Non-injection drug use and Hepatitis C Virus: A systematic review. Drug and Alcohol Dependence. 2007.
67. Urbanus AT, Van De Laar TJ, Stolte IG, Schinkel J, Heijman T, Coutinho RA, et al. Hepatitis C virus infections among HIV-infected men who have sex with men: An expanding epidemic. AIDS. 2009;
68. Giraudon I, Ruf M, Maguire H, Charlett A, Ncube F, Turner J, et al. Increase in diagnosed newly acquired hepatitis C in HIV-positive men who have sex with men across London and Brighton, 2002-2006: Is this an outbreak? Sex Transm Infect. 2008;
69. Fierer DS, Uriel AJ, Carriero DC, Klepper A, Dieterich DT, Mullen MP, et al. Liver Fibrosis during an Outbreak of Acute Hepatitis C Virus Infection in HIV-Infected Men: A Prospective Cohort Study. J Infect Dis. 2008;
70. Taylor LE, Holubar M, Wu K, Bosch RJ, Wyles DL, Davis JA, et al. Incident hepatitis C virus infection among US HIV-infected men enrolled in clinical trials. Clin Infect Dis. 2011;
71. Raska M, Takahashi K, Czernekova L, Zachova K, Hall S, Moldoveanu Z, et al. Glycosylation Patterns of HIV-1 gp120 Depend on the Type of Expressing Cells and Affect Antibody Recognition. J Biol Chem. 2010 Jul 2;285(27):20860–9.
72. Matthews G V., Hellard M, Kaldor J, Lloyd A, Dore GJ. Further evidence of HCV sexual transmission among HIV-positive men who have sex with men:

Response to Danta et al. [2]. AIDS. 2007.

73. Yaphe S, Bozinoff N, Kyle R, Shivkumar S, Pai NP, Klein M. Incidence of acute hepatitis C virus infection among men who have sex with men with and without HIV infection: A systematic review. Sexually Transmitted Infections. 2012.
74. Quan VM, Go VF, Nam L Van, Bergenstrom A, Thuoc NP, Zenilman J, et al. Risks for HIV, HBV, and HCV infections among male injection drug users in northern Vietnam: A case-control study. AIDS Care - Psychol Socio-Medical Asp AIDS/HIV. 2009;
75. Chemaitelly H, Mahmud S, Rahmani AM, Abu-Raddad LJ. The epidemiology of hepatitis C virus in Afghanistan: Systematic review and meta-analysis. International Journal of Infectious Diseases. 2015.
76. Thursz M, Fontanet A. HCV transmission in industrialized countries and resource-constrained areas. Nature Reviews Gastroenterology and Hepatology. 2014.
77. Frank C, Mohamed MK, Strickland GT, Lavanchy D, Arthur RR, Magder LS, et al. The role of parenteral antischistosomal therapy in the spread of hepatitis C virus in Egypt. Lancet. 2000;
78. Nerrienet E, Pouillot R, Lachenal G, Njouom R, Mfoupouendoun J, Bilong C, et al. Hepatitis C virus infection in Cameroon: A cohort-effect. J Med Virol. 2005;
79. Iles JC, Abby Harrison GL, Lyons S, Djoko CF, Tamoufe U, Lebreton M, et al. Hepatitis C virus infections in the Democratic Republic of Congo exhibit a cohort effect. Infect Genet Evol. 2013;
80. Njouom R, Caron M, Besson G, Ndong-Atome GR, Makuwa M, Pouillot R, et al. Phylogeography, risk factors and genetic history of hepatitis C virus in Gabon, Central Africa. PLoS One. 2012;
81. Lavanchy D. The global burden of hepatitis C. In: Liver International. 2009.
82. Gower E, Estes C, Blach S, Razavi-Shearer K, Razavi H. Global epidemiology and genotype distribution of the hepatitis C virus infection. Journal of Hepatology. 2014.
83. Younossi Z, Kallman J, Kincaid J. Global hepatitis report, 2017. Hepatology. 2007.
84. Mohd Hanafiah K, Groeger J, Flaxman AD, Wiersma ST. Global epidemiology of hepatitis C virus infection: New estimates of age-specific antibody to HCV

seroprevalence. Hepatology. 2013;

85. Aly Abd Elrazek AEM, Bilasy SE, Elbanna AEM, Elsherif AEA. Prior to the oral therapy, what do we know about HCV-4 in Egypt: A randomized survey of prevalence and risks using data mining computed analysis. Med (United States). 2014;
86. Umer M, Iqbal M. Hepatitis C virus prevalence and genotype distribution in Pakistan: Comprehensive review of recent data. World Journal of Gastroenterology. 2016.
87. Riou J, Aït Ahmed M, Blake A, Vozlinsky S, Brichler S, Eholié S, et al. Hepatitis C virus seroprevalence in adults in Africa: A systematic review and meta-analysis. Journal of Viral Hepatitis. 2016.
88. Sharvadze L, Nelson KE, Imnadze P, Karchava M, Tsertsvadze T. Prevalence of HCV and genotypes distribution in general population of Georgia. Georgian Med News. 2008;
89. Messina JP, Humphreys I, Flaxman A, Brown A, Cooke GS, Pybus OG, et al. Global distribution and prevalence of hepatitis C virus genotypes. Hepatology. 2015;
90. Smith DB, Pathirana S, Davidson F, Lawlor E, Power J, Yap PL, et al. The origin of hepatitis C virus genotypes. J Gen Virol. 1997;
91. Rao MR, Naficy AB, Darwish MA, Darwish NM, Schisterman E, Clemens JD, et al. Further evidence for association of hepatitis C infection with parenteral schistosomiasis treatment in Egypt. BMC Infect Dis. 2002;
92. Magiorkinis G, Magiorkinis E, Paraskevis D, Ho SYW, Shapiro B, Pybus OG, et al. The global spread of hepatitis C virus 1a and 1b: A phylodynamic and phylogeographic analysis. PLoS Med. 2009;
93. Simmonds P. The origin and evolution of hepatitis viruses in humans. J Gen Virol. 2001;
94. Pybus OG, Barnes E, Taggart R, Lemey P, Markov P V., Rasachak B, et al. Genetic History of Hepatitis C Virus in East Asia. J Virol. 2009;
95. Costella A, Harris H, Mandal S, Ramsay M. Hepatitis C in England 2017 report Working to eliminate hepatitis C as a major public health threat. Public Health England. 2017.
96. Harris RJ, Harris HE, Mandal S, Ramsay M, Vickerman P, Hickman M, et al. Monitoring the hepatitis C epidemic in England and evaluating intervention

scale-up using routinely collected data. J Viral Hepat. 2019;

97. Mohsen AH, Green ST, Irving WL, Jones DA, McKendrick MW, Mohsen A, et al. The epidemiology of hepatitis C in a UK health regional population of 5.12 million. Gut. 2001;
98. McLauchlan J, Innes H, Dillon JF, Foster G, Holtham E, McDonald S, et al. Cohort Profile: The Hepatitis C Virus (HCV) Research UK Clinical Database and Biobank. Int J Epidemiol. 2017;
99. Hollander A, Glaumann H, Weiland O. Histological Findings, Genotype Distribution and Percentage of Patients Fulfilling the Treatment Criteria among Patients with Chronic Hepatitis C Virus Infection in a Single Swedish Centre. Scand J Gastroenterol. 2004;
100. Zhou YH, Yao ZH, Liu FL, Li H, Jiang L, Zhu JW, et al. High prevalence of HIV, HCV, HBV and co-infection and associated risk factors among injecting drug users in Yunnan Province, China. PLoS One. 2012;
101. Mcnaughton AL, Thomson EC, Templeton K, Gunson RN, Leitch ECM. Mixed genotype hepatitis C infections and implications for treatment. Hepatology. 2014.
102. Falade-Nwulia O, Sulkowski MS, Merkow A, Latkin C, Mehta SH. Understanding and addressing hepatitis C reinfection in the oral direct-acting antiviral era. Journal of Viral Hepatitis. 2018.
103. Welsch C, Jesudian A, Zeuzem S, Jacobson I. New direct-acting antiviral agents for the treatment of hepatitis C virus infection and perspectives. Gut. 2012.
104. Fried MW, Shiffman ML, Rajender Reddy K, Smith C, Marinos G, Gonçales FL, et al. Peginterferon alfa-2a plus ribavirin for chronic hepatitis C virus infection. N Engl J Med. 2002;
105. Ghany MG, Strader DB, Thomas DL, Seeff LB. Diagnosis, management, and treatment of hepatitis C: An update. Hepatology. 2009;
106. Mchutchison JG, Gordon SC, Schiff ER, Shiffman ML, Lee WM, Rustgi VK, et al. Interferon alfa-2b alone or in combination with ribavirin as initial treatment for chronic hepatitis C. N Engl J Med. 1998;
107. Zoratti MJ, Siddiqua A, Morassut RE, Zeraatkar D, Chou R, van Holten J, et al. Pangenotypic direct acting antivirals for the treatment of chronic hepatitis C virus infection: A systematic literature review and meta-analysis.

EClinicalMedicine. 2020;
108. Zoulim F, Liang TJ, Gerbes AL, Aghemo A, Deuffic-Burban S, Dusheiko G, et al. Hepatitis C virus treatment in the real world: Optimising treatment and access to therapies. Gut. 2015;
109. Sundberg I, Lannergård A, Ramklint M, Cunningham JL. Direct-acting antiviral treatment in real world patients with hepatitis C not associated with psychiatric side effects: A prospective observational study. BMC Psychiatry. 2018;
110. WHO G. Monitoring and evaluation for viral hepatitis b and c: 2016;40.
111. Terrault NA. Hepatitis C elimination: Challenges with under-diagnosis and under-treatment [version 1; referees: 2 approved]. F1000Research. 2019.
112. Alimohammadi A, Holeksa J, Thiam A, Truong D, Conway B. Real-world efficacy of direct-acting antiviral therapy for HCV infection affecting people who inject drugs delivered in a multidisciplinary setting. Open Forum Infect Dis. 2018;
113. Scott N, Wilson DP, Thompson AJ, Barnes E, El-Sayed M, Benzaken AS, et al. The case for a universal hepatitis C vaccine to achieve hepatitis C elimination. BMC Med. 2019;
114. Gastaminza P, Dryden KA, Boyd B, Wood MR, Law M, Yeager M, et al. Ultrastructural and Biophysical Characterization of Hepatitis C Virus Particles Produced in Cell Culture. J Virol. 2010;
115. Merz A, Long G, Hiet MS, Brügger B, Chlanda P, Andre P, et al. Biochemical and morphological properties of hepatitis C virus particles and determination of their lipidome. J Biol Chem. 2011;
116. Catanese MT, Uryu K, Kopp M, Edwards TJ, Andrus L, Rice WJ, et al. Ultrastructural analysis of hepatitis C virus particles. Proc Natl Acad Sci U S A. 2013;
117. Bassendine MF, Sheridan DA, Felmlee DJ, Bridge SH, Toms GL, Neely RDG. HCV and the hepatic lipid pathway as a potential treatment target. Journal of Hepatology. 2011.
118. Meunier J-C, Russell RS, Engle RE, Faulk KN, Purcell RH, Emerson SU. Apolipoprotein C1 Association with Hepatitis C Virus. J Virol. 2008;
119. Piver E, Boyer A, Gaillard J, Bull A, Beaumont E, Roingeard P, et al. Ultrastructural organisation of HCV from the bloodstream of infected patients revealed by electron microscopy after specific immunocapture. Gut. 2017;

120. Aizawa Y, Seki N, Nagano T, Abe H. Chronic hepatitis C virus infection and lipoprotein metabolism. World Journal of Gastroenterology. 2015.
121. Wrensch F, Crouchet E, Ligat G, Zeisel MB, Keck ZY, Foung SKH, et al. Hepatitis C virus (HCV)-apolipoprotein interactions and immune evasion and their impact on HCV vaccine design. Frontiers in Immunology. 2018.
122. Rehermann B. Hepatitis C virus versus innate and adaptive immune responses: A tale of coevolution and coexistence. Journal of Clinical Investigation. 2009.
123. Jopling CL, Yi M, Lancaster AM, Lemon SM, Sarnow P. Modulation of Hepatitis C Virus RNA Abundance by a. Science (80-). 2005;
124. Shimakami T, Yamane D, Jangra RK, Kempf BJ, Spaniel C, Barton DJ, et al. Stabilization of hepatitis C virus RNA by an Ago2-miR-122 complex. Proc Natl Acad Sci U S A. 2012;
125. Lohmann V, Körner F, Koch JO, Herian U, Theilmann L, Bartenschlager R. Replication of subgenomic hepatitis C virus RNAs in a hepatoma cell line. Science (80-). 1999;
126. Kuiken C, Combet C, Bukh J, Shin-I T, Deleage G, Mizokami M, et al. A comprehensive system for consistent numbering of HCV sequences, proteins and epitopes. Hepatology. 2006.
127. Alazard-Dany N, Denolly S, Boson B, Cosset FL. Overview of hcv life cycle with a special focus on current and possible future antiviral targets. Viruses. 2019.
128. Popescu CI, Callens N, Trinel D, Roingeard P, Moradpour D, Descamps V, et al. NS2 protein of hepatitis C virus interacts with structural and non-structural proteins towards virus assembly. PLoS Pathog. 2011;
129. Kim JL, Morgenstern KA, Lin C, Fox T, Dwyer MD, Landro JA, et al. Crystal structure of the hepatitis C virus NS3 protease domain complexed with a synthetic NS4A cofactor peptide. Cell. 1996;
130. Paul D. Architecture and biogenesis of plus-strand RNA virus replication factories. World J Virol. 2013;
131. Niepmann M, Shalamova LA, Gerresheim GK, Rossbach O. Signals involved in regulation of hepatitis C virus RNA genome translation and replication. Frontiers in Microbiology. 2018.
132. Elazar M, Liu P, Rice CM, Glenn JS. An N-Terminal Amphipathic Helix in

Hepatitis C Virus (HCV) NS4B Mediates Membrane Association, Correct Localization of Replication Complex Proteins, and HCV RNA Replication. J Virol. 2004;

133. Miller S, Krijnse-Locker J. Modification of intracellular membrane structures for virus replication. Nature Reviews Microbiology. 2008.
134. Einav S, Gerber D, Bryson PD, Sklan EH, Elazar M, Maerkl SJ, et al. Discovery of a hepatitis C target and its pharmacological inhibitors by microfluidic affinity analysis. Nat Biotechnol. 2008;
135. Tellinghuisen TL, Marcotrigiano J, Gorbalenya AE, Rice CM. The NS5A protein of hepatitis C virus is a zinc metalloprotein. J Biol Chem. 2004;
136. Ross-Thriepland D, Harris M. Hepatitis C virus NS5A: Enigmatic but still promiscuous 10 years on! Journal of General Virology. 2015.
137. Berger KL, Cooper JD, Heaton NS, Yoon R, Oakland TE, Jordan TX, et al. Roles for endocytic trafficking and phosphatidylinositol 4-kinase III alpha in hepatitis C virus replication. Proc Natl Acad Sci U S A. 2009;
138. Vicinanza M, D'Angelo G, Di Campli A, De Matteis MA. Function and dysfunction of the PI system in membrane trafficking. EMBO Journal. 2008.
139. Madan V, Paul D, Lohmann V, Bartenschlager R. Inhibition of HCV replication by cyclophilin antagonists is linked to replication fitness and occurs by inhibition of membranous web formation. Gastroenterology. 2014;
140. Quinkert D, Bartenschlager R, Lohmann V. Quantitative Analysis of the Hepatitis C Virus Replication Complex. J Virol. 2005;
141. Lohmann V. Hepatitis C Virus RNA Replication. In 2013.
142. Lindenbach BD, Rice CM. The ins and outs of hepatitis C virus entry and assembly. Nat Rev Micro. 2013;11(10):688–700.
143. Miyanari Y, Atsuzawa K, Usuda N, Watashi K, Hishiki T, Zayas M, et al. The lipid droplet is an important organelle for hepatitis C virus production. Nat Cell Biol. 2007;
144. Jones DM, McLauchlan J. Hepatitis C virus: Assembly and release of virus particles. Journal of Biological Chemistry. 2010.
145. Zayas M, Long G, Madan V, Bartenschlager R. Coordination of Hepatitis C Virus Assembly by Distinct Regulatory Regions in Nonstructural Protein 5A. PLoS Pathog. 2016;
146. Denolly S, Mialon C, Bourlet T, Amirache F, Penin F, Lindenbach B, et al. The

amino-terminus of the hepatitis C virus (HCV) p7 viroporin and its cleavage from glycoprotein E2-p7 precursor determine specific infectivity and secretion levels of HCV particle types. PLoS Pathog. 2017;

147. Ma Y, Anantpadma M, Timpe JM, Shanmugam S, Singh SM, Lemon SM, et al. Hepatitis C Virus NS2 Protein Serves as a Scaffold for Virus Assembly by Interacting with both Structural and Nonstructural Proteins. J Virol. 2011;
148. Boson B, Granio O, Bartenschlager R, CossetFranç FL. A concerted action of hepatitis C virus P7 and nonstructural protein 2 regulates core localization at the endoplasmic reticulum and virus assembly. PLoS Pathog. 2011;
149. Stapleford KA, Lindenbach BD. Hepatitis C Virus NS2 Coordinates Virus Particle Assembly through Physical Interactions with the E1-E2 Glycoprotein and NS3-NS4A Enzyme Complexes. J Virol. 2011;
150. Barouch-Bentov R, Neveu G, Xiao F, Beer M, Bekerman E, Schor S, et al. Hepatitis C virus proteins interact with the endosomal sorting complex required for transport (ESCRT) machinery via ubiquitination to facilitate viral envelopment. MBio. 2016;
151. Corless L, Crump CM, Griffin SDC, Harris M. Vps4 and the ESCRT-III complex are required for the release of infectious Hepatitis C virus particles. J Gen Virol. 2010;
152. Tamai K, Shiina M, Tanaka N, Nakano T, Yamamoto A, Kondo Y, et al. Regulation of hepatitis C virus secretion by the Hrs-dependent exosomal pathway. Virology. 2012;
153. Vieyres G, Thomas X, Descamps V, Duverlie G, Patel AH, Dubuisson J. Characterization of the Envelope Glycoproteins Associated with Infectious Hepatitis C Virus. J Virol. 2010 Oct 1;84(19):10159–68.
154. Falcón V, Acosta-Rivero N, González S, Dueñas-Carrera S, Martinez-Donato G, Menéndez I, et al. Ultrastructural and biochemical basis for hepatitis C virus morphogenesis. Virus Genes. 2017.
155. Gastaminza P, Cheng G, Wieland S, Zhong J, Liao W, Chisari F V. Cellular Determinants of Hepatitis C Virus Assembly, Maturation, Degradation, and Secretion. J Virol. 2008;
156. Gastaminza P, Kapadia SB, Chisari F V. Differential Biophysical Properties of Infectious Intracellular and Secreted Hepatitis C Virus Particles. J Virol. 2006;
157. Gerold G, Bruening J, Weigel B, Pietschmann T. Protein interactions during

the Flavivirus and hepacivirus life cycle. Molecular and Cellular Proteomics. 2017.
158. Adams RL, Pirakitikulr N, Pyle AM. Functional RNA structures throughout the Hepatitis C Virus genome. Current Opinion in Virology. 2017.
159. Heim MH, Thimme R. Innate and adaptive immune responses in HCV infections. Journal of Hepatology. 2014.
160. Klenerman P, Thimme R. T cell responses in hepatitis C: The good, the bad and the unconventional. Gut. 2012.
161. Sioud M. Innate sensing of self and non-self RNAs by Toll-like receptors. Trends in Molecular Medicine. 2006.
162. Heim MH. HCV innate immune responses. Viruses. 2009.
163. Wang B, Trippler M, Pei R, Lu M, Broering R, Gerken G, et al. Toll-like receptor activated human and murine hepatic stellate cells are potent regulators of hepatitis C virus replication. J Hepatol. 2009;
164. Sen GC. Viruses and interferons. Annual Review of Microbiology. 2001.
165. Ferreira AR, Ramos B, Nunes A, Ribeiro D. Hepatitis C Virus: Evading the Intracellular Innate Immunity. J Clin Med. 2020;
166. Li XD, Sun L, Seth RB, Pineda G, Chen ZJ. Hepatitis C virus protease NS3/4A cleaves mitochondrial antiviral signaling protein off the mitochondria to evade innate immunity. Proc Natl Acad Sci U S A. 2005;
167. Horner SM, Gale M. Regulation of hepatic innate immunity by hepatitis C virus. Nature Medicine. 2013.
168. Cheent K, Khakoo SI. Natural killer cells and hepatitis C: Action and reaction. Gut. 2011.
169. Rehermann B. Natural Killer Cells in Viral Hepatitis. CMGH. 2015.
170. Abel AM, Yang C, Thakar MS, Malarkannan S. Natural killer cells: Development, maturation, and clinical utilization. Frontiers in Immunology. 2018.
171. Amadei B, Urbani S, Cazaly A, Fisicaro P, Zerbini A, Ahmed P, et al. Activation of Natural Killer Cells During Acute Infection With Hepatitis C Virus. Gastroenterology. 2010;
172. Palm AKE, Henry C. Remembrance of Things Past: Long-Term B Cell Memory After Infection and Vaccination. Frontiers in immunology. 2019.
173. Larrubia JR, Moreno-Cubero E, Lokhande MU, García-Garzón S, Lázaro A,

Miquel J, et al. Adaptive immune response during hepatitis C virus infection. World J Gastroenterol. 2014;

174. Mueller M, Spangenberg HC, Kersting N, Altay T, Blum HE, Klenerman P, et al. Virus-specific CD4+ T cell responses in chronic HCV infection in blood and liver identified by antigen-specific upregulation of CD154. J Hepatol. 2010;
175. Schulze zur Wiesch J, Lauer GM, Day CL, Kim AY, Ouchi K, Duncan JE, et al. Broad Repertoire of the CD4 + Th Cell Response in Spontaneously Controlled Hepatitis C Virus Infection Includes Dominant and Highly Promiscuous Epitopes . J Immunol. 2005;
176. Urbani S, Amadei B, Fisicaro P, Tola D, Orlandini A, Sacchelli L, et al. Outcome of acute hepatitis C is related to virus-specific CD4 function and maturation of antiviral memory CD8 responses. Hepatology. 2006;
177. Cabrera R, Tu Z, Xu Y, Firpi RJ, Rosen HR, Liu C, et al. An immunomodulatory role for CD4+CD25+ regulatory T lymphocytes in hepatitis C virus infection. Hepatology. 2004;
178. Keoshkerian E, Hunter M, Cameron B, Nguyen N, Sugden P, Bull R, et al. Hepatitis C-specific effector and regulatory CD4 T-cell responses are associated with the outcomes of primary infection. J Viral Hepat. 2016;
179. Jo J, Bengsch B, Seigel B, Rau SJ, Schmidt J, Bisse E, et al. Low perforin expression of early differentiated HCV-specific CD8+ T cells limits their hepatotoxic potential. J Hepatol. 2012;
180. Lechner F, Gruener NH, Urbani S, Uggeri J, Santantonio T, Kammer AR, et al. CD8+ T lymphocyte responses are induced during acute hepatitis C virus infection but are not sustained. Eur J Immunol. 2000;
181. Grüner NH, Gerlach TJ, Jung MC, Diepolder HM, Schirren CA, Schraut WW, et al. Association of hepatitis C virus-specific CD8+ T cells with viral clearance in acute hepatitis C. J Infect Dis. 2000;
182. Bowen DG, Walker CM. Adaptive immune responses in acute and chronic hepatitis C virus infection. Nature. 2005.
183. Bull RA, Leung P, Gaudieri S, Deshpande P, Cameron B, Walker M, et al. Transmitted/Founder Viruses Rapidly Escape from CD8 + T Cell Responses in Acute Hepatitis C Virus Infection . J Virol. 2015;
184. Urbani S, Amadei B, Tola D, Massari M, Schivazappa S, Missale G, et al. PD-1 Expression in Acute Hepatitis C Virus (HCV) Infection Is Associated with

HCV-Specific CD8 Exhaustion. J Virol. 2006;

185. Saeidi A, Zandi K, Cheok YY, Saeidi H, Wong WF, Lee CYQ, et al. T-cell exhaustion in chronic infections: Reversing the state of exhaustion and reinvigorating optimal protective immune responses. Front Immunol. 2018;
186. Janda A, Bowen A, Greenspan NS, Casadevall A. Ig constant region effects on variable region structure and function. Frontiers in Microbiology. 2016.
187. Füst G, Tóth FD, Kiss J, Ujhelyi E, Nagy I, Bánhegyi D. Neutralizing and enhancing antibodies measured in complement-restored serum samples from HIV-1-infected individuals correlate with immunosuppression and disease. AIDS. 1994;
188. Hessell AJ, Hangartner L, Hunter M, Havenith CEG, Beurskens FJ, Bakker JM, et al. Fc receptor but not complement binding is important in antibody protection against HIV. Nature. 2007;
189. Osburn WO, Fisher BE, Dowd KA, Urban G, Liu L, Ray SC, et al. Spontaneous Control of Primary Hepatitis C Virus Infection and Immunity Against Persistent Reinfection. Gastroenterology. 2010;
190. Raghuraman S, Park H, Osburn WO, Winkelstein E, Edlin BR, Rehermann B. Spontaneous clearance of chronic hepatitis C virus infection is associated with appearance of neutralizing antibodies and reversal of T-cell exhaustion. J Infect Dis. 2012;
191. Pestka JM, Zeisel MB, Blaser E, Schurmann P, Bartosch B, Cosset F-L, et al. Rapid induction of virus-neutralizing antibodies and viral clearance in a single-source outbreak of hepatitis C. Proc Natl Acad Sci. 2007 Apr 3;104(14):6025–30.
192. Dimitrov DS. Virus entry: Molecular mechanisms and biomedical applications. Nature Reviews Microbiology. 2004.
193. Marsh M, Helenius A. Virus entry: Open sesame. Cell. 2006.
194. Earnest JT, Hantak MP, Li K, McCray PB, Perlman S, Gallagher T. The tetraspanin CD9 facilitates MERS-coronavirus entry by scaffolding host cell receptors and proteases. PLoS Pathog. 2017;
195. Grove J, Marsh M. The cell biology of receptor-mediated virus entry. Journal of Cell Biology. 2011.
196. El Omari K, Iourin O, Harlos K, Grimes JM, Stuart DI. Structure of a Pestivirus Envelope Glycoprotein E2 Clarifies Its Role in Cell Entry. Cell Rep. 2013;

197. Li Y, Wang J, Kanai R, Modis Y. Crystal structure of glycoprotein E2 from bovine viral diarrhea virus. Proc Natl Acad Sci U S A. 2013;
198. Pileri P, Uematsu Y, Campagnoli S, Galli G, Falugi F, Petracca R, et al. Binding of hepatitis C virus to CD81. Science. 1998;282(5390):938–41.
199. Zimmerman B, Kelly B, McMillan BJ, Seegar TCM, Dror RO, Kruse AC, et al. Crystal Structure of a Full-Length Human Tetraspanin Reveals a Cholesterol-Binding Pocket. Cell. 2016;167(4):1041-1051.e11.
200. Zimmerman B, Kelly B, McMillan BJ, Seegar TCM, Dror RO, Kruse AC, et al. Crystal Structure of a Full-Length Human Tetraspanin Reveals a Cholesterol-Binding Pocket. Cell. 2016;167(4):1041-1051.e11.
201. Termini CM, Gillette JM. Tetraspanins function as regulators of cellular signaling. Frontiers in Cell and Developmental Biology. 2017.
202. Flint M, von Hahn T, Zhang J, Farquhar M, Jones CT, Balfe P, et al. Diverse CD81 Proteins Support Hepatitis C Virus Infection. J Virol. 2006;
203. Palor M, Stejskal L, Mandal P, Lenman A, Alberione MP, Kirui J, et al. Cholesterol sensing by CD81 is important for hepatitis C virus entry. J Biol Chem. 2020;
204. Roccasecca R, Ansuini H, Vitelli A, Meola A, Scarselli E, Acali S, et al. Binding of the Hepatitis C Virus E2 Glycoprotein to CD81 Is Strain Specific and Is Modulated by a Complex Interplay between Hypervariable Regions 1 and 2. J Virol. 2003;
205. Keck Z, Li SH, Xia J, von Hahn T, Balfe P, McKeating JA, et al. Mutations in Hepatitis C Virus E2 Located outside the CD81 Binding Sites Lead to Escape from Broadly Neutralizing Antibodies but Compromise Virus Infectivity. J Virol. 2009;
206. Drummer HE, Boo I, Maerz AL, Poumbourios P. A Conserved Gly436-Trp-Leu-Ala-Gly-Leu-Phe-Tyr Motif in Hepatitis C Virus Glycoprotein E2 Is a Determinant of CD81 Binding and Viral Entry. J Virol. 2006;
207. Krieger M. Scavenger receptor class b type I is a multiligand hdl receptor that influences diverse physiologic systems. Journal of Clinical Investigation. 2001.
208. Shen WJ, Azhar S, Kraemer FB. SR-B1: A Unique Multifunctional Receptor for Cholesterol Influx and Efflux. Annual Review of Physiology. 2018.
209. Neculai D, Schwake M, Ravichandran M, Zunke F, Collins RF, Peters J, et al. Structure of LIMP-2 provides functional insights with implications for SR-BI and

CD36. Nature. 2013;
210. Hoekstra M, van Berkel TJC, van Eck M. Scavenger receptor BI: A multi-purpose player in cholesterol and steroid metabolism. World Journal of Gastroenterology. 2010.
211. Scarselli E, Ansuini H, Cerino R, Roccasecca RM, Acali S, Filocamo G, et al. The human scavenger receptor class B type I is a novel candidate receptor for the hepatitis C virus. EMBO J. 2002;
212. Bartosch B, Vitelli A, Granier C, Goujon C, Dubuisson J, Pascale S, et al. Cell Entry of Hepatitis C Virus Requires a Set of Co-receptors that Include the CD81 Tetraspanin and the SR-B1 Scavenger Receptor. J Biol Chem. 2003;
213. Bartosch B, Verney G, Dreux M, Donot P, Morice Y, Penin F, et al. An Interplay between Hypervariable Region 1 of the Hepatitis C Virus E2 Glycoprotein, the Scavenger Receptor BI, and High-Density Lipoprotein Promotes both Enhancement of Infection and Protection against Neutralizing Antibodies. J Virol. 2005;
214. Dreux M, Pietschmann T, Granier C, Voisset C, Ricard-Blum S, Mangeot PE, et al. High density lipoprotein inhibits hepatitis C virus-neutralizing antibodies by stimulating cell entry via activation of the scavenger receptor BI. J Biol Chem. 2006;
215. Voisset C, Op de Beeck A, Horellou P, Dreux M, Gustot T, Duverlie G, et al. High-density lipoproteins reduce the neutralizing effect of hepatitis C virus (HCV)-infected patient antibodies by promoting HCV entry. J Gen Virol. 2006;
216. Zahid MN, Turek M, Xiao F, Dao Thi VL, Guérin M, Fofana I, et al. The postbinding activity of scavenger receptor class B type I mediates initiation of hepatitis C virus infection and viral dissemination. Hepatology. 2013;57(2):492–504.
217. Thi VLD, Granier C, Zeisel MB, Guérin M, Mancip J, Granio O, et al. Characterization of hepatitis C virus particle subpopulations reveals multiple usage of the scavenger receptor BI for entry steps. J Biol Chem. 2012;287(37):31242–57.
218. Yamamoto S, Fukuhara T, Ono C, Uemura K, Kawachi Y, Shiokawa M, et al. Lipoprotein Receptors Redundantly Participate in Entry of Hepatitis C Virus. PLoS Pathog. 2016;
219. Kalemera M, Mincheva D, Grove J, Illingworth CJR. Building a mechanistic

mathematical model of hepatitis C virus entry. Wilke CO, editor. PLOS Comput Biol. 2019 Mar 18;15(3):e1006905.

220. Popescu CI, Riva L, Vlaicu O, Farhat R, Rouillé Y, Dubuisson J. Hepatitis C virus life cycle and lipid metabolism. Biology. 2014.
221. Colpitts CC, Tsai PL, Zeisel MB. Hepatitis C virus entry: An intriguingly complex and highly regulated process. International Journal of Molecular Sciences. 2020.
222. Evans MJ, Von Hahn T, Tscherne DM, Syder AJ, Panis M, Wölk B, et al. Claudin-1 is a hepatitis C virus co-receptor required for a late step in entry. Nature. 2007;
223. Ploss A, Evans MJ, Gaysinskaya VA, Panis M, You H, De Jong YP, et al. Human occludin is a hepatitis C virus entry factor required for infection of mouse cells. Nature. 2009;
224. Zihni C, Mills C, Matter K, Balda MS. Tight junctions: From simple barriers to multifunctional molecular gates. Nature Reviews Molecular Cell Biology. 2016.
225. Baktash Y, Madhav A, Coller KE, Randall G. Single Particle Imaging of Polarized Hepatoma Organoids upon Hepatitis C Virus Infection Reveals an Ordered and Sequential Entry Process. Cell Host Microbe. 2018;
226. Martin DN, Uprichard SL. Identification of transferrin receptor 1 as a hepatitis C virus entry factor. Proc Natl Acad Sci U S A. 2013;
227. Qing J, Wu M, Luo R, Chen J, Cao L, Zeng D, et al. Identification of interferon receptor ifnar2 as a novel hcv entry factor by using chemical probes. ACS Chem Biol. 2020;
228. Lupberger J, Zeisel MB, Xiao F, Thumann C, Fofana I, Zona L, et al. EGFR and EphA2 are host factors for hepatitis C virus entry and possible targets for antiviral therapy. Nat Med. 2011;
229. Sainz B, Barretto N, Martin DN, Hiraga N, Imamura M, Hussain S, et al. Identification of the Niemann-Pick C1-like 1 cholesterol absorption receptor as a new hepatitis C virus entry factor. Nat Med. 2012;
230. Monazahian M, Böhme I, Bonk S, Koch A, Scholz C, Grethe S, et al. Low density lipoprotein receptor as a candidate receptor for hepatitis C virus. J Med Virol. 1999;
231. Koutsoudakis G, Kaul A, Steinmann E, Kallis S, Lohmann V, Pietschmann T, et al. Characterization of the Early Steps of Hepatitis C Virus Infection by

Using Luciferase Reporter Viruses. J Virol. 2006;

232. Zeisel MB, Koutsoudakis G, Schnober EK, Haberstroh A, Blum HE, Cosset FL, et al. Scavenger receptor class B type I is a key host factor for hepatitis C virus infection required for an entry step closely linked to CD81. Hepatology. 2007;46(6):1722–31.
233. Bertaux C, Dragic T. Different Domains of CD81 Mediate Distinct Stages of Hepatitis C Virus Pseudoparticle Entry. J Virol. 2006;
234. Krieger SE, Zeisel MB, Davis C, Thumann C, Harris HJ, Schnober EK, et al. Inhibition of hepatitis c virus infection by anti-claudin-1 antibodies is mediated by neutralization of E2-CD81-claudin-1 associations. Hepatology. 2010;
235. Diao J, Pantua H, Ngu H, Komuves L, Diehl L, Schaefer G, et al. Hepatitis C Virus Induces Epidermal Growth Factor Receptor Activation via CD81 Binding for Viral Internalization and Entry. J Virol. 2012;
236. Dreux M, Thi VLD, Fresquet J, Guérin M, Julia Z, Verney G, et al. Receptor complementation and mutagenesis reveal SR-BI as an essential HCV entry factor and functionally imply its intra- and extra-cellular domains. PLoS Pathog. 2009;
237. Zona L, Lupberger J, Sidahmed-Adrar N, Thumann C, Harris HJ, Barnes A, et al. HRas signal transduction promotes hepatitis C virus cell entry by triggering assembly of the host tetraspanin receptor complex. Cell Host Microbe. 2013;
238. Cukierman L, Meertens L, Bertaux C, Kajumo F, Dragic T. Residues in a Highly Conserved Claudin-1 Motif Are Required for Hepatitis C Virus Entry and Mediate the Formation of Cell-Cell Contacts. J Virol. 2009;
239. Douam F, Dao Thi VL, Maurin G, Fresquet J, Mompelat D, Zeisel MB, et al. Critical interaction between E1 and E2 glycoproteins determines binding and fusion properties of hepatitis C virus during cell entry. Hepatology. 2014;
240. Sourisseau M, Michta ML, Zony C, Israelow B, Hopcraft SE, Narbus CM, et al. Temporal Analysis of Hepatitis C Virus Cell Entry with Occludin Directed Blocking Antibodies. PLoS Pathog. 2013;
241. Sharma NR, Mateu G, Dreux M, Grakoui A, Cosset FL, Melikyan GB. Hepatitis C virus is primed by CD81 protein for low pH-dependent fusion. J Biol Chem. 2011;
242. Thi VLD, Granier C, Zeisel MB, Guérin M, Mancip J, Granio O, et al. Characterization of hepatitis C virus particle subpopulations reveals multiple

usage of the scavenger receptor BI for entry steps. J Biol Chem. 2012;
243. Farquhar MJ, Hu K, Harris HJ, Davis C, Brimacombe CL, Fletcher SJ, et al. Hepatitis C Virus Induces CD81 and Claudin-1 Endocytosis. J Virol. 2012;
244. Niepmann M. Hepatitis C virus RNA translation. Curr Top Microbiol Immunol. 2013;
245. Dubuisson J, Cosset FL. Virology and cell biology of the hepatitis C virus life cycle - An update. Journal of Hepatology. 2014.
246. Timpe JM, Stamataki Z, Jennings A, Hu K, Farquhar MJ, Harris HJ, et al. Hepatitis C virus cell-cell transmission in hepatoma cells in the presence of neutralizing antibodies. Hepatology. 2008;
247. Brimacombe CL, Grove J, Meredith LW, Hu K, Syder AJ, Flores M V., et al. Neutralizing Antibody-Resistant Hepatitis C Virus Cell-to-Cell Transmission. J Virol. 2011;
248. Catanese MT, Loureiro J, Jones CT, Dorner M, von Hahn T, Rice CM. Different Requirements for Scavenger Receptor Class B Type I in Hepatitis C Virus Cell-Free versus Cell-to-Cell Transmission. J Virol. 2013;
249. Wieland S, Makowska Z, Campana B, Calabrese D, Dill MT, Chung J, et al. Simultaneous detection of hepatitis C virus and interferon stimulated gene expression in infected human liver. Hepatology. 2014;
250. Ramakrishnaiah V, Thumann C, Fofana I, Habersetzer F, Pan Q, De Ruiter PE, et al. Exosome-mediated transmission of hepatitis C virus between human hepatoma Huh7.5 cells. Proc Natl Acad Sci U S A. 2013;
251. Kielian M, Rey FA. Virus membrane-fusion proteins: More than one way to make a hairpin. Nature Reviews Microbiology. 2006.
252. Rey FA, Lok SM. Common Features of Enveloped Viruses and Implications for Immunogen Design for Next-Generation Vaccines. Cell. 2018.
253. Wilson IA, Skehel JJ, Wiley DC. Structure of the haemagglutinin membrane glycoprotein of influenza virus at 3 Å resolution. Nature. 1981;
254. Doms RW. What Came First—the Virus or the Egg? Cell. 2017.
255. Yamauchi Y, Helenius A. Virus entry at a glance. Journal of Cell Science. 2013.
256. Shaik MM, Peng H, Lu J, Rits-Volloch S, Xu C, Liao M, et al. Structural basis of coreceptor recognition by HIV-1 envelope spike. Nature. 2019;
257. White JM, Whittaker GR. Fusion of Enveloped Viruses in Endosomes. Traffic.

2016.

258. Key T, Sarker M, De Antueno R, Rainey JK, Duncan R. The p10 FAST protein fusion peptide functions as a cystine noose to induce cholesterol-dependent liposome fusion without liposome tubulation. Biochim Biophys Acta - Biomembr. 2015;
259. Leikin S. Hydration Forces. Annu Rev Phys Chem. 1993;
260. Chernomordik L V., Kozlov MM. Mechanics of membrane fusion. Nature Structural and Molecular Biology. 2008.
261. Vigant F, Santos NC, Lee B. Broad-spectrum antivirals against viral fusion. Nature Reviews Microbiology. 2015.
262. Harrison SC. Viral membrane fusion. Virology. 2015.
263. Lavialle C, Cornelis G, Dupressoir A, Esnault C, Heidmann O, Vernochet C, et al. Paleovirology of “syncytins”, retroviral env genes exapted for a role in placentation. Philosophical Transactions of the Royal Society B: Biological Sciences. 2013.
264. Sha M, Lee X, Li X ping, Veldman GM, Finnerty H, Racie L, et al. Syncytin is a captive retroviral envelope protein involved in human placental morphogenesis. Nature. 2000;
265. Pérez-Vargas J, Krey T, Valansi C, Avinoam O, Haouz A, Jamin M, et al. Structural basis of eukaryotic cell-cell fusion. Cell. 2014;
266. Fédry J, Liu Y, Péhau-Arnaudet G, Pei J, Li W, Tortorici MA, et al. The Ancient Gamete Fusogen HAP2 Is a Eukaryotic Class II Fusion Protein. Cell. 2017;
267. Baquero E, Albertini AAV, Gaudin Y. Recent mechanistic and structural insights on class III viral fusion glycoproteins. Current Opinion in Structural Biology. 2015.
268. Vollmer B, Prazák V, Vasishtan D, Jefferys EE, Hernandez-Duran A, Vallbracht M, et al. The prefusion structure of herpes simplex virus glycoprotein B. Sci Adv. 2020;
269. Liu Y, Heim KP, Che Y, Chi X, Qiu X, Han S, et al. Prefusion structure of human cytomegalovirus glycoprotein B and structural basis for membrane fusion. Sci Adv. 2021;
270. Lavie M, Goffard A, Dubuisson J. HCV Glycoproteins: Assembly of a Functional E1–E2 Heterodimer. Hepatitis C Viruses: Genomes and Molecular Biology. 2006.

271. Falson P, Bartosch B, Alsaleh K, Tews BA, Loquet A, Ciczora Y, et al. Hepatitis C Virus Envelope Glycoprotein E1 Forms Trimers at the Surface of the Virion. J Virol. 2015;
272. Lavie M, Goffard A, Dubuisson J. Assembly of a functional HCV glycoprotein heterodimer. Current Issues in Molecular Biology. 2007.
273. Kong L, Giang E, Nieusma T, Kadam RU, Cogburn KE, Hua Y, et al. Hepatitis C virus e2 envelope glycoprotein core structure. Sci (New York, NY). 2013;342(6162):1090–4.
274. Khan AG, Whidby J, Miller MT, Scarborough H, Zatorski A V., Cygan A, et al. Structure of the core ectodomain of the hepatitis C virus envelope glycoprotein 2. Nature. 2014 May 19;509(7500):381–4.
275. Helle F, Vieyres G, Elkrief L, Popescu C-I, Wychowski C, Descamps V, et al. Role of N-Linked Glycans in the Functions of Hepatitis C Virus Envelope Proteins Incorporated into Infectious Virions. J Virol. 2010 Nov 15;84(22):11905–15.
276. Goffard A, Dubuisson J. Glycosylation of hepatitis C virus envelope proteins. Biochimie. 2003.
277. Ball JK, Tarr AW, McKeating JA. The past, present and future of neutralizing antibodies for hepatitis C virus. Antiviral Research. 2014.
278. Kobayashi Y, Suzuki Y. Evidence for N-Glycan Shielding of Antigenic Sites during Evolution of Human Influenza A Virus Hemagglutinin. J Virol. 2012 Apr 1;86(7):3446–51.
279. Lavie M, Hanoulle X, Dubuisson J. Glycan Shielding and Modulation of Hepatitis C Virus Neutralizing Antibodies. Front Immunol. 2018 Apr 27;9.
280. Flyak AI, Ruiz S, Colbert MD, Luong T, Crowe JE, Bailey JR, et al. HCV Broadly Neutralizing Antibodies Use a CDRH3 Disulfide Motif to Recognize an E2 Glycoprotein Site that Can Be Targeted for Vaccine Design. Cell Host Microbe. 2018;
281. Bartosch B, Dubuisson J, Cosset F-L. Infectious Hepatitis C Virus Pseudo-particles Containing Functional E1–E2 Envelope Protein Complexes. J Exp Med. 2003 Mar 3;197(5):633–42.
282. Wakita T, Pietschmann T, Kato T, Date T, Miyamoto M, Zhao Z, et al. Production of infectious hepatitis C virus in tissue culture from a cloned viral genome. Nat Med. 2005 Jul 12;11(7):791–6.

283. Lindenbach BD, Evans MJ, Syder AJ, Wölk B, Tellinghuisen TL, Liu CC, et al. Virology: Complete replication of hepatitis C virus in cell culture. Science (80-). 2005;
284. Yost SA, Wang Y, Marcotrigiano J. Hepatitis C Virus Envelope Glycoproteins: A Balancing Act of Order and Disorder. Frontiers in immunology. 2018.
285. Drummer HE. Challenges to the development of vaccines to hepatitis C virus that elicit neutralizing antibodies. Frontiers in Microbiology. 2014.
286. Tong Y, Lavillette D, Li Q, Zhong J. Role of hepatitis C virus envelope glycoprotein E1 in virus entry and assembly. Frontiers in Immunology. 2018.
287. Moustafa RI, Dubuisson J, Lavie M. Function of the HCV E1 envelope glycoprotein in viral entry and assembly. Future Virology. 2019.
288. Walker LM, Phogat SK, Wagner D, Goss JL, Wrin T, Simek MD, et al. NIH Public Access. 2012;326(5950):285–9.
289. Zhang M, Gaschen B, Blay W, Foley B, Haigwood N, Kuiken C, et al. Tracking global patterns of N-linked glycosylation site variation in highly variable viral glycoproteins: HIV, SIV, and HCV envelopes and influenza hemagglutinin. Glycobiology. 2004.
290. Fournillier A, Wychowski C, Boucreux D, Baumert TF, Meunier J-C, Jacobs D, et al. Induction of Hepatitis C Virus E1 Envelope Protein-Specific Immune Response Can Be Enhanced by Mutation of N-Glycosylation Sites. J Virol. 2001;
291. Liu M, Chen H, Luo F, Li P, Pan Q, Xia B, et al. Deletion of N-glycosylation sites of hepatitis C virus envelope protein E1 enhances specific cellular and humoral immune responses. Vaccine. 2007;
292. Ren Y, Min YQ, Liu M, Chi L, Zhao P, Zhang XL. N-glycosylation-mutated HCV envelope glycoprotein complex enhances antigen-presenting activity and cellular and neutralizing antibody responses. Biochim Biophys Acta - Gen Subj. 2016;
293. Kong L, Giang E, Nieusma T, Kadam RU, Cogburn KE, Hua Y, et al. Hepatitis C virus E2 envelope glycoprotein core structure. Science (80-). 2013;
294. El Omari K, Iourin O, Kadlec J, Sutton G, Harlos K, Grimes JM, et al. Unexpected structure for the N-terminal domain of hepatitis C virus envelope glycoprotein E1. Nat Commun. 2014;
295. Perin PM, Haid S, Brown RJP, Doerrbecker J, Schulze K, Zeilinger C, et al.

Flunarizine prevents hepatitis C virus membrane fusion in a genotype-dependent manner by targeting the potential fusion peptide within E1. Hepatology. 2016;

296. Lavillette D, Pécheur E-I, Donot P, Fresquet J, Molle J, Corbau R, et al. Characterization of Fusion Determinants Points to the Involvement of Three Discrete Regions of Both E1 and E2 Glycoproteins in the Membrane Fusion Process of Hepatitis C Virus. J Virol. 2007;
297. Wahid A, Helle F, Descamps V, Duverlie G, Penin F, Dubuisson J. Disulfide Bonds in Hepatitis C Virus Glycoprotein E1 Control the Assembly and Entry Functions of E2 Glycoprotein. J Virol. 2013;
298. Moustafa RI, Haddad JG, Linna L, Hanoulle X, Descamps V, Mesalam AA, et al. Functional Study of the C-Terminal Part of the Hepatitis C Virus E1 Ectodomain. J Virol. 2018;
299. Bailey JR, Barnes E, Cox AL. Approaches, Progress, and Challenges to Hepatitis C Vaccine Development. Gastroenterology. 2019;
300. Flint M, Dubuisson J, Maidens C, Harrop R, Guile GR, Borrow P, et al. Functional Characterization of Intracellular and Secreted Forms of a Truncated Hepatitis C Virus E2 Glycoprotein. J Virol. 2000;
301. Whidby J, Mateu G, Scarborough H, Demeler B, Grakoui A, Marcotrigiano J. Blocking Hepatitis C Virus Infection with Recombinant Form of Envelope Protein 2 Ectodomain. J Virol. 2009 Nov 1;83(21):11078–89.
302. Douam F, Fusil F, Enguehard M, Dib L, Nadalin F, Schwaller L, et al. A protein coevolution method uncovers critical features of the Hepatitis C Virus fusion mechanism. PLoS Pathog. 2018;
303. Li Y, Modis Y. A novel membrane fusion protein family in Flaviviridae? Trends in Microbiology. 2014.
304. Dao Thi VL, Dreux M, Cosset FL. Scavenger receptor class B type I and the hypervariable region-1 of hepatitis C virus in cell entry and neutralisation. Expert Rev Mol Med. 2011;
305. Voisset C, Callens N, Blanchard E, Op De Beeck A, Dubuisson J, Vu-Dac N. High density lipoproteins facilitate hepatitis C virus entry through the scavenger receptor class B type I. J Biol Chem. 2005;
306. Bankwitz D, Vieyres G, Hueging K, Bitzegeio J, Doepke M, Chhatwal P, et al. Role of Hypervariable Region 1 for the Interplay of Hepatitis C Virus with Entry

Factors and Lipoproteins. J Virol. 2014;

307. Cuevas JM, Gonzalez M, Torres-Puente M, Jiménez-Hernández N, Bracho MA, García-Robles I, et al. The role of positive selection in hepatitis C virus. Infect Genet Evol. 2009;
308. Palmer BA, Schmidt-Martin D, Dimitrova Z, Skums P, Crosbie O, Kenny-Walsh E, et al. Network Analysis of the Chronic Hepatitis C Virome Defines Hypervariable Region 1 Evolutionary Phenotypes in the Context of Humoral Immune Responses. J Virol. 2016;
309. Chen F, Nagy K, Chavez D, Willis S, McBride R, Giang E, et al. Antibody Responses to Immunization With HCV Envelope Glycoproteins as a Baseline for B-Cell–Based Vaccine Development. Gastroenterology. 2020;
310. Prentoe J, Velázquez-Moctezuma R, Foung SKH, Law M, Bukh J. Hypervariable region 1 shielding of hepatitis C virus is a main contributor to genotypic differences in neutralization sensitivity. Hepatology. 2016;
311. Prentoe J, Velázquez-Moctezuma R, Augestad EH, Galli A, Wang R, Law M, et al. Hypervariable region 1 and N-linked glycans of hepatitis C regulate virion neutralization by modulating envelope conformations. Proc Natl Acad Sci U S A. 2019;
312. Law JLM, Logan M, Wong J, Kundu J, Hockman D, Landi A, et al. Role of the E2 Hypervariable Region (HVR1) in the Immunogenicity of a Recombinant Hepatitis C Virus Vaccine. J Virol. 2018;
313. McCaffrey K, Boo I, Poumbourios P, Drummer HE. Expression and Characterization of a Minimal Hepatitis C Virus Glycoprotein E2 Core Domain That Retains CD81 Binding. J Virol. 2007;
314. McCaffrey K, Gouklani H, Boo I, Poumbourios P, Drummer HE. The variable regions of hepatitis C virus glycoprotein E2 have an essential structural role in glycoprotein assembly and virion infectivity. J Gen Virol. 2011;
315. Helenius A. Intracellular Functions of N-Linked Glycans. Science (80-). 2001 Mar 23;291(5512):2364–9.
316. Dubuisson J, Rice CM. Hepatitis C virus glycoprotein folding: disulfide bond formation and association with calnexin. J Virol. 1996;
317. Choukhi A, Ung S, Wychowski C, Dubuisson J. Involvement of Endoplasmic Reticulum Chaperones in the Folding of Hepatitis C Virus Glycoproteins. J Virol. 1998;

318. Goffard A, Callens N, Bartosch B, Wychowski C, Cosset F-L, Montpellier C, et al. Role of N-Linked Glycans in the Functions of Hepatitis C Virus Envelope Glycoproteins. J Virol. 2005 Jul 1;79(13):8400–9.
319. Falkowska E, Kajumo F, Garcia E, Reinus J, Dragic T. Hepatitis C Virus Envelope Glycoprotein E2 Glycans Modulate Entry, CD81 Binding, and Neutralization. J Virol. 2007;
320. Vigerust DJ, Shepherd VL. Virus glycosylation: role in virulence and immune interactions. Trends in Microbiology. 2007.
321. Crispin M, Ward AB, Wilson IA. Structure and Immune Recognition of the HIV Glycan Shield. Annu Rev Biophys. 2018 May 20;47(1):499–523.
322. Tzarum N, Wilson IA, Law M. The neutralizing face of hepatitis C virus E2 envelope glycoprotein. Frontiers in Immunology. 2018.
323. Kong L, Lee DE, Kadam RU, Liu T, Giang E, Nieusma T, et al. Structural flexibility at a major conserved antibody target on hepatitis C virus E2 antigen. Proc Natl Acad Sci. 2016 Nov 8;113(45):12768–73.
324. Goo L, VanBlargan LA, Dowd KA, Diamond MS, Pierson TC. A single mutation in the envelope protein modulates flavivirus antigenicity, stability, and pathogenesis. PLoS Pathog. 2017;
325. Lu M, Ma X, Castillo-Menendez LR, Gorman J, Alsahafi N, Ermel U, et al. Associating HIV-1 envelope glycoprotein structures with states on the virus observed by smFRET. Nature. 2019;
326. Wei G, Xi W, Nussinov R, Ma B. Protein Ensembles: How Does Nature Harness Thermodynamic Fluctuations for Life? the Diverse Functional Roles of Conformational Ensembles in the Cell. Chemical Reviews. 2016.
327. Lee HS, Qi Y, Im W. Effects of N-glycosylation on protein conformation and dynamics: Protein Data Bank analysis and molecular dynamics simulation study. Sci Rep. 2015;
328. Krey T, D'Alayer J, Kikuti CM, Saulnier A, Damier-Piolle L, Petitpas I, et al. The disulfide bonds in glycoprotein E2 of hepatitis C virus reveal the tertiary organization of the molecule. PLoS Pathog. 2010;
329. Fraser J, Boo I, Poumbourios P, Drummer HE. Hepatitis C virus (HCV) envelope glycoproteins E1 and E2 contain reduced cysteine residues essential for virus entry. J Biol Chem. 2011;
330. Stejskal L, Lees WD, Moss DS, Palor M, Bingham RJ, Shepherd AJ, et al.

Flexibility and intrinsic disorder are conserved features of hepatitis C virus E2 glycoprotein. Wei G, editor. PLOS Comput Biol. 2020 Feb 28;16(2):e1007710.

331. McCaffrey K, Boo I, Tewierek K, Edmunds ML, Poumbourios P, Drummer HE. Role of Conserved Cysteine Residues in Hepatitis C Virus Glycoprotein E2 Folding and Function. J Virol. 2012;
332. Johansson DX, Voisset C, Tarr AW, Aung M, Ball JK, Dubuisson J, et al. Human combinatorial libraries yield rare antibodies that broadly neutralize hepatitis C virus. Proc Natl Acad Sci U S A. 2007;
333. Keck Z-Y, Li T-K, Xia J, Gal-Tanamy M, Olson O, Li SH, et al. Definition of a Conserved Immunodominant Domain on Hepatitis C Virus E2 Glycoprotein by Neutralizing Human Monoclonal Antibodies. J Virol. 2008;
334. Keck Z-Y, Saha A, Xia J, Wang Y, Lau P, Krey T, et al. Mapping a Region of Hepatitis C Virus E2 That Is Responsible for Escape from Neutralizing Antibodies and a Core CD81-Binding Region That Does Not Tolerate Neutralization Escape Mutations. J Virol. 2011;
335. Keck Z-Y, Op De Beeck A, Hadlock KG, Xia J, Li T-K, Dubuisson J, et al. Hepatitis C Virus E2 Has Three Immunogenic Domains Containing Conformational Epitopes with Distinct Properties and Biological Functions. J Virol. 2004;
336. Pierce BG, Keck Z-Y, Lau P, Fauvelle C, Gowthaman R, Baumert TF, et al. Global mapping of antibody recognition of the hepatitis C virus E2 glycoprotein: Implications for vaccine design. Proc Natl Acad Sci. 2016;201614942.
337. Meunier J-C, Russell RS, Goossens V, Priem S, Walter H, Depla E, et al. Isolation and Characterization of Broadly Neutralizing Human Monoclonal Antibodies to the E1 Glycoprotein of Hepatitis C Virus. J Virol. 2008 Jan 15;82(2):966–73.
338. Haberstroh A, Schnober EK, Zeisel MB, Carolla P, Barth H, Blum HE, et al. Neutralizing Host Responses in Hepatitis C Virus Infection Target Viral Entry at Postbinding Steps and Membrane Fusion. Gastroenterology. 2008;
339. Giang E, Dorner M, Prentoe JC, Dreux M, Evans MJ, Bukh J, et al. Human broadly neutralizing antibodies to the envelope glycoprotein complex of hepatitis C virus. Proc Natl Acad Sci. 2012 Apr 17;109(16):6205–10.
340. Sabo MC, Luca VC, Prentoe J, Hopcraft SE, Blight KJ, Yi M, et al. Neutralizing

Monoclonal Antibodies against Hepatitis C Virus E2 Protein Bind Discontinuous Epitopes and Inhibit Infection at a Postattachment Step. J Virol. 2011;

341. Brimacombe CL, Grove J, Meredith LW, Hu K, Syder AJ, Flores M V., et al. Neutralizing Antibody-Resistant Hepatitis C Virus Cell-to-Cell Transmission. J Virol. 2011;
342. Shimizu YK, Hijikata M, Iwamoto A, Alter HJ, Purcell RH, Yoshikura H. Neutralizing antibodies against hepatitis C virus and the emergence of neutralization escape mutant viruses. J Virol. 1994;
343. Tarr AW, Owsianka AM, Timms JM, McClure CP, Brown RJP, Hickling TP, et al. Characterization of the hepatitis C virus E2 epitope defined by the broadly neutralizing monoclonal antibody AP33. Hepatology. 2006;
344. Tarr AW, Owsianka AM, Jayaraj D, Brown RJP, Hickling TP, Irving WL, et al. Determination of the human antibody response to the epitope defined by the hepatitis C virus-neutralizing monoclonal antibody AP33. J Gen Virol. 2007;
345. Keck Z, Wang W, Wang Y, Lau P, Carlsen THR, Prentoe J, et al. Cooperativity in Virus Neutralization by Human Monoclonal Antibodies to Two Adjacent Regions Located at the Amino Terminus of Hepatitis C Virus E2 Glycoprotein. J Virol. 2013;
346. Augestad EH, Castelli M, Clementi N, Ströh LJ, Krey T, Burioni R, et al. Global and local envelope protein dynamics of hepatitis C virus determine broad antibody sensitivity. Sci Adv. 2020;
347. Pierce BG, Boucher EN, Piepenbrink KH, Ejemel M, Rapp CA, Thomas WD, et al. Structure-Based Design of Hepatitis C Virus Vaccines That Elicit Neutralizing Antibody Responses to a Conserved Epitope. J Virol. 2017;
348. Sandomenico A, Leonardi A, Berisio R, Sanguigno L, Focà G, Focà A, et al. Generation and Characterization of Monoclonal Antibodies against a Cyclic Variant of Hepatitis C Virus E2 Epitope 412-422. J Virol. 2016;
349. Owsianka AM, Timms JM, Tarr AW, Brown RJP, Hickling TP, Szwejk A, et al. Identification of Conserved Residues in the E2 Envelope Glycoprotein of the Hepatitis C Virus That Are Critical for CD81 Binding. J Virol. 2006;
350. Gu J, Hardy J, Boo I, Vietheer P, McCaffrey K, Alhammad Y, et al. Escape of Hepatitis C Virus from Epitope I Neutralization Increases Sensitivity of Other Neutralization Epitopes. J Virol. 2018;

351. Kong L, Giang E, Nieusma T, Robbins JB, Deller MC, Stanfield RL, et al. Structure of Hepatitis C Virus Envelope Glycoprotein E2 Antigenic Site 412 to 423 in Complex with Antibody AP33. J Virol. 2012;
352. Kong L, Giang E, Robbins JB, Stanfield RL, Burton DR, Wilson IA, et al. Structural basis of hepatitis C virus neutralization by broadly neutralizing antibody HCV1. Proc Natl Acad Sci U S A. 2012;
353. Potter JA, Owsianka AM, Jeffery N, Matthews DJ, Keck Z-Y, Lau P, et al. Toward a Hepatitis C Virus Vaccine: the Structural Basis of Hepatitis C Virus Neutralization by AP33, a Broadly Neutralizing Antibody. J Virol. 2012;
354. Pantua H, Diao J, Ultsch M, Hazen M, Mathieu M, McCutcheon K, et al. Glycan shifting on hepatitis C virus (HCV) E2 glycoprotein is a mechanism for escape from broadly neutralizing antibodies. J Mol Biol. 2013;
355. Meola A, Tarr AW, England P, Meredith LW, McClure CP, Foung SKH, et al. Structural Flexibility of a Conserved Antigenic Region in Hepatitis C Virus Glycoprotein E2 Recognized by Broadly Neutralizing Antibodies. J Virol. 2015;
356. Li Y, Pierce BG, Wang Q, Keck ZY, Fuerst TR, Foung SKH, et al. Structural basis for penetration of the glycan shield of hepatitis C virus E2 glycoprotein by a broadly neutralizing human antibody. J Biol Chem. 2015;
357. Balasco N, Barone D, Iaccarino E, Sandomenico A, De Simone A, Ruvo M, et al. Intrinsic structural versatility of the highly conserved 412–423 epitope of the Hepatitis C Virus E2 protein. Int J Biol Macromol. 2018;
358. Ströh LJ, Nagarathinam K, Krey T. Conformational flexibility in the CD81-binding site of the hepatitis C virus glycoprotein E2. Frontiers in Immunology. 2018.
359. Krey T, Meola A, Keck Z yong, Damier-Piolle L, Foung SKH, Rey FA. Structural Basis of HCV Neutralization by Human Monoclonal Antibodies Resistant to Viral Neutralization Escape. PLoS Pathog. 2013;
360. Keck ZY, Wang Y, Lau P, Lund G, Rangarajan S, Fauvelle C, et al. Affinity maturation of a broadly neutralizing human monoclonal antibody that prevents acute hepatitis C virus infection in mice. Hepatology. 2016;
361. Deng L, Ma L, Virata-Theimer ML, Zhong L, Yan H, Zhao Z, et al. Discrete conformations of epitope II on the hepatitis C virus E2 protein for antibody-mediated neutralization and nonneutralization. Proc Natl Acad Sci U S A. 2014;

362. Deng L, Zhong L, Struble E, Duan H, Li M, Harman C, et al. Structural evidence for a bifurcated mode of action in the antibody-mediated neutralization of hepatitis C virus. Proc Natl Acad Sci U S A. 2013;
363. Tzarum N, Giang E, Kadam RU, Chen F, Nagy K, Augestad EH, et al. An alternate conformation of HCV E2 neutralizing face as an additional vaccine target. Sci Adv. 2020;
364. Vasiliauskaite I, Owsianka A, England P, Khan AG, Cole S, Bankwitz D, et al. Conformational Flexibility in the Immunoglobulin-Like Domain of the Hepatitis C Virus Glycoprotein E2. Palese P, editor. MBio. 2017 Jul 5;8(3).
365. Freedman H, Logan MR, Hockman D, Koehler Leman J, Law JLM, Houghton M. Computational Prediction of the Heterodimeric and Higher-Order Structure of gpE1/gpE2 Envelope Glycoproteins Encoded by Hepatitis C Virus. J Virol. 2017;
366. Cao L, Yu B, Kong D, Cong Q, Yu T, Chen Z, et al. Functional expression and characterization of the envelope glycoprotein E1E2 heterodimer of hepatitis C virus. PLoS Pathog. 2019;
367. Alhammad Y, Gu J, Boo I, Harrison D, McCaffrey K, Vietheer PT, et al. Monoclonal Antibodies Directed toward the Hepatitis C Virus Glycoprotein E2 Detect Antigenic Differences Modulated by the N-Terminal Hypervariable Region 1 (HVR1), HVR2, and Intergenotypic Variable Region. J Virol. 2015;
368. Rogers TF, Zhao F, Huang D, Beutler N, Burns A, He WT, et al. Isolation of potent SARS-CoV-2 neutralizing antibodies and protection from disease in a small animal model. Science (80-). 2020;
369. Culley S, Towers GJ, Selwood DL, Henriques R, Grove J. Infection counter: Automated quantification of in vitro virus replication by fluorescence microscopy. Viruses. 2016;
370. Aisyah D, Shallcross L, Kozlakidis Z, Vlachou MK, Hayward A. Assessing HCV distribution among ‘Hard to Reach’ populations in London using whole genome sequencing: Report from the TB reach study. Int J Infect Dis. 2020;
371. Manso CF, Bibby DF, Lythgow K, Mohamed H, Myers R, Williams D, et al. Technical Validation of a Hepatitis C Virus Whole Genome Sequencing Assay for Detection of Genotype and Antiviral Resistance in the Clinical Pathway. Front Microbiol. 2020;
372. Bolger AM, Lohse M, Usadel B. Trimmomatic: A flexible trimmer for Illumina

sequence data. Bioinformatics. 2014;

373. Li H, Durbin R. Fast and accurate short read alignment with Burrows-Wheeler transform. Bioinformatics. 2009;
374. Schindelin J, Arganda-Carreras I, Frise E, Kaynig V, Longair M, Pietzsch T, et al. Fiji: An open-source platform for biological-image analysis. Nature Methods. 2012.
375. Kalemera MD, Capella-Pujol J, Chumbe A, Underwood A, Bull RA, Schinkel J, et al. Optimized cell systems for the investigation of hepatitis C virus E1E2 glycoproteins. J Gen Virol. 2021;
376. Webb B, Sali A. Comparative protein structure modeling using MODELLER. Curr Protoc Bioinforma. 2016;
377. Case DA, Cheatham TE, Darden T, Gohlke H, Luo R, Merz KM, et al. The Amber biomolecular simulation programs. Journal of Computational Chemistry. 2005.
378. Pettersen EF, Goddard TD, Huang CC, Couch GS, Greenblatt DM, Meng EC, et al. UCSF Chimera - A visualization system for exploratory research and analysis. J Comput Chem. 2004;
379. Grove J, Nielsen S, Zhong J, Bassendine MF, Drummer HE, Balfe P, et al. Identification of a Residue in Hepatitis C Virus E2 Glycoprotein That Determines Scavenger Receptor BI and CD81 Receptor Dependency and Sensitivity to Neutralizing Antibodies. J Virol. 2008;
380. Zhu H, Wong-Staal F, Lee H, Syder A, McKelvy J, Schooley RT, et al. Evaluation of ITX 5061, a scavenger receptor B1 antagonist: Resistance selection and activity in combination with other hepatitis C virus antivirals. J Infect Dis. 2012;
381. Pileri P, Uematsu Y, Campagnoli S, Galli G, Falugi F, Petracca R, et al. Binding of hepatitis C virus to CD81. Science (80-). 1998;
382. Grove J, Nielsen S, Zhong J, Bassendine MF, Drummer HE, Balfe P, et al. Identification of a residue in hepatitis C virus E2 glycoprotein that determines scavenger receptor BI and CD81 receptor dependency and sensitivity to neutralizing antibodies. J Virol. 2008;82(24):12020–9.
383. Grove J, Hu K, Farquhar MJ, Goodall M, Walker L, Jamshad M, et al. A new panel of epitope mapped monoclonal antibodies recognising the prototypical tetraspanin CD81. Wellcome Open Res. 2017;

384. Allison AC, Valentine RC. Virus particle adsorption. III. Adsorption of viruses by cell monolayers and effects of some variables on adsorption. BBA - Biochim Biophys Acta. 1960;
385. Andreadis S, Lavery T, Davis HE, Le Doux JM, Yarmush ML, Morgan JR. Erratum in the print version of “Toward a More Accurate Quantitation of the Activity of Recombinant Retroviruses: Alternatives to Titer and Multiplicity of Infection.” J Virol. 2000;
386. Seisenberger G, Ried MU, Endreß T, Büning H, Hallek M, Bräuchle C. Real-time single-molecule imaging of the infection pathway of anadeno-associated virus. Science (80-). 2001;
387. Haim H, Steiner I, Panet A. Time frames for neutralization during the human immunodeficiency virus type 1 entry phase, as monitored in synchronously infected cell cultures. J Virol. 2007;81(7):3525–34.
388. Keck M-L, Wrensch F, Pierce BG, Baumert TF, Foung SKH. Mapping Determinants of Virus Neutralization and Viral Escape for Rational Design of a Hepatitis C Virus Vaccine. Front Immunol. 2018;
389. Kinchen VJ, Massaccesi G, Flyak AI, Mankowski MC, Colbert MD, Osburn WO, et al. Plasma deconvolution identifies broadly neutralizing antibodies associated with hepatitis C virus clearance. J Clin Invest. 2019;
390. Song H, Ren F, Li J, Shi S, Yan L, Gao F, et al. A laboratory-adapted HCV JFH-1 strain is sensitive to neutralization and can gradually escape under the selection pressure of neutralizing human plasma. Virus Res. 2012;
391. Tao W, Xu C, Ding Q, Li R, Xiang Y, Chung J, et al. A single point mutation in E2 enhances hepatitis C virus infectivity and alters lipoprotein association of viral particles. Virology. 2009;395(1):67–76.
392. Fontana A, De Laureto PP, Spolaore B, Frare E, Picotti P, Zambonin M. Probing protein structure by limited proteolysis. In: Acta Biochimica Polonica. 2004.
393. El-Diwany R, Cohen VJ, Mankowski MC, Wasilewski LN, Brady JK, Snider AE, et al. Extra-epitopic hepatitis C virus polymorphisms confer resistance to broadly neutralizing antibodies by modulating binding to scavenger receptor B1. PLoS Pathog. 2017;
394. Sautto G, Tarr AW, Mancini N, Clementi M. Structural and antigenic definition of hepatitis C virus E2 glycoprotein epitopes targeted by monoclonal

antibodies. Clinical and Developmental Immunology. 2013.

395. Zeisel MB, Fofana I, Fafi-Kremer S, Baumert TF. Hepatitis C virus entry into hepatocytes: Molecular mechanisms and targets for antiviral therapies. Journal of Hepatology. 2011.
396. Sakai A, Takikawa S, Thimme R, Meunier J-C, Spangenberg HC, Govindarajan S, et al. In Vivo Study of the HC-TN Strain of Hepatitis C Virus Recovered from a Patient with Fulminant Hepatitis: RNA Transcripts of a Molecular Clone (pHC-TN) Are Infectious in Chimpanzees but Not in Huh7.5 Cells. J Virol. 2007;
397. Quadeer AA, Louie RHY, McKay MR. Identifying immunologically-vulnerable regions of the HCV E2 glycoprotein and broadly neutralizing antibodies that target them. Nat Commun. 2019;
398. Lu M, Uchil PD, Li W, Zheng D, Terry DS, Gorman J, et al. Real-Time Conformational Dynamics of SARS-CoV-2 Spikes on Virus Particles. Cell Host Microbe. 2020;
399. Hollingsworth SA, Dror RO. Molecular Dynamics Simulation for All. Neuron. 2018.
400. Prentoe J, Bukh J. Hypervariable Region 1 in Envelope Protein 2 of Hepatitis C Virus: A Linchpin in Neutralizing Antibody Evasion and Viral Entry. Frontiers in immunology. 2018.
401. Smyda MR, Harvey SC. The entropic cost of polymer confinement. J Phys Chem B. 2012;
402. Zuiani A, Chen K, Schwarz MC, White JP, Luca VC, Fremont DH, et al. A Library of Infectious Hepatitis C Viruses with Engineered Mutations in the E2 Gene Reveals Growth-Adaptive Mutations That Modulate Interactions with Scavenger Receptor Class B Type I. J Virol. 2016;
403. Prentoe J, Jensen TB, Meuleman P, Serre SBN, Scheel TKH, Leroux-Roels G, et al. Hypervariable Region 1 Differentially Impacts Viability of Hepatitis C Virus Strains of Genotypes 1 to 6 and Impairs Virus Neutralization. J Virol. 2011;
404. Prentoe J, Serre SBN, Ramirez S, Nicosia A, Gottwein JM, Bukh J. Hypervariable Region 1 Deletion and Required Adaptive Envelope Mutations Confer Decreased Dependency on Scavenger Receptor Class B Type I and Low-Density Lipoprotein Receptor for Hepatitis C Virus. J Virol. 2014;

405. Bitzegeio J, Bankwitz D, Hueging K, Haid S, Brohm C, Zeisel MB, et al. Adaptation of Hepatitis C Virus to mouse CD81 permits infection of mouse cells in the absence of human entry factors. PLoS Pathog. 2010;
406. Lavie M, Sarrazin S, Montserret R, Descamps V, Baumert TF, Duverlie G, et al. Identification of Conserved Residues in Hepatitis C Virus Envelope Glycoprotein E2 That Modulate Virus Dependence on CD81 and SRB1 Entry Factors. J Virol. 2014;
407. Fofana I, Fafi-Kremer S, Carolla P, Fauvelle C, Zahid MN, Turek M, et al. Mutations that alter use of hepatitis C virus cell entry factors mediate escape from neutralizing antibodies. Gastroenterology. 2012;143(1):223-233.e9.
408. Tomlinson JE, Wolfisberg R, Fahnøe U, Patel RS, Trivedi S, Kumar A, et al. Pathogenesis, miR-122 gene-regulation, and protective immune responses after acute equine hepacivirus infection. Hepatology. 2021 Mar 13;hep.31802.
409. Weiner AJ, Geysen HM, Christopherson C, Hall JE, Mason TJ, Saracco G, et al. Evidence for immune selection of hepatitis C virus (HCV) putative envelope glycoprotein variants: Potential role in chronic HCV infections. Proc Natl Acad Sci U S A. 1992;
410. Wong JAJ-X, Bhat R, Hockman D, Logan M, Chen C, Levin A, et al. Recombinant hepatitis C virus envelope glycoprotein vaccine elicits antibodies targeting multiple epitopes on the envelope glycoproteins associated with broad cross-neutralization. J Virol. 2014;88(24):14278–88.
411. Crank MC, Ruckwardt TJ, Chen M, Morabito KM, Phung E, Costner PJ, et al. A proof of concept for structure-based vaccine design targeting RSV in humans. Science (80-). 2019;
412. Hsieh CL, Goldsmith JA, Schaub JM, DiVenere AM, Kuo HC, Javanmardi K, et al. Structure-based design of prefusion-stabilized SARS-CoV-2 spikes. Science (80-). 2020;
413. Sanders RW, Van Gils MJ, Derking R, Sok D, Ketas TJ, Burger JA, et al. HIV-1 neutralizing antibodies induced by native-like envelope trimers. Science (80-). 2015;
414. Uversky VN. Intrinsically disordered proteins and their “Mysterious” (meta)physics. Frontiers in Physics. 2019.
415. Uversky VN. Unusual biophysics of intrinsically disordered proteins. Biochimica et Biophysica Acta - Proteins and Proteomics. 2013.

416. Gutierrez B, Escalera-Zamudio M, Pybus OG. Parallel molecular evolution and adaptation in viruses. Current Opinion in Virology. 2019.
417. Burton DR, Poignard P, Stanfield RL, Wilson IA. Broadly Neutralizing Antibodies Present New Prospects to Counter Highly Antigenically Diverse Viruses. Science (80-). 2012 Jul 13;337(6091):183–6.
418. deCamp A, Hraber P, Bailer RT, Seaman MS, Ochsenbauer C, Kappes J, et al. Global Panel of HIV-1 Env Reference Strains for Standardized Assessments of Vaccine-Elicited Neutralizing Antibodies. J Virol. 2014 Mar 1;88(5):2489–507.
419. Pietschmann T, Kaul A, Koutsoudakis G, Shavinskaya A, Kallis S, Steinmann E, et al. Construction and characterization of infectious intragenotypic and intergenotypic hepatitis C virus chimeras. Proc Natl Acad Sci. 2006 May 9;103(19):7408–13.
420. Hsu M, Zhang J, Flint M, Logvinoff C, Cheng-Mayer C, Rice CM, et al. Hepatitis C virus glycoproteins mediate pH-dependent cell entry of pseudotyped retroviral particles. Proc Natl Acad Sci. 2003;
421. Zhong J, Gastaminza P, Cheng G, Kapadia S, Kato T, Burton DR, et al. Robust hepatitis C virus infection in vitro. Proc Natl Acad Sci. 2005 Jun 28;102(26):9294–9.
422. Riva L, Dubuisson J. Similarities and Differences Between HCV Pseudoparticle (HCVpp) and Cell Culture HCV (HCVcc) in the Study of HCV. In: Methods in Molecular Biology. 2019. p. 33–45.
423. Catanese MT, Dorner M. Advances in experimental systems to study hepatitis C virus in vitro and in vivo. Virology. 2015 May;479–480:221–33.
424. Bartosch B, Cosset F-L. Studying HCV Cell Entry with HCV Pseudoparticles (HCVpp). In: Methods in molecular biology (Clifton, NJ). 2009. p. 279–93.
425. Wasilewski LN, Ray SC, Bailey JR. Hepatitis C virus resistance to broadly neutralizing antibodies measured using replication-competent virus and pseudoparticles. J Gen Virol. 2016 Nov 10;97(11):2883–93.
426. Sliepen K, Han BW, Bontjer I, Mooij P, Garces F, Behrens AJ, et al. Structure and immunogenicity of a stabilized HIV-1 envelope trimer based on a group-M consensus sequence. Nat Commun. 2019;
427. Marín MQ, Sliepen K, García-Arriaza J, Koekkoek SM, Pérez P, Sorzano CÓS, et al. Optimized Hepatitis C Virus (HCV) E2 Glycoproteins and their

Immunogenicity in Combination with MVA-HCV. Vaccines. 2020;

428. Struwe WB, Chertova E, Allen JD, Seabright GE, Watanabe Y, Harvey DJ, et al. Site-Specific Glycosylation of Virion-Derived HIV-1 Env Is Mimicked by a Soluble Trimeric Immunogen. Cell Rep. 2018 Aug;24(8):1958-1966.e5.
429. Urbanowicz RA, McClure CP, King B, Mason CP, Ball JK, Tarr AW. Novel functional hepatitis C virus glycoprotein isolates identified using an optimized viral pseudotype entry assay. J Gen Virol. 2016 Sep 1;97(9):2265–79.
430. Merat SJ, Molenkamp R, Wagner K, Koekkoek SM, van de Berg D, Yasuda E, et al. Hepatitis C virus Broadly Neutralizing Monoclonal Antibodies Isolated 25 Years after Spontaneous Clearance. Ray R, editor. PLoS One. 2016 Oct 24;11(10):e0165047.
431. Urbanowicz RA, McClure CP, Brown RJP, Tsoleridis T, Persson MAA, Krey T, et al. A Diverse Panel of Hepatitis C Virus Glycoproteins for Use in Vaccine Research Reveals Extremes of Monoclonal Antibody Neutralization Resistance. Diamond MS, editor. J Virol. 2016 Apr 1;90(7):3288–301.
432. Cunningham EB, Hajarizadeh B, Bretana NA, Amin J, Betz-Stablein B, Dore GJ, et al. Ongoing incident hepatitis C virus infection among people with a history of injecting drug use in an Australian prison setting, 2005-2014: The HITS-p study. J Viral Hepat. 2017 Sep;24(9):733–41.
433. Lavillette D, Tarr AW, Voisset C, Donot P, Bartosch B, Bain C, et al. Characterization of host-range and cell entry properties of the major genotypes and subtypes of hepatitis C virus. Hepatology. 2005 Feb;41(2):265–74.
434. Keck Z, Xia J, Wang Y, Wang W, Krey T, Prentoe J, et al. Human Monoclonal Antibodies to a Novel Cluster of Conformational Epitopes on HCV E2 with Resistance to Neutralization Escape in a Genotype 2a Isolate. Diamond MS, editor. PLoS Pathog. 2012 Apr 12;8(4):e1002653.
435. Urbanowicz RA, Wang R, Schiel JE, Keck Z, Kerzic MC, Lau P, et al. Antigenicity and Immunogenicity of Differentially Glycosylated Hepatitis C Virus E2 Envelope Proteins Expressed in Mammalian and Insect Cells. James Ou J-H, editor. J Virol. 2019 Jan 16;93(7).
436. Hadlock KG, Lanford RE, Perkins S, Rowe J, Yang Q, Levy S, et al. Human Monoclonal Antibodies That Inhibit Binding of Hepatitis C Virus E2 Protein to CD81 and Recognize Conserved Conformational Epitopes. J Virol. 2000 Nov 15;74(22):10407–16.

437. McKeating JA, Zhang LQ, Logvinoff C, Flint M, Zhang J, Yu J, et al. Diverse Hepatitis C Virus Glycoproteins Mediate Viral Infection in a CD81-Dependent Manner. J Virol. 2004 Aug 15;78(16):8496–505.
438. Lavillette D, Pecheur E-I, Donot P, Fresquet J, Molle J, Corbau R, et al. Characterization of Fusion Determinants Points to the Involvement of Three Discrete Regions of Both E1 and E2 Glycoproteins in the Membrane Fusion Process of Hepatitis C Virus. J Virol. 2007;
439. Bailey JR, Urbanowicz RA, Ball JK, Law M, Foung SKH. Standardized Method for the Study of Antibody Neutralization of HCV Pseudoparticles (HCVpp). In: Methods in Molecular Biology. 2019. p. 441–50.
440. Soares HR, Ferreira-Fernandes M, Almeida AI, Marchel M, Alves PM, Coroadinha AS. Enhancing Hepatitis C virus pseudoparticles infectivity through p7NS2 cellular expression. J Virol Methods. 2019 Dec;274:113714.
441. Shukla P, Faulk KN, Emerson SU. The entire core protein of HCV JFH1 is required for efficient formation of infectious JFH1 pseudoparticles. J Med Virol. 2010 May;82(5):783–90.
442. Masciopinto F, Giovani C, Campagnoli S, Galli-Stampino L, Colombatto P, Brunetto M, et al. Association of hepatitis C virus envelope proteins with exosomes. Eur J Immunol. 2004 Oct;34(10):2834–42.
443. Flint M, Logvinoff C, Rice CM, McKeating JA. Characterization of Infectious Retroviral Pseudotype Particles Bearing Hepatitis C Virus Glycoproteins. J Virol. 2004 Jul 1;78(13):6875–82.
444. Soares HR, Castro R, Tomás HA, Carrondo MJT, Alves PM, Coroadinha AS. Pseudotyping retrovirus like particles vaccine candidates with Hepatitis C virus envelope protein E2 requires the cellular expression of CD81. AMB Express. 2019;
445. Earnest JT, Hantak MP, Park J-E, Gallagher T. Coronavirus and Influenza Virus Proteolytic Priming Takes Place in Tetraspanin-Enriched Membrane Microdomains. J Virol. 2015;
446. Li W, Moore MJ, Vasllieva N, Sui J, Wong SK, Berne MA, et al. Angiotensin-converting enzyme 2 is a functional receptor for the SARS coronavirus. Nature. 2003;
447. Hoffmann M, Kleine-Weber H, Schroeder S, Krüger N, Herrler T, Erichsen S, et al. SARS-CoV-2 Cell Entry Depends on ACE2 and TMPRSS2 and Is

Blocked by a Clinically Proven Protease Inhibitor. Cell. 2020;

448. Coller KE, Heaton NS, Berger KL, Cooper JD, Saunders JL, Randall G. Molecular Determinants and Dynamics of Hepatitis C Virus Secretion. Ou JJ, editor. PLoS Pathog. 2012 Jan 5;8(1):e1002466.
449. Binley JM, Sanders RW, Clas B, Schuelke N, Master A, Guo Y, et al. A Recombinant Human Immunodeficiency Virus Type 1 Envelope Glycoprotein Complex Stabilized by an Intermolecular Disulfide Bond between the gp120 and gp41 Subunits Is an Antigenic Mimic of the Trimeric Virion-Associated Structure. J Virol. 2000 Jan 15;74(2):627–43.
450. Malm M, Saghaleyni R, Lundqvist M, Giudici M, Chotteau V, Field R, et al. Evolution from adherent to suspension – systems biology of HEK293 cell line development. bioRxiv. 2020;
451. Behrens A-J, Vasiljevic S, Pritchard LK, Harvey DJ, Andev RS, Krumm SA, et al. Composition and Antigenic Effects of Individual Glycan Sites of a Trimeric HIV-1 Envelope Glycoprotein. Cell Rep. 2016 Mar;14(11):2695–706.
452. Mahley RW, Innerarity TL. Lipoprotein receptors and cholesterol homeostasis. Biochim Biophys Acta - Rev Biomembr. 1983 May;737(2):197–222.
453. Streuli CH. Integrins and cell-fate determination. J Cell Sci. 2009 Jan 15;122(2):171–7.
454. Henry B. DRUG PRICING & CHALLENGES TO HEPATITIS C TREATMENT ACCESS. J Heal Biomed law. 2018;
455. Abdel-Razek W, Hassany M, El-Sayed MH, El-Serafy M, Doss W, Esmat G, et al. Hepatitis C Virus in Egypt: Interim Report From the World's Largest National Program. Clinical Liver Disease. 2019.
456. Geneva SWHO. Progress report on access to hepatitis C treatment: focus on overcoming barriers in low- and middle-income countries, March 2018. Who. 2018;
457. Swadling L, Capone S, Antrobus RD, Brown A, Richardson R, Newell EW, et al. A human vaccine strategy based on chimpanzee adenoviral and MVA vectors that primes, boosts, and sustains functional HCV-specific T cell memory. Sci Transl Med. 2014;
458. Barnes E, Folgori A, Capone S, Swadling L, Aston S, Kurioka A, et al. Novel adenovirus-based vaccines induce broad and sustained T cell responses to HCV in man. Sci Transl Med. 2012;

459. Frey SE, Houghton M, Coates S, Abrignani S, Chien D, Rosa D, et al. Safety and immunogenicity of HCV E1E2 vaccine adjuvanted with MF59 administered to healthy adults. Vaccine. 2010;
460. Page K, Melia MT, Veenhuis RT, Winter M, Rousseau KE, Massaccesi G, et al. Randomized Trial of a Vaccine Regimen to Prevent Chronic HCV Infection. N Engl J Med. 2021;
461. Swadling L, Halliday J, Kelly C, Brown A, Capone S, Ansari MA, et al. Highly-immunogenic virally-vectored T-cell vaccines cannot overcome subversion of the T-cell response by HCV during chronic infection. Vaccines. 2016;
462. López S, Arias CF. Multistep entry of rotavirus into cells: A Versaillesque dance. Trends in Microbiology. 2004.
463. Smith AE, Helenius A. How Viruses Enter Animal Cells. Science. 2004.
464. Spear PG, Manoj S, Yoon M, Jogger CR, Zago A, Myscofski D. Different receptors binding to distinct interfaces on herpes simplex virus gD can trigger events leading to cell fusion and viral entry. Virology. 2006.
465. Ujino S, Nishitsuji H, Hishiki T, Sugiyama K, Takaku H, Shimotohno K. Hepatitis C virus utilizes VLDLR as a novel entry pathway. Proc Natl Acad Sci U S A. 2016;
466. Mankowski MC, Kinchen VJ, Wasilewski LN, Flyak AI, Ray SC, Crowe JE, et al. Synergistic anti-HCV broadly neutralizing human monoclonal antibodies with independent mechanisms. Proc Natl Acad Sci. 2018 Jan 2;115(1):E82–91.
467. Zeisel MB, Koutsoudakis G, Schnober EK, Haberstroh A, Blum HE, Cosset FL, et al. Scavenger receptor class B type I is a key host factor for hepatitis C virus infection required for an entry step closely linked to CD81. Hepatology. 2007;
468. Brazzoli M, Bianchi A, Filippini S, Weiner A, Zhu Q, Pizza M, et al. CD81 Is a Central Regulator of Cellular Events Required for Hepatitis C Virus Infection of Human Hepatocytes. J Virol. 2008;
469. Padmanabhan P, Dixit NM. Mathematical model of viral kinetics in vitro estimates the number of E2-CD81 complexes necessary for hepatitis C virus entry. PLoS Comput Biol. 2011;
470. Duncan JD, Urbanowicz RA, Tarr AW, Ball JK. Hepatitis C virus vaccine: Challenges and prospects. Vaccines. 2020.
471. Sabo MC, Luca VC, Ray SC, Bukh J, Fremont DH, Diamond MS. Hepatitis C

virus epitope exposure and neutralization by antibodies is affected by time and temperature. Virology. 2012;

472. Lok SM, Kostyuchenko V, Nybakken GE, Holdaway HA, Battisti AJ, Sukupolvi-Petty S, et al. Binding of a neutralizing antibody to dengue virus alters the arrangement of surface glycoproteins. Nat Struct Mol Biol. 2008;
473. Gromowski GD, Roehrig JT, Diamond MS, Lee JC, Pitcher TJ, Barrett ADT. Mutations of an antibody binding energy hot spot on domain III of the dengue 2 envelope glycoprotein exploited for neutralization escape. Virology. 2010;
474. Pierson TC, Kuhn RJ. Capturing a virus while it catches its breath. Structure. 2012.
475. Cockburn JJB, Navarro Sanchez ME, Fretes N, Urvoas A, Staropoli I, Kikuti CM, et al. Mechanism of dengue virus broad cross-neutralization by a monoclonal antibody. Structure. 2012;
476. Bressanelli S, Stiasny K, Allison SL, Stura EA, Duquerroy S, Lescar J, et al. Structure of a flavivirus envelope glycoprotein in its low-pH-induced membrane fusion conformation. EMBO J. 2004;
477. Fibriansah G, Ng T-S, Kostyuchenko VA, Lee J, Lee S, Wang J, et al. Structural Changes in Dengue Virus When Exposed to a Temperature of 37 C. J Virol. 2013;
478. Lieberman PM. Epigenetics and Genetics of Viral Latency. Cell Host and Microbe. 2016.
479. Leoni MC, Ustianowski A, Farooq H, Arends JE. HIV, HCV and HBV: A Review of Parallels and Differences. Infectious Diseases and Therapy. 2018.
480. Xu C, Wang Y, Liu C, Zhang C, Han W, Hong X, et al. Conformational dynamics of SARS-CoV-2 trimeric spike glycoprotein in complex with receptor ACE2 revealed by cryo-EM. Sci Adv. 2021;
481. Pallesen J, Wang N, Corbett KS, Wrapp D, Kirchdoerfer RN, Turner HL, et al. Immunogenicity and structures of a rationally designed prefusion MERS-CoV spike antigen. Proc Natl Acad Sci U S A. 2017;
482. Kwong PD, Doyle ML, Casper DJ, Cicala C, Leavitt SA, Majeed S, et al. HIV-1 evades antibody-mediated neutralization through conformational masking of receptor-binding sites. Nature. 2002;
483. Walls AC, Tortorici MA, Frenz B, Snijder J, Li W, Rey FA, et al. Glycan shield and epitope masking of a coronavirus spike protein observed by cryo-electron

microscopy. Nat Struct Mol Biol. 2016;
484. Ridpath JF. Immunology of BVDV vaccines. Biologicals. 2013;
485. Kwong PD, Mascola JR. HIV-1 Vaccines Based on Antibody Identification, B Cell Ontogeny, and Epitope Structure. Immunity. 2018.
486. Chen F, Tzarum N, Wilson IA, Law M. V H 1-69 antiviral broadly neutralizing antibodies: genetics, structures, and relevance to rational vaccine design. Current Opinion in Virology. 2019.
487. Keck ZY, Pierce BG, Lau P, Lu J, Wang Y, Underwood A, et al. Broadly neutralizing antibodies from an individual that naturally cleared multiple hepatitis c virus infections uncover molecular determinants for E2 targeting and vaccine design. PLoS Pathog. 2019;
488. Underwood AP, Walker MR, Brasher NA, Eltahla AA, Maher L, Luciani F, et al. Understanding the determinants of BnAb induction in acute HCV infection. Viruses. 2018;
489. Penin F, Combet C, Germanidis G, Frainais P-O, Deléage G, Pawlotsky J-M. Conservation of the Conformation and Positive Charges of Hepatitis C Virus E2 Envelope Glycoprotein Hypervariable Region 1 Points to a Role in Cell Attachment. J Virol. 2001;
490. Krammer F. SARS-CoV-2 vaccines in development. Nature. 2020.
491. Moore JP, Offit PA. SARS-CoV-2 Vaccines and the Growing Threat of Viral Variants. JAMA - Journal of the American Medical Association. 2021.
492. Zon I, Chumbe A, Crispin M, Schinkel J, Lander GC, Sanders RW. 2,4# ,. 2021;